frontiers | Research Topics

Advances in precision diagnosis and therapy of pediatric rare diseases

Edited by
Jian Gao, Jian Wang, Yang Zhou, Yimin Cui and Xue-Ning Li

Published in
Frontiers in Medicine
Frontiers in Pediatrics
Frontiers in Pharmacology

ISSN 1664-8714
ISBN 978-2-8325-3540-0
DOI 10.3389/978-2-8325-3540-0

About Frontiers

Frontiers is more than just an open access publisher of scholarly articles: it is a pioneering approach to the world of academia, radically improving the way scholarly research is managed. The grand vision of Frontiers is a world where all people have an equal opportunity to seek, share and generate knowledge. Frontiers provides immediate and permanent online open access to all its publications, but this alone is not enough to realize our grand goals.

Frontiers journal series

The Frontiers journal series is a multi-tier and interdisciplinary set of open-access, online journals, promising a paradigm shift from the current review, selection and dissemination processes in academic publishing. All Frontiers journals are driven by researchers for researchers; therefore, they constitute a service to the scholarly community. At the same time, the *Frontiers journal series* operates on a revolutionary invention, the tiered publishing system, initially addressing specific communities of scholars, and gradually climbing up to broader public understanding, thus serving the interests of the lay society, too.

Dedication to quality

Each Frontiers article is a landmark of the highest quality, thanks to genuinely collaborative interactions between authors and review editors, who include some of the world's best academicians. Research must be certified by peers before entering a stream of knowledge that may eventually reach the public - and shape society; therefore, Frontiers only applies the most rigorous and unbiased reviews. Frontiers revolutionizes research publishing by freely delivering the most outstanding research, evaluated with no bias from both the academic and social point of view. By applying the most advanced information technologies, Frontiers is catapulting scholarly publishing into a new generation.

What are Frontiers Research Topics?

Frontiers Research Topics are very popular trademarks of the *Frontiers journals series*: they are collections of at least ten articles, all centered on a particular subject. With their unique mix of varied contributions from Original Research to Review Articles, Frontiers Research Topics unify the most influential researchers, the latest key findings and historical advances in a hot research area.

Find out more on how to host your own Frontiers Research Topic or contribute to one as an author by contacting the Frontiers editorial office: frontiersin.org/about/contact

Advances in precision diagnosis and therapy of pediatric rare diseases

Topic editors

Jian Gao — Shanghai Children's Medical Center, China
Jian Wang — International Peace Maternity and Child Health Hospital, China
Yang Zhou — Brown University, United States
Yimin Cui — Peking University, China
Xue-Ning Li — Fudan University, China

Citation

Gao, J., Wang, J., Zhou, Y., Cui, Y., Li, X.-N., eds. (2023). *Advances in precision diagnosis and therapy of pediatric rare diseases*. Lausanne: Frontiers Media SA. doi: 10.3389/978-2-8325-3540-0

Table of contents

frontiers | Frontiers in Medicine

TYPE Case Report
PUBLISHED 18 July 2022
DOI 10.3389/fmed.2022.922347

OPEN ACCESS

EDITED BY
Jian Gao,
Shanghai Children's Medical Center, China

REVIEWED BY
Feng Hu,
Shanghai Jiao Tong University, China
Jiajia Yang,
University of South Florida, United States

*CORRESPONDENCE
Yifei Li
liyfwcsh@scu.edu.cn
Shuhua Luo
luoshuhua@scu.edu.cn

†These authors have contributed equally to this work

SPECIALTY SECTION
This article was submitted to Precision Medicine, a section of the journal Frontiers in Medicine

RECEIVED 17 April 2022
ACCEPTED 23 June 2022
PUBLISHED 18 July 2022

CITATION
Wang Y, Fang Y, Zhang D, Li Y and Luo S (2022) A rare case of arrhythmogenic right ventricular cardiomyopathy associated with *LAMA2* mutation: A case report and literature review. *Front. Med.* 9:922347. doi: 10.3389/fmed.2022.922347

A rare case of arrhythmogenic right ventricular cardiomyopathy associated with *LAMA2* mutation: A case report and literature review

Yue Wang[1†], Yibing Fang[2†], Dan Zhang[3], Yifei Li[4*] and Shuhua Luo[1*]

[1]Department of Cardiovascular Surgery, West China Hospital, Sichuan University, Chengdu, China, [2]Department of Cardiovascular Surgery, Southwest Hospital, Army Medical University, Chongqing, China, [3]Key Laboratory of Medical Electrophysiology, Ministry of Education, Medical Electrophysiological Key Laboratory of Sichuan Province, Institute of Cardiovascular Research, Southwest Medical University, Luzhou, China, [4]Key Laboratory of Birth Defects and Related Diseases of Women and Children of MOE, Department of Pediatrics, West China Second University Hospital, Sichuan University, Chengdu, China

Background: Arrhythmogenic right ventricular cardiomyopathy (ARVC) is a heritable heart muscle disorder that predominantly affects the right ventricle. Mutations in genes that encode components of desmosomes, the adhesive junctions that connect cardiomyocytes, are the predominant cause of ARVC. A case with novel heterozygous mutation in the *LAMA2* gene is reported here. The protein encoded by *LAMA2* gene is the α2 chain of laminin-211 protein, which establishes a stable relationship between the muscle fiber membrane and the extracellular matrix. We explored the potential mechanism and the relationship between the mutation and ARVC.

Case Presentation: At the age of 8, the patient developed syncope and palpitation after exercise. Dynamic electrocardiogram recorded continuous premature ventricular beats, and MRI showed the right ventricle was significantly enlarged and there were many localized distensions at the edge of the right ventricular wall. The patient was diagnosed with ARVC and received heart transplantation at the age of 14 due to severe heart dysfunction. The myocardial histological pathological staining revealed a large amount of fibrosis and adipose migration. Whole exome sequencing (WES) identified the heterozygous mutation in the *LAMA2* gene [NM_000426.3: c.8842G > A (p.G2948S)]. This is the first report of these variants. Analysis was performed on genetic disorders to reveal splice site changes and damage to protein structure. *LAMA2 p.G2948S* predicted unstable protein structure and impaired function. Induced pluripotent stem cell-derived cardiomyocytes (iPSC-CMs) were established. RNA-seq and the western blot were performed on IPSC-CMs to explore the ARVC-related signaling pathway.

Conclusion: This is the first case report to describe an ARVC phenotype in patients possessing a novel *LAMA2 c.8842G > A* (*p.G2948S*) mutation. Our results aid in understanding of the pathogenesis of ARVC. The molecular mechanism of *LAMA2* leading to ARVC disease still needs further study.

KEYWORDS

***LAMA2*, ARVC, iPSC, case report, literature review**

Introduction

Arrhythmogenic right ventricular cardiomyopathy is an inherited cardiomyopathy characterized by the fibrofatty replacement of the myocardium predominantly in the right ventricle. Progressive loss of right ventricular myocardium and its replacement by fibrofatty tissue is the pathological hallmark of the disease (1, 2). Mutations in the genes encoding desmosome complex, which is important in regulating cell-to-cell adhesion and maintain cellular integrity, may affect protein structure of desmosome complex. The degradation of desmosome has been believed to be involved in the pathogenesis of ARVC. Until now, most of the ARVC-related genetic variants have been located in the desmosome complex. In addition, other non-desmosome genes, which participate in mediating cellular adhesion and intercellular connection, would also contribute to induce ARVC, and increasing numbers of mutations have been underlined. In detail, the reported genetic mutations of ARVC encoding proteins cover a large diverse range of biological functions, including cytoskeletal architecture formation, calcium handling, sodium transport, and cytokine signaling (2). Nevertheless, negative genetic results have been found in 35–50% of patients, suggesting that there may be unknown genes involved in the pathogenesis of ARVC (3, 4).

The *LAMA2* gene encodes the α2 chain of laminin-211 protein, which establishes a stable relationship between the muscle fiber membrane and the extracellular matrix (ECM). Laminin 211 is dominantly expressed in the basement membrane of myocytes and Schwann cells. The mutations of *LAMA2* have been proved to be involved in the initial of congenital muscular dystrophy type 1a (MDC1A) and limb girdle muscular dystrophy (LGMD) (5, 6). Laminin-α2 has also been proved to be expressed in other organ tissues, such as the heart (7). However, current evidence suggests that only a small proportion of patients with MDC1A is associated with cardiac-related clinical manifestations, and the correlation between *LAMA2* mutation and ARVC remains unknown (8, 9). And only one record from the ClinicalVar database demonstrated *LAMA2* might be related with primary dilated cardiomyopathy. Induced pluripotent stem cell-derived cardiomyocytes (iPSC-CMs) have been used as a fully mimic platform to study the biological and molecular mechanism of any identified uncertain genetic variant. Several cell lines had been established to demonstrate the essential changes on ARVC-related genetic mutations. Thus, we attempt to explore the relationship between *LAMA2* mutation and ARVC *via* iPSC-CMs.

Herein, we report a rare case with ARVC carrying a novel heterozygous mutation in the *LAMA2* gene. This should be the first case report of ARVC due to a *LAMA2* mutation, and we also established the first iPSC line of *LAMA2* associated with ARVC, which would be differentiation into cardiomyocytes to address the potential activated ARVC-related pathogenic signaling pathways.

Case presentation

Ethics compliance

The parents of the patient provided written consent for participating in the study carried out at the West China Hospital, Sichuan University, China. This research study was approved by the Ethics Committee of West China Second University Hospital, Sichuan University, China (2014–034).

Clinical presentation and outcomes

This proband was a male who had been admitted to our hospital due to aggressive fatigue, chest tightness, and fainting for 2 years. He experienced significant chest pain and palpitations shortly before syncope, with a decrease in tolerance of daily activities. A pale face, dull heart sound, and third-degree systolic murmur in the fourth intercostal space were observed. Results of physical examination of the respiratory and nervous systems were negative. The parents of the patient declined any cardiovascular symptoms. Myocarditis has been excluded at first due to the patient, and his parents declined any no related nearby infection history. Furthermore, the patient declined any symptoms of muscular dystrophy. Then, any potential virus antibodies were negative after serum analysis. Electrocardiogram (ECG) demonstrated inversion of T waves in leads V1–V5, and epsilon waves were visible in some leads (**Figure 1A**). Holter presented 5,443 premature

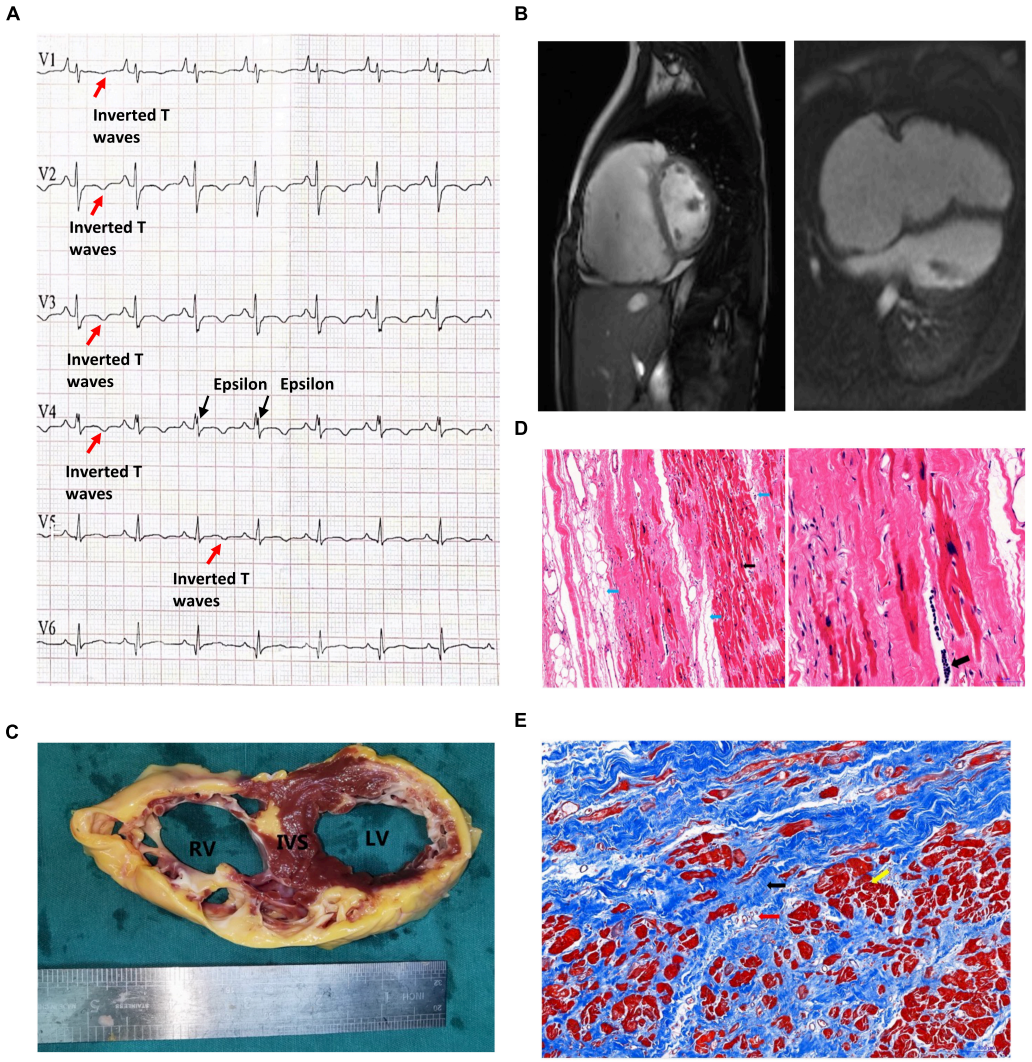

FIGURE 1
Clinical presentation of the proband. **(A)** The patient's preoperative ECG showed inverted T waves in lead V1, V2, V3, V4, and V5, with typical Epsilon waves visible in V4. **(B)** Preoperative cardiac MRI of the patient indicated that the right atrium was significantly enlarged, the right ventricular wall was thinner, the right ventricular wall edge was localized in many places, and the amplitude of myocardial contraction of the right ventricle was significantly reduced. **(C)** The myocardium was replaced by extensive fibrous adipose tissue in the wall of the right ventricle (RV), the right ventricle was bag like and thinly dilated, part of the ventricular septum (IVS) was adipose, and part of the myocardium in the anterior and lateral wall of the left ventricle (LV) was replaced by adipose fibers. **(D)** HE staining of the myocardium of the right ventricle: Left: the blue arrow indicates the adipose tissue, and the myocardium of the right ventricle is surrounded by the adipose tissue and divided into cords. The black arrow shows abnormal hypertrophic cardiomyocytes with large, dark-stained nuclei and oddly shaped nuclei, broken muscle fibers in the cytoplasm of the cardiomyocytes (magnified 100×). Right: The black arrow indicates the presence of inflammatory cell infiltration between cardiomyocytes at magnified 200×. **(E)** Masson staining of the myocardium of the right ventricle. Note that the myocardium (the yellow arrow) is surrounded by large amount of fibrous adipocytes (the black arrow) and divided into cords or islands. The collagenous fiber bundles around small blood vessels (red arrows) are increased.

multisource ventricular beats in 24 h, with unequal pairing intervals, ventricular fusion wave, and insertion ventricular premature beats. MRI identified enlargement of the right ventricle, the thinner right ventricular wall, and localized distensions at the edge of the right ventricular wall. The myocardial contraction of the right ventricle was significantly reduced, and ejection fraction of the right ventricle was 15%. Right ventricular end-diastolic volume index = 142 ml/m^2 (Figure 1B), so that, according to Task Force Criteria (10), this patient received a clinical diagnosis of ARVC based on his clinical manifestation, classic ECG presentation, and a cardiac phenomenon recorded by MRI.

Unfortunately, due to severe and irreversible heart dysfunction, the patient received heart transplantation at the age of 14. The examination of the heart tissue revealed generally adipose infiltration in the interventricular septum

and partial fiber-adipose infiltration in the myocardial tissue of the posterior wall of the left ventricle (Figure 1C). The wall of the right ventricle is extensively fiber-adipose, and only a small amount of myocardial tissue remains. The whole right ventricle is obviously dilated. And the myocardial histological pathological staining revealed a large amount of fibrosis and adipose migration (Figures 1D,E).

After the heart transplantation, the patient had a good quality of life and was followed for 3 years.

Molecular results

A peripheral blood sample was obtained from the patients in an EDTA anticoagulant blood sample tube stored at 4°C for less than 6 h, and DNA was extracted. Protein-coding exome enrichment was performed using the Agilent SureSelect Human All Exon V6. The whole exon sequencing (WES) of the patient and his parents were performed using the NovaSeq 6000 platform (Illumina, San Diego, CA, United States), and the raw data were processed using FastP to remove adapters and filter out low-quality reads. Paired-end reads were aligned with the ENSEMBL GRCh38/hg38 reference genome using the BWA software (version 0.7.12-r1039). Then, the SAMtools software (Version 1.3.1) was used to compare and order the results, and Sambamba (Version 0.7.1) was used to mark the repeated reads. Variant annotation was performed in accordance with database-sourced minor allele frequencies (MAFs) and practical guidelines on pathogenicity issued by the American College of Medical Genetics. The annotation of MAFs was performed based on the 1,000 Genomes, dbSNP, ESP, ExAC, Provean, Sift, Polypen2_hdiv, Polypen2_hvar, and Chigene in-house MAF databases using R software (R Foundation for Statistical Computing, Vienna, Austria). The sequencing data have been deposited in the GSA database.

Whole exon sequencing identified *de novo* heterozygous mutations in the *LAMA2* gene at c.8842G > A, which has not been reported in any publication. This mutation was absent from the patients' parents (Figure 2). This mutation site could be retrieved in 1000G and the ExAC database. There were 3 records of allele carriers in 1000G and 46 records of allele carriers in ExAC. Its clinical associations were found in congenital muscular dystrophy (RCV000764636.1), *LAMA2*-related dystrophy (RCV001086813.1), and primary dilated cardiomyopathy (RCV001293224.1). All the records were submitted by a gene sequencing company, and no available publication demonstrated the molecular mechanism and provided a detailed clinical report. Until now, no research has declaimed a clear relationship between *LAMA2 c.8842G > A* and ARVC. According to the American College of Medical Genetics, the variant has uncertain pathogenicity. SIFT, Polyphen_HumDiv, Polyphen_HumVar, and Mutation Taster were used for mutation locus screening. Analysis performed with MutationTaster revealed that this mutation was considered disease causing due to amino acid sequence changes, protein features affected, and splice site changes (probability = 0.999). The PolyPhen tool predicted protein structural and functional damaging for p.G2948S (Polyphen_HumDiv score = 1.000, the Polyphen_HumVar score = 0.999). The SIFT prediction on the protein batch demonstrated a damaging change as a score of 0.006. And the PROVEAN prediction on the protein batch revealed a deleterious change as a score of −4.34. All analyses were based on the P24043 FASTA sequence of the G2948S variant. However, it failed to identify any other known ARVC-related gene mutations both in exons and introns.

To understand the molecular architecture of the human *LAMA2* gene, we performed comparative modeling using the SWISS-MODEL[1]. We estimated the change in the free energy of the model using the mutation cut-off scanning matrix (mCSM) method[2], the Site Directed Mutator (SDM)[3], and the DyanMut method, which can be used to analyze and visualize protein dynamics by sampling conformations and assess the impact of mutations on protein dynamics and stability[4]. To assess the impacts of mutations on the stability of *LAMA2*. We also used the DUET server[5] that integrates mCSM and SDM to improve the overall prediction accuracy of the mutations under consideration. The signature vector that was ultimately generated was employed to train the predictive classification and the regression model used to calculate the change induced by mutations in terms of Gibbs folding free energy ($\Delta\Delta G$).

The SWISS-MODEL tool was used to analyze stability after amino acid changes. Ramachandran plots indicated that amino acid positions were altered (Figure 3A). Rebuilding molecular structure based on a 1okq.1.A template resulted in residue changes between Gly and Alaat 2948 (Figure 3B). Five types of calculation methods all demonstrated significant destabilizing change (DynaMut −0.950 Kcal/mol; NMA-Based Predictions, 0.298 Kcal/mol; mCSM, −1.404 Kcal/mol; DUET, −1.505 Kcal/mol; SDM, −2.480 Kcal/mol; Figure 3C). Besides, change in vibrational entropy energy between wild-type and mutant Figure 3D demonstrated a decrease of molecule flexibility as −0.372 kcal/mol K. The blue-colored amino acids sequence according to the vibrational entropy change upon mutation represented a rigidification of the structure.

Induced pluripotent stem cell reprogramming and validation

Peripheral blood mononuclear cells (PBMCs) were isolated from 20 ml of blood obtained from the patient with *LAMA2 c.8842G > A*. And the wild-type control was obtained

1 https://swissmodel.expasy.org/
2 http://biosig.unimelb.edu.au/mcsm/
3 http://marid.bioc.cam.ac.uk/sdm2
4 http://biosig.unimelb.edu.au/dynamut/
5 http://biosig.unimelb.edu.au/duet/

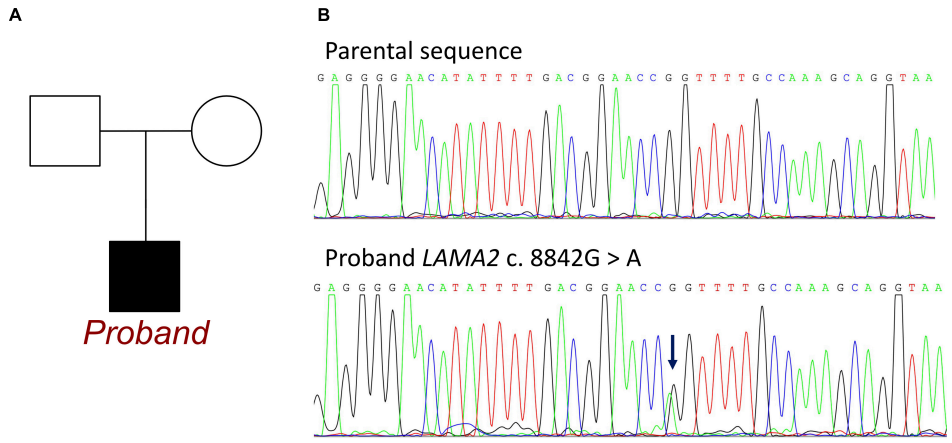

FIGURE 2
Information of *LAMA2* c.8842G > A in the family of the proband. **(A)** Family map of gene mutation. **(B)** Sequencing of mutations. Blue arrow: The normal group showed single peak of base G, while the patient showed heterozygous state of base G peak and A peak.

from a healthy donor, who was confirmed without any pathogenic variant, including *LAMA2*, by another WES. The third-generation PBMCs cells with good growth status were induced to differentiate into pluripotent stem cells. The PBMCs cells were cultured in a StemPro-34 complete medium containing cytokines IL-3, IL-6, SCF, and FLT-3 for 4 days. Sendai virus containing four reprogramming transcription factors [OCT3/4 (MOI = 3), SOX2 (MOI = 5), KLF4 (MOI = 3), and C-MYC (MOI = 5)] was added into the StemPro-34 complete culture medium (provided with a Sendai virus reprogramming kit) and cultured in a cell incubator for 24 h. For the first 3 days after transfection, the cells were maintained in the StemPro-34 complete culture medium without virus. Sendai virus-infected PBMCs were transferred to Matrigel-coated 12-well plate containing an E8 medium. iPSCs, (WCHi002-A) were manually picked at around day 20 post transfection and plated onto a Matrigel-coated 12- well plate. iPSCs differentiated to cardiomyocytes by modulating WNT signaling with CHIR99021 and IWR-1. iPSC-CMs were enriched by culture in lactate-containing media. Spontaneous beating activity can be observed in iPSC-CMs and the expression of myosin light chain 2 (MYL2) and cardiac troponin T (CTNT) can be detected by immunofluorescent staining.

Induced pluripotent stem cell-derived CMs were fixed in 4% paraformaldehyde overnight. The cells were incubated in a blocking medium (PBS containing 5% donkey serum, 0.2% Triton X-100) at 4°C overnight. For immunostaining, the sections were incubated with primary antibodies at 4°C overnight and secondary antibodies for 2 h. The primary antibodies used were as follows: sarcomeric alpha-actinin (1:200, Abcam, ab137346). After washing with a blocking buffer, the slices were incubated with optimal secondary antibodies with DAPI at room temperature for 2 h. After washing, the samples were imaged using an Olympus FV1000 confocal microscope (**Figure 4A**). Flow cytometry had been applied to demonstrate the purity of iPSC-CMs. Non-differentiated iPSC and differentiated iPSC were stained with cardiac troponin I (1:200, Abcam, ab56357). More than 80% of CMs had been identified (**Figure 4B**).

The TRIzol method was used to extract total RNA from iPSC-CMs of ARVC (n = 3) and WT (n = 3) groups, and the DNase I method was used to remove DNA in the samples. An Illumina HiSeq XTEN/NovaSeq 6000 sequencing platform was used for high-throughput sequencing. Transcript abundance was determined by TopHat alignment followed by HTSeq-Count and statistical analysis by DESeq2. Enrichment analysis of differentially expressed genes (DEGs) was implemented by the clusterProfiler R package, in which gene length bias was corrected. KEGG pathways with corrected P-value less than 0.05 were considered significantly enriched by DEGs. According to the established pathophysiological characteristics of ARVC, five enrichment sets were established, including fibrosis, adipogenesis, apoptosis, intracellular calcium, and cellular connectivity (**Figure 5A**). The KEGG pathways of fibrosis were enriched in PI3K-Akt signaling and regulation of actin cytoskeleton (**Supplementary Figure 1**). The enrichment analysis for lipid metabolism revealed a general alternation of lipid metabolic dysfunction (**Supplementary Figure 2**). In addition, apoptosis had been recorded by KEGG enrichment (**Supplementary Figure 3**). Most important, ARVC was characterized as misleading calcium handling and cellular connection disorders. After KEGG analysis based on DEGs, the significant calcium signaling pathway and cGMP-PKG signaling pathway were identified (**Supplementary Figure 4**). Furthermore, the changes in adherens junction, cell adhesion molecules, and the hippo signaling pathway had been proved to be participated in pathological remodeling of cardiomyocyte

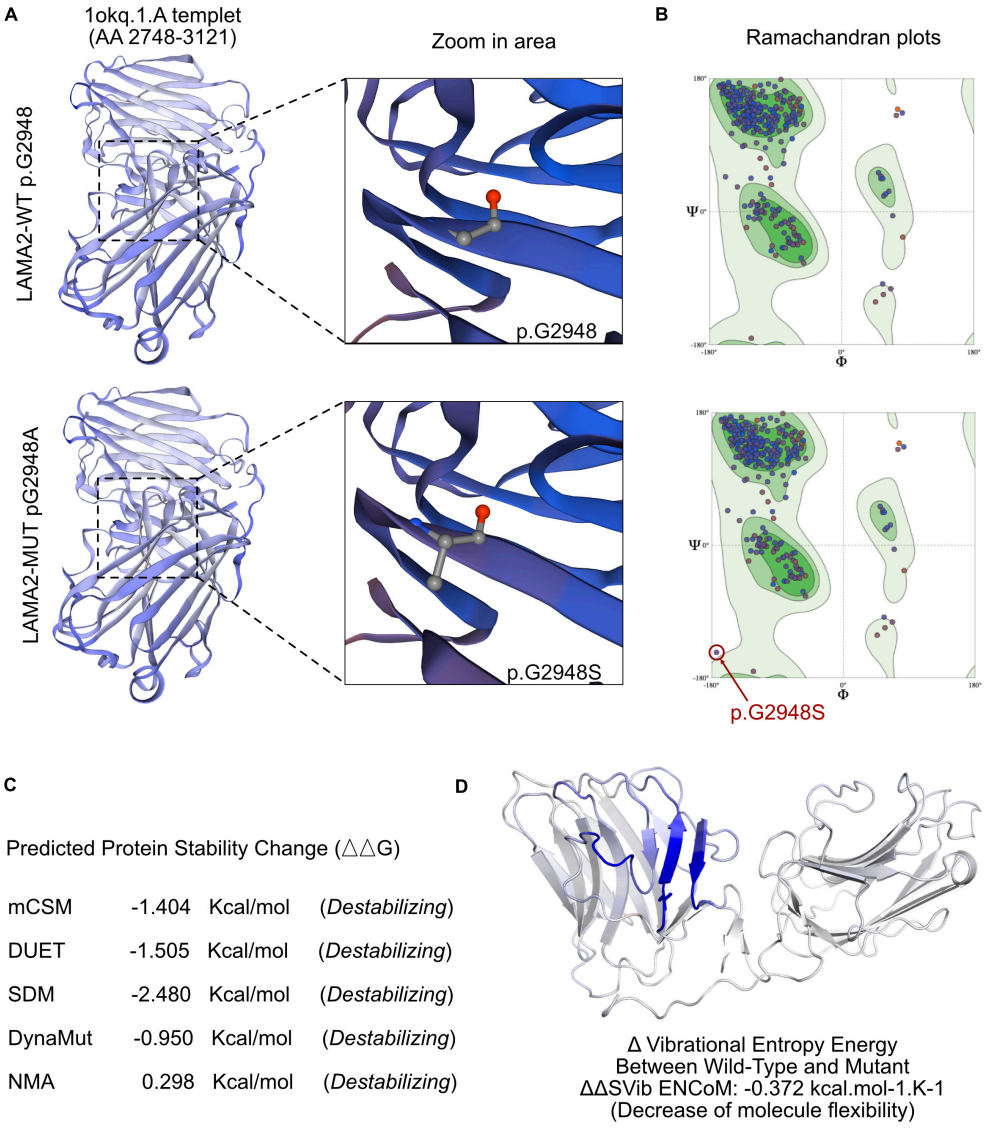

FIGURE 3
The effects of *LAMA2* c.8842G > A mutation on the molecular structure of the protein. **(A)** Individual crystal structures of wild type and G2948S according to the 1okq.1.A model template. **(B)** Ramachandran plots of amino acid with wild type and p.G2948A. **(C)** The comparisons of free energy on crystal structure of the wild type sequence and the p.G2948A variant. **(D)** The structural changes due to the mutation of *LAMA2* G2948S.

due to *LAMA2* mutation. And the enrichment of ARVC was definitely identified among all DEGs (Figure 5B).

We queried all possible related signaling pathways of ARVC through KEGG website[6], and found the *LAMA2* and its related proteins integrin beta 1 (ITGB1) and β-muscle dystroglycan 1 (β-DG) are involved in the ARVC signaling pathway. The protein expressions of LAMA2, ITGB1, and β-DG were further detected by the Western blot. Normal healthy human PBMCs were successfully reprogrammed and inversely differentiated into iPSCs according to the above scheme, and were induced into cardiomyocytes as the control group. Both groups were continuously cultured in a myocardial maintenance medium for 50 days. Differentiated iPSC-CMs were lysed in RIPA lysis buffer system (Santa Cruz Biotechnology, sc-24948) with Mini Protease Inhibitor Cocktail Tablets (cOmplete, 4693124001). Total protein concentrations were normalized using BCA analysis (Life Technologies, 23227). After boiling with a 4X loading buffer for 5 min, 20-μl cell lysate of each sample was separated on a 10% gel, transferred to a PDVF membrane, and blocked by 4% BSA/TBST. Primary antibodies of LAMA2 (1:2,000, Abcam, ab140482), β-DG (1:2,000, Abcam, ab3125),

6 https://www.genome.jp/kegg

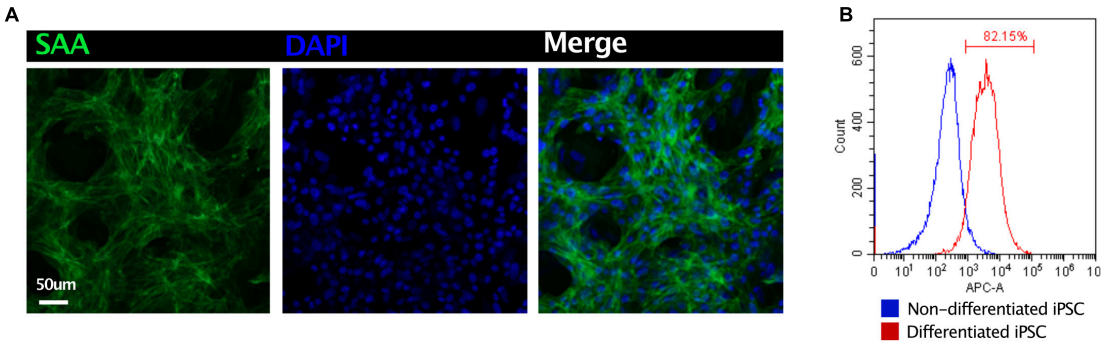

FIGURE 4
Quality control of iPSC-derived CMs. **(A)** Immunostaining of sarcomeric alpha-actinin (SAA) demonstrated the high ratio of CMs. **(B)** Flow cytometry revealed 82.5% iPSC had been differentiated into CMs.

ITGB1 (1:2,000, Abcam, ab52971), Adiponectin (1:2,000, Abcam, ab181281), FABP4 (1:2,000, Abcam, ab92501), CTGF (1:2,000, Abcam, ab209780), and GAPDH (1:2,000, ProteinTech, 60004-1-lg). The data were analyzed with GraphPad Prism 8.0 statistical software by *t*-test. LAMA2 protein expression in the ARVC group demonstrated significant decreased (p = 0.02), ITGB1 (p = 0.001), and β-DG (p = 0.004) protein expressions were significantly upregulated (Figures 5C,D).

Discussion

This study demonstrated a rare clinical case with a *LAMA2* genetic heterozygous mutation (c.8842G > A, p.G2948S). The patient was initially diagnosed with ARVC based on clinical presentation and radiological images examinations according to Task Force Criteria. After several years of medication administration, the irreversible heart failure and aggressive cardiac pathological remodeling led this patient to receive a heart transplantation at the age of 14. Before the heart transplantation, WES had been applied to this boy. Interestingly, the *LAMA2* c.8842G > A variant had been identified at the first time among patients with ARVC. However, the patient was absent from any other potential-related variants. So that it is critical to demonstrate the relationship between *LAMA2* and ARVC. Within this research, we enrolled histological section assessment to explore the pieces of evidence on standard ARVC changes. Most important, we reprogrammed the PBMCs of this proband to iPSC. After differentiating iPSC-CMs successfully, bulk RNA-seq was involved to reveal the molecular alternations post *LAMA2* mutation, which would definitely help to underline the association between *LAMA2* and ARVC.

Arrhythmogenic right ventricular cardiomyopathy has been characterized as a heritable disorder with palpitations, syncope, ventricular tachycardia (VT), or fibrillation. Ventricular dysfunction and heart failure can also develop can be found in some patients. This kind of disease was initially considered to be a developmental abnormality of the right ventricle. With the emerging pieces of evidence on molecular diagnosis, a novel genotype-based clinicopathology classification of arrhythmogenic cardiomyopathy (ACM) has been well established. Several specific mutations within desmosome would result in biventricular or only left ventricular phenotype, such as DSP, PLN, and CTNNA3. Besides, large unknown mutations have been claimed to be associated with left ventricular failure, leading to heart transplantation. For this patient, *LAMA2* c.8842C > A could be one of the potential mutations to cause cluster 4 ACM. After the research database, only four reports have been retrieved on *LAMA2* c.8842C > A. Three of them were identified among patients with muscular dystrophy, and only one record demonstrated a potential link with primary dilated cardiomyopathy. In addition, the iPSC-CMs provided a good platform to study the molecular mechanisms due to an uncertain mutation. The bulk RNA-seq results demonstrated alternations among calcium handling, impaired cell-cell interaction, reduced cellular adhesion, and dysfunction of lipid metabolism. All the changes in gene expressions and regulation fall within the pathological remodeling of ARVC. Taking the histological studies of the proband's abandoned heart, it would draw a highly convinced association between *LAMA2* c.8842C > A and ARVC.

After reviewing all the published cases of *LAMA2* missense mutation, a case series of 57 particular variants was assembled and summarized in Table 1. Most of the mutations were correlated with the symptom of muscular dystrophy, and there was no association with cardiac-related clinical manifestations in theses mutations. Among them, 15 variants were located in the N-terminal domain, 18 variants were located in EGF-like domains, and 16 variants were located in LG domains. But there was no reported pathogenic missense mutation in the LG5 domain.

The laminin-211 structure consists of α2, β1, and γ1 chains. The polymeric activity of laminin-211 maps to three domains of LN: nidogen binds γ 1-Leb3, agrin binds the curl γ1

TABLE 1 A summary of reported cases of *LAMA2* missense mutation.

References	Exon	Variants	Predicted amino acid change	Protein domains	Phenotype
Oliveira	1	c.112G > A	p.Gly38Ser	N-terminal	MDC1A
Oliveira	2	c.245A > T	p.Gln82Leu	N-terminal	Late-onset LAMA2-related MD
Ganapathy	2	c.250C > T	p.Arg84Ter	N-terminal	MDC1A
Oliveira	3	c.437C > T	p.Ser146Phe	N-terminal	MDC1A
Gavassini	4	c.454T > G	p.Trp152Gly	N-terminal	LGMD
Geranmayeh	4	c.470C > T	p.Ser157Phe	N-terminal	MDC1A
Di Blasi	4	c.500A > C	p.Gln167Pro	N-terminal	MDC1A
Harris	4	c.611C > T	p.Ser204Phe	N-terminal	LGMD
Dean	5	c.713C > A	p.Ala238Asp	N-terminal	LGMD
Gavassini	5	c.728T > C	p.Leu243Pro	N-terminal	LGMD
Oliveira	5	c.745C > T	p.Arg249Cys	N-terminal	MDC1A
Marques	5	c.812C > T	p.Thr271Ile	N-terminal	Epileptic encephalopathy
Oliveira	5	c.818G > A	p.Arg273Lys	N-terminal	MDC1A
Beytía	6	c.830C > T	p.Ser277Leu	N-terminal	MDC1A
Gavassini	6	c.850G > A	p.Gly284Arg	N-terminal	LGMD
Oliveira	10	c.1326T > G	p.Cys442Trp	EGF-like 3	MDC1A
Töpf	10	c.1466A > G	p.Lys489Arg	EGF-like 4	LGMD
Xiong H	11	c.1553G > A	p.Cys518Tyr	EGF-like 5; first part	MDC1A
Tezak/Valencia	11	c.1580G > A	p.Cys527Tyr	EGF-like 5; first part	MDC1A
Ganapathy	12	c.1749C > G	p.Tyr583Ter	IV type A 1	MDC1A
Beytía	14	c.2089A > G	p.Ile697Val	IV type A 1	MDC1A
Marques	18	c.2461A > C	p.Thr821Pro	EGF-like 7	Epileptic encephalopathy
Xiong H	18	c.2462C > T	p.Thr821Met	EGF-like 7	MDC1A
Tezak	19	c.2584T > C	p.Cys862Arg	EGF-like 7	MDC1A
Allamand	21	c.2954G > A	p.Cys985Tyr	EGF-like 10	MDC1A
Guicheney	21	c.2986T > C	p.Cys996Arg	EGF-like 10	MDC1A
Valencia	22	c.3154A > G	p.Ser1052Gly	EGF-like 11	MDC1A
Töpf	23	c.3235T > C	p.Cys1079Arg	EGF-like 12	LGMD
Oliveira	23	c.3235T > G	p.Cys1079Gly	EGF-like 12	Late-onset LAMA2-related MD
Xiong H	27	c.3931T > G	p.Trp1311Gly	IV type A 2	MDC1A
Ganapathy	27	c.4048C > T	p.Arg1350Ter	IV type A 2	MDC1A
Ganapathy	29	c.4198C > T	p.Arg1400Ter	EGF-like 14; second part	MDC1A
Di Blasi	30	c.4405T > C	p.Cys1469Arg	EGF-like 16	MDC1A
Oliveira	31	c.4523G > A	p.Arg1508Lys	EGF-like 16	MDC1A
Wang	32	c.4640C > T	p.Thr1547Met	EGF-like 17	MDC1A
Oliveira	32	c.4654G > A	p.Ala1552Thr	EGF-like 17	MDC1A
Allamand	32	c.4690C > T	p.His1564Tyr	EGF-like 17	MDC1A
Tezak	33	c.4750G > A	p.Gly1584Ser	Domain II and I	MDC1A
Afshin	33	c.4840A > G	p.Asn1614Asp	Domain II and I	MDC1A
Geranmayeh	38	c.5530C > A	p.Arg1844Ser	Domain II and I	MDC1A
Oliveira	46	c.6548T > G	p.Leu2183Arg	G-like 1	MDC1A
Giugliano	47	c.6599G > A	p.Arg2200His	G-like 1	MDC1A
Töpf	47	c.6624G > C	p.Trp2208Cys	G-like 1	LGMD
Oliveira	47	c.6707G > A	p.Arg2236Lys	G-like 1	LGMD
Töpf	49	c.7040G > T	p.Gly2347Val	G-like 2	LGMD
Ganapathy	50	c.7147C > T	p.Arg2383Ter	G-like 2	MDC1A
Gavassini	52	c.7431A > T	p.Arg2477Ser	G-like 2	LGMD
Oliveira	54	c.7571A > T	p.Glu2524Val	–	MDC1A
Afshin	55	c.7681G > A	p. Gly2561Ser	G-like 3	MDC1A
He	55	c.7691T > C	p.Leu2564Pro	G-like 3	MDC1A
Ganapathy	56	c.7816del	p.Met2606Ter	G-like 3	MDC1A
Geranmayeh	56	c.7881T > G	p.His2627Gln	G-like 3	MDC1A
Xiong H	56	c.7898G > C	p.Gly2633Ala	G-like 3	MDC1A
Magri	60	c.8544C > G	p.His2848Gln	G-like 4	LGMD
Töpf	61	c.8654T > A	p.Leu2885Gln	G-like 4	LGMD
Liang	61	c.8654T > C	p.Leu2885Pro	G-like 4	MDC1A
Fattahi	61	c.8665G > A	p.Gly2889Arg	G-like 4	MDC1A

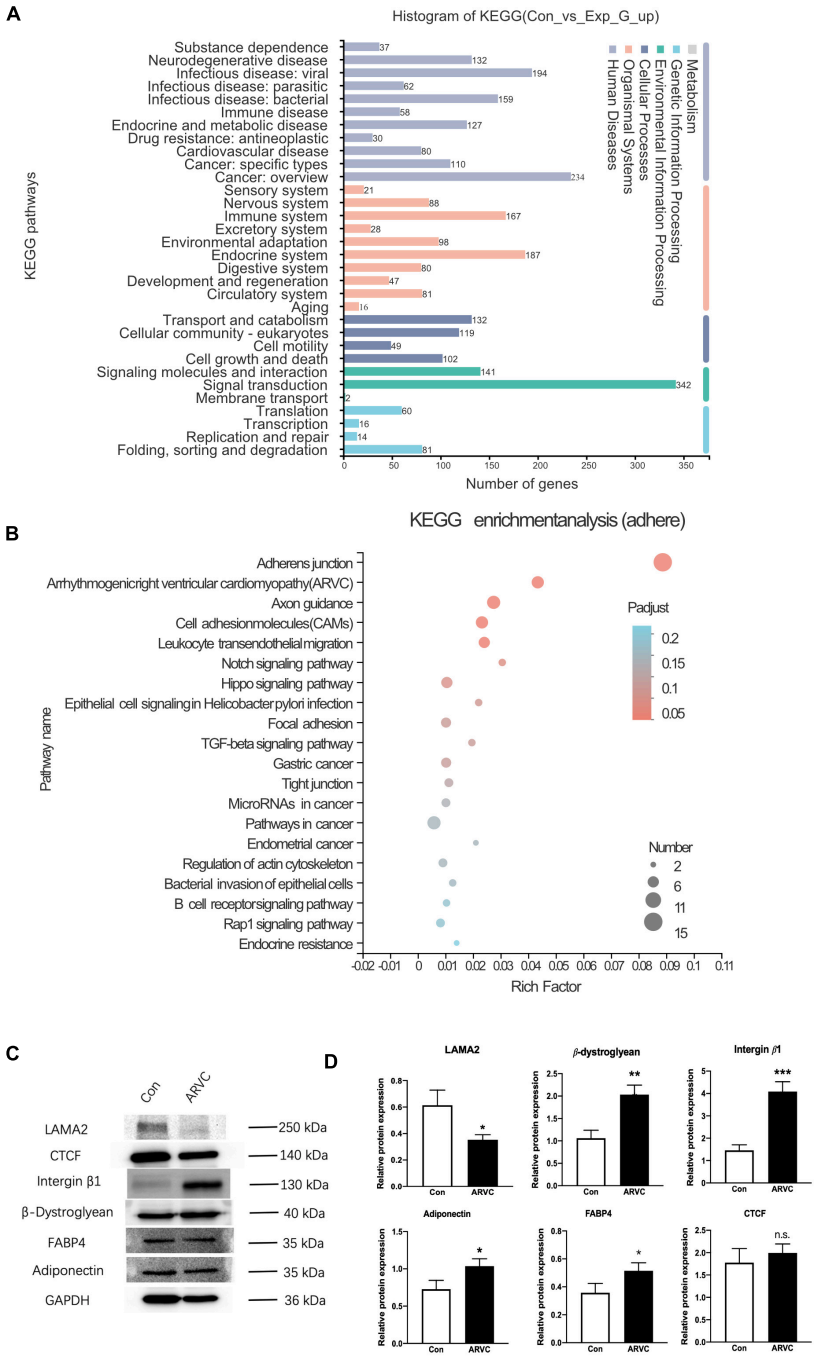

FIGURE 5
The analysis of iPSC-derived CMs indicated an ARVC-associated phenotype. **(A)** Histogram of KEGG signaling pathway classification. **(B)** KEGG enrichment analysis of the adherent signaling pathway. **(C)** Western blot results showed the protein expressions of LAMA2, CTCF, Integrin-β1, β-Dystroglycan, FABP4, and Adiponectin in myocardium cells of the control group and the ARVC group, with GAPDH as internal reference. **(D)** Histogram shows the protein expression differences of LAMA2, CTCF, Integrin-β1, β-Dystroglycan, FABP4, and Adiponectin between the control group and the ARVC group (N.S. The difference is meaningless; *$p < 0.05$; **$p < 0.01$; ***$p < 0.001$).

subunit, integrin α7β1 binds LG1-3, α-dystroglycan (α-DG) binds to LG4-5 with sulfated glycolipids. LG interactions provide anchoring for the cell membrane and cytoskeleton. α-DG is coupled to transmembrane β-DG, β-DG binds to cytoskeletal dystrophin, and dystrophin binds to the actin-rich cytoskeleton; this critical interaction creates a link from the basement membrane to actin cytoskeleton (11). Previous studies demonstrated homozygous or compound heterozygous

mutations that result in deletion of the α2 subunit or diverse aggregation of laminin-211 lead to muscular dystrophy with peripheral nerve defects like MDC1A or LGMD.

In this case, the heterozygous mutation was located in the LG5 domain. We used SFIT, PolyPhen-2, and MutationTaster to predict the impact of this mutation on protein structure and function, showing that p.G2948S is a diseasing-causing and protein-damaging mutation. The Western blot showed that the expression of LAMA2 protein decreased in the ARVC group, and the expression of LAMA2-interacting proteins (ITGB1, β-DG) increased as a compensatory regulation. Using bulk RNA-seq, it confirmed that DEGs in iPSC-CMs of the ARVC group were abundant in signaling pathways of inflammation, fibrosis, adipose, cell connection, and apoptosis. Thus, we elucidated that p.G2948S of *LAMA2* induced the change of the LG5 domain and induce the compensatory expression of ITGB1 and β-DG, and led to the activation of ARVC changes. Moreover, the impaired binding function of the LG5 domain would reshape the cytoskeleton, leading cardiac failure as a major clinical concern. There are still some limitations in this study. We did not perform the isogenic iPSC line based on this patient. At the same time, the distribution of LAMA2 by immunostaining of iPSC-CM had not been investigated, which we would carry out further analysis in the following studies.

Conclusion

In summary, this is the first case report to describe an ARVC phenotype with a *LAMA2* mutation of c.8842G > A (p.G2948S), which is located in the LG5 domain. In addition, the first iPSC cell line has been established based on the proband. Histological studies and bulk RNA-seq have demonstrated a convinced association between *LAMA2* c.8842C > A and ARVC. Considering 35–50% of patients with a clinical diagnosis of ARVC fail to address a particular disease-causing gene mutation, this research expands the understanding of the pathogenesis of ARVC. However, the molecular mechanism of *LAMA2* mutation inducing ARVC still requires further study.

Ethics statement

The studies involving human participants were reviewed and approved by the Ethics Committee of West China Second Hospital of Sichuan University (2014-034). Written informed consent to participate in this study was provided by the participants' legal guardian/next of kin. Written informed consent was obtained from the individual(s), and minor(s)' legal guardian/next of kin, for the publication of any potentially identifiable images or data included in this article.

Author contributions

SL was the patient's physician and responsible for the revision of the manuscript for important intellectual content. YW reviewed the literature and contributed to manuscript drafting. YW and YL performed the mutation analysis. DZ and YF contributed to the iPSC-related experiments. YL and SL conceptualized and designed the study, coordinated and supervised the data collection, and critically reviewed the manuscript for important intellectual content. All authors issued final approval for the version to be submitted.

Funding

This work was supported by grants from the National Natural Science Foundation of China (No. 81700360) and Technology Project of Sichuan Province of China (Nos. 2020YFS0101 and 2020YFS0102).

Conflict of interest

The authors declare that the research was conducted in the absence of any commercial or financial relationships that could be construed as a potential conflict of interest.

Publisher's note

Supplementary material

The Supplementary Material for this article can be found online at: https://www.frontiersin.org/articles/10.3389/fmed.2022.922347/full#supplementary-material

SUPPLEMENTARY FIGURE 1
KEGG enrichment analysis of the fibrosis signaling pathway.

SUPPLEMENTARY FIGURE 2
KEGG enrichment analysis of the lipidation signaling pathway.

SUPPLEMENTARY FIGURE 3
KEGG enrichment analysis of the apoptosis signaling pathway.

SUPPLEMENTARY FIGURE 4
KEGG enrichment analysis of the calcium signaling pathway.

References

1. Corrado D, Link MS, Calkins H. Arrhythmogenic right ventricular cardiomyopathy. *N Engl J Med.* (2017) 376:61–72. doi: 10.1056/NEJMra1509267

2. Austin KM, Trembley MA, Chandler SF, Sanders SP, Saffitz JE, Abrams DJ, et al. Molecular mechanisms of arrhythmogenic cardiomyopathy. *Nat Rev Cardiol.* (2019) 16:519–37. doi: 10.1038/s41569-019-0200-7

3. Groeneweg JA, Bhonsale A, James CA, te Riele AS, Dooijes D, Tichnell C, et al. Clinical presentation, long-term follow-up, and outcomes of 1001 arrhythmogenic right ventricular dysplasia/cardiomyopathy patients and family members. *Circ Cardiovasc Genet.* (2015) 8:437–46.

4. Lazzarini E, Jongbloed JD, Pilichou K, Thiene G, Basso C, Bikker H, et al. The ARVD/C genetic variants database: 2014 update. *Hum Mutat.* (2015) 36:403–10.

5. Yurchenco PD, Patton BL. Developmental and pathogenic mechanisms of basement membrane assembly. *Curr Pharm Des.* (2009) 15:1277–94. doi: 10.2174/138161209787846766

6. Yurchenco PD. Basement membranes: cell scaffoldings and signaling platforms. *Cold Spring Harb Perspect Biol.* (2011) 3:a004911. doi: 10.1101/cshperspect.a004911

7. Sasaki T, Giltay R, Talts U, Timpl R, Talts JF. Expression and distribution of laminin alpha1 and alpha2 chains in embryonic and adult mouse tissues: an immunochemical approach. *Exp Cell Res.* (2002) 275:185–99. doi: 10.1006/excr.2002.5499

8. Geranmayeh F, Clement E, Feng LH, Sewry C, Pagan J, Mein R, et al. Genotype–phenotype correlation in a large population of muscular dystrophy patients with LAMA2 mutations. *Neuromusc Disord.* (2010) 20:241–50. doi: 10.1016/j.nmd.2010.02.001

9. Jones KJ, Morgan G, Johnston H, Tobias V, Ouvrier RA, Wilkinson I, et al. The expanding phenotype of laminin 2 chain (Merosin) abnormalities: case series and review. *Med Genet.* (2001) 38:649–57. doi: 10.1136/jmg.38.10.649

10. Marcus FI, McKenna WJ, Sherrill D, Basso C, Bauce B, Bluemke DA, et al. Diagnosis of arrhythmogenic right ventricular cardiomyopathy/dysplasia: proposed modification of the Task Force Criteria. *Eur Heart J.* (2010) 31:806–14. doi: 10.1093/eurheartj/ehq025

11. Yurchenco PD, McKee KK. Linker protein repair of LAMA2 dystrophic neuromuscular basement membranes. *Front Mol Neurosci.* (2019) 12:305. doi: 10.3389/fnmol.2019.00305

frontiers | Frontiers in Pharmacology

TYPE Review
PUBLISHED 22 July 2022
DOI 10.3389/fphar.2022.956397

OPEN ACCESS

EDITED BY
Jian Gao,
Shanghai Children's Medical Center, China

REVIEWED BY
Li Zhiling,
Shanghai Jiao Tong University, China
Liang Huang,
Sichuan University, China

*CORRESPONDENCE
Wei Xiong,
857915113@qq.com
Yong Yang,
yyxpower@163.com

SPECIALTY SECTION
This article was submitted to Obstetric and Pediatric Pharmacology, a section of the journal Frontiers in Pharmacology

RECEIVED 30 May 2022
ACCEPTED 27 June 2022
PUBLISHED 22 July 2022

CITATION
Yang X, Li Q, He Y, Zhu Y, Yang R, Zhu X, Zheng X, Xiong W and Yang Y (2022), Individualized medication based on pharmacogenomics and treatment progress in children with IgAV nephritis. *Front. Pharmacol.* 13:956397. doi: 10.3389/fphar.2022.956397

Individualized medication based on pharmacogenomics and treatment progress in children with IgAV nephritis

Xuerong Yang[1,2], Qi Li[1,2], Yuanyuan He[1,2], Yulian Zhu[3], Rou Yang[1,2], Xiaoshi Zhu[4], Xi Zheng[1,2], Wei Xiong[5]* and Yong Yang[1,2]*

[1]Department of Pharmacy, Sichuan Academy of Medical Sciences & Sichuan Provincial People's Hospital, School of Medicine, University of Electronic Science and Technology of China, Chengdu, China, [2]Personalized Drug Therapy Key Laboratory of Sichuan Province, School of Medicine, University of Electronic Science and Technology of China, Chengdu, China, [3]Department of Pharmacy, Ziyang People's Hospital, Ziyang, China, [4]Department of Pediatrics, Sichuan Academy of Medical Sciences & Sichuan Provincial People's Hospital, Chengdu, China, [5]Department of Hepatobiliary Surgery, Sichuan Academy of Medical Sciences & Sichuan Provincial People's Hospital, Chengdu, China

Immunoglobulin A vasculitis (IgAV) nephritis, also known as Henoch-Schönlein purpura nephritis (HSPN), is a condition in which small blood vessel inflammation and perivascular IgA deposition in the kidney caused by neutrophil activation, which more often leads to chronic kidney disease and accounts for 1%–2% of children with end-stage renal disease (ESRD). The treatment principles recommended by the current management guidelines include general drug treatment, support measures and prevention of sequelae, among which the therapeutic drugs include corticosteroids, immunosuppressive agents and angiotensin system inhibitors. However, the concentration range of immunosuppressive therapy is narrow and the individualized difference is large, and the use of corticosteroids does not seem to improve the persistent nephropathy and prognosis of children with IgAV. Therefore, individualized maintenance treatment of the disease and stable renal prognosis are still difficult problems. Genetic information helps to predict drug response in advance. It has been proved that most gene polymorphisms of cytochrome oxidase P450 and drug transporter can affect drug efficacy and adverse reactions (ADR). Drug therapy based on genetics and pharmacogenomics is beneficial to providing safer and more effective treatment for children. Based on the pathogenesis of IgAV, this paper summarizes the current therapeutic drugs, explores potential therapeutic drugs, and focuses on the therapeutic significance of corticosteroids and immunosuppressants in children with IgAV nephritis at the level of pharmacogenomics. In addition, the individualized application of corticosteroids and immunosuppressants in children with different genotypes was analyzed, in order to provide a more comprehensive reference for the individualized treatment of IgAV nephritis in children.

KEYWORDS

IgA vasculitis nephritis, Henoch-Schönlein purpura nephritis, treatment, immunosuppressants, personalized medicine, pharmacogenomics, gene polymorphism, paediatric

1 Introduction

Immunoglobulin A vasculitis (IgAV), previously known as Henoch-Schönlein purpura, is the most common systemic vessel vasculitis in children. It's a kind of immune sediment dominated by IgA and usually self-limiting, which often affects the skin (which can touch purpura), gastrointestinal tract, lungs, joints, nervous system, urinary system, and renal (Nicoara and Twombley, 2019). The incidence of IgAV is about 3–27 cases in every 100,000 children (Piram et al., 2017), and it can appear at any age, with the highest incidence being about four to 6 years old and 90% of cases happening under 10 years old (Oni and Sampath, 2019). Males are slightly dominant (the ratio of men to women is 1.5: 1), and the incidence tends to decrease with age (Gardner-Medwin et al., 2002). The prognosis for IgAV in children is generally reasonable. However, serious complications can still occur, including renal involvement, with IgAV nephritis progressing in the acute phase of IgAV involving the kidneys, which can occur in 20%–80% of IgAV cases (Ozen et al., 2019). Most children with IgAV nephritis are slightly ill, exhibiting only hematuria or light proteinuria, and likely to recover independently. However, the long-term prognosis of patients with IgAV is determined by the severity of renal involvement; a small percentage of patients develop nephrotic syndrome or renal impairment that may progress to renal failure or end-stage renal disease. Therefore, it is very crucial for children and families to choose the most appropriate therapeutic drugs based on a clear understanding of the pathogenesis and clinical manifestations of IgAV nephritis. The management of IgAV is still highly controversial, with few international management guidelines and no consensus between regions.

Currently, in addition to the widely recognized renin-angiotensin system (RAS) inhibitors, drugs such as corticosteroids (CS) and various immunosuppressive agents are often recommended for IgAV nephritis in the presence of proteinuria to stifle renal damage (Ozen et al., 2019). However, the therapeutic range of immunosuppressive drugs is very narrow, which suggests that immunosuppression can easily fall between efficacy and toxicity (Casati et al., 2017). Since the dosage and monitoring target concentrations of drugs used to treat IgAV nephritis in children are inferred from experience with adults, these drugs have not been sufficiently validated for use in children and are prone to imprecise dosages, which can adversely affect growth and development in children.

Genetics is and mayone of the most common factors associated with drug response, and having genetic information about patients can help predict drug response in advance. Due to the narrow concentration range of immunosuppressive drug therapy, pharmacogenomics is expected to be one of the most promising tools in the field of immunosuppressive drug therapy. It may help select appropriate drugs for children with IgAV nephritis and individualize the dose (Collins and Varmus, 2015).

In this review, we compare the current major international guidelines, summarize the current therapeutic use based on the analysis of the mechanisms of IgAV occurrence and explore potential therapeutic agents. We focus on the impact of genetic polymorphisms of cytochrome oxidase P450, drug transporters, and pharmacodynamic drug targets on hormones and immunosuppressants, and analyze the individualized application of hormones and immunosuppressants in children with different genotypes in order to achieve precise drug use in children with IgAV nephritis and provide a more comprehensive reference for the individualized treatment of IgAV nephritis in children. This review is dedicated to supplying some information for future individualized treatment based on pharmacogenomics and pharmacogenetics.

2 Immunoglobulin A vasculitis nephritis

2.1 Pathogenesis of immunoglobulin A vasculitis nephritis

IgAV nephritis is a typical acute glomerular inflammatory disease caused by autolytic vasculitis. It is due to mesangial proliferative changes caused by aberrant glycosylation of IgA1 sedimentation in the glomerulus. At present, the precise mechanism for this situation is unclear. Kiryluk et al. (2017) proposed that crucial gene abnormalities may cause it in the glycosylation pathway. Such aberrant glycosylation leads to the exposure of residues in the IgA hinge region, which constitutes antigens and triggers humoral autoimmune responses, and its cycle immunity compound and immune deposition include IgA1. Aberrant glycosylation may be associated with serum galactose deficiency variation, which is seldom seen in normal circulating IgA1 but is more frequently seen in IgAV people. Specifically, transferrin receptors preferentially bind to galactose deficient IgA1 in the renal and express it on its mesangial cells, forming deposits through enhanced cell multiplication, cytokine release, completement activation, induction of Pro cell-extracellular matrices (ECM), ultimately leading to local renal tissue inflammation (Oni and Sampath, 2019). Studies have shown that the primary circulating sediment is a large (>19S) circulating IgA1-o-sugar-containing immune complex (IgA-IC) (Nicoara and Twombley, 2019). It is unclear whether these circulating complexes and immune deposits are temporary phenomena in the acute phase or even present in the quiescent phase of the disease (Nicoara and Twombley, 2019; Oni and Sampath, 2019).

In addition to IgA1 deposition, IgAV nephritis has also been found to be correlated with immune factors, including immune complexes, and its incidence is positively correlated with plasma IgG and IgE levels and type 1 allergic reactions (Nicoara and Twombley, 2019).

2.2 Clinical manifestations of immunoglobulin A vasculitis nephritis

IgAV is a vasculitis of small vessel leukocyte fragmentation; compared with the clinical manifestations of adult IgAV nephritis, children's IgAV nephritis clinical manifestations are different (Oni and Sampath, 2019). In 95% of patients, a skin rash will have a symmetrical red spot or palpable purpura rash; most start in the legs and hips and can extend to the arms and less common trunk (Oni and Sampath, 2019). Facial involvement is sporadic. With the exception of skin symptoms, the disease is characterized by typical triad symptoms, namely, involving the skeletal, muscle and kidney systems, rarely involving the respiratory system, and very rarely involving the nervous system. In the brachychronic phase, patients with musculoskeletal involvement up to 70%–90%, manifested as joint pain or arthritis. The incidence of arthritis is relatively low, about 61%–64%; the most common involvement is lower limb joints, which are likely to occur in the same area as rashes, but joint symptoms are usually transient and do not cause long-term abnormalities (Oni and Sampath, 2019). As many as 72% of patients develop gastrointestinal symptoms, usually gastrointestinal colic, which may precede skin manifestations for several days or even a week. In severe cases, acute gastrointestinal bleeding, such as melena, or severe and life-threatening vomiting may be developed. However, asymptomatic fecal occults are common (Oni and Sampath, 2019). Renal involvement, called IgAV nephritis, is the most severe manifestation of IgAV. About 20%–80% of children may be involved in the renal, which is usually asymptomatic and requires activity screening.

IgAV nephritis can be manifested as hematuria with or without albumin urine, nephropathy and/or idiopathic nephrotic syndrome under the microscope (and/or visible to the naked eye), and/or purpura, colic, bloody stools, edema, and joint pain. In general, IgAV nephritis is somewhat self-limited and may recover without treatment. Children with mild IgAV nephritis have a good prognosis but may develop permanent renal damage and scarring if not diagnosed and treated early (Chan et al., 2016). IgAV nephritis in children is generally restricted to abnormal urine, but there are no clinical symptoms. At the same time, the blood pressure and renal function of children are standard, making it difficult to monitor and manage IgAV nephritis in children. Indeed, the long-run risk of lasting renal dysfunction in patients with minor urinary abnormalities is low but significantly higher in children with nephrotic and/or nephrotic syndrome (Narchi, 2005). The risk of developing chronic kidney disease in children with mild renal involvement is only between 5 and 20 percent (Bogdanovic, 2009). Therefore, it is important for all children suspected of IgAV to be actively examined for renal involvement during diagnosis. At least 6–12 months of monitoring and follow-up are required, even though the original blood pressure and urine test are not abnormal.

Renal involvement needs to be evaluated by measuring blood pressure, morning urine test, and glomerular filtration rate (GFR) to evaluate the comprehensive renal function. Urine analysis (morning urine samples) should confirm hematuria, proteinuria, and/or proteinuria quantification and urine protein: urine creatinine ratio (UP: UC ratio) (Foster and Brogan, 2018). The calculation method of GFR in children is different from that in adults. The simplest and most commonly used method is the improved Schwartz formula to estimate the renal function of children aged 1–17. The accuracy of calculation and diagnostic accuracy of the formula has been verified, that is, eGFR (ml/min/1.73 m^2) = 36.2 × height (cm)/serum creatinine (μmol/L). However, the formula is derived from GFR in children 15–75 ml/min/1.73 m^2, and it may be invalid if GFR exceeds this range (Bhowmick et al., 2022). The classical Schwartz formula was used to estimate renal function in 0–12 months infants. The GFR of low-birth-weight infants with a birth weight less than 2.5 kg was 29.1 × body length (cm)/serum creatinine (μmol/L), and the GFR of full-term infants was 39.7 × body length (cm)/serum creatinine (μmol/L). At the same time, renal biopsy should be performed for histological classification based on GFR impairment or severe or persistent proteinuria to more accurately assess the severity of IgAV nephritis.

3 Genetic susceptibility to immunoglobulin A vasculitis nephritis

Recent studies have confirmed that individuals with IgAV nephritis have a strong genetic susceptibility. It is correlated with human leukocyte antigen (HLA), especially in its type II region (Gonzalez-Gay et al., 2018). Currently, genetic susceptibility to IgAV nephritis is mainly studied in The European population. A study of 349 patients with IgAV showed that Caucasian people have associated with HLA type I alleles, especially HLA-B*41:02. This study is inconsistent with the previous research (Lopez-Mejias et al., 2015b), which was relevant to the HLA-DRB1*01 allele (Lopez-Mejias et al., 2015a). The claim that HLA Class II regions constitute a significant susceptibility locus for IgAV has been supported by the largest ever genetic study of IgAV patients of European descent, which confirmed that the mapping of a link disequilibrium region between HLA-dqa1 and HLA-dqb1 to the intergenic region (IGR) of HLA class II was closely related to the susceptibility of disease. The values of HLA-DRB1*13 and HLA-DRB1*11 were very high; weak correlation with HLA class I regions and latent signals other than HLA were found (Lopez-Mejias et al., 2017).

Other studies have also shown that susceptibility to IgAV nephritis is associated with genetic polymorphisms outside the HLA region, containing genetic polymorphisms that regulate vascular homeostasis, new angiogenesis, and gene polymorphisms that encode aberrant glycosylation of IgA1(Lopez-Mejias et al., 2018). It was also confirmed that

T cells, pro-inflammatory cytokines, or homocysteine metabolism might be related to the susceptibility to IgAV and the universality of IgAV (Lopez-Mejias et al., 2018). Another study evaluated the relevance of cytokines and immune globulin with glomerulonephritis in IgAV children and observed IgA1 levels in serum galactose deficiency and IgA, IgG, IgM, IL-6, IL-8, and IL-10 complex levels in urine were predictors of glomerulonephritis in IgAV children (Berthelot et al., 2018).

4 Drug therapy for immunoglobulin A vasculitis nephritis in children

4.1 Renin-angiotensin system blockers

It has been shown that blocking the RAS is beneficial to renal function (Selvaskandan et al., 2019). Regardless of whether prednisolone or other immunosuppressants are used in treatment, the panel recommended that angiotensin-converting enzyme inhibitors (ACEI) or angiotensin II receptor blockers (ARBs) for IgAV in children with continuous proteinuria (>3 months) and renal involvement to prevent or restrict subsequent glomerular injury (Coppo et al., 2007). Also, the Kidney Disease Improving Global Outcomes (KDIGO) group approved RAS blockers for treating persistent proteinuria, and the KDIGO guidelines (Rovin et al., 2021) recommend that children with persistent proteinuria with IgAV nephritis (defined as > 0.5–1 g/d/1.73 m^2) should be treated with ACEI or ARBs.

The efficacy of RAS blockers on IgAV cannot be clearly demonstrated. Still, clinical studies suggest that RAS blocker use has a favorable impact on the nephritic outcomes of patients with IgAV. In a recent study (Nagai et al., 2022), proteinuria was resolved in cases of moderate-to-severe IgAV nephritis with RAS inhibitors as the initial treatment regimen, regardless of relapse. Irrespective of the status of pathological findings in children diagnosed with IgAV, RAS inhibitor therapy at an early stage has shown excellent results and beneficial effects on renal outcomes (Kurt-Sukur et al., 2021; Nagai et al., 2022). This suggests that timely assessment of patients' clinical and pathologic outcomes prior to therapeutic intervention and early introduction of RAS inhibitors as a treatment strategy for IgAV nephritis is exceptionally beneficial. Some guidelines recommend that in the absence of crescentic nephritis (>50% of crescents) with worsening renal function and nephrotic syndrome, treatment with only ACEI or ARBs alone may be used initially for 3–6 months (Radhakrishnan and Cattran, 2012). Other experts, however, believe this approach may leave acute and potentially aggressive glomerulonephritis undetermined or its immunosuppressive management deferred for months, leading to undertreatment (Davin and Coppo, 2013). Relapse is more likely with RAS blockers alone, especially when the patient has global/segmental sclerosis or tubular atrophy/interstitial fibrosis (Nagai et al., 2022). Therefore, RAS blockers combined with other therapies such as CS and immunosuppressive agents can be considered in more complex cases.

4.2 Corticosteroids

The potent anti-inflammatory effect of CS can inhibit the rapid deterioration of renal pathology in the IgAV patients' population to a certain extent, especially in diminishing urinary protein and postponing the renal function decline. In patients' serum, CS can reduce the aberrant o-glycosylation of IgA1, thereby reducing the latter's deposition in the glomerular capillary wall and mesangial. The guideline of 2012 KDIGO recommended that patients with persistent proteinuria be treated with CS for 6 months after using ACEI or ARBs (KDIGO, 2012). In the latest guidelines of KDIGO in 2021, oral prednisone/prednisone or pulsed intravenous (IV) methylprednisolone (MP) were recommended for the treatment of patients with mild and moderate IgAV nephritis (Rovin et al., 2021). Recommendations for CS use in China are basically consistent with the 2012 KDIGO. For children with severe clinical symptoms, diffuse renal pathological changes, or with > 50% crescent formation, methylprednisolone can be used for shock therapy in addition to oral CS (see Table 1 for the severity of the condition) (Subspecialty Group of Renal Diseases and Chinese Medical Association, 2017). The SHARE (Single Hub and Access Point for Paediatric Rheumatology in Europe) initiative issued first the international evidence-based recommendation on treating IgAV in children, and CS application in children with kidney injury was made more evident (Ozen et al., 2019). Oral or IV CS runs through severe, moderate, and even mild IgAV nephritis treatment, with a 10–30 mg/kg recommended dosage of pulsed MP. Patients can use it for 3 days, up to 1 g daily. Subsequently, in the latest evidence-based consensus in Egypt, oral prednisolone or pulsed MP is recommended for mild, moderate, and severe nephritis (see Table 1: Comparison of guidelines for the severity of the condition) (Abu-Zaid et al., 2021). The publication of these guidelines and consensus has given the international community a clearer understanding of the treatment of IgAV in children. However, there are still many problems here.

Significantly, long-term CS administration can induce the inhibition of growth and development, osteoporosis, diabetes, adrenal inhibition, and Cushing syndrome (Caplan et al., 2017; Adami and Saag, 2019; Tan et al., 2019). More importantly, a considerable number of patients in the clinical use of CS will not respond or show increased disease, CS resistance phenomenon, which may be related to pharmacogenomics. Pharmacogenomics of CS has been extensively studied in many conditions. Related studies have shown that the key reasons for the individualized diversity of CS in humans are single nucleotide polymorphisms (SNPs) of nuclear receptor subfamily 3 group C member 1

TABLE 1 Comparison of guidelines.

Guideline	Severity of IgAV nephritis and definition	Treatment recommendations
Evidence-based guideline for diagnosis and treatment of Henoch-Schönlein purpura nephritis (2016) Subspecialty Group of Renal Diseases and Chinese Medical Association (2017)	Isolated hematuria or pathological grade I (slight glomerular abnormality).	Only complementary treatment for HSP.
	Isolated microalbuminuria or combined with microscopic hematuria or pathological grade II a (focal segmental simple mesangial hyperplasia).	ACEI or ARBs can be routinely used.
	Non-nephropathic proteinuria or pathological grade II b (diffuse simple mesangial hyperplasia), grade III a (focal segmental mesangial hyperplasia, with < 50% glomerular crescent formation/segmental lesions).	CS for 6 months.
	Nephropathy level proteinuria, nephrotic syndrome, acute nephritis syndrome or pathological grade III b (diffuse mesangial hyperplasia, with < 50% crescent formation/segmental glomerular lesions), grade IV (lesions the same as grade III, 50%–75% glomeruli with the above lesions).	Available regimens: 1. CS combined with CYC pulse therapy: prednisone 1.5–2 mg/kg/d, oral administration for 4 weeks, and then oral administration every other day for 4 weeks, followed by IV pulse therapy with CYC based on CS. CYC accumulation ≤ 168 mg/kg. 2. CS combined with CyA: CyA was taken orally four times at 6 mg/kg/d every 12 h. The serum concentration was measured 1–2 weeks after administration, and the trough concentration was maintained at 100–200 μg/L. The induction period was 3 μg/L for 6 months. 3. CS combined with MMF: MMF 20–30 mg/kg/d was taken orally twice and gradually decreased after 3–6 months. The complete course of treatment was 12–24 months. 4. CS combined with AZA: AZA 2 mg/kg/d, the general course of treatment was 8 months to 1 year.
	Acute nephritis or pathological grade V (lesions the same as grade III, > 75% of glomeruli with the above lesions), grade VI (mesangial proliferative glomerulonephritis).	A combination of 3–4 drugs: 1. Prednisone + CYC (or other immunosuppressants) + heparin + dipyridamole were taken orally after 1–2 courses of MP pulse therapy. 2. MP combined with urokinase shock therapy + oral prednisone + CYC + heparin + dipyridamole.
European consensus-based recommendations for diagnosis and treatment of immunoglobulin A vasculitis—the SHARE initiative Ozen et al. (2019)	Mild IgAV nephritis: normal GFR (>80 ml/min/1.73 m^2) and mild proteinuria (UP: UC ratio < 100 mg/mmol) or moderate proteinuria (UP: UC ratio 100–250 mg/mmol). UP: UC is tested in an early morning urine sample.	1st line: oral prednisolone. 2nd line: AZA, MMF, pulsed MP. ACEI can be considered a preventive drug for (persistent) albuminuria.
	Moderate IgAV nephritis: < 50% crescents on renal biopsy and GFR damage (<80 ml/min/1.73 m^2) or severe persistent proteinuria (>250 mg/mmol for 4 weeks).	1st line: oral prednisolone (1–2 mg/kg/d) or pulsed MP (10–30 mg/kg, up to 1 g/d for 3 days). 2nd line: AZA, MMF, IV CYC. Oral CyA or CYC is not routinely indicated.
	Severe IgAV nephritis: > 50% crescents on renal biopsy and GFR damage or severe persistent proteinuria. (The definition is the same as the corresponding in Moderate IgAV nephritis.)	1st line: High-dose CS and IV CYC as induced therapy. 2nd line: Low-dose CS + AZA/MMF as maintenance therapy.
Executive summary of the KDIGO 2021 guideline for the management of glomerular diseases Rovin et al. (2021)	Persistent proteinuria (>0.5–1 g/d/1.73 m^2) for more than 3 months.	ACEI or ARBs (the combination of these two drugs is not recommended). Glucocorticoids are not recommended to prevent nephritis in patients with isolated extrarenal IgAV.
	Mild or Moderate nephritis	Oral prednisone/prednisolone or pulsed MP.
	Nephrotic syndrome or rapid deterioration of renal function	CYC + glucocorticoids (usually as pulsed MP). 1st line: oral prednisolone.

(Continued on following page)

TABLE 1 (*Continued*) Comparison of guidelines.

Guideline	Severity of IgAV nephritis and definition	Treatment recommendations
Consensus evidence-based recommendations for treat-to-target management of immunoglobulin A vasculitis Abu-Zaid et al. (2021)	Mild nephritis: normal eGFR (>90 ml/min) and mild or moderate proteinuria, microscopic hematuria.	2nd line: AZA, MMF, pulsed MP (drug-resistant cases with no response).
	Moderate nephritis: < 50% crescents on renal biopsy and eGFR damage (60–89 ml/min/1.73 m^2) or severe persistent proteinuria.	1st line: oral prednisolone and/or pulsed MP. 2nd line: AZA, MMF, IV CYC.
	Severe nephritis: > 50% crescents on renal biopsy and eGFR damage (<60 ml/min) or severe persistent proteinuria.	1st line: IV CYC + pulsed MP and oral prednisolone for 6–9 months as induction therapy. 2nd line: AZA/MMF + CS as maintenance therapy.
	Persistent proteinuria (UP: UC ratio > 250 mg/mmol for 4 weeks or UP: UC ratio > 100 mg/mmol for 3 months or UP: UC ratio > 50 mg/mmol for 6 months), drug-resistant cases, incurable or recurrent IgAV.	1. Children with persistent proteinuria (0.5–1.0 g/d) should be treated with ACEI or ARBs. 2. After ACEI or ARBs tests, children with persistent proteinuria > 1 g/d and GFR > 50 ml/min/1.73 m^2 should be treated with CS for 6 months (oral administration of 0.5 mg/kg prednisone or 0.8–1 mg/kg prednisone every other day for 2 months, followed by a monthly decrease of 0.2 mg/kg/d in the next 4 months). 3. Plasmapheresis and IV immunoglobulin can be used in drug-resistant cases. 4. Rituximab is recommended as replacement therapy for recurrent or incurable IgAV.

IgAV, IgA vasculitis; HSP, Henoch-Schönlein purpura; ACEI, angiotensin-converting enzyme inhibitors; ARBs, angiotensin II, receptor blockers; CS, corticosteroids; CYC, cyclophosphamide; IV, intravenous; CyA, cyclosporine A; MMF, mycophenolate mofetil; AZA, azathioprine; MP, methylprednisolone; GFR, glomerular filtration rate; UP, UC; urine protein, urine creatinine ratio; eGFR, estimated glomerular filtration rate.

(NR3C1), corticotropin-releasing hormone receptor 1 (CRHR1), glucocorticoid-induced transcript 1 gene (GLCC1), stress-induced phosphoprotein 1 (STIP1), histone deacetylase (HDAC), ATP-binding cassette transporter (ABC), and plasminogen activator inhibitor-1 (PAI-1). We also summarized the impact of intermediate target mutations on drug outcomes in Supplementary Table S1.

Glucocorticoid is a kind of CS classification, and NR3C1 is a gene that codes glucocorticoid receptor (GR). NR3C1 mutations can reduce the transcriptional activity of genes or even lose the activity of protein expression products, affecting GR's formation and then impacting GR's response to CS, resulting in CS resistance. Many studies have shown that NR3C1 is closely related to CS resistance in nephrotic syndrome (Ye et al., 2003; Liu et al., 2018; Parvin et al., 2021). These SNPs sites that mainly affect the sensitivity of GR include Tth111I, BclI, ER22/23EK, and N363S (Panek et al., 2015; Cheng et al., 2016).

CRHR1 is the key factor that mediates corticotropin-releasing hormone (CRH) to stimulate adrenocorticotropic hormone (ATCH) to secrete CS, which is indispensable in the secretion of human CS. If the CRHR1 gene is mutated, it can reduce or lose the gene's function and inhibit the increased secretion of CS stimulated by inflammation by decreasing the secretion of ACTH. Therefore, the genetic variation of CRHR1 may be the most useful marker to identify the deficiency of endogenous CS and respond better to exogenous CS. Based on this theory, studies have shown that CRHR1 gene variants (including rs739645, rs1876831, rs1876829, and rs1876828) can enhance the efficacy of CS in asthma (Mougey et al., 2013).

Moreover, a variety of GLCCI1 mutated alleles are mainly associated with the efficacy of CS (Tantisira et al., 2011; Izuhara et al., 2014). Current studies have focused on asthma, where GLCCI1 gene variability is related to a noticeable decline in response to inhaled glucocorticoids in asthmatic patients (Tantisira et al., 2011). Current studies have focused on asthma, where GLCCI1 gene variability is related to a noticeable decline in response to inhaled glucocorticoids in asthmatic patients (Cheong et al., 2012). Whether this applies equally to IgA vasculitis is unknown.

STIP1 is a coordinated GR receptor chaperone protein that participates in CS binding and activating of intracellular GR complex and plays an anti-inflammatory role. STIP1 gene variation may regulate the CS response of asthma patients with impaired pulmonary function (Hawkins et al., 2009). Furthermore, HDAC is related to the activation mechanism of CS. The recruitment of HDAC2 is an essential step in the process of CS inhibiting inflammatory genes. In some diseases, the activity of HDAC2 is low, resulting in a weak answer to glucocorticoids (Barnes et al., 2004). Therefore, HDAC2 may become the target medium for predicting CS reactions in the future.

In addition, in idiopathic nephrotic syndrome pediatric, the 1236C > T polymorphism, one of the ABCB1 (belonging to ABC) gene mutations, may be associated with CS resistance, and the T allele and TT genotype may be closely associated with resistance

and may require other therapeutic strategies (Safan et al., 2017). Here, we highlight the genetic polymorphisms associated with CS-induced osteonecrosis of the femoral head (ONFH), an essential gene for which several meta-analyses have shown its mutant phenotype (3435C > T) is a protective gene for CS-induced ONFH (Zhang et al., 2017; Chen et al., 2018; Lee et al., 2022). In other words, the T allele can significantly reduce the risk of CS-induced ONFH compared to the C allele. However, in a meta-analysis in 2015, ABCB1 rs1045642, the mutant phenotype (3435C > T), was an increased risk factor for the development of ONFH in women under the allele model. Still, this association was not found under the dominant model (Zhou et al., 2015). Another gene known to be associated with CS-induced ONFH is PAI-1. The well-studied mutant PAI-1 4G/5G (rs1799889) increases the risk of CS-induced ONFH development (Sobhan et al., 2018). A recent meta-analysis concluded that patients with 5G were at a lower risk than those with 4G during CS-induced ONFH development (Lee et al., 2022). Further studies are yet to be done in the future.

4.3 Immunosuppressants

4.3.1 Cyclophosphamide

Cyclophosphamide (CYC) can inhibit the function of T cells and B cells and then reduce or prevent abnormal immune complexes sludging in glomeruli (Kanigicherla et al., 2018). CYC is one of the immunosuppressants with high-quality evidence and has been widely recognized by scholars at home and abroad for treating IgAV nephritis. As the only immunosuppressant recommended by KDIGO in 2012, CYC combined with CS can be used in children with crescentic IgAV nephritis complicated with nephrotic syndrome and/or renal function deterioration (KDIGO, 2012). Fortunately, with the continuous development of relevant research, the guidelines and consensus on using CYC recommendations are also more positive. The latest KDIGO guideline published in 2021 suggests that CYC should be used for IgAV nephritis with nephrotic syndrome or rapid deterioration of renal function (Rovin et al., 2021). IV CYC can be taken into account as second-line therapy for moderate IgAV nephritis and induction therapy (6–9 months) for severe IgAV nephritis (Ozen et al., 2019; Abu-Zaid et al., 2021), and second-line therapy for mild IgAV nephritis (Ozen et al., 2019). Considering the adverse reactions (ADR) of CYC, sequential maintenance therapy with other immunosuppressants after induction therapy is recommended. It is worth mentioning that the guidelines do not recommend oral CYC therapy because of insufficient evidence.

Although using CYC in IgAV nephritis has been more widely recognized and recommended, it varies significantly among individuals. The exposure of metabolites *in vivo* can be ten times different when ordinary people take the same amount of CYC (de Jonge et al., 2005). Moreover, the drug is prone to hemorrhagic cystitis, ovarian toxicity, leukopenia, male semen toxicity, and other ADR (Chong et al., 1983; Koetter, 2009; Rocha et al., 2009; Sharma et al., 2020). CYC is an inactive prodrug that needs to be metabolized into active 4-hydroxycyclophosphamide (4-OHCPA) through CYP2B6, 2C9, 2C19, and 3A4 *in vivo* (Roy et al., 1999), and then glutathione S-transferase (GST) will inactivate the latter. Besides, multidrug resistance-associated proteins (MRPs, such as MRP1 and MRP4) and ALDHs play an essential role in CYC transport and metabolism.

There are many types of CYP2B6 gene mutations, and studies have shown that many kinds of SNPs are related to their efficacy and safety. In terms of the coding region, CYP2B6*2 (c.64C > T) and CYP2B6*4 (c.785A > G) mutations increased enzyme activity, which significantly increased the risk of ADR (hemorrhagic cystitis and oral mucositis, respectively) for people with these allele mutations (Rocha et al., 2009). In contrast, CYP2B6*5 (c.1459C > T) mutation led to a decline in enzymatic activity and prominently increased the risk of reduced efficacy (Takada et al., 2004; Uppugunduri et al., 2014). Also, similar results have been obtained in breast cancer group patients treated with CYC, with CYP2B6*2, *4, *8, and *9 alleles related to poor clinical outcomes (Bray et al., 2010). Interestingly, the same CYP2B6 (c.516G > T) can increase or decrease enzyme activity in different researches (Xie et al., 2006; Joy et al., 2012), showing contradictory results. The conflicting results may be related to the diseases studied, the research methods, the mode of administration, the medication timing, and the medicine combination. Except for the coding region, a study in Japan found that CYP2B6 (g.−2320T > C, g.18492T > C, and g.−750T > C) in the non-coding region was also significantly associated with ADR (including leukopenia) of CYC (Nakajima et al., 2007).

The metabolism of CYC in CYP2C19 is less than that in CYP2B6, and it has a more negligible effect on the activation of CYC. CYP2C19*2 can induce a deficit of enzyme activity, which reduces the activation level of CYC and the risk of ADR (ovarian toxicity) (Singh et al., 2007; Tatarunas et al., 2014). Whereas, if the dose of CYC exceeds 1 g/m^2, the mutation does not affect the metabolic level of CYC (Timm et al., 2005). It is speculated that the reason may be that the offset of CYP2B6 induced by CYC itself even exceeds the loss of enzyme activity caused by CYP2C19*2 (Martin et al., 2003). Oppositely, homozygous individuals carrying CYP2C19*1/*1 show an increased risk of ovarian toxicity (Ngamjanyaporn et al., 2011).

CYP2C9 and CYP3A4 play fewer roles in CYC activation. CYP2C9*2 (c.430C > T) and *3 (c.1075A > C) may increase the risk of leukopenia, but, interestingly, they may have a preferable effect on the therapeutic regimen (Schirmer et al., 2016). A better therapeutic response may be since the higher 4-hydroxylase activity of wild-type proteins than those encoded by CYP2C9*2 and *3, and the lower activity leads to slower activation of its intermediates by prodrug CYC (Timm et al., 2005). Notably, the formation of chloroacetaldehyde, a toxic

metabolite of CYC, can be significantly reduced in combination with CYP3A4 inhibitors such as triptolide and ketoconazole, reducing the risk of nephrotoxicity and neurotoxicity (Zhang X. F. et al., 2014; Yang et al., 2018). This drug interaction seems to be beneficial to children.

Glutathione S-transferase (GST) is a phase II metabolic enzyme that can inactivate CYC and its intermediate metabolites, including GSTA1, GSTP1, GSTT1, and GSTM1. In a recent study on the mutation of GSTA1, it was found that compared with wild-type and heterozygous carriers carrying GSTA1 (−69C > T, rs3957356) T allele, patients with a homozygous mutation of GSTA1 (−69C > T, rs3957356) T allele were prone to unresponsiveness to CYC and more likely to be toxic (Attia et al., 2021). Increased risk of severe leukopenia was found in GSTA1*B carriers (Afsar et al., 2012). Compared with wild-type GSTM1 allele, only defective GSTM1 alleles are associated with more ADR (Hajdinak et al., 2020). Inversely, the GSTP1 I105V allele can reduce the enzyme activity, and the response rate of mutant individuals to CYC treatment is significantly higher. In addition, some studies have found that a mutation in ABCC4 (rs9561778) encoding MRP4 is significantly correlated with CYC-induced ADR (gastrointestinal toxicity and leukopenia/neutropenia) (Low et al., 2009).

4.3.2 Mycophenolate mofetil and azathioprine

Mycophenolate mofetil (MMF) and azathioprine (AZA) are often regarded as immunosuppressants of the same recommended level in IgAV glomerulonephritis, and both are prodrugs. *In vivo*, a vital substance first converted from MMF is Mycophenolic acid (MPA). The MPA can downregulate the activity of inosine monophosphate dehydrogenase (IMPDH) in the critical pathway of purine synthesis, blocking the T and B lymphocytes proliferation and differentiation, thus effectively inhibiting the renal damage caused by abnormal immune reactions (Allison and Eugui, 2000). After entering our body, AZA is activated into cytotoxic thioguanine nucleotides. The latter can alleviate inflammation by restraining DNA replication and arresting CD28 co-stimulatory signals but will be inactivated by thiopurine methyltransferase (TPMT).

Compared with the 2012 KDIGO guidelines, the recommendations of immunosuppressants such as CYC, MMF, and AZA were more positive by subsequent evidence-based consensus or guidelines. In China, experts support CS combined with immunosuppressants in treating severe IgAV nephritis in children (Subspecialty Group of Renal Diseases and Chinese Medical Association, 2017). The recommended usage of MMF/AZA combined with CS was as follows: MMF 20–30 mg/kg/d, oral twice, gradually reduced after 3–6 months, and the entire course of treatment was 12–24 months, or the dose of AZA is 2 mg/kg/d for 8 months to 1 year. AZA and MMF can be taken into account as second-line therapy for mild IgAV nephritis and the first-line or second-line therapy for moderate patients. Considering the ADR of CYC, it is suggested that MMF or AZA should be the maintenance therapy after CYC induction treatment for the severe IgAV nephritis group (Ozen et al., 2019; Abu-Zaid et al., 2021). Besides CYC, KDIGO was skeptical about immunosuppressants, so no other immunosuppressants were recommended. The SHARE initiative and the consensus of Egyptian experts agreed that effective immunosuppressants could prevent/minimize the risk of renal kidney disease or renal failure, especially in rapidly progressive acute vasculitis (Ozen et al., 2019; Abu-Zaid et al., 2021), so the recommended intensity of immunosuppressants was also stronger. However, for MMF or AZA, which is more suitable for priority recommendation, there is a lack of corresponding research, and high-quality evidence is needed to distinguish the advantages and disadvantages.

MPA has biological activity as an intermediate from MMF and can inhibit IMPDH. It is catalyzed and transformed by uridine diphosphate glucuronosyltransferase (UGT). Most MPA is transformed by UGT1A9 into 7-O-MPA-glucuronide (7-O-MPAG) without activity, and a small part of MPA is transformed into Acyl-MPA-glucuronide (AcMPAG) by UGT2B7 (Picard et al., 2005). Remarkably, MPAG has the characteristic of the enterohepatic circulation process. Part of MPAG can be secreted into the bile and then converted into MPA in the intestine, which enters the body again after entering the blood through the portal vein. The transporters involved include organic anion transporting polypeptide (OATP) and multidrug-resistant protein-2 (MRP2) (Barraclough et al., 2010). In conclusion, IMPDH involved in the pharmacodynamics of MMF, UGT involved in metabolism, and OATP and MRP2 engaged in the transport process are related to the individual differences of MMF in patients.

It is reported that IMPDH can be divided into IMPDH type I and type II (Natsumeda et al., 1990). A study on renal transplant patients demonstrated that a mutation of IMPDH type II (3757T > C, rs11706052) was related to improving IMPDH bioactivity, which explained 8.0% of the patient-to-patient variance of IMPDH bioactivity (Sombogaard et al., 2009). The increase in IMPDH bioactivity is detrimental to MPA immunosuppression. Furthermore, studies have shown that IMPDH type I (rs2278293 and rs2278294) is related to a decrease in acute rejection 1 year after renal transplantation (Keown et al., 1996). Paradoxically, in an extensive research on 1,040 renal transplant patients, the results suggested that the above three IMPDH variants had no significant effect on acute rejection, MMF tolerance dose, 1-year allograft function, and 5-year allograft survival (Shah et al., 2012). The researchers believe that the main reason for the difference in the results may be longer follow-up (5 years) and a larger population cohort (1,040 patients) than in previous studies. Besides, they also found that patients carrying IMPDH type I (rs2278294) mutant A allele had a remarkable difference in the 2-year

graft survival rate compared with other genotypes but was not proved at 5 years. It is the above research that demonstrated the essentiality of long-term follow-up. Of course, the differences in medical level and ethnicity between studies also contribute to differences in the results. Therefore, the current research results do not support the prior detection of IMPDH allele polymorphism in renal transplant recipients, let alone children with IgAV nephritis.

Among the mutants of UGT, UGT1A9 is the most studied. UGT1A9 is one of the most studied UGT variants. Firstly, the decrease in MPA exposure was found in the renal transplant population carrying the UGT1A9 (−2152C > T, rs17868320) or UGT1A9 (−275T > A, rs6714486) mutation genes located in the gene promoter region (Kuypers et al., 2005; Mazidi et al., 2013), which may be due to the blocking of the intestinal and liver circulation process of MPAG. Secondly, several studies have shown that in the same region of the gene coding UGT1A9, the other two SNPs (−440C > T and −331T > C) significantly impact the *in vivo* metabolic process of MPA in patients with renal transplantation (Baldelli et al., 2007; Levesque et al., 2008). However, the subjects are also renal transplant recipients. In a new Chinese renal transplantation study, researchers have not found that various SNPs of UGT1A9 are related to the pharmacokinetics of MPA or MPAG (Yang et al., 2021). This difference remains to be discussed. The sample size is too small, there are differences in the combination of drugs, and even the sampling methods may affect the study results. The polymorphisms of UGT1A1, UGT1A7, and UGT1A8, and the polymorphisms of MMF transporters including OATP, MRP2, ABCC2, and SLCO, all contribute to the individualized differences of MMF. Still, the evidence quality of clinical studies is not high enough to influence clinical decision-making.

AZA is prone to myelosuppression, mainly caused by excessive induction of thioguanine nucleotides, an intermediate metabolite. The prevailing view is that the TPMT alleles are critical in this step because mutations in the TPMT gene result in reduced or absent enzyme activity, causing a considerable accumulation of approximately 90% of thioguanine nucleotides that cannot be converted. Compared with adults, the TPMT activity of children is almost the same as that of adults (Schaeffeler et al., 2004). Although 40 variants of the TPMT allele (Appell et al., 2013) have been identified, more than 90% of the decrease in enzyme activity is mainly associated with TPMT*2 (c.238G > C), *3A (c.460G > A, c.719A > G), *3B (c.460G > A) and *3C (c.719A > G) polymorphisms. Patients with homozygous TPMT mutations had low TPMT activity. In contrast, patients with heterozygous TPMT mutations had moderate TPMT activity, and those without mutations had high TPMT activity. TPMT has good genotypic and phenotypic consistency (inconsistencies may be due to blood transfusion since TPMT is measured in red blood cells) (Yates et al., 1997). Myelosuppression is more prone in patients with low and moderate TPMT activity than in those with high TPMT activity. Nevertheless, the latter population needs more doses to resist rapid intermediate metabolite inactivation (Yates et al., 1997). Studies have shown that TPMT genotyping and dose adjustment before using AZA can reduce the incidence of ADR in intermediate metabolites to a level similar to normal metabolism in the Spanish population (Casajus et al., 2022).

Furthermore, mutations in the nucleoside diphosphate-linked moiety X-type motif 15 (NUDT15) gene have been reported as a more predictive predictor of AZA-induced leukocytopenia in Asian patients than TPMT. The low frequency of TPMT mutations in Asian populations may make NUDT15 more dominant in the use of AZA. A meta-analysis found that NUDT15*2 and *3 were critical genetic markers of early myelotoxicity elicited by thiopurine drugs (including AZA) in Asians (Khaeso et al., 2021). The NUDT15*3 mutant is a predictive factor for AZA-elicited myelosuppression in Chinese, so it has been suggested that patients carrying homozygous NUDT15*3 should avoid using AZA (Chen et al., 2021; Miao et al., 2021). Compared with TPMT, NUDT15 variant genotyping has higher accuracy in predicting AZA-induced leukopenia in the Indian population and can be used to optimize azathioprine dose (Banerjee et al., 2020).

In addition to the gene polymorphisms of TPMT and NUDT15, the allelic variation of inosine triphosphate pyrophosphatase (ITPA) during AZA metabolism also affects ADR. Most mutations in ITPA genes lead to a decrease in the bioactivity of ITPA, and the primary mutations are ITPA (c.94C > A, IVS2 + 21A > C, c.138G > A, IVS3+101G > A), in which c.94C > A pure and mutation almost inactivate the enzyme (Marsh et al., 2004; Simone et al., 2013). Low ITPA activity increases the risk of granulocytopenia, liver damage, or influenza-like symptoms, rash, fever, nausea, and vomiting (Simone et al., 2013; Wang et al., 2014). Nevertheless, a trial of about 550 adults with inflammatory bowel disease (IBD) showed that the ITPA allele has nothing to do with treatment-related ADR (Steponaitiene et al., 2016). Whether this is related to the sample size needs more research to prove the hypothesis.

4.3.3 Cyclosporin A

Cyclosporin A (CyA) has rich application experience in various immune diseases and organ transplantation as a calcineurin inhibitor, but few studies have been conducted in children with IgAV nephritis. Koskela et al. (2019) studied 42 children with IgAV nephritis who used the MP and 20 children who used CyA and found that the long-term efficacy of the two groups was better. In the study, 5 years later, 38% of patients receiving MP treatment and 10% of

patients receiving CyA treatment needed additional immunosuppressive therapy because of their condition. Therefore, Koskela et al. (2019) believed that these children with poor responses to MP maybe require long-term CyA therapy to inhibit the progression of IgAV nephritis. Jauhola et al. (2011) also followed up 24 children with severe IgAV for an average of 6 years and found that CyA treatment achieved the goal of complete remission of proteinuria faster than the MP group, while 6 of 13 MP patients needed additional immunosuppressive therapy, one of them had ESRD and received renal transplantation. This study suggests that CyA is more effective and safer than MP in treating severe IgAV. Studies have also shown that CyA may be effective in patients with CS resistance (Ohara et al., 2013). However, CyA treatment is easy to develop into CyA-dependent nephritis (Ronkainen et al., 2003; Park et al., 2011). Moreover, most researches have few cases and insufficient evidence, so the guidelines pointed out that CyA cannot be routinely recommended for moderate IgAV nephritis patients. However, CyA should be considered in patients with CS resistance or other immunosuppressants that are ineffective and relapsed.

The ADR of CyA includes hepatorenal toxicity, hypertension, neurotoxicity, gastrointestinal symptoms, and hairiness (Phan et al., 2021), especially hepatorenal toxicity showing a significant dose-effect relationship. CyA is biotransformed mainly by CYP3A4 and CYP3A5 into primary metabolites, including AM1, AM9, and AM4N, and then into secondary and tertiary metabolites AM1c, AM19, and AM1c9 (Lensmeyer et al., 1988; Christians et al., 1991a; Christians et al., 1991b). CyA principally relies on CYP3A4 metabolism *in vivo*, while a similar drug, Tacrolimus (TAC), is mainly metabolized by CYP3A5. Compared with CYP3A5, which mainly plays a role in the kidney, CYP3A4 metabolizes most CyA in the liver, and its variant CYP3A4*22 (c.522-191C > T, rs35599367) was related to the decline of enzyme bioactivity expressed in the liver, which is also related to individual clearance declining and renal toxicity (Elens et al., 2011; Wang and Sadee, 2016), such as worse creatinine clearance rate. As for CYP3A5, it is generally believed that carrying wild-type CYP3A5*1 allele (including homozygous and heterozygous) is considered CYP3A5 expression type, while CYP3A5*3 and *6 are considered to be CYP3A5 low expression or non-expression type due to incorrect mRNA splicing (Kuehl et al., 2001; Lin et al., 2002). Zheng et al. (2013) observed that individuals with CYP3A5 expression type (including homozygous and heterozygous) showed an enhanced formation of secondary metabolites AM19 and AM1c9, which may augment the risk of nephrotoxicity (Dai et al., 2004; Zheng et al., 2013).

Except for CYP3A4 and 3A5, P-gp and P450 oxidoreductase genes (POR) also have affected the pharmacokinetics (PK) of CyA. As one of the sensitive substrates of P-gp, the bioavailability of CyA is low. P-gp, a member of the ABC membrane transporter family (including ABCC2 and ABCG2), is a product of human multidrug resistance gene 1 (MDR1). It has been discovered that adults carrying the POR*28 allele require more CsA dose (Cvetkovic et al., 2017), while ABCC2 (c.-24C > T, rs717620) and ABCG2 (c.421C > A, rs2231142) may increase the exposure of CyA *in vivo*, which in turn increases the risk of hepatorenal toxicity (Wang et al., 2021).

4.3.4 Other immunosuppressants

4.3.4.1 Tacrolimus

TAC is a widely used immunosuppressive drug whose mechanism of action is to bind to the cytosolic receptor FK-binding protein 12 in T lymphocytes to form a composite that combines with calcium-regulated neurophosphatase to prevent dephosphorylation and nucleus translocation of nuclear factors in inflamed T cells, eventually inhibiting the expression of interleukin 2 and activation of T lymphocytes (Bowman and Brennan, 2008). The demethylation and hydroxylation occur *via* CYP3A isoforms (CYP3A4 and CYP3A5) in the hepar and intestine, while TAC is the substrate of the multidrug efflux transporter P-glycoprotein which is epitomized by the ABCB1 gene and previously known as MDR1; and it is represented on a multitude of epithelial cells, endotheliocyte, and lymphocytes (Birdwell et al., 2015). The restricted therapeutic index and pharmacokinetic differences between patients with TAC are partly due to the CYP3A5 gene variation, and CYP3A5 is the primary enzyme of TAC metabolism (Dai et al., 2006). Although TAC is currently used empirically in the treatment of childhood IgAV nephritis (Ichiyama et al., 2017; Zhang et al., 2018) and is believed to be a prospective non-steroidal medicine for treating severe IgAV nephritis, proof-based clinical information available are still modest. As a calcium-regulated neurophosphatase inhibitor (CNI), the critical mechanistic effects of TAC in childhood IgAV nephritis include inhibition of calcium-regulated neurophosphatase redistribution in the cleft septum, which may potentially reduce proteinuria (Namgoong, 2020). TAC has been proposed to potentially alleviate proteinuria through stabilization of the podocyte cytoskeleton primarily by inhibiting the expression of calcium-regulated neurophosphatase (Zhang et al., 2012). A recent retrospective clinical study concluded that TAC for the treatment of IgAV nephropathy in children was shown to reduce proteinuria, hematuria and improve renal function with relatively mild side effects, with major adverse events likely to include respiratory and urinary tract infections (Wu et al., 2022). The evidence for the safety of TAC in the treatment of IgAV nephritis in children is insufficient, however, if proteinuria persists after a course of CS, tacrolimus may also be considered for the immunosuppressive treatment of children with IgAV

nephritis, with attention to the detection of relevant indicators and clinical symptoms in the child at the time of use.

The CYP3A5 expression phenotype exhibits negative or mildly decreased levels of CYP3A5 mRNA and expressed analogous vasoactive protein CYP3A5; in contrast, the CYP3A5 non-expression phenotype expresses low expression of the vasoactive CYP3A5 protein due to a CYP3A5*3 allelic variant encoding an enzyme with reduced activity (Hustert et al., 2001; Kuehl et al., 2001). This variant is most common in whites, with 80%–85% of whites being CYP3A5 non-expression (Van Schaik et al., 2002). Zhang et al. (2018) performed a study on the use of TAC beyond instructions in children with IgAV nephritis. They found that children with the CYP3A5*1 allelic variant had significantly lower dose-adjusted trough concentrations than children with the CYP3A5*3/*3 allelic variant. However, there was no difference in short-term efficacy between the two groups, probably due to the small sample size. Massive retrospective studies of current TAC use in renal transplant patients have shown that CYP3A5 expression renal transplant recipients require approximately twice the dose of TAC than non-expression patients (Birdwell et al., 2012). A controlled trial indicated that patients carrying the CYP3A5*1/*1 or CYP3A5*1/*3 genes (CYP3A5 expression) required an equal dose of TAC compared to patients carrying the CYP3A5*3/*3 genes (CYP3A5 non-expression) patients, with comparable blood intensities requiring 1.5 to 2 times the dose (Haufroid et al., 2004). And in the immediate first year after kidney transplantation, patients carrying the CYP3A5*3/*3 gene had 1.8–2.5 fold higher dose-adjusted trough concentrations than patients expressing CYP3A5 (Rojas et al., 2015). This proved that patients with CYP3A5 expression phenotypes metabolize TAC more strongly than patients with CYP3A5 non-expression phenotypes and that the required dose to maintain the target blood concentration should be higher. Based on the impact of CYP3A5 genotyping on the pharmacokinetic parameters of TAC, the guideline (Birdwell et al., 2015) gives recommendations for the dose of TAC to be used, with CYP3A5 expression patients will demand an upper recommended initial dose, while patients who do not express CYP3A5 will demand the standard recommended initial dose, and for faster achievement of therapeutic drug concentrations, it is recommended that taking TAC CYP3A5*3 allele testing is recommended for patients taking TAC prior to initiation of TAC. Also, considering risks of arterial constriction, hypertension, and renal toxicity that may develop with supra therapeutic concentrations of TAC, dose adjustment based on observed serum concentrations should be made for intermediate (CYP3A5*1/*3) or rapid (CYP3A5*1/*1) metabolizers using TDM.

There is still a lack of evidence that CYP3A5 genotyping guides the efficacy of TAC dosing in pediatric IgAV nephritis patients, and CYP3A5 genotyping does not replace therapeutic TDM due to the existence of many other factors that influence the dosing requirements of TAC, such as drug interactions with glucocorticoids and immunosuppressants commonly used in the treatment of IgAV nephritis and genetic variants that affect TAC pharmacodynamics. The two methods should be used in combined for individualized treatment of pediatric IgAV nephritis patients. Future clinical trials on the affection of CYP3A5 genotyping in guiding the effectiveness of using TAC in pediatric IgAV nephritis patients are needed, which will be of great significance for the precise dosing of TAC in pediatric IgAV nephritis patients.

4.3.4.2 Mizoribine and leflunomide

Mizoribine (MZB) is an antimetabolic drug that exerts immunosuppressive effects by inhibiting lymphocyte proliferation (Yokota, 2002). The reported immunosuppressive effect of MZB is due to the suppression of DNA in the S phase of the cell cycle. There are clinical cases of using MZB instead of CYC in combination with pulsed MP as part of the treatment of severe IgAV nephritis in children, and this therapy has shown improvement in histological severity as well proteinuria in children with IgAV nephritis (Kawasaki et al., 2011). A clinical trial using MZB as a complementary therapy to prednisolone monotherapy in patients with IgAV nephritis showed that MZB may have a prophylactic effect in patients with IgAV nephritis at risk of relapse (Kawakami et al., 2010). MZB is a reliable and well-tolerated drug, and no significant adverse effects, including bone marrow suppression, have been reported in the treatment of children with IgAV nephritis. This suggests that MZB is likely to be a potential drug for managing IgAV nephritis in children.

In clinical experience, many patients and their families are reluctant to undergo treatment with CTX primarily because of its gonadal toxicity. The high cost of MMF may have an impact on treatment choice. Leflunomide (LEF) is a comparatively new oral immunosuppressant that disrupts T and B cell function by inhibiting dihydronucleic acid dehydrogenase (the rate-limiting enzyme for ab initio synthesis of pyrimidine nucleotides), specifically inhibits T-dependent autoantibody formation; and a few tyrosine kinase signaling molecules involved in immune function are also inhibited by LEF (Siemasko et al., 1996; Lou et al., 2006). The current clinical trial results showed that LEF combined with steroids improved the renal prognosis of patients with IgAV nephritis with nephrotic proteinuria more significantly than steroids alone, with no apparent adverse effects (Zhang Y. et al., 2014; Hou et al., 2021). LEF, which has been reported to be rapidly biotransformed to its active metabolite, is usually undetectable in plasma and therefore has only a tiny *in vivo* exposure (and no pharmacological activity). *In vitro* studies suggest that activation of LEF may be associated with CYP4501A2, CYP2C19, and CYP3A4 (Rozman, 2002; Kalgutkar et al., 2003), and only limited pharmacogenetic data are available for LEF or its active metabolite. When LEF is used for the treatment of rheumatoid arthritis (RA), individuals carrying the CYP1A2*1F CC gene are more likely to have a 9.7-fold higher risk of overall toxicity than those carrying the CYP1A2*1F A

allele (Bohanec Grabar et al., 2008). Furthermore, ABCG2, as an efflux transporter, is involved in the disposal of various chemotherapeutic drugs, and it has been reported that LEF and its active metabolites are substrates of ABCG2 *in vitro* (Kis et al., 2009). So ABCG2 gene polymorphism may be a major determinant of interindividual differences in the disposition of the active metabolite of LEF-teflunomide. A study investigated the effect of the ABCG2 (c.421C > A and c.34G > A) gene on teflunomide PK in 24 healthy volunteers and concluded that ABCG2 c.421C > A polymorphism seems to be the main determinant of inter-individual pharmacokinetic differences in teflunomide (Kim et al., 2011). Overall, LEF can be considered an alternative drug with good efficacy and safety profile in pediatric patients with IgAV nephritis who are intolerant to commonly used immunosuppressive agents.

4.3.4.3 Monoclonal antibodies

Rituximab (RTX), a monoclonal antibody against the B-cell CD20 antigen, was initially conceived and endorsed in 1997 for the therapy of non-Hodgkin's B-cell lymphoma and, as such, has been used in many immune-mediated diseases, for example, has become the standard therapy for inducing remission and maintaining resolution in patients with anti-neutrophil cytoplasmic antibody (ANCA)-associated vasculitis (Modena et al., 2013; Clark, 2020). Studies evaluated the major lymphocyte subsets in the peripheral blood of children with IgAV and showed an increased percentage of B lymphocytes as well as increased serum IgA in children with IgAV (Wiercinski et al., 2001), and RTX, by depleting B cells, may reduce the formation of IgA-containing immune complexes and limit the activity of IgA disease (Fenoglio et al., 2017). Although RTX should not deplete terminally differentiated, immunoglobulin-secreting plasma cells, the benefit of depleting B cells by RTX in other B cell-mediated diseases guarantees its use in refractory IgAV (Donnithorne et al., 2009). RTX has therefore been suggested as an alternative therapy for refractory or recurrent IgAV (Abu-Zaid et al., 2021) and is a potential therapeutic tool for IgAV nephritis that is attractive in refractory IgAV nephritis.

In case reports with adult patients with IgAV nephritis (Pindi Sala et al., 2014; Bellan et al., 2016; Fenoglio et al., 2017), RTX was primarily used as a salvage treatment for the onset of IgAV nephritis, where patients received RTX for refractory/recurrent disease or because conventional CS/immunosuppressive therapy was contraindicated, and complete renal remission was achieved after treatment, during which all patients were in sustained remission. No serious adverse events associated with RTX were usually observed, and only a minimal number of patients experienced gastrointestinal norovirus infection in patients 3 months after RTX. However, this infection may have been associated not only with RTX treatment but also with other immunosuppressive therapies previously received. Meanwhile, a report by Katherine et al. (Donnithorne et al., 2009) demonstrated the effectiveness of RTX in children with severe IgAV nephritis who had failed to respond to conventional interventions. A clinical study on IgA nephropathy (IgAN) patients conducted by Richard et al. (Lafayette et al., 2017) yielded different results, with RTX treatment failing to significantly reduce proteinuria or improve renal function in IgAN patients during the period studied. When RTX was used for renal disease, the older the patient was used, the better the outcome, such as the lower risk of relapse, longer B-cell recovery, and lower risk of hypogammaglobulinemia; however, these associations have not been universally confirmed (Sinha et al., 2021). Overall, RTX is a potential therapeutic agent for severe childhood IgAV nephritis where conventional interventions have failed. However, pediatric data regarding the use of RTX for IgAV nephritis in children are still sparse. The lack of randomized controlled trials is insufficient to conclude that RTX is equally secure and effective in pediatric patients, and more clinical data are needed.

4.4 Others

4.4.1 Complement inhibitors

The complement system, a critical player in the body's response to defense, exerts a powerful effect upon many physiological systems. However, unintentional activation of the complement system may turn the scales in favor of self-aggression, leading to an over-reaction to self-aggression and auto-inflammatory illnesses (Ort et al., 2020), where the kidney is particularly vulnerable, and abnormal complement activation is associated with many renal diseases. Patients with IgAV have an increased number of IgA immune complexes that are deposited on the glomerular thylakoid because of the lack of C1q binding sites IgA fails to activate the classical pathway of complement but activates the complement system *via* the alternative or lectin pathway (Chen and Mao, 2015; Heineke et al., 2017), ultimately leading to podocyte and glomerular injury, fibrosis and ESRD (Ort et al., 2020).

The availability of eculizumab (eculizumab) in 2007 demonstrated that complement inhibitors could treat rare (auto) inflammatory diseases (Ort et al., 2020). Many next-generation complement inhibitors, including humanized monoclonal antibodies, small proteins that bind to specific complement components, and recombinant proteins, are currently being evaluated in clinical trials (Zipfel et al., 2019). Mannan-binding lectin-associated serine protease 2 (MASP-2), an effector enzyme activated by the complement lectin pathway, is a potential drug target for IgAV nephritis (Lafayette et al., 2020). Narsoplimab, a fully human monoclonal antibody, is designed to treat diseases mediated by the complement agglutinin pathway by inhibiting of MASP-2. The classical complement activation pathway, which is not interfered with by inhibition of MASP-2, plays a vital role in the immune response to acquired infections (Lafayette et al., 2020);

therefore, the use of narsoplimab has not increased the risk of infection or autoimmune disease. Currently, guidelines suggest that patients need meningococcal vaccination and appropriate prophylaxis when complement deficient or treated with complementing inhibitors (Rovin et al., 2021).

The current results of many basic studies support the idea that complement activation can play a critical role in the development and progression of IgAN disease; for example, narsoplimab appears to significantly reduce proteinuria and increase the stability of EGFR in renal function in high-risk IgAN patients (Edström Halling et al., 2010). Since the pathophysiology of IgAV nephritis is similar or identical to that of IgAN (Chen and Mao, 2015) and is also accompanied by IgA deposition, complement factors, and massive neutrophil infiltration (Heineke et al., 2017), narsoplimab would be equally very promising as a complement inhibitor in patients with IgAV nephritis.

4.4.2 Anticoagulants and antiplatelet drugs

Abnormalities in the coagulation and fibrinolytic systems can contribute to the development of IgAV nephritis (Prandota et al., 2001); and activation of intra-glomerular coagulation is an aggravating factor in IgAV nephritis, which may be related to fibrin deposition in the glomerulus contributing to the crescent formation (Shin et al., 2005). In experimental models, defibrinolysis reduced the number of crescent bodies and the severity of renal insufficiency (Tipping et al., 1986). Therefore, the use of appropriate fibrinolytic and anticoagulant drugs may have significance for preventing and treating IgAV nephritis in children. Although still controversial, evidence-based guidelines in China suggest that anticoagulants and/or antiplatelet aggregating agents can be used to treat IgAV nephritis (Subspecialty Group of Renal Diseases and Chinese Medical Association, 2017). Common anticoagulants and antiplatelet agents, including warfarin, heparin, pentoxifylline, and aspirin (Chartapisak et al., 2009), and the fibrinolytic drug urokinase.

Iijima et al. (1998) suggested that various combinations of glucocorticoids and anti-immune drugs with heparin/warfarin and pansentin are effective in histologically severe IgAV nephritis. However, a recent case report (Kalay-Yildizhan et al., 2020) reported the development of skin ulcerated plaques and proteinuria in IgAV patients treated with warfarin, as well as a rare complication with heparin, namely heparin-induced thrombocytopenia (HIT), which activates platelets and leads to thrombocytopenia and a prothrombotic state. Treatment with anticoagulants in patients with IgAV should be vigilant for these rare but serious consequences, and immediate discontinuation of the drug is essential to prevent renal failure and other organ involvement. Watanabe et al. (Kawasaki et al., 2004b) affirmed urokinase's efficacy in treating severe IgAV nephritis and recommended fibrinolytic therapy to alleviate the intra-glomerular hypercoagulable state resulting from renal injury to protect renal function in patients with severe IgAV nephritis. A clinical trial (Kawasaki et al., 2003) showed that hypercoagulable in IgAV nephritis improved with urokinase shock treatment compared to pre-treatment, with lower urinary protein excretion and lower volume of cases of renal disfunction after treatment, and no ADR such as bleeding tendency were observed. Meanwhile, a study (Shin et al., 2005) found that children with IgAV nephritis who develop the disease at an age older than 9 years have relatively severe fibrinogen deposition, suggesting that age of onset affects the process and prognosis of fibrinogen deposition. Moreover, childhood IgAV nephritis is a heterogeneous disease with multiple histopathological manifestations. The increase of crescent bodies in children with IgAV nephritis is not always dependent on fibrinogen, so fibrinolytic therapy should be tailored to the child's characteristics to achieve individualized treatment.

4.4.3 Chinese medicine

Chinese medicine treatment has been considered an effective treatment for children with IgAV nephritis; its combination with immunosuppressants and CS produces additional positive effects, such as alleviating blood hypercoagulability in children, reducing proteinuria, and decreasing the recurrence rate of IgAV nephritis in children (Ding et al., 2019; Jin et al., 2021). Tripterygium wilfordii, a vine grown in southeastern China for thousands of years, is the most widely used Chinese medicine in children with IgAV nephritis. Tripterygium glycosides, a natural active ingredient extracted from tripterygium wilfordii, could inhibit delayed metabolic reactions, reduce the secretion of cytokine IL-1, and inhibit the function, division, and replication of T lymphocytes (Wang et al., 2019). Furthermore, the tripterygium glycosides antagonize the binding of inflammatory factors to receptors, inhibiting the release of inflammatory transmitters (Han et al., 2016). The ability of tripterygium glycosides to alleviate hematuria and proteinuria in IgA deposition nephropathy has been demonstrated in a previous study (Liu X. et al., 2019). Tripterygium glycosides also possess some anti-inflammatory effects, and their combination with TAC can reduce the dosage of TAC, thus reducing the risk of complications such as hepatotoxicity and neutropenia. However, the time required to treat IgAV nephritis in children is longer than that of TAC alone, which may be related to the slow onset of action of the herbal medicine (Zhang et al., 2021). ADR to tripterygium glycosides is widespread and can involve multiple systems, including hematologic, cardiovascular, and neurologic. Although several clinical reports demonstrate favorable effects of tripterygium glycosides in children with IgAV nephritis for whom conventional therapy is ineffective, they are still insufficient to verify the safety of tripterygium glycosides. Based on the safety considerations of pediatric use, the current drug instructions for tripterygium glycosides explicitly indicate that it is prohibited in children. Therefore, the Chinese expert group did not

recommend tripterygium glycosides for the treatment of IgAV nephritis in children in the 2017 guidelines (Subspecialty Group of Renal Diseases and Chinese Medical Association, 2017). As a potential drug for the treatment of IgAV nephritis in children, it is expected that more relevant randomized controlled clinical studies and prolonged follow-up will emerge in the future to help the decision on the use of tripterygium glycosides.

5 Non-drug treatment of immunoglobulin A vasculitis nephritis in children

5.1 Plasmapheresis

Plasmapheresis (PP) has become a typical extracorporeal circulation blood purification therapy, and studies on the treatment of IgAV nephritis in children with PP or PP combined with drug therapy have proved beneficial.

Hattori et al. (1999) retrospectively evaluated 9 cases of rapidly progressing IgAV nephritis in children treated with PP as the only treatment. All the children had proteinuria and decreased GFR, and renal biopsy indicated that the crescent shape was over 50%. The PP regimen was three times weekly for 2 weeks and then once a week for 6 weeks. The study showed that all patients responded quickly to PP treatment, with clinical symptoms improving, proteinuria decreasing, GFR improving, purpuric rash, and abdominal pain alleviating. Kawasaki et al. (2004a) retrospectively studied six rapidly progressive IgAV nephritis cases in children treated with PP combined with multiple drugs. PP regimen for all patients consisted of five courses for 2 weeks, three times every other day in the first week and two times every other day in the second week. No increase in urinary protein and crescents, glomerulosclerosis, and renal failure was observed during multidrug therapy after PP treatment, which has been shown to be beneficial for rapidly progressive IgAV nephritis in children. Liu N. et al. (2019) studied the clinical therapeutic effect and reliability of dual filter plasma exchange (DFPP) combined with drugs to treat severe IgAV nephritis in children. All children had severe IgAV nephritis and received DFPP for three courses on the basis of the drug treatment regimen of MP and CYC dual pulse therapy. The decrease in urinary protein, immunoglobulin, serum creatinine, and urea nitrogen was notably higher than those in the control group. There was non-differentiation in the incidence of ADR. The study results confirmed that DFPP combined with drugs could improve clinical symptoms and reduce renal injury without increasing the incidence of side effects.

The mechanism of PP treatment for IgAV nephritis in children is still unclear. The results of test indicators and immunology show that PP can remove IgA-containing immune complexes or accumulations of pro-inflammatory mediators, and reduce fibrous protein or other blood coagulable factors. It is speculated that these mechanisms are related (Kawasaki et al., 2004a). Overall, early PP treatment can effectively improve the prognosis of children with IgAV nephritis, especially in children with rapid progression and severe IgAV nephritis, which can significantly improve urinary protein, GFR, and other indicators, prevent and reduce renal injury, reduce purpura and other clinical symptoms (Kawasaki, 2011).

5.2 Tonsillectomy

Several current studies have shown that tonsillectomy is not only related to the reduction of urinary protein excretion but also can effectively treat IgAV nephritis in children and prevent the recurrence of IgAV nephritis in children (Yang et al., 2016; Umeda et al., 2020). There was a case of IgAV nephritis in children with ISKDC VI-grade. After tonsillectomy, the proteinuria was significantly reduced, and the renal pathological results were improved in this patient. Tonsillectomy was performed on 5 cases of IgAV nephritis in adults and children with ISKDC grade II-VI (Ohara et al., 2011). The study showed that the pathological results of renal biopsy after tonsillectomy were improved with or without methylprednisolone pulse therapy, and the prognosis was good, confirming that tonsillectomy can successfully treat IgAV nephritis in children with severe ISKDC grade VI. A study (Umeda et al., 2020) retrospectively analyzed 71 cases of IgAV nephritis in Japanese children, 31 of whom underwent tonsillectomy after methylprednisolone pulse therapy and 40 of whom received methylprednisolone pulse therapy alone. The study showed that 2 years after methylprednisolone pulse therapy, the recurrence rate of IgAV nephritis in children undergoing tonsillectomy was significantly lower than that in children without tonsillectomy, which confirmed that tonsillectomy was conducive to preventing the recurrence of IgAV nephritis in children.

The mechanism of tonsillectomy in the treatment of children with IgAV nephritis is not yet clear. According to the remarkable influence of tonsillectomy on proteinuria in children's IgAV nephritis, it can cut down the production of IgA and the aberrant immunoreaction and inflammation after glomerular deposit IgA, which is different from the IgA immune compound removed by PP, suggesting that tonsil may act the part of the pathogenesis of IgAV nephritis (Kawasaki et al., 2006). On the other hand, chronic bacterial colonization of the upper airway or chronic inflammation has been considered to be the triggering factor of IgA vasculitis, and intervention measures to remove major lymphatic organs and reduce the recurrence of chronic inflammation may be helpful in reducing the induction of IgAV (Kronbichler et al., 2015). Therefore, tonsillectomy can significantly reduce the occurrence of proteinuria and hematuria and improve the pathological results of renal biopsy substantially,

and other aspects the benefits. Tonsillectomy is also a good choice for treating IgAV nephritis in children, especially severe pathological grade IgAV nephritis, and prevention of recurrence of IgAV nephritis.

6 Discussion

IgAV nephritis is mainly due to renal involvement caused by aberrant o-glycosylation of IgA1 deposition in the renal. The ultimate object of its therapy is to relieve or even eliminate the long-term harm of IgAV to the kidney. Drug therapy for IgAV nephritis includes ACEI/ARBs, CS, CYC, MMF, and AZA. The evidence quality of these drugs is high, and the guidelines recommend. Potential drug therapy includes CyA, TAC, MEB, LEF, RTX, complement inhibitors, anticoagulant antiplatelet drugs, and traditional Chinese medicine. Non-drug therapy is mainly PP and tonsillectomy, which can be used as an alternative treatment or potential treatment for drug-resistant cases, recurrent cases, and refractory cases. This paper also emphatically discusses the therapeutic significance of CS and immunosuppressants on children with IgAV nephritis at the level of pharmacogenomics and analyzes the individualized application of CS and immunosuppressants on children with different genotypes to provide a more comprehensive reference for individualized treatment of children with IgAV nephritis. Pre-identification of genes that affect drug efficacy and toxicity can predict the response of individual patients to drug treatment in advance, thus helping to determine a more effective initial dose and maintenance dose and even choose a more appropriate treatment for IgAV nephritis. It can also provide genetic evidence for post hoc analysis of drug resistance and ADR. The implementation of pharmacogenomics detection can help many Chinese children achieve better treatment outcomes (Qin et al., 2020). Therefore, this article focuses on linking pharmacogenomics and children with IgAV nephritis, which will draw more attention and thinking about the precise dosing of immunosuppressants in children with IgAV nephritis. We will also pay more attention to the pharmacogenomics related to the use of CS and immunosuppressants and encourage you to actively explore the pharmacogenomics of CS and immunosuppressants in children with IgAV nephritis.

CS-related gene polymorphism is associated chiefly with CS resistance, especially NR3C1 gene polymorphism, but there is a lack of related research in patients with IgAV nephritis, especially in children. Therefore, NR3C1 and other related gene polymorphisms on CS responsiveness in other diseases apply to IgAV glomerulonephritis, which still needs further research to confirm its universality.

Most CYC-related genetic variations are associated with ADR, such as the higher risk of hemorrhagic cystitis and leukopenia associated with CYP2B6 and GST gene polymorphism (Rocha et al., 2009; Afsar et al., 2012). Unfortunately, these results of most related pharmacogenomics studies about CYC have poor repeatability and cannot be applied to clinical practice.

The most significant advantage of MMF is that it is safer than other immunosuppressants, and its gene polymorphism is more associated with curative effects than toxicity and is often studied in patients with renal transplantation. The research is still immature. For example, the research results in IMPDH and UGT1A9 have some contradictions and differences.

The Clinical Pharmacogenetics Implementation Consortium (CPIC) suggested that TPMT deficiency was detected by identifying TPMT allele variants or TPMT phenotypes associated with the inactivation of AZA active metabolites and gave strong dose recommendations for the use of AZA in IBD patients (Relling et al., 2011; Woillard et al., 2017). These recommendations also apply to children (Relling et al., 2013). In the updated 2018 CPIC guidelines, AZA dosage guidance based on TPMT activity is no longer limited to a few diseases; CPIC has extrapolated it to all diseases. In some non-malignant cases, those with moderate TPMT activity and low TPMT activity may avoid AZA in favor of other alternative drugs (Relling et al., 2019). For high TPMT activity, use the standard starting dose recommended according to the guidelines for the respective disease. For patients with moderate TPMT activity and low TPMT activity who must use AZA, a dose reduction of 30%–80% for moderate TPMT activity and a 10-fold decrease in daily dose for low TPMT activity is recommended (Relling et al., 2019). In addition to TPMT, the NUDT15 gene polymorphism is more instructive in Asians. Similar to AZA, regular starting doses are used for those with normal NUDT15 metabolism (i.e., NUDT15*1 pure-hybrid individuals) and those with intermediate NUDT15 metabolism (i.e., NUDT15*1-containing heterozygotes), starting doses should be reduced by 30%–80% (Relling et al., 2019). In contrast, those with poor NUDT15 metabolism (not carrying the NUDT15*1 allele) should substantially lessen the regular initial dose or avoid AZA (Relling et al., 2019). The initial dose should be determined according to disease-specific and race-specific guidelines. Furthermore, an initial screening for TPMT and NUDT15 can predict the drug response in advance, give an appropriate initial dose, and be used for post-mortem detection of severe myelotoxicity, liver failure, and drug resistance to find the genetic causes of ADR and drug resistance (Woillard et al., 2017). If the child has a homozygous mutation of TPMT or NUDT15, MMF can be selected in advance instead of AZA for treatment. If the child

has a heterozygous mutation, a low dose of AZA is more recommended.

Several studies have shown that CYP3A4, CYP3A5, POR, ABC, and other gene polymorphisms are related to the individual differences of CyA to a certain extent, and they all can become factors that predict CyA response in advance. Unfortunately, the uncertainty of efficacy and toxicity of CyA in the IgAV population is an indispensable reason limiting the expansion of such research in the past and future.

Like AZA, the research on the relationship between gene polymorphism of TAC metabolizing enzyme CYP3A5 and drug dose is relatively mature in the renal transplantation population. Therefore, to use TAC more safely, it is recommended that prior CYP3A5 typing be performed before some solid organ transplants such as heart, kidney, and lung transplants (Woillard et al., 2017). CPIC also strongly proposed that patients with CYP3A5 non-expression start treatment of the standard commended dosage (0.15 mg/kg/d), while patients with CYP3A5 expression increase the initiation dosage to 1.5–2 times the commended initiation dosage to guide dosage adjustment by therapeutic drug monitoring (Birdwell et al., 2015). However, these are not recommended for children with IgAV nephritis.

For the objects of gene detection, there is no guiding principle for gene detection of children with IgAV nephritis, and there is no relevant research. However, according to the AZA genotyping guidelines (Woillard et al., 2017), genetic post hoc probing and validation should be performed when patients present with drug resistance, serious adverse effects (e.g., myelosuppression and nephrotoxicity), and abnormal blood levels values. Of course, ex-ante genotyping should be considered when patients are planning to use high-quality evidence like AZA and TAC and have genotyped dosing recommendations in other diseases to seek safe and effective initial and maintenance doses.

There are still some limitations here. The most important of these is the lack of drug-related genetic polymorphism studies in children with IgAV nephritis, which are currently limited to studies in other diseases, such as AZA in IBD and TAC in the renal transplant population, and the paucity of authoritative guidelines for patient genotype-based drug use and clinical evidence for physicians and pharmacists. Indeed, genetic testing increases the cost of treatment for children. It is unclear whether the increase in treatment cost is proportional to the improvement in therapeutic efficacy and safety. Despite the relative maturity of genetic testing technology, many medical institutions have not been able to implement this technology, which is related to the lack of pharmacy technicians, small patient populations, and physician attitudes toward genetic testing.

In conclusion, it may not be the best time for pharmacogenomics to guide the dosing of children with IgAV nephritis, but with the vision of precision dosing, our attention to pharmacogenomics should not be diminished, especially for drugs like AZA, which can already guide dosing based on patient genotype. Therefore, the future treatment of IgAV nephritis in children urgently needs high-quality pharmacogenomics-related clinical trials to provide more evidence-based medical and pharmacological evidence for clinical diagnosis and treatment.

Author contributions

XY, QL, YH, YZ, and RY were involved in the literature review, discussion, manuscript creation. XsZ and XZ participated in manuscript revision. YY and WX guided the manuscript writing and participated in manuscript modification. All authors reviewed and approved the manuscript.

Funding

This research is supported by the Key Research and Development Project of the Science & Technology Department of Sichuan Provincial, China (No. 2022YFS0059).

Acknowledgments

We recognize the support from Sichuan Academy of Medical Sciences & Sichuan Provincial People's Hospital, University of Electronic Science and Technology of China, and Ziyang People's Hospital.

Conflict of interest

The authors declare that the research was conducted in the absence of any commercial or financial relationships that could be construed as a potential conflict of interest.

Publisher's note

Supplementary material

The Supplementary Material for this article can be found online at: https://www.frontiersin.org/articles/10.3389/fphar.2022.956397/full#supplementary-material

References

Abu-Zaid, M. H., Salah, S., Lotfy, H. M., El Gaafary, M., Abdulhady, H., Tabra, S. A. A., et al. (2021). Consensus evidence-based recommendations for treat-to-target management of immunoglobulin a vasculitis. *Ther. Adv. Musculoskelet. Dis.* 13, 1759720X211059610. doi:10.1177/1759720x211059610

Adami, G., and Saag, K. G. (2019). Glucocorticoid-induced osteoporosis: 2019 concise clinical review. *Osteoporos. Int.* 30 (6), 1145–1156. doi:10.1007/s00198-019-04906-x

Afsar, N. A., Ufer, M., Haenisch, S., Remmler, C., Mateen, A., Usman, A., et al. (2012). Relationship of drug metabolizing enzyme genotype to plasma levels as well as myelotoxicity of cyclophosphamide in breast cancer patients. *Eur. J. Clin. Pharmacol.* 68 (4), 389–395. doi:10.1007/s00228-011-1134-0

Allison, A. C., and Eugui, E. M. (2000). Mycophenolate mofetil and its mechanisms of action. *Immunopharmacology* 47 (2-3), 85–118. doi:10.1016/s0162-3109(00)00188-0

Appell, M. L., Berg, J., Duley, J., Evans, W. E., Kennedy, M. A., Lennard, L., et al. (2013). Nomenclature for alleles of the thiopurine methyltransferase gene. *Pharmacogenet Genomics* 23 (4), 242–248. doi:10.1097/FPC.0b013e32835f1cc0

Attia, D. H. S., Eissa, M., Samy, L. A., and Khattab, R. A. (2021). Influence of glutathione S transferase A1 gene polymorphism (-69C > T, rs3957356) on intravenous cyclophosphamide efficacy and side effects: a case-control study in Egyptian patients with lupus nephritis. *Clin. Rheumatol.* 40 (2), 753–762. doi:10.1007/s10067-020-05276-0

Baldelli, S., Merlini, S., Perico, N., Nicastri, A., Cortinovis, M., Gotti, E., et al. (2007). C-440T/T-331C polymorphisms in the UGT1A9 gene affect the pharmacokinetics of mycophenolic acid in kidney transplantation. *Pharmacogenomics* 8 (9), 1127–1141. doi:10.2217/14622416.8.9.1127

Banerjee, R., Ravikanth, V. V., Pal, P., Bale, G., Avanthi, U. S., Goren, I., et al. (2020). NUDT15 C415T variant compared with TPMT genotyping in predicting azathioprine-induced leucopenia: prospective analysis of 1014 inflammatory bowel disease patients in India. *Aliment. Pharmacol. Ther.* 52 (11-12), 1683–1694. doi:10.1111/apt.16137

Barnes, P. J., Ito, K., and Adcock, I. M. (2004). Corticosteroid resistance in chronic obstructive pulmonary disease: inactivation of histone deacetylase. *Lancet* 363 (9410), 731–733. doi:10.1016/s0140-6736(04)15650-x

Barraclough, K. A., Lee, K. J., and Staatz, C. E. (2010). Pharmacogenetic influences on mycophenolate therapy. *Pharmacogenomics* 11 (3), 369–390. doi:10.2217/pgs.10.9

Bellan, M., Pirisi, M., and Sainaghi, P. P. (2016). Long-term remission of corticosteroid- and cyclophosphamide-resistant Henoch-Schönlein purpura with rituximab. *Scand. J. Rheumatol.* 45 (1), 83–84. doi:10.3109/03009742.2015.1058417

Berthelot, L., Jamin, A., Viglietti, D., Chemouny, J. M., Ayari, H., Pierre, M., et al. (2018). Value of biomarkers for predicting immunoglobulin a vasculitis nephritis outcome in an adult prospective cohort. *Nephrol. Dial. Transpl.* 33 (9), 1579–1590. doi:10.1093/ndt/gfx300

Bhowmick, R., Rameshkumar, R., Ponnusamy, M., Rajaraman, V., Chidambaram, M., Sheriff, A., et al. (2022). Modified Schwartz formula and 99mTc-DTPA plasma clearance methods to calculate glomerular filtration rate in critically ill children. *Pediatr. Nephrol.* 37 (4), 899–906. doi:10.1007/s00467-021-05197-3

Birdwell, K. A., Grady, B., Choi, L., Xu, H., Bian, A., Denny, J. C., et al. (2012). The use of a DNA biobank linked to electronic medical records to characterize pharmacogenomic predictors of tacrolimus dose requirement in kidney transplant recipients. *Pharmacogenet Genomics* 22 (1), 32–42. doi:10.1097/FPC.0b013e32834e1641

Birdwell, K. A., Decker, B., Barbarino, J. M., Peterson, J. F., Stein, C. M., Sadee, W., et al. (2015). Clinical Pharmacogenetics implementation Consortium (CPIC) guidelines for CYP3A5 genotype and tacrolimus Dosing. *Clin. Pharmacol. Ther.* 98 (1), 19–24. doi:10.1002/cpt.113

Bogdanovic, R. (2009). Henoch-Schönlein purpura nephritis in children: risk factors, prevention and treatment. *Acta Paediatr.* 98 (12), 1882–1889. doi:10.1111/j.1651-2227.2009.01445.x

Bohanec Grabar, P., Rozman, B., Tomsic, M., Suput, D., Logar, D., and Dolzan, V. (2008). Genetic polymorphism of CYP1A2 and the toxicity of leflunomide treatment in rheumatoid arthritis patients. *Eur. J. Clin. Pharmacol.* 64 (9), 871–876. doi:10.1007/s00228-008-0498-2

Bowman, L. J., and Brennan, D. C. (2008). The role of tacrolimus in renal transplantation. *Expert Opin. Pharmacother.* 9 (4), 635–643. doi:10.1517/14656566.9.4.635

Bray, J., Sludden, J., Griffin, M. J., Cole, M., Verrill, M., Jamieson, D., et al. (2010). Influence of pharmacogenetics on response and toxicity in breast cancer patients treated with doxorubicin and cyclophosphamide. *Br. J. Cancer* 102 (6), 1003–1009. doi:10.1038/sj.bjc.6605587

Caplan, A., Fett, N., Rosenbach, M., Werth, V. P., and Micheletti, R. G. (2017). Prevention and management of glucocorticoid-induced side effects: a comprehensive review: gastrointestinal and endocrinologic side effects. *J. Am. Acad. Dermatol* 76 (1), 11–16. doi:10.1016/j.jaad.2016.02.1239

Casajus, A., Zubiaur, P., Méndez, M., Campodónico, D., Gómez, A., Navares-Gómez, M., et al. (2022). Genotype-guided prescription of azathioprine reduces the incidence of adverse drug reactions in TPMT intermediate metabolizers to a similar incidence as normal metabolizers. *Adv. Ther.* 39 (4), 1743–1753. doi:10.1007/s12325-022-02067-8

Casati, C., Menegotto, A., Querques, M. L., Ravera, F., and Colussi, G. (2017). Immunosuppression in kidney transplantation: a way between efficacy and toxicity. *G. Ital. Nefrol.* 34 (2), 29–39.

Chan, H., Tang, Y. L., Lv, X. H., Zhang, G. F., Wang, M., Yang, H. P., et al. (2016). Risk factors associated with renal involvement in childhood henoch-schönlein Purpura: A meta-analysis. *Plos One* 11 (11), e0167346. doi:10.1371/journal.pone.0167346

Chartapisak, W., Opastirakul, S., Hodson, E. M., Willis, N. S., and Craig, J. C. (2009). Interventions for preventing and treating kidney disease in Henoch-Schonlein Purpura (HSP) (Review). *Cochrane Database Syst. Rev.* 5 (3), CD005128. doi:10.1002/14651858.CD005128.pub2

Chen, J. Y., and Mao, J. H. (2015). Henoch-Schönlein purpura nephritis in children: incidence, pathogenesis and management. *World J. Pediatr.* 11 (1), 29–34. doi:10.1007/s12519-014-0534-5

Chen, X., Zhang, L., Liang, D., Li, J., Liu, F., and Ma, H. (2018). Lipid transporter activity-related genetic Polymorphisms are associated with steroid-induced osteonecrosis of the femoral head: An updated meta-analysis based on the GRADE guidelines. *Front. Physiol.* 9, 1684. doi:10.3389/fphys.2018.01684

Chen, Z. Y., Zhu, Y. H., Zhou, L. Y., Shi, W. Q., Qin, Z., Wu, B., et al. (2021). Association between genetic Polymorphisms of metabolic enzymes and azathioprine-induced myelosuppression in 1,419 Chinese Patients: A retrospective study. *Front. Pharmacol.* 12, 672769. doi:10.3389/fphar.2021.672769

Cheng, Z., Dai, L. L., Liu, Q., Liu, M., Wang, Q., Li, P. F., et al. (2016). Correlation between polymorphisms in the glucocorticoid receptor gene NR3C1 and susceptibility to asthma in a Chinese population from the Henan Province. *Genet. Mol. Res.* 15 (2). doi:10.4238/gmr.15028507

Cheong, H. I., Kang, H. G., and Schlondorff, J. (2012). GLCCI1 single nucleotide polymorphisms in pediatric nephrotic syndrome. *Pediatr. Nephrol.* 27 (9), 1595–1599. doi:10.1007/s00467-012-2197-6

Chong, A. P., Walters, C. A., and Weinrieb, S. A. (1983). The neglected laboratory test. The semen analysis. *J. Androl.* 4 (4), 280–282. doi:10.1002/j.1939-4640.1983.tb02368.x

Christians, U., Strohmeyer, S., Kownatzki, R., Schiebel, H. M., Bleck, J., Greipel, J., et al. (1991a). Investigations on the metabolic pathways of cyclosporine: I. Excretion of cyclosporine and its metabolites in human bile--isolation of 12 new cyclosporine metabolites. *Xenobiotica* 21 (9), 1185–1198. doi:10.3109/00498259109039559

Christians, U., Strohmeyer, S., Kownatzki, R., Schiebel, H. M., Bleck, J., Kohlhaw, K., et al. (1991b). Investigations on the metabolic pathways of cyclosporine: II. Elucidation of the metabolic pathways *in vitro* by human liver microsomes. *Xenobiotica* 21 (9), 1199–1210. doi:10.3109/00498259109039560

Clark, A. (2020). Rituximab versus azathioprine for maintenance therapy in ANCA-associated vasculitis. *Lancet Rheumatol.* 2 (1), E12. doi:10.1016/s2665-9913(19)30139-0

Collins, F. S., and Varmus, H. (2015). A new initiative on Precision medicine. *N. Engl. J. Med.* 372 (9), 793–795. doi:10.1056/NEJMp1500523

Coppo, R., Peruzzi, L., Amore, A., Piccoli, A., Cochat, P., Stone, R., et al. (2007). IgACE: A placebo-controlled, randomized trial of angiotensin-converting enzyme inhibitors in children and young people with IgA nephropathy and moderate proteinuria. *J. Am. Soc. Nephrol.* 18 (6), 1880–1888. doi:10.1681/asn.2006040347

Cvetković, M., Zivković, M., Bundalo, M., Gojković, I., Spasojević-Dimitrijeva, B., Stanković, A., et al. (2017). Effect of age and allele variants of CYP3A5, CYP3A4, and POR genes on the Pharmacokinetics of cyclosporin A in Pediatric renal transplant recipients from Serbia. *Ther. Drug Monit.* 39 (6), 589–595. doi:10.1097/ftd.0000000000000442

Dai, Y., Iwanaga, K., Lin, Y. S., Hebert, M. F., Davis, C. L., Huang, W., et al. (2004). *In vitro* metabolism of cyclosporine A by human kidney CYP3A5. *Biochem. Pharmacol.* 68 (9), 1889–1902. doi:10.1016/j.bcp.2004.07.012

Dai, Y., Hebert, M. F., Isoherranen, N., Davis, C. L., Marsh, C., Shen, D. D., et al. (2006). Effect of CYP3A5 polymorphism on tacrolimus metabolic clearance *in vitro*. *Drug Metab. Dispos.* 34 (5), 836–847. doi:10.1124/dmd.105.008680

Davin, J. C., and Coppo, R. (2013). Pitfalls in recommending evidence-based guidelines for a protean disease like Henoch-Schönlein purpura nephritis. *Pediatr. Nephrol.* 28 (10), 1897–1903. doi:10.1007/s00467-013-2550-4

de Jonge, M. E., Huitema, A. D., Rodenhuis, S., and Beijnen, J. H. (2005). Clinical pharmacokinetics of cyclophosphamide. *Clin. Pharmacokinet.* 44 (11), 1135–1164. doi:10.2165/00003088-200544110-00003

Ding, Y., Zhang, X., Ren, X., Zhai, W., He, L., Liu, J., et al. (2019). Traditional Chinese medicine versus regular therapy in henoch-schönlein purpura nephritis in children: study protocol for a randomized controlled trial. *Trials* 20 (1), 538. doi:10.1186/s13063-019-3484-3

Donnithorne, K. J., Atkinson, T. P., Hinze, C. H., Nogueira, J. B., Saeed, S. A., Askenazi, D. J., et al. (2009). Rituximab therapy for severe refractory chronic Henoch-Schönlein purpura. *J. Pediatr.* 155 (1), 136–139. doi:10.1016/j.jpeds.2008.12.049

Edström Halling, S., Söderberg, M. P., and Berg, U. B. (2010). Predictors of outcome in Henoch-Schönlein nephritis. *Pediatr. Nephrol.* 25 (6), 1101–1108. doi:10.1007/s00467-010-1444-y

Elens, L., van Schaik, R. H., Panin, N., de Meyer, M., Wallemacq, P., Lison, D., et al. (2011). Effect of a new functional CYP3A4 polymorphism on calcineurin inhibitors' dose requirements and trough blood levels in stable renal transplant patients. *Pharmacogenomics* 12 (10), 1383–1396. doi:10.2217/pgs.11.90

Fenoglio, R., Naretto, C., Basolo, B., Quattrocchio, G., Ferro, M., Mesiano, P., et al. (2017). Rituximab therapy for IgA-vasculitis with nephritis: a case series and review of the literature. *Immunol. Res.* 65 (1), 186–192. doi:10.1007/s12026-016-8827-5

Foster, H. B., and Brogan, P. (2018). *Oxford handbook of paediatric rheumatology*. 2nd edn. New York: Oxford University Press.

Gardner-Medwin, J. M., Dolezalova, P., Cummins, C., and Southwood, T. R. (2002). Incidence of Henoch-Schönlein purpura, Kawasaki disease, and rare vasculitides in children of different ethnic origins. *Lancet* 360 (9341), 1197–1202. doi:10.1016/s0140-6736(02)11279-7

González-Gay, M. A., López-Mejías, R., Pina, T., Blanco, R., and Castañeda, S. (2018). IgA vasculitis: Genetics and clinical and therapeutic management. *Curr. Rheumatol. Rep.* 20 (5), 24. doi:10.1007/s11926-018-0735-3

Hajdinák, P., Szabó, M., Kiss, E., Veress, L., Wunderlich, L., and Szarka, A. (2020). Genetic Polymorphism of GSTP-1 affects cyclophosphamide treatment of autoimmune Diseases. *Molecules* 25 (7), 1542. doi:10.3390/molecules25071542

Han, B., Ge, C. Q., Zhang, H. G., Zhou, C. G., Ji, G. H., Yang, Z., et al. (2016). Effects of tripterygium glycosides on restenosis following endovascular treatment. *Mol. Med. Rep.* 13 (6), 4959–4968. doi:10.3892/mmr.2016.5149

Hattori, M., Ito, K., Konomoto, T., Kawaguchi, H., Yoshioka, T., and Khono, M. (1999). Plasmapheresis as the sole therapy for rapidly progressive Henoch-Schönlein purpura nephritis in children. *Am. J. Kidney Dis.* 33 (3), 427–433. doi:10.1016/s0272-6386(99)70178-2

Haufroid, V., Mourad, M., Van Kerckhove, V., Wawrzyniak, J., De Meyer, M., Eddour, D. C., et al. (2004). The effect of CYP3A5 and MDR1 (ABCB1) polymorphisms on cyclosporine and tacrolimus dose requirements and trough blood levels in stable renal transplant patients. *Pharmacogenetics* 14 (3), 147–154. doi:10.1097/00008571-200403000-00002

Hawkins, G. A., Lazarus, R., Smith, R. S., Tantisira, K. G., Meyers, D. A., Peters, S. P., et al. (2009). The glucocorticoid receptor heterocomplex gene STIP1 is associated with improved lung function in asthmatic subjects treated with inhaled corticosteroids. *J. Allergy Clin. Immunol.* 123 (6), 1376–e7. doi:10.1016/j.jaci.2009.01.049

Heineke, M. H., Ballering, A. V., Jamin, A., Ben Mkaddem, S., Monteiro, R. C., and Van Egmond, M. (2017). New insights in the pathogenesis of immunoglobulin A vasculitis (Henoch-Schönlein purpura). *Autoimmun. Rev.* 16 (12), 1246–1253. doi:10.1016/j.autrev.2017.10.009

Hou, L., Zhang, Z., and Du, Y. (2021). Leflunomide therapy for IgA vasculitis with nephritis in children. *BMC Pediatr.* 21 (1), 391. doi:10.1186/s12887-021-02866-y

Hustert, E., Haberl, M., Burk, O., Wolbold, R., He, Y. Q., Klein, K., et al. (2001). The genetic determinants of the CYP3A5 polymorphism. *Pharmacogenetics* 11 (9), 773–779. doi:10.1097/00008571-200112000-00005

Ichiyama, S., Matayoshi, T., Kaneko, T., Shimizu, A., Osada, S. I., Watanabe, A., et al. (2017). Successful multitarget therapy using prednisolone, mizoribine and tacrolimus for Henoch-Schönlein purpura nephritis in children. *J. Dermatol.* 44 (4), E56–E57. doi:10.1111/1346-8138.13614

Iijima, K., Ito-Kariya, S., Nakamura, H., and Yoshikawa, N. (1998). Multiple combined therapy for severe Henoch-Schönlein nephritis in children. *Pediatr. Nephrol.* 12 (3), 244–248. doi:10.1007/s004670050447

Izuhara, Y., Matsumoto, H., Kanemitsu, Y., Izuhara, K., Tohda, Y., Horiguchi, T., et al. (2014). GLCCI1 variant accelerates pulmonary function decline in patients with asthma receiving inhaled corticosteroids. *Allergy* 69, 668–673. doi:10.1111/all.12400

Jauhola, O., Ronkainen, J., Autio-Harmainen, H., Koskimies, O., Ala-Houhala, M., Arikoski, P., et al. (2011). Cyclosporine A vs. methylprednisolone for Henoch-Schönlein nephritis: a randomized trial. *Pediatr. Nephrol.* 26 (12), 2159–2166. doi:10.1007/s00467-011-1919-5

Jin, Y., Wang, Y., Wang, S., Zhao, Q., Zhang, D., and Feng, X. (2021). The efficacy of tripterygium glycosides combined with LMWH in treatment of HSPN in children. *Evid. Based Complement. Altern. Med.* 2021, 7223613. doi:10.1155/2021/7223613

Joy, M. S., La, M., Wang, J., Bridges, A. S., Hu, Y., Hogan, S. L., et al. (2012). Cyclophosphamide and 4-hydroxycyclophosphamide pharmacokinetics in patients with glomerulonephritis secondary to lupus and small vessel vasculitis. *Br. J. Clin. Pharmacol.* 74 (3), 445–455. doi:10.1111/j.1365-2125.2012.04223.x

Kalay-Yildizhan, I., Akay, B. N., Boyvat, A., and Heper, A. (2020). Ulcerative IgA vasculitis in the setting of warfarin therapy. *Dermatol Online J.* 26 (9). doi:10.5070/d3269050166

Kalgutkar, A. S., Nguyen, H. T., Vaz, A. D., Doan, A., Dalvie, D. K., McLeod, D. G., et al. (2003). *In vitro* metabolism studies on the isoxazole ring scission in the anti-inflammatory agent lefluonomide to its active alpha-cyanoenol metabolite A771726: mechanistic similarities with the cytochrome P450-catalyzed dehydration of aldoximes. *Drug Metab. Dispos.* 31 (10), 1240–1250. doi:10.1124/dmd.31.10.1240

Kanigicherla, D. A. K., Hamilton, P., Czapla, K., and Brenchley, P. E. (2018). Intravenous pulse cyclophosphamide and steroids induce immunological and clinical remission in New-incident and relapsing primary membranous nephropathy. *Nephrol. Carlt.* 23 (1), 60–68. doi:10.1111/nep.12955

Kawakami, T., Shirai, S., Kimura, K., and Soma, Y. (2010). Successful use of mizoribine to treat recurrent corticosteroid-resistant Palpable Purpura in a Patient with Henoch-Schonlein Purpura nephritis. *Arch. Dermatol* 146 (2), 212–213. doi:10.1001/archdermatol.2009.371

Kawasaki, Y., Suzuki, J., Nozawa, R., Suzuki, S., and Suzuki, H. (2003). Efficacy of methylprednisolone and urokinase pulse therapy for severe Henoch-Schönlein nephritis. *Pediatrics* 111 (4), 785–789. doi:10.1542/peds.111.4.785

Kawasaki, Y., Suzuki, J., Murai, M., Takahashi, A., Isome, M., Nozawa, R., et al. (2004a). Plasmapheresis therapy for rapidly progressive Henoch-Schönlein nephritis. *Pediatr. Nephrol.* 19 (8), 920–923. doi:10.1007/s00467-004-1514-0

Kawasaki, Y., Suzuki, J., and Suzuki, H. (2004b). Efficacy of methylprednisolone and urokinase pulse therapy combined with or without cyclophosphamide in severe henoch-schoenlein nephritis: a clinical and histopathological study. *Nephrol. Dial. Transpl.* 19 (4), 858–864. doi:10.1093/ndt/gfg617

Kawasaki, Y., Takano, K., Suyama, K., Isome, M., Suzuki, H., Sakuma, H., et al. (2006). Efficacy of tonsillectomy pulse therapy versus multiple-drug therapy for IgA nephropathy. *Pediatr. Nephrol.* 21 (11), 1701–1706. doi:10.1007/s00467-006-0272-6

Kawasaki, Y., Suyama, K., Hashimoto, K., and Hosoya, M. (2011). Methylprednisolone pulse plus mizoribine in children with Henoch-Schoenlein purpura nephritis. *Clin. Rheumatol.* 30 (4), 529–535. doi:10.1007/s10067-010-1572-6

Kawasaki, Y. (2011). The pathogenesis and treatment of pediatric Henoch-Schönlein purpura nephritis. *Clin. Exp. Nephrol.* 15 (5), 648–657. doi:10.1007/s10157-011-0478-1

KDIGO (2012). Chapter 11: Henoch-Schönlein purpura nephritis. *Kidney Int. Suppl. (2011)* 2 (2), 218–220. doi:10.1038/kisup.2012.24

Keown, P., Hayry, P., Mathew, T., Morris, P., Stiller, C., Barker, C., et al. (1996). A blinded, randomized clinical trial of mycophenolate mofetil for the prevention of acute rejection in cadaveric renal transplantation. The Tricontinental Mycophenolate Mofetil Renal Transplantation Study Group. *Transplantation* 61 (7), 1029–1037.

Khaeso, K., Udayachalerm, S., Komvilaisak, P., Chainansamit, S. O., Suwannaying, K., Laoaroon, N., et al. (2021). Meta-analysis of NUDT15 genetic Polymorphism on thiopurine-induced myelosuppression in asian Populations. *Front. Pharmacol.* 12, 784712. doi:10.3389/fphar.2021.784712

Kim, K. A., Joo, H. J., and Park, J. Y. (2011). Effect of ABCG2 genotypes on the pharmacokinetics of A771726, an active metabolite of prodrug leflunomide, and association of A771726 exposure with serum uric acid level. *Eur. J. Clin. Pharmacol.* 67 (2), 129–134. doi:10.1007/s00228-010-0916-0

Kiryluk, K., Li, Y., Moldoveanu, Z., Suzuki, H., Reily, C., Hou, P., et al. (2017). GWAS for serum galactose-deficient IgA1 implicates critical genes of the O-glycosylation pathway. *PLoS Genet.* 13 (2), e1006609. doi:10.1371/journal.pgen.1006609

Kis, E., Nagy, T., Jani, M., Molnár, E., Jánossy, J., Ujhellyi, O., et al. (2009). Leflunomide and its metabolite A771726 are high affinity substrates of BCRP:

implications for drug resistance. *Ann. Rheum. Dis.* 68 (7), 1201–1207. doi:10.1136/ard.2007.086264

Koetter, I. (2009). Pulse versus daily oral cyclophosphamide for induction of remission in antineutrophil cytoplasmic antibody-associated vasculitis (CYCLOPS study). *Z. Fur Rheumatol.* 68 (7), 575–577. doi:10.1007/s00393-009-0509-4

Koskela, M., Jahnukainen, T., Endén, K., Arikoski, P., Kataja, J., Nuutinen, M., et al. (2019). Methylprednisolone or cyclosporine a in the treatment of Henoch-Schönlein nephritis: a nationwide study. *Pediatr. Nephrol.* 34 (8), 1447–1456. doi:10.1007/s00467-019-04238-2

Kronbichler, A., Kerschbaum, J., and Mayer, G. (2015). The influence and role of microbial factors in autoimmune kidney Diseases: a systematic review. *J. Immunol. Res.* 2015, 1–13. doi:10.1155/2015/858027

Kuehl, P., Zhang, J., Lin, Y., Lamba, J., Assem, M., Schuetz, J., et al. (2001). Sequence diversity in CYP3A promoters and characterization of the genetic basis of polymorphic CYP3A5 expression. *Nat. Genet.* 27 (4), 383–391. doi:10.1038/86882

Kurt-Şükür, E. D., Sekar, T., and Tullus, K. (2021). Biopsy-proven Henoch-Schönlein purpura nephritis: a single center experience. *Pediatr. Nephrol.* 36 (5), 1207–1215. doi:10.1007/s00467-020-04809-8

Kuypers, D. R., Naesens, M., Vermeire, S., and Vanrenterghem, Y. (2005). The impact of uridine diphosphate-glucuronosyltransferase 1A9 (UGT1A9) gene promoter region single-nucleotide polymorphisms T-275A and C-2152T on early mycophenolic acid dose-interval exposure in de novo renal allograft recipients. *Clin. Pharmacol. Ther.* 78 (4), 351–361. doi:10.1016/j.clpt.2005.06.007

Lafayette, R. A., Canetta, P. A., Rovin, B. H., Appel, G. B., Novak, J., Nath, K. A., et al. (2017). A randomized, controlled trial of rituximab in IgA nephropathy with Proteinuria and renal Dysfunction. *J. Am. Soc. Nephrol.* 28 (4), 1306–1313. doi:10.1681/asn.2016060640

Lafayette, R. A., Rovin, B. H., Reich, H. N., Tumlin, J. A., Floege, J., and Barratt, J. (2020). Safety, tolerability and efficacy of narsoplimab, a novel MASP-2 inhibitor for the treatment of IgA nephropathy. *Kidney Int. Rep.* 5 (11), 2032–2041. doi:10.1016/j.ekir.2020.08.003

Lee, S., Yoo, J. I., and Kang, Y. J. (2022). Integrative analyses of genes related to femoral head osteonecrosis: an umbrella review of systematic reviews and meta-analyses of observational studies. *J. Orthop. Surg. Res.* 17 (1), 182. doi:10.1186/s13018-022-03079-4

Lensmeyer, G. L., Wiebe, D. A., and Carlson, I. H. (1988). Deposition of nine metabolites of cyclosporine in human tissues, bile, urine, and whole blood. *Transpl. Proc.* 20 (2 Suppl. 2), 614–622.

Lévesque, E., Benoit-Biancamano, M. O., Delage, R., Couture, F., and Guillemette, C. (2008). Pharmacokinetics of mycophenolate mofetil and its glucuronide metabolites in healthy volunteers. *Pharmacogenomics* 9 (7), 869–879. doi:10.2217/14622416.9.7.869

Lin, Y. S., Dowling, A. L., Quigley, S. D., Farin, F. M., Zhang, J., Lamba, J., et al. (2002). Co-regulation of CYP3A4 and CYP3A5 and contribution to hepatic and intestinal midazolam metabolism. *Mol. Pharmacol.* 62 (1), 162–172. doi:10.1124/mol.62.1.162

Liu, J., Wan, Z., Song, Q., Li, Z., He, Y., Tang, Y., et al. (2018). NR3C1 gene polymorphisms are associated with steroid resistance in patients with primary nephrotic syndrome. *Pharmacogenomics* 19 (1), 45–60. doi:10.2217/pgs-2017-0084

Liu, N., Ma, Z. Z., Yan, H. F., Li, Q., Lyu, X. Q., Kang, W. L., et al. (2019). Clinical effect of double filtration plasmapheresis combined with glucocorticoid and immunosuppressant in treatment of children with severe Henoch-Schönlein purpura nephritis. *Zhongguo Dang Dai Er Ke Za Zhi* 21 (10), 955–959.

Liu, X., Gao, C., Liu, X., and Gao, T. (2019). Efficacy and safety of tripterygium glycosides for graves ophthalmopathy: A systematic review and meta-analysis. *Med. Baltim.* 98 (50), e18242. doi:10.1097/md.0000000000018242

Lopez-Mejias, R., Genre, F., Pérez, B. S., Castañeda, S., Ortego-Centeno, N., Llorca, J., et al. (2015a). Association of HLA-B*41:02 with henoch-schönlein Purpura (IgA vasculitis) in Spanish individuals irrespective of the HLA-DRB1 status. *Arthritis Res. Ther.* 17, 102. doi:10.1186/s13075-015-0622-5

Lopez-Mejias, R., Genre, F., Pérez, B. S., Castañeda, S., Ortego-Centeno, N., Llorca, J., et al. (2015b). Brief report: Association of HLA-DRB1*01 with IgA vasculitis (Henoch-Schönlein). *Arthritis & Rheumatology* 67 (3), 823–827. doi:10.1002/art.38979

Lopez-Mejias, R., Carmona, F. D., Castañeda, S., Genre, F., Remuzgo-Martínez, S., Sevilla-Perez, B., et al. (2017). A genome-wide association study suggests the HLA class II region as the major susceptibility locus for IgA vasculitis. *Sci. Rep.* 7, 5088. doi:10.1038/s41598-017-03915-2

Lopez-Mejias, R., Castañeda, S., Genre, F., Remuzgo-Martínez, S., Carmona, F. D., Llorca, J., et al. (2018). Genetics of immunoglobulin-A vasculitis (Henoch-Schönlein purpura): An updated review. *Autoimmun. Rev.* 17 (3), 301–315. doi:10.1016/j.autrev.2017.11.024

Lou, T., Wang, C., Chen, Z., Shi, C., Tang, H., Liu, X., et al. (2006). Randomised controlled trial of leflunomide in the treatment of immunoglobulin A nephropathy. *Nephrol. Carlt.* 11 (2), 113–116. doi:10.1111/j.1440-1797.2006.00547.x

Low, S. K., Kiyotani, K., Mushiroda, T., Daigo, Y., Nakamura, Y., and Zembutsu, H. (2009). Association study of genetic polymorphism in ABCC4 with cyclophosphamide-induced adverse drug reactions in breast cancer patients. *J. Hum. Genet.* 54 (10), 564–571. doi:10.1038/jhg.2009.79

Marsh, S., King, C. R., Ahluwalia, R., and McLeod, H. L. (2004). Distribution of ITPA P32T alleles in multiple world populations. *J. Hum. Genet.* 49 (10), 579–581. doi:10.1007/s10038-004-0183-y

Martin, H., Sarsat, J. P., de Waziers, I., Housset, C., Balladur, P., Beaune, P., et al. (2003). Induction of cytochrome P450 2B6 and 3A4 expression by phenobarbital and cyclophosphamide in cultured human liver slices. *Pharm. Res.* 20 (4), 557–568. doi:10.1023/a:1023234429596

Mazidi, T., Rouini, M. R., Ghahremani, M. H., Dashti-Khavidaki, S., Lessan-Pezeshki, M., Ahmadi, F. L., et al. (2013). Impact of UGT1A9 Polymorphism on mycophenolic acid Pharmacokinetic Parameters in stable renal transplant Patients. *Iran. J. Pharm. Res.* 12 (3), 547–556.

Miao, Q., Yan, L., Zhou, Y., Li, Y., Zou, Y., Wang, L., et al. (2021). Association of genetic variants in TPMT, ITPA, and NUDT15 with azathioprine-induced myelosuppression in southwest China patients with autoimmune hepatitis. *Sci. Rep.* 11 (1), 7984. doi:10.1038/s41598-021-87095-0

Modena, V., Bianchi, G., and Roccatello, D. (2013). Cost-effectiveness of biologic treatment for rheumatoid arthritis in clinical practice: An achievable target? *Autoimmun. Rev.* 12 (8), 835–838. doi:10.1016/j.autrev.2012.11.009

Mougey, E. B., Chen, C., Tantisira, K. G., Blake, K. V., Peters, S. P., Wise, R. A., et al. (2013). Pharmacogenetics of asthma controller treatment. *Pharmacogenomics J.* 13 (3), 242–250. doi:10.1038/tpj.2012.5

Nagai, S., Horinouchi, T., Ninchoji, T., Kondo, A., Aoto, Y., Ishiko, S., et al. (2022). Use of renin-angiotensin system inhibitors as initial therapy in children with Henoch-Schönlein purpura nephritis of moderate severity. *Pediatr. Nephrol.* 37 (8), 1845–1853. doi:10.1007/s00467-021-05395-z

Nakajima, M., Komagata, S., Fujiki, Y., Kanada, Y., Ebi, H., Itoh, K., et al. (2007). Genetic polymorphisms of CYP2B6 affect the pharmacokinetics/pharmacodynamics of cyclophosphamide in Japanese cancer patients. *Pharmacogenet. Genomics* 17 (6), 431–445. doi:10.1097/FPC.0b013e328045c4fb

Namgoong, M. (2020). Management of IgA vasculitis nephritis (Henoch-Schonlein purpura nephritis) in Children. *Child. Kidney Dis.* 24 (1), 1–13. doi:10.3339/jkspn.2020.24.1.1

Narchi, H. (2005). Risk of long term renal impairment and duration of follow up recommended for henoch-schonlein purpura with normal or minimal urinary findings: a systematic review. *Arch. Dis. Child.* 90 (9), 916–920. doi:10.1136/adc.2005.074641

Natsumeda, Y., Ohno, S., Kawasaki, H., Konno, Y., Weber, G., and Suzuki, K. (1990). Two distinct cDNAs for human IMP dehydrogenase. *J. Biol. Chem.* 265 (9), 5292–5295. doi:10.1016/s0021-9258(19)34120-1

Ngamjanyaporn, P., Thakkinstian, A., Verasertniyom, O., Chatchaipun, P., Vanichapuntu, M., Nantiruj, K., et al. (2011). Pharmacogenetics of cyclophosphamide and CYP2C19 polymorphism in Thai systemic lupus erythematosus. *Rheumatol. Int.* 31 (9), 1215–1218. doi:10.1007/s00296-010-1420-7

Nicoara, O., and Twombley, K. (2019). Immunoglobulin A nephropathy and immunoglobulin A vasculitis. *Pediatr. Clin. North Am.* 66 (1), 101–110. doi:10.1016/j.pcl.2018.08.008

Ohara, S., Kawasaki, Y., Matsuura, H., Oikawa, T., Suyama, K., and Hosoya, M. (2011). Successful therapy with tonsillectomy for severe ISKDC grade VI Henoch-Schönlein purpura nephritis and persistent nephrotic syndrome. *Clin. Exp. Nephrol.* 15 (5), 749–753. doi:10.1007/s10157-011-0463-8

Ohara, S., Kawasaki, Y., Miyazaki, K., Ono, A., Suzuki, Y., Suyama, K., et al. (2013). Efficacy of cyclosporine A for steroid-resistant severe Henoch-Schönlein purpura nephritis. *Fukushima J. Med. Sci.* 59 (2), 102–107. doi:10.5387/fms.59.102

Oni, L., and Sampath, S. (2019). Childhood IgA vasculitis (henoch schonlein Purpura)-advances and knowledge gaps. *Front. Pediatr.* 7, 257. doi:10.3389/fped.2019.00257

Ort, M., Dingemanse, J., van den Anker, J., and Kaufmann, P. (2020). Treatment of rare inflammatory kidney Diseases: Drugs targeting the terminal complement Pathway. *Front. Immunol.* 11, 599417. doi:10.3389/fimmu.2020.599417

Ozen, S., Marks, S. D., Brogan, P., Groot, N., de Graeff, N., Avcin, T., et al. (2019). European consensus-based recommendations for diagnosis and treatment of immunoglobulin A vasculitis-the SHARE initiative. *Rheumatol. Oxf.* 58 (9), 1607–1616. doi:10.1093/rheumatology/kez041

Panek, M., Pietras, T., Fabijan, A., Zioło, J., Wieteska, Ł., Małachowska, B., et al. (2015). The NR3C1 glucocorticoid receptor gene Polymorphisms may modulate the TGF-beta mRNA expression in asthma Patients. *Inflammation* 38 (4), 1479–1492. doi:10.1007/s10753-015-0123-3

Park, J. M., Won, S. C., Shin, J. I., Yim, H., and Pai, K. S. (2011). Cyclosporin A therapy for Henoch-Schönlein nephritis with nephrotic-range proteinuria. *Pediatr. Nephrol.* 26 (3), 411–417. doi:10.1007/s00467-010-1723-7

Parvin, M. N., Aziz, M. A., Rabbi, S. N. I., Al-Mamun, M. M. A., Hanif, M., Islam, M. S., et al. (2021). Assessment of the link of ABCB1 and NR3C1 gene polymorphisms with the prednisolone resistance in pediatric nephrotic syndrome patients of Bangladesh: A genotype and haplotype approach. *J. Adv. Res.* 33, 141–151. doi:10.1016/j.jare.2021.02.001

Phan, K., Charlton, O., Baker, C., Foley, P., and Smith, S. D. (2021). Dermatologist attitudes toward ciclosporin use in atopic dermatitis. *J. Dermatol. Treat.* 32 (8), 922–924. doi:10.1080/09546634.2020.1724251

Picard, N., Ratanasavanh, D., Prémaud, A., Le Meur, Y., and Marquet, P. (2005). Identification of the UDP-glucuronosyltransferase isoforms involved in mycophenolic acid phase II metabolism. *Drug Metab. Dispos.* 33 (1), 139–146. doi:10.1124/dmd.104.001651

Pindi Sala, T., Michot, J. M., Snanoudj, R., Dollat, M., Estève, E., Marie, B., et al. (2014). Successful outcome of a corticodependent henoch-schönlein purpura adult with rituximab. *Case Rep. Med.* 2014, 619218. doi:10.1155/2014/619218

Piram, M., Maldini, C., Biscardi, S., De Suremain, N., Orzechowski, C., Georget, E., et al. (2017). Incidence of IgA vasculitis in children estimated by four-source capture-recapture analysis: a population-based study. *Rheumatol. Oxf.* 56 (8), 1358–1366. doi:10.1093/rheumatology/kex158

Prandota, J., Pankow-Prandota, L., and Kotecki, L. (2001). Impaired activation of the fibrinolytic system in children with henoch-schönlein purpura: Beneficial effect of hydrocortisone plus sigma-aminocaproic acid therapy on disappearance rate of cutaneous vasculitis and fibrinolysis. *Am. J. Ther.* 8 (1), 11–19. doi:10.1097/00045391-200101000-00004

Qin, W., Du, Z., Xiao, J., Duan, H., Shu, Q., and Li, H. (2020). Evaluation of clinical impact of pharmacogenomics knowledge involved in CPIC guidelines on Chinese pediatric patients. *Pharmacogenomics* 21 (3), 209–219. doi:10.2217/pgs-2019-0153

Radhakrishnan, J., and Cattran, D. C. (2012). The KDIGO practice guideline on glomerulonephritis: reading between the (guide)lines--application to the individual patient. *Kidney Int.* 82 (8), 840–856. doi:10.1038/ki.2012.280

Relling, M. V., Gardner, E. E., Sandborn, W. J., Schmiegelow, K., Pui, C. H., Yee, S. W., et al. (2011). Clinical Pharmacogenetics Implementation Consortium guidelines for thiopurine methyltransferase genotype and thiopurine dosing. *Clin. Pharmacol. Ther.* 89 (6), 387–391. doi:10.1038/clpt.2011.15210.1038/clpt.2010.320

Relling, M. V., Gardner, E. E., Sandborn, W. J., Schmiegelow, K., Pui, C.-H., Yee, S. W., et al. (2013). Clinical Pharmacogenetics implementation Consortium guidelines for thiopurine methyltransferase genotype and thiopurine Dosing: 2013 update. *Clin. Pharmacol. Ther.* 93 (4), 324–325. doi:10.1038/clpt.2013.4

Relling, M. V., Schwab, M., Whirl-Carrillo, M., Suarez-Kurtz, G., Pui, C. H., Stein, C. M., et al. (2019). Clinical Pharmacogenetics implementation Consortium guideline for thiopurine Dosing based on TPMT and NUDT15 genotypes: 2018 update. *Clin. Pharmacol. Ther.* 105 (5), 1095–1105. doi:10.1002/cpt.1304

Rocha, V., Porcher, R., Fernandes, J. F., Filion, A., Bittencourt, H., Silva, W., Jr., et al. (2009). Association of drug metabolism gene polymorphisms with toxicities, graft-versus-host disease and survival after HLA-identical sibling hematopoietic stem cell transplantation for patients with leukemia. *Leukemia* 23 (3), 545–556. doi:10.1038/leu.2008.323

Rojas, L., Neumann, I., Herrero, M. J., Bosó, V., Reig, J., Poveda, J. L., et al. (2015). Effect of CYP3A5*3 on kidney transplant recipients treated with tacrolimus: a systematic review and meta-analysis of observational studies. *Pharmacogenomics J.* 15 (1), 38–48. doi:10.1038/tpj.2014.38

Ronkainen, J., Autio-Harmainen, H., and Nuutinen, M. (2003). Cyclosporin A for the treatment of severe Henoch-Schönlein glomerulonephritis. *Pediatr. Nephrol.* 18 (11), 1138–1142. doi:10.1007/s00467-003-1245-7

Rovin, B. H., Adler, S. G., Barratt, J., Bridoux, F., Burdge, K. A., Chan, T. M., et al. (2021). Executive summary of the KDIGO 2021 guideline for the management of glomerular Diseases. *Kidney Int.* 100 (4), 753–779. doi:10.1016/j.kint.2021.05.015

Roy, P., Yu, L. J., Crespi, C. L., and Waxman, D. J. (1999). Development of a substrate-activity based approach to identify the major human liver P-450 catalysts of cyclophosphamide and ifosfamide activation based on cDNA-expressed activities and liver microsomal P-450 profiles. *Drug Metab. Dispos.* 27 (6), 655–666.

Rozman, B. (2002). Clinical pharmacokinetics of leflunomide. *Clin. Pharmacokinet.* 41 (6), 421–430. doi:10.2165/00003088-200241060-00003

Safan, M. A., Elhelbawy, N. G., Midan, D. A., and Khader, H. F. (2017). ABCB1 polymorphisms and steroid treatment in children with idiopathic nephrotic syndrome. *Br. J. Biomed. Sci.* 74 (1), 36–41. doi:10.1080/09674845.2016.1220707

Schaeffeler, E., Fischer, C., Brockmeier, D., Wernet, D., Moerike, K., Eichelbaum, M., et al. (2004). Comprehensive analysis of thiopurine S-methyltransferase phenotype-genotype correlation in a large population of German-Caucasians and identification of novel TPMT variants. *Pharmacogenetics* 14 (7), 407–417. doi:10.1097/01.fpc.0000114745.08559.db

Schirmer, J. H., Bremer, J. P., Moosig, F., Holle, J. U., Lamprecht, P., Wieczorek, S., et al. (2016). Cyclophosphamide treatment-induced leukopenia rates in ANCA-associated vasculitis are influenced by variant CYP450 2C9 genotypes. *Pharmacogenomics* 17 (4), 367–374. doi:10.2217/pgs.15.176

Selvaskandan, H., Cheung, C. K., Muto, M., and Barratt, J. (2019). New strategies and perspectives on managing IgA nephropathy. *Clin. Exp. Nephrol.* 23 (5), 577–588. doi:10.1007/s10157-019-01700-1

Shah, S., Harwood, S. M., Döhler, B., Opelz, G., and Yaqoob, M. M. (2012). Inosine monophosphate Dehydrogenase Polymorphisms and renal allograft outcome. *Transplantation* 94 (5), 486–491. doi:10.1097/TP.0b013e31825b7654

Sharma, S. K., Jain, S., Bahl, P., Potturi, P., Rathi, M., Naidu, S., et al. (2020). Ovarian dysfunction with moderate-dose intravenous cyclophosphamide (modified NIH regimen) and mycophenolate mofetil in young adults with severe lupus: a prospective cohort study. *Arthritis Res. Ther.* 22 (1), 189. doi:10.1186/s13075-020-02292-y

Shin, J. I., Park, J. M., Shin, Y. H., Lee, J. S., and Jeong, H. J. (2005). Role of mesangial fibrinogen deposition in the pathogenesis of crescentic Henoch-Schonlein nephritis in children. *J. Clin. Pathol.* 58 (11), 1147–1151. doi:10.1136/jcp.2005.027409

Siemasko, K. F., Chong, A. S., Williams, J. W., Bremer, E. G., and Finnegan, A. (1996). Regulation of B cell function by the immunosuppressive agent leflunomide. *Transplantation* 61 (4), 635–642. doi:10.1097/00007890-199602270-00020

Simone, P. D., Pavlov, Y. I., and Borgstahl, G. E. (2013). ITPA (inosine triphosphate pyrophosphatase): From surveillance of nucleotide pools to human disease and pharmacogenetics. *Mutat. Res.* 753 (2), 131–146. doi:10.1016/j.mrrev.2013.08.001

Singh, G., Saxena, N., Aggarwal, A., and Misra, R. (2007). Cytochrome P450 polymorphism as a predictor of ovarian toxicity to pulse cyclophosphamide in systemic lupus erythematosus. *J. Rheumatol.* 34 (4), 731–733. doi:10.1016/S0973-3698(10)60212-9

Sinha, R., Agrawal, N., Xue, Y., Chanchlani, R., Pradhan, S., Raina, R., et al. (2021). Use of rituximab in paediatric nephrology. *Arch. Dis. Child.* 106 (11), 1058–1065. doi:10.1136/archdischild-2020-321211

Sobhan, M. R., Mahdinezhad-Yazdi, M., Moghimi, M., Aghili, K., Jafari, M., Zare-Shehneh, M., et al. (2018). Plasminogen activator inhibitor-1 4G/5G Polymorphism contributes to osteonecrosis of the femoral head susceptibility: Evidence from a systematic review and meta-analysis. *Arch. Bone Jt. Surg.* 6 (6), 468–477.

Sombogaard, F., van Schaik, R. H., Mathot, R. A., Budde, K., van der Werf, M., Vulto, A. G., et al. (2009). Interpatient variability in IMPDH activity in MMF-treated renal transplant patients is correlated with IMPDH type II 3757T > C polymorphism. *Pharmacogenet Genomics* 19 (8), 626–634. doi:10.1097/FPC.0b013e32832f5f1b

Steponaitiene, R., Kupcinskas, J., Survilaite, S., Varkalaite, G., Jonaitis, L., Kiudelis, G., et al. (2016). TPMT and ITPA genetic variants in Lithuanian inflammatory bowel disease patients: Prevalence and azathioprine-related side effects. *Adv. Med. Sci.* 61 (1), 135–140. doi:10.1016/j.advms.2015.09.008

Subspecialty Group of Renal Diseases; Chinese Medical Association (2017). Evidence-based guideline for diagnosis and treatment of Henoch-Schonlein purpura nephritis (2016). *Zhonghua Er Ke Za Zhi* 55 (9), 647–651. doi:10.3760/cma.j.issn.0578-1310.2017.09.003

Takada, K., Arefayene, M., Desta, Z., Yarboro, C. H., Boumpas, D. T., Balow, J. E., et al. (2004). Cytochrome P450 pharmacogenetics as a predictor of toxicity and clinical response to pulse cyclophosphamide in lupus nephritis. *Arthritis Rheum.* 50 (7), 2202–2210. doi:10.1002/art.20338

Tan, J., Tang, Y., Zhong, Z., Yan, S., Tan, L., Tarun, P., et al. (2019). The efficacy and safety of immunosuppressive agents plus steroids compared with steroids alone in the treatment of henoch-schönlein purpura nephritis: A meta-analysis. *Int. Urol. Nephrol.* 51 (6), 975–985. doi:10.1007/s11255-019-02092-7

Tantisira, K. G., Lasky-Su, J., Harada, M., Murphy, A., Litonjua, A. A., Himes, B. E., et al. (2011). Genomewide association between GLCCI1 and response to glucocorticoid therapy in asthma. *N. Engl. J. Med.* 365 (13), 1173–1183. doi:10.1056/NEJMoa0911353

Tatarunas, V., Jankauskiene, L., Kupstyte, N., Skipskis, V., Gustiene, O., Grybauskas, P., et al. (2014). The role of clinical parameters and of CYP2C19 G681 and CYP4F2 G1347A polymorphisms on platelet reactivity during dual antiplatelet therapy. *Blood Coagul. Fibrinolysis* 25 (4), 369–374. doi:10.1097/mbc.0000000000000053

Timm, R., Kaiser, R., Lötsch, J., Heider, U., Sezer, O., Weisz, K., et al. (2005). Association of cyclophosphamide pharmacokinetics to polymorphic cytochrome P450 2C19. *Pharmacogenomics J.* 5 (6), 365–373. doi:10.1038/sj.tpj.6500330

Tipping, P. G., Thomson, N. M., and Holdsworth, S. R. (1986). A comparison of fibrinolytic and defibrinating agents in established experimental glomerulonephritis. *Br. J. Exp. Pathol.* 67 (4), 481–491.

Umeda, C., Fujinaga, S., Endo, A., Sakuraya, K., Asanuma, S., and Hirano, D. (2020). Preventive effect of tonsillectomy on recurrence of henoch-schönlein Purpura nephritis after intravenous methylprednisolone Pulse therapy. *Tohoku J. Exp. Med.* 250 (1), 61–69. doi:10.1620/tjem.250.61

Uppugunduri, C. R., Rezgui, M. A., Diaz, P. H., Tyagi, A. K., Rousseau, J., Daali, Y., et al. (2014). The association of cytochrome P450 genetic polymorphisms with sulfolane formation and the efficacy of a busulfan-based conditioning regimen in pediatric patients undergoing hematopoietic stem cell transplantation. *Pharmacogenomics J.* 14 (3), 263–271. doi:10.1038/tpj.2013.38

Van Schaik, R. H., Van Der Heiden, I. P., Van Den Anker, J. N., and Lindemans, J. (2002). CYP3A5 variant allele frequencies in Dutch Caucasians. *Clin. Chem.* 48 (10), 1668–1671. doi:10.1093/clinchem/48.10.1668

Wang, D., and Sadee, W. (2016). CYP3A4 intronic SNP rs35599367 (CYP3A4*22) alters RNA splicing. *Pharmacogenet Genomics* 26 (1), 40–43. doi:10.1097/fpc.0000000000000183

Wang, T.-S., Chiu, H.-Y., Wu, L. S.-H., Chu, C.-Y., and Tsai, T.-F. (2014). Correlation of thiopurine methyltransferase and inosine triphosphate pyrophosphatase polymorphisms and adverse effects induced by azathioprine treatment in Taiwanese dermatology patients. *Dermatol. Sin.* 32 (1), 13–18. doi:10.1016/j.dsi.2013.07.001

Wang, J. X., Liu, C. F., Li, Y. Q., Su, X. H., Liu, L. L., Tian, Y. G., et al. (2019). Effect of tripterygium glycosides tablets on synovial angiogenesis in rats with type Ⅱ collagen induced arthritis. *Zhongguo Zhong Yao Za Zhi* 44 (16), 3441–3447. doi:10.19540/j.cnki.cjcmm.20190625.401

Wang, L., Zeng, G., Li, J., Luo, J., Li, H., and Zhang, Z. (2021). Association of polymorphism of CYP3A4, ABCB1, ABCC2, ABCG2, NFKB1, POR, and PXR with the concentration of cyclosporin A in allogeneic haematopoietic stem cell transplantation recipients. *Xenobiotica* 51 (7), 852–858. doi:10.1080/00498254.2021.1928791

Wierciński, R., Zoch-Zwierz, W., Wasilewska, A., Tomaszewska, B., Winiecka, W., Stasiak-Barmuta, A., et al. (2001). Lymphocyte subpopulations of peripheral blood in children with Schönlein-Henoch purpura and IgA nephropathy. *Pol. Merkur Lek.* 10 (58), 244–246.

Woillard, J. B., Chouchana, L., Picard, N., Loriot, M. A., and French Network, P. (2017). Pharmacogenetics of immunosuppressants: State of the art and clinical implementation - recommendations from the French National Network of Pharmacogenetics (RNPGx). *Therapie* 72 (2), 285–299. doi:10.1016/j.therap.2016.09.016

Wu, D., Ma, R., Wang, X., and Yang, Y. (2022). Efficacy and safety of tacrolimus in the treatment of Pediatric henoch-schönlein Purpura nephritis. *Paediatr. Drugs* 24 (4), 389–401. doi:10.1007/s40272-022-00506-1

Xie, H., Griskevicius, L., Ståhle, L., Hassan, Z., Yasar, U., Rane, A., et al. (2006). Pharmacogenetics of cyclophosphamide in patients with hematological malignancies. *Eur. J. Pharm. Sci.* 27 (1), 54–61. doi:10.1016/j.ejps.2005.08.008

Yang, D., He, L., Peng, X., Liu, H., Peng, Y., Yuan, S., et al. (2016). The efficacy of tonsillectomy on clinical remission and relapse in patients with IgA nephropathy: a randomized controlled trial. *Ren. Fail* 38 (2), 242–248. doi:10.3109/0886022x.2015.1128251

Yang, L., Yan, C., Zhang, F., Jiang, B., Gao, S., Liang, Y., et al. (2018). Effects of ketoconazole on cyclophosphamide metabolism: evaluation of CYP3A4 inhibition effect using the *in vitro* and *in vivo* models. *Exp. Anim.* 67 (1), 71–82. doi:10.1538/expanim.17-0048

Yang, C. L., Sheng, C. C., Liao, G. Y., Su, Y., Feng, L. J., Xia, Q., et al. (2021). Genetic polymorphisms in metabolic enzymes and transporters have no impact on mycophenolic acid pharmacokinetics in adult kidney transplant patients co-treated with tacrolimus: A population analysis. *J. Clin. Pharm. Ther.* 46 (6), 1564–1575. doi:10.1111/jcpt.13488

Yates, C. R., Krynetski, E. Y., Loennechen, T., Fessing, M. Y., Tai, H. L., Pui, C. H., et al. (1997). Molecular diagnosis of thiopurine S-methyltransferase deficiency: Genetic basis for azathioprine and mercaptopurine intolerance. *Ann. Intern Med.* 126 (8), 608–14. doi:10.7326/0003-4819-126-8-199704150-00003

Ye, J. W., Ding, J., Huang, J. P., Chen, Y., Yao, Y., Xiao, H. J., et al. (2003). Analysis on association of glucocorticoid receptor gene polymorphism with steroid-resistance in idiopathic nephrotic syndrome of children. *Zhonghua Er Ke Za Zhi* 41 (9), 661–665.

Yokota, S. (2002). Mizoribine: Mode of action and effects in clinical use. *Pediatr. Int.* 44 (2), 196–198. doi:10.1046/j.1328-8067.2002.01536.x

Zhang, Q., Shi, S. F., Zhu, L., Lv, J. C., Liu, L. J., Chen, Y. Q., et al. (2012). Tacrolimus improves the Proteinuria remission in Patients with refractory IgA nephropathy. *Am. J. Nephrol.* 35 (4), 312–320. doi:10.1159/000337175

Zhang, Y., Xie, H., Zhao, D., Wang, B., Yang, L., and Meng, Q. (2017). Association of ABCB1 C3435T polymorphism with the susceptibility to osteonecrosis of the femoral head: A meta-analysis. *Med. Baltim.* 96 (20), e6049. doi:10.1097/md.0000000000006049

Zhang, D. F., Hao, G. X., Li, C. Z., Yang, Y. J., Liu, F. J., Liu, L., et al. (2018). Off-label use of tacrolimus in children with henoch-schönlein purpura nephritis: a pilot study. *Arch. Dis. Child.* 103 (8), 772–775. doi:10.1136/archdischild-2017-313788

Zhang, H., Li, X., Xu, H., Ran, F., and Zhao, G. (2021). Effect and safety evaluation of tacrolimus and tripterygium glycosides combined therapy in treatment of Henoch-Schönlein purpura nephritis. *Int. J. Urol.* 28 (11), 1157–1163. doi:10.1111/iju.14665

Zhang, X. F., Liu, J., Ye, F., Ji, S. G., Zhang, N., Cao, R. S., et al. (2014). Effects of triptolide on the pharmacokinetics of cyclophosphamide in rats: a possible role of cytochrome P3A4 inhibition. *Chin. J. Integr. Med.* 20 (7), 534–539. doi:10.1007/s11655-014-1710-0

Zhang, Y., Gao, Y., Zhang, Z., Liu, G., He, H., and Liu, L. (2014). Leflunomide in addition to steroids improves proteinuria and renal function in adult Henoch-Schoenlein nephritis with nephrotic proteinuria. *Nephrol. Carlt.* 19 (2), 94–100. doi:10.1111/nep.12175

Zheng, S., Tasnif, Y., Hebert, M. F., Davis, C. L., Shitara, Y., Calamia, J. C., et al. (2013). CYP3A5 gene variation influences cyclosporine A metabolite formation and renal cyclosporine Disposition. *Transplantation* 95 (6), 821–827. doi:10.1097/TP.0b013e31827e6ad9

Zhou, Z. C., Gu, S. Z., Wu, J., and Liang, Q. W. (2015). VEGF, eNOS, and ABCB1 genetic polymorphisms may increase the risk of osteonecrosis of the femoral head. *Genet. Mol. Res.* 14 (4), 13688–13698. doi:10.4238/2015.October.28.31

Zipfel, P. F., Wiech, T., Rudnick, R., Afonso, S., Person, F., and Skerka, C. (2019). Complement inhibitors in clinical trials for glomerular Diseases. *Front. Immunol.* 10, 2166. doi:10.3389/fimmu.2019.02166

frontiers | Frontiers in Medicine

TYPE Original Research
PUBLISHED 11 August 2022
DOI 10.3389/fmed.2022.941468

OPEN ACCESS

EDITED BY
Jian Wang,
Shanghai Children's Medical Center, China

REVIEWED BY
Augusto Rojas-Martinez,
Escuela de Medicina y Ciencias de la Salud TecSalud del Tecnológico de Monterrey, Mexico
Raquel Cruz Guerrero,
Centro de Investigación Biomédica en Red de Enfermedades Raras (CIBERER), Spain

*CORRESPONDENCE
Xuejun Zhang
zhang-x-j04@163.com
Chanjuan Hao
hchjhchj@163.com

†These authors have contributed equally to this work and share first authorship

SPECIALTY SECTION
This article was submitted to Precision Medicine, a section of the journal Frontiers in Medicine

RECEIVED 11 May 2022
ACCEPTED 14 July 2022
PUBLISHED 11 August 2022

CITATION
Zhang W, Yao Z, Guo R, Li H, Zhao S, Li W, Zhang X and Hao C (2022) Molecular identification of T-box transcription factor 6 and prognostic assessment in patients with congenital scoliosis: A single-center study. *Front. Med.* 9:941468. doi: 10.3389/fmed.2022.941468

Molecular identification of T-box transcription factor 6 and prognostic assessment in patients with congenital scoliosis: A single-center study

Wenyan Zhang[1,2†], Ziming Yao[3†], Ruolan Guo[1,2,4], Haichong Li[3], Shuang Zhao[1,2], Wei Li[1,2,4], Xuejun Zhang[3*] and Chanjuan Hao[1,2,4*]

[1]Beijing Key Laboratory for Genetics of Birth Defects, Beijing Pediatric Research Institute, Beijing, China, [2]Ministry of Education of the People's Republic of China (MOE) Key Laboratory of Major Diseases in Children, National Center for Children's Health, Beijing Children's Hospital, Capital Medical University, Beijing, China, [3]Department of Orthopedics, National Center for Children's Health, Beijing Children's Hospital, Capital Medical University, Beijing, China, [4]Henan Key Laboratory of Pediatric Inherited and Metabolic Diseases, Henan Children's Hospital, Zhengzhou Hospital of Beijing Children's Hospital, Zhengzhou, China

Background: Congenital scoliosis (CS) is characterized by vertebral malformations. The precise etiology of CS is not fully defined. A compound inheritance of *TBX6* was identified in 10% of patients with CS in Han Chinese and formed a distinguishable subtype named *TBX6*-associated congenital scoliosis (TACS).

Methods: To investigate the variants and risk haplotype of *TBX6*, we recruited 121 patients with CS at Beijing Children's Hospital. We collected the clinical characteristics and surgical treatment options and followed their postoperative prognoses.

Results: Eight patients (6.6%) were molecularly diagnosed with TACS and carried the previously defined pathogenic *TBX6* compound heterozygous variants. All the eight patients with TACS had the typical TACS clinical feature of hemivertebrae in the lower part of the spine. These patients received posterior hemivertebra resection combined with segmental fusion. Follow-ups revealed satisfactory correction without postoperative complications.

Conclusion: We observed a 6.6% prevalence of TACS in our CS cohort. Follow-ups further highlighted that surgical treatment of hemivertebra resection combined with segmental fusion performed well with prognosis for patients with TACS. This could provide valuable information for CS individuals with compound heterozygosity in *TBX6*.

KEYWORDS

congenital scoliosis (CS), T-box transcription factor 6 (*TBX6*), surgical treatment, prognosis, rare disease

Introduction

With an incidence rate of 0.5–1/1,000 of live births, congenital scoliosis (CS) is the most frequent congenital deformity of the spine that causes birth defects (1,2). CS is caused by vertebral deformities including defects of formation or segmentation, or a combination of both. Patients present unbalanced body axis growth and curvature of the spine, and scoliosis progresses rapidly with the patient's growth. Because of progressive scoliosis and secondary thoracic insufficiency caused by rib deformity, the patient quality of life is considerably compromised. Thus, most patients require more than one timely and effective treatment to correct scoliosis and avoid limitations of lung function (3).

Genetic studies have identified a series of genes, including Notch signaling pathway genes, genes encoding enzymes that regulate vertebral metabolism, ion channel genes, and ciliopathy-associated genes, associated with vertebral malformations and CS (4). Among these genes, T-box transcription factor 6 (*TBX6*), involved in activating the expression of HES family bHLH transcription factor 7 (*HES7*), mesoderm posterior basic helix-loop-helix transcription factor 2 (*MESP2*), and RIPPLY transcriptional repressor 2 (*RIPPLY2*) and regulating the cyclical activation of Notch signaling (5–10), has been identified as an essential regulator in the development of somites (11). Deleterious homozygote or compound heterozygote mutations in the *TBX6* gene could lead to spondylocostal dysostosis 5 [online mendelian inheritance in man (OMIM) 122600] (12–14) (**Supplementary Table 1**). Patients with *TBX6*-related spondylocostal dysostosis 5 present with rib deformities and a short trunk, which is caused by extensive vertebral deformities such as hemivertebrae, butterfly vertebrae, and vertebral fusion (12–14). A CS cohort study in Han Chinese showed that the compound inheritance of *TBX6* included a rare null mutation and a common risk haplotype T-C-A (composed of the three single-nucleotide polymorphisms, namely, rs2289292, rs3809624, and rs3809627) could lead to *TBX6*-associated congenital scoliosis (TACS), which accounted for 10% of patients with CS in this cohort (15). Patients with TACS presented with hemivertebrae in the lower half of the spine with or without mild rib deformities. The TACScore scoring system was developed to evaluate the likelihood of TACS (16). Subsequent studies in Japanese and European populations revealed similar inheritance patterns, population frequency, and clinical features of TACS (13,17). In contrast, the frequency of TACS in Hong Kong and Texas, United States was as low as 4.5% (18,19). However, published studies have mainly focused on adolescent patients (15,19), while those patients who present in childhood and receive effective surgical treatment are rarely studied. Moreover, the surgical treatment of patients with TACS has not been systematically reported and patient prognosis has not been followed.

In this study, we enrolled 121 patients with CS who visited Beijing Children's Hospital for surgical treatment and genetic counseling. In the single-center cohort, eight (6.6%) patients were genetically diagnosed with TACS. We collected information on clinical manifestations and postoperative prognoses during follow-up. All the patients with TACS had one or more malformed vertebrae in the lower part of the spine and consented to posterior hemivertebra resection combined with segmental fusion surgery, which effectively corrected scoliosis in patients with TACS with a mean correction rate of 90.84% and no feedback about complications. This finding could provide valuable information to guide clinical genetic counseling and the identification of treatment options, and provide further assurance to patients with TACS and their families.

Materials and methods

Ethical compliance

The study was approved by the Institutional Medical Ethics Committee of Beijing Children's Hospital, Capital Medical University (Approval No. 2015-26). All the patients or legal guardians provided written informed consent for this study.

Subjects

We enrolled patients that were diagnosed with CS by at least two independent surgeons in the Department of Orthopedics of Beijing Children's Hospital from January 2019 to December 2021. Patients were referred to the Orthopedics Department for surgical and genetic consults. A panel of trained physicians and geneticists at Beijing Children's Hospital assessed patients for genomic testing. We collected peripheral blood samples of patients and their parents, documented surgical treatment, and followed prognoses until January 2022. Images, including CT, X-ray, and MRI, were collected before and after surgery to evaluate prognosis. The Cobb angle was measured using Surgimap version 2.3.2.1 software (Nemaris Incorporation, New York, United States). TACScore was calculated as previously described (16). The correction rate was calculated using the following equation.

$$\text{Correction rate} = \frac{\text{Cobb angle before surgery} - \text{Cobb angle in latest follow} - \text{up}}{\text{Cobb angle before surgery}} \times 100\%$$

Exome sequencing

Deoxyribonucleic acid was isolated from peripheral blood samples obtained from probands and their parents using the Gentra Puregene Blood Kit (Qiagen, Hilden, Germany). A total of 200 ng genomic DNA from each individual was sheared using Biorupter (Diagenode, Liège, Belgium) to acquire 150–200 bp fragments. The ends of the DNA fragment were

repaired and Illumina Adaptors (Agilent Technologies, Santa Clara, United States) were added. After the sequencing library was constructed, the whole exome was captured using the SureSelect Human All Exon Kit (Agilent Technologies, Santa Clara, United States) and sequenced on Illumina NovaSeq 6000 (Illumina, San Diego, United States) with 150 base paired-end reads. Raw reads were filtered to remove low-quality reads using FastQC. Exome sequencing (ES) resulted in over 12 Gb of clean data. The average sequencing depth was greater than 100 X. Clean reads were mapped to the reference genome sequence Genome Reference Consortium Human Build 37 (GRCh37)/hg19 using Burrows–Wheeler Aligner and bam files were created using Picard. The Genome Analysis Toolkit software was used to perform variant calling (**Figure 1**).

Variant analysis and copy number variation calling based on exome sequencing data

Single-nucleotide variants (SNVs) were annotated and filtered using TGex.[1] Variants with a frequency of over 1% in the Genome Aggregation Database (gnomAD), NHLBI Exome Sequencing Project (ESP), or 1,000 G databases were excluded. Variants that lacked segregation in family members were also filtered. The main disease reference databases were Human Gene Mutation Database (HGMD) Professional, ClinVar, OMIM, and MalaCards. The pathogenicity of the missense variants found in patients was evaluated using the following bioinformatics tools: PolyPhen-2 (version 2.2.2),[2] protein variation effect analyzer (PROVEAN) (version 1.03),[3] MutationTaster,[4] and VarCards[5] (20). Variants were classified following the interpretation standards and guidelines of the American College of Medical Genetics and Genomics and the Association for Molecular Pathology (21). Putative pathogenic variants detected by next-generation sequencing were confirmed by Sanger sequencing. eXome-Hidden Markov Model (XHMM) software was used to detect copy number variations (CNVs) based on ES data (22) (**Figure 1**).

Copy number variation sequencing

To confirm CNVs, part of the library without capture was sequenced directly onto Illumina NovaSeq 6000; each sample yielded 1 Gb of raw data (QC: average read length: > 0.3 × Whole-genome sequencing). An in-house pipeline was applied to map and call CNVs based on CNV sequencing software. Clean reads were mapped to the reference genome GRCh37/hg19. CNVs called from parental low-depth whole-genome sequencing data were used as controls. The following were excluded: (1) CNVs reported in multiple peer-reviewed publications as benign or likely benign; (2) CNVs annotated in curated databases as benign or likely benign; (3) CNVs observed frequently in the general population; and (4) CNVs that did not cover the coding regions of genes. The Database of Genomic Variants (DGVs), the DECIPHER database, ClinVar, OMIM, and ClinGen were used for the interpretation and classification of the clinical significance of candidate CNVs according to previously reported guidelines (23,24) (**Figure 1**).

T-box transcription factor 6 T-C-A haplotype sequencing

Previously isolated DNA from patients and their parents was used for T-C-A haplotype sequencing, a technique first defined by Wu et al. (15). Among the three common single nucleotide polymorphisms (SNPs), C (rs3809624) and A (rs3809627) are located at the 5' untranslated region and are close to one another (i.e., at a distance of 358 nt). In contrast, T (rs2289292) is located at the eighth exon of *TBX6*. Thus, we designed the amplifying and Sanger sequencing primers for C-A and T, respectively (**Supplementary Table 2** and **Figure 1**).

Statistical analysis

The Cobb angles were measured before and after surgery. Correction rates of patients were analyzed using SPSS version 20.0 software (IBM Incorporation, New York, United States). Graphs were drawn using Microsoft Excel (Microsoft Corporation, Washington, United States) and GraphPad Prism 8 (GraphPad Software, San Diego, United States).

Results

Demographics and clinical characteristics

We enrolled a total of 121 Chinese patients with CS nationwide (male:female = 57:64) (**Figures 2A,B**). Over 86% of patients were diagnosed with CS before the age of 5 years (**Figure 2C**). The spinal deformities of 121 patients originated from a vertebral formation defect and involved the entire spine, although T6–T10 were mostly affected (**Figure 2D**).

1 https://fa.shanyint.com
2 http://genetics.bwh.harvard.edu/pph2/
3 http://provean.jcvi.org/
4 http://www.mutationtaster.org/
5 http://varcards.biols.ac.cn/

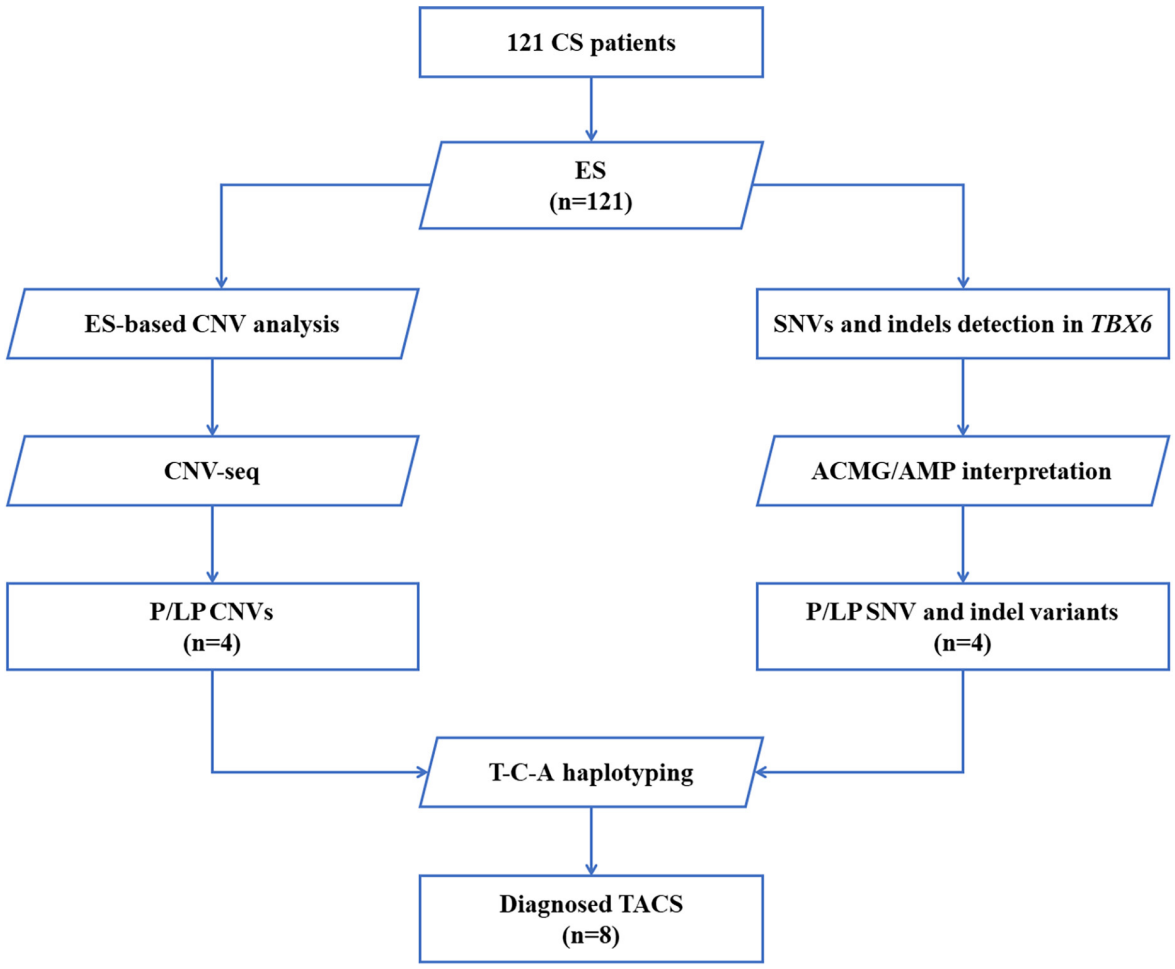

FIGURE 1
Flow diagram of patients with CS who were enrolled and received genetic testing. A total of 121 patients were recruited, and exome sequencing was performed. SNVs and indels in *TBX6* were evaluated by American College of Medical Genetics and Genomics (ACMG)/Association for Molecular Pathology (AMP) guidelines. CNVs were first analyzed based on ES data, further confirmed by CNV-seq, and classified by reported guidelines. The DNA of patients with pathogenic/likely pathogenic *TBX6* variants (right branch) or *TBX6*-involving CNVs (left branch) was amplified and sequenced to verify their T-C-A haplotypes. CS, congenital scoliosis; ES, exome sequencing; SNV, single nucleotide variation; indel, inversion and deletion; CNVs, copy number variations; ACMG/AMP interpretation, American College of Medical Genetics and Genomics and the Association for Molecular Pathology interpretation standards and guidelines; P, pathogenic; LP, likely pathogenic; T-C-A, rs2289292 (C > T) - rs3809624 (T > C) - rs3809627 (C > A); TACS, *TBX6*-associated congenital scoliosis.

Exome sequencing findings of T-box transcription factor 6

Exome sequencing was applied to all the patients and revealed one missense variant (Patient 1: c.745G > A/p.Val249Met), one nonsense variant (Patient 8: c.903T > G/p.Tyr301*), and two frameshift variants (Patient 6: c.271dupG/p.Val91fs × 79; Patient 7: c.1115_1130dupAGGCTCCAGACTCCGG/p.Arg378fs × 66) of *TBX6* (Table 1). All the four variants were not recorded in the gnomAD, ExAC, or 1,000 G databases, indicating that the population frequencies of these variants were extremely low. *In silico* analyses indicated that the unreported *TBX6* missense variant from patient 1 was deleterious (Supplementary Table 3). Thus, all the four variants were pathogenic mimicking a 16p11.2 microdeletion.

Copy number variation analysis of T-box transcription factor 6

Copy number variation calling based on ES data suggested that four of the 121 patients with CS (patients 2–5) had a heterozygous deletion of the 16p11.2 region. Further CNV sequencing tests confirmed the deletions. Patients 2–5 consistently carried 0.52–0.56 Mb of heterozygous deletions of *TBX6* and all the deleted regions covered the entire *TBX6* gene (Table 1 and Supplementary Figure 1).

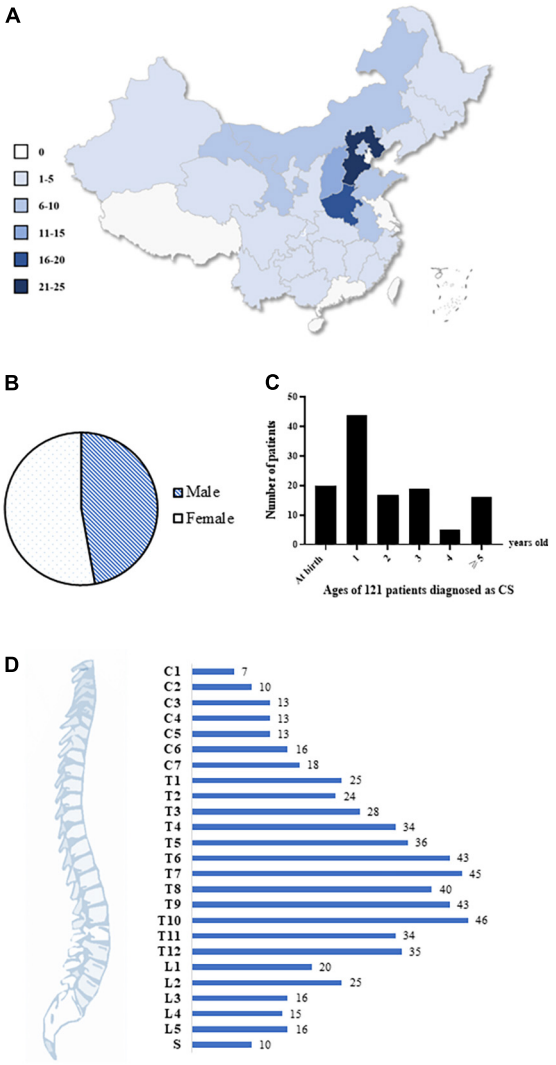

FIGURE 2
Demographics and clinical characteristics of the cohort. **(A)** The geographical characteristic of our cohort. A total of 121 Chinese patients with CS were recruited from all over the country. Different colors represent different patient numbers from the corresponding region, and the darker color, the more patients. **(B)** The gender ratio. A total of 57 males and 64 females were enrolled. **(C)** Age of 121 patients when they were diagnosed as CS. 87% of patients were diagnosed with CS before 5 years old. **(D)** The distribution of malformed vertebrae in all the patients. The numbers of patients were labeled. CS, congenital scoliosis; C, cervical; T, thoracic; L, lumbar; S, sacral.

Haplotyping of T-box transcription factor 6 variants

To determine whether the T-C-A haplotype existed in patients, T and C-A were amplified and PCR productions were sequenced separately. All the eight patients carried the T-C-A haplotype with in-trans *TBX6* deleterious variants, representing typical TACS compound inheritance (Table 1 and Figure 3).

Clinical characteristics of patients with T-box transcription factor 6-associated congenital scoliosis

Eight patients (five boys and three girls) were diagnosed with TACS, which accounted for 6.6% of our CS cohort. All the patients had malformed vertebrae located in the lower half of the spine (below T8) and only patient 7 had an additional butterfly vertebra at C7 (Figure 4). Patients 2, 3, and 8 had mildly deformed ribs. In addition, patient 5 exhibited mild developmental delay and patient 8 had bilateral radial polydactyly. In summary, these patients displayed the typical clinical characteristics of TACS despite only four patients scoring $\geq$ 3, the cutoff point, according to the TACScore algorithm (Table 2).

Surgical strategy and patient prognosis

All the patients with TACS were diagnosed with scoliosis before the age of 1 year and underwent surgery at varying ages. Because of the presence of simple hemivertebrae, all the patients received corresponding hemivertebra resection combined with short segmental fusion. Patients 1, 5, and 7 underwent surgery twice for two malformed vertebrae each, which progressed as patients grew. Before surgery, patients' Cobb angles ranged from 22.0 to 53.0° with a mean angle of 38.28 ± 12.28°. In the most recent follow-up (i.e., at 3 years and 3 months), the Cobb angles ranged from 0 to 6.0° and the mean angle was 3.57 ± 2.22°. Correction rates ranged from 86.4 to 100% with a mean rate of 90.84 ± 4.71% and no complications were reported (Table 2 and Figure 4).

Discussion

In this study, we enrolled 121 patients with CS who visited Beijing Children's Hospital for surgical treatment and genetic counseling; eight of these patients were molecularly diagnosed with TACS. Patients with TACS accounted for 6.6% of CS. Our study retrospectively summarized the clinical characteristics of patients with TACS and the surgical strategies adopted for these patients. The study is the first study to report the postsurgical prognosis of patients with TACS and suggests that all the patients had positive outcomes.

The 6.6% prevalence of TACS among patients with CS was slightly different from that reported in the following CS cohorts of previous studies: 10% in Han Chinese (15), 9.6% in a Japanese cohort (17), 7.2% in a European cohort (13), and 4.5% in a Hong Kong, Southern China cohort (19). Several explanations for this difference are proposed. First, ethnic differences in these regional populations likely contribute to different allele frequencies. Second, with the development

TABLE 1 The genotypes of patients.

Patient	Allele 1	Allele 2
	Deleterious variant	Common haplotype
Patient 1	c.745G > A / p.Val249Met	T-C-A
Patient 2	16p11.2 deletion 0.54 Mb (chr16:29660000–30200000)	T-C-A
Patient 3	16p11.2 deletion 0.56 Mb (chr16:29640000–30200000)	T-C-A
Patient 4	16p11.2 deletion 0.52 Mb (chr16:29680000-30200000)	T-C-A
Patient 5	16p11.2 deletion 0.56 Mb (chr16:29640000–30200000)	T-C-A
Patient 6	c.271dupG / p.Val91fs*79	T-C-A
Patient 7	c.1115_1130dupAGGCTCCAGACTCCGG /p.Arg378fs*66	T-C-A
Patient 8	c.903T > G/p.Tyr301*	T-C-A

The haplotype defined by three common *TBX6* SNPs (reference/non-reference): rs2289292 (C/T)–rs3809624 (T/C)–rs3809627 (C/A).
The "*" was one of the genetic terms. In "c.271dupG / p.Val91fs*79" it means frameshift occurs at the 91st amino acid, translation is stopped after 79 amino acids. So does "c.1115_1130dupAGGCTCCAGACTCCGG /p.Arg378fs*66". In "c.903T > G/p.Tyr301*", it means the 301st amino acid turns into a termination codon and translation is stopped.

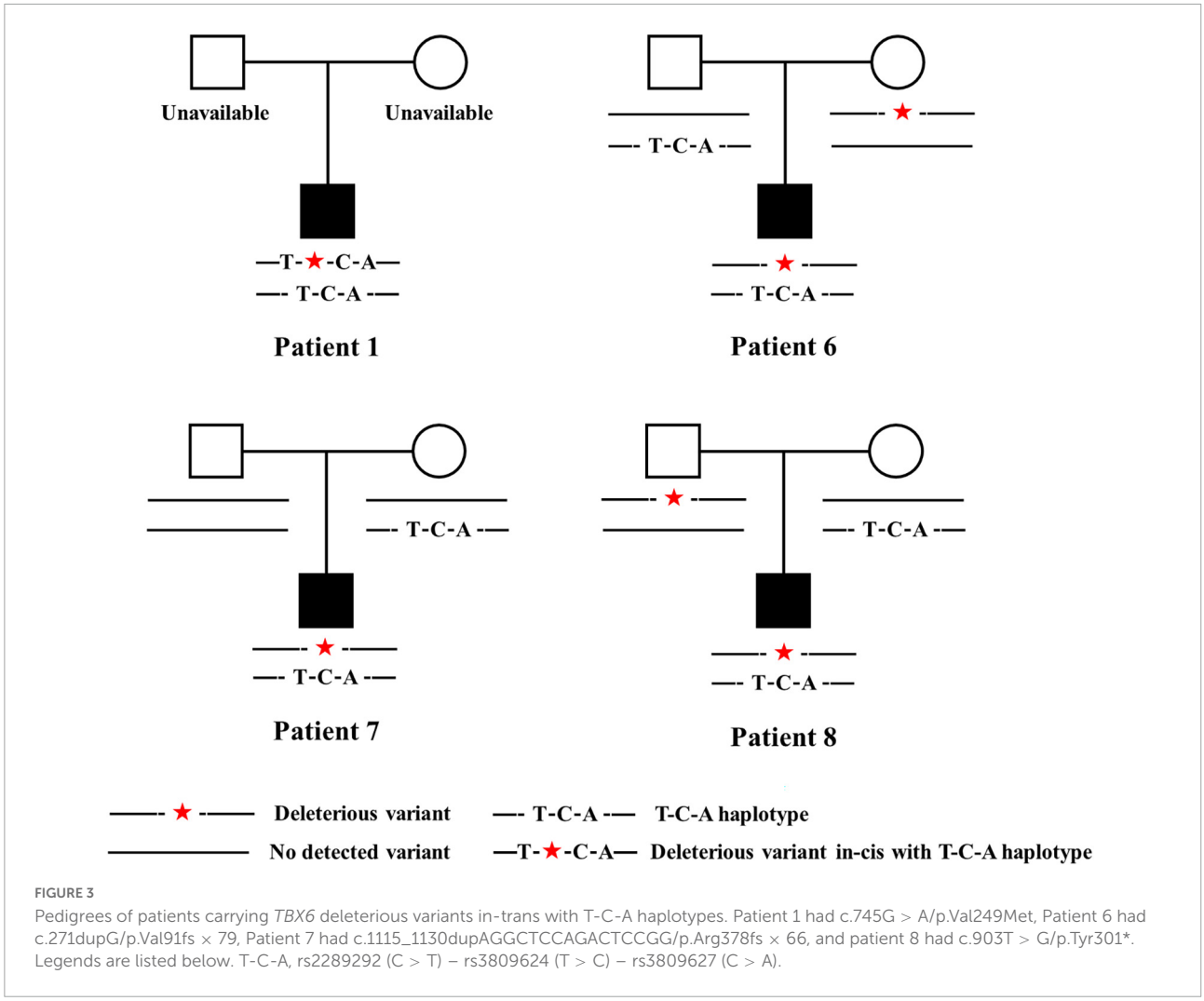

FIGURE 3
Pedigrees of patients carrying *TBX6* deleterious variants in-trans with T-C-A haplotypes. Patient 1 had c.745G > A/p.Val249Met, Patient 6 had c.271dupG/p.Val91fs × 79, Patient 7 had c.1115_1130dupAGGCTCCAGACTCCGG/p.Arg378fs × 66, and patient 8 had c.903T > G/p.Tyr301*. Legends are listed below. T-C-A, rs2289292 (C > T) – rs3809624 (T > C) – rs3809627 (C > A).

of prenatal ultrasound diagnostic technology, fetuses with CS accompanied by severe structural malformations can be identified and pregnancy terminated. Third, the TACS ratio may have been altered with the enlargement of our cohort.

Previous Deciphering Disorders Involving Scoliosis and Comorbidities (DISCO) studies have revealed that the TACScore is a cost-effective and time-saving tool for screening patients with TACS and shows considerable sensitivity (93.9%),

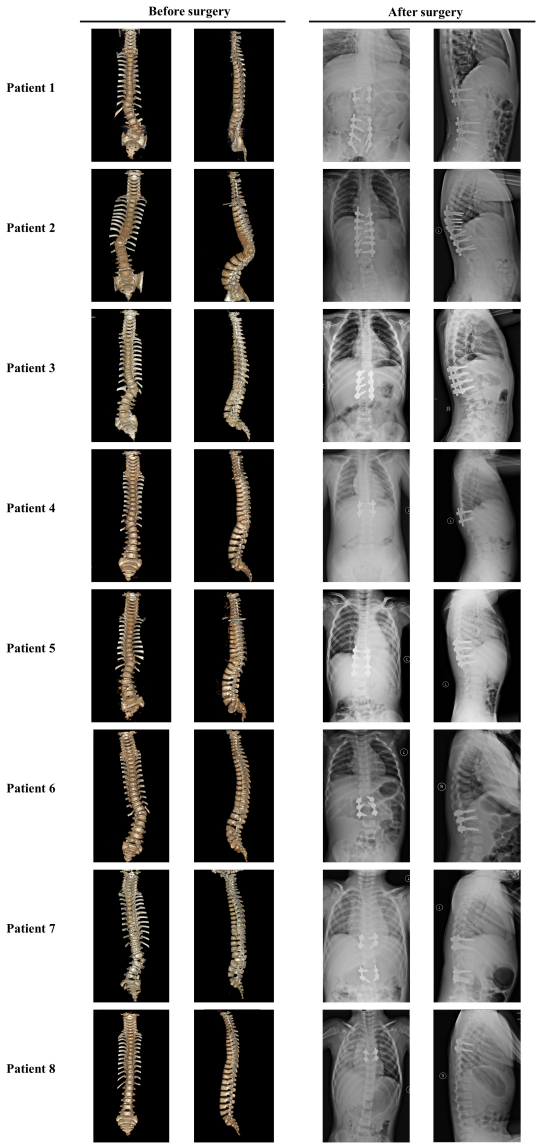

FIGURE 4
Images of patients with TACS before and after surgeries suggested well outcomes. **Patient 1** had hemivertebrae at T12 and L5 with the Cobb angle of 26°; after surgery, the Cobb angle was reduced to 2°. **Patient 2** had hemivertebrae at T11 with the Cobb angle of 53°; after surgery, the Cobb angle was reduced to 87°. **Patient 3** had hemivertebrae at T12 and butterfly vertebrae at T11 with the Cobb angle of 50°; after surgery, the Cobb angle was reduced to 5°. **Patient 4** had hemivertebrae at T11 with the Cobb angle of 41°; after surgery, the Cobb angle was reduced to 0°. **Patient 5** had hemivertebrae at T11 and butterfly vertebrae at L4 and S3 with the Cobb angle of 30°; after surgery, the Cobb angle was reduced to 3°. **Patient 6** had hemivertebrae at T12 and butterfly vertebrae at L5 with the Cobb angle of 46°; after surgery, the Cobb angle was reduced to 6°. **Patient 7** had unsegmented hemivertebrae at T10 and L3 and butterfly vertebrae at C7 and T9 with the Cobb angle of 22°; after surgery, the Cobb angle was reduced to 3°. **Patient 8** had hemivertebrae at T8 with the Cobb angle of 26°; after surgery, the Cobb angle was reduced to 4°. Images before and after surgeries were obtained by CT and X-ray, respectively. TACS, *TBX6*-associated congenital scoliosis.

specificity (90.9%), and accuracy (91.2%). However, the sensitivity, specificity, and accuracy of the TACScore were 50, 85.8, and 83.5%, respectively, in our cohort, far lower than the values in DISCO studies. We inferred that results could be due to our smaller cohort size and that findings may more closely match those in previous reports if our cohort is expanded (16, 25).

In clinical practice, the selection of surgical treatment comprehensively considers three indicators: patient age, the Cobb angle magnitude, and the type of malformation. These indicators predict the surgical correction rate and operative and postoperative complications. For hemivertebrae-induced CS, posterior hemivertebra resection combined with segmental fusion was the most common choice of surgery. Its correction rate varied from 46 to 87% (26–35). The frequency of complications ranged from 0 to 41% (27,28,32,33,35–42) and complications included wound infection, adding-on phenomenon, pseudoarticulation formation, postoperative progression of scoliosis, the offset of the internal fixation, and pedicle fractures. In our previous study (43), it showed that 14 patients with CS younger than 5 years of age accepted short fixation for posterior hemivertebra resection, which had a mean correction rate of 77.86% and no surgery-related complications. With a mean correction rate of 90.84%, posterior hemivertebra resection combined with segmental fusion was more effective in patients with TACS. Taken together, our findings implied that the optimal surgical choice for patients with TACS is posterior hemivertebra resection combined with segmental fusion, which should be a first treatment option for patients with TACS.

As a complex genetic disorder, CS is often accompanied by multisystem abnormalities. For example, patient 5 with 16p11.2 deletion presented with mild developmental delay and intellectual disability. The 16p11.2 deletion is considered to be related to autism, obesity, developmental delay, and intellectual disability (13,44–46). Comprehensive and systematic physical examination is required for clinical diagnosis and treatment and CS may present a considerable psychological and financial burden to children and their families (3). Although the clinical phenotypes of patients with TACS are less complicated than those of other malformations, most orthopedic clinicians find TACS difficult to distinguish from other forms of non-syndromic scoliosis. Genetic testing for *TBX6* can rapidly identify the etiology and reduce unnecessary physical examination (15). In addition, CS caused by different gene mutations exhibits varying patterns of progression. A definite molecular diagnosis can further predict complications and long-term prognosis and can guide the identification of appropriate intervention time and surgical options (47). In our study, all the molecularly diagnosed patients with TACS received posterior hemivertebra resection combined with short-stage fusion and the prognoses were followed for at least 1 year. All the patients ultimately presented with the Cobb angle of less than 10°, an average correction rate of 90.84%, and no complications to date.

TABLE 2 Clinical information of patients.

	Patient 1	Patient 2	Patient 3	Patient 4	Patient 5	Patient 6	Patient 7	Patient 8
Gender	Male	Female	Female	Female	Male	Male	Male	Male
Delivery	Uneventful	Uneventful	Uneventful	Uneventful	Cesarean section because of macrosomia	Uneventful	Uneventful	Uneventful
Age of finding scoliosis	1 year	1 year	5 month	2 month	1 year	1 year	1 year	Intrauterine 7 month
Age of undergoing surgeries	3 year	2, 8 year	8 year	4 year	6 year 4 month, 6 year 7 month	2 year	2, 5 year	4 year 2 month
Hemivertebra	T12, L5	T11	T12	T11	T11	T12	T10, L3 (unsegmented)	T8
Butterfly-vertebra	–	–	T11	–	L4, S3	L5	C7, T9	–
Fusional vertebra	–	T7–L2	–	–	–	–	T9–10, L3–4	–
Rib malformation	–	Yes	Yes	–	–	–	–	Yes
Other clinical features	–	Kyphosis	–	–	Mildly developmental delay	–	–	Polydactyly at bilateral thumb radial
TACScore	3	2	4	3	2	3	2	3
Cobb angel before surgery (°)	26	53	50	41	30	46	22	26
Number of operations	2	1	1	1	2	1	2	1
Cobb angel after last surgery (°)	2	6	5	0	3	6	3	4
Correction rate (%)	93.8	88.7	90.0	100.0	90.0	87.0	86.4	84.6
Fusion occurs at last follow-up	Yes	Yes	Yes	Yes	Yes	Yes	Yes	Yes
Complication	No	No	No	No	No	No	No	No
Follow-up time after surgery	3 year 3 month	3 year	3 year	3 year	2 year 9 month	1 year	2 year 3 month	3 month
Surgery	Posterior hemivertebra resection and segmental fusion	Posterior hemivertebra resection and segmental fusion	Posterior hemivertebra resection and segmental fusion	Posterior hemivertebra resection and segmental fusion	Posterior hemivertebra resection and segmental fusion†	Posterior hemivertebra resection and segmental fusion	Posterior hemivertebra resection and segmental fusion†	Posterior hemivertebra resection and segmental fusion

Y, year; M, month; C, cervical; T, thoracic; L, lumbar; S, sacral; TACScore, TBX6-associated congenital scoliosis score.
†Patient 5 and 7 underwent twice surgeries of posterior hemivertebra resection and segmental fusion.

10.3389/fmed.2022.941468

Thus, our results indicated that hemivertebrae caused by the compound inheritance of *TBX6* can be corrected effectively by hemivertebra resection combined with segmental fusion—a finding that may reassure CS children and their parents.

Conclusion

In conclusion, we recruited 121 patients with CS in Beijing Children's Hospital and diagnosed eight (6.6%) of these patients with TACS with *TBX6* deleterious and hypomorphic allele in trans. Follow-up revealed that hemivertebra resection and segmental fusion resulted in positive outcomes. Our study can guide risk evaluation for patients with TACS and their families.

Data availability statement

The data that support the findings of this study are openly available. Raw data were uploaded and public to gsa-human [Genome Sequence Archive for Human (https://ngdc.cncb.ac.cn/gsa-human/)], under accession PRJCA010512.

Ethics statement

The studies involving human participants were reviewed and approved by the Institutional Medical Ethics Committee of Beijing Children's Hospital, Capital Medical University (BCH, Approval No. 2015-26). Written informed consent to participate in this study was provided by the participants' legal guardian/next of kin.

Author contributions

CH and XZ conceived and designed the study. ZY, HL, and XZ recruited their respective patients for this study and provided clinical data. WZ conducted the experiments, analyzed the data, and wrote the manuscript. RG and SZ contributed to the analysis of sequencing data. CH and WL were involved in manuscript editing. All authors reviewed and approved the final version of the manuscript.

Funding

This study was partially supported by grants from the Beijing Municipal Commission of Health and Family Planning Foundation (2022-2-1142 and 2020-4-1144), the Special Fund of the Pediatric Medical Coordinated Development Center of Beijing Hospitals Authority (XTCX201807), and the Beihang University and Capital Medical University Advanced Innovation Center for Big Data-based Precision Medicine Plan (BHME-201905).

Conflict of interest

The authors declare that the research was conducted in the absence of any commercial or financial relationships that could be construed as a potential conflict of interest.

Publisher's note

Supplementary material

The Supplementary Material for this article can be found online at: https://www.frontiersin.org/articles/10.3389/fmed.2022.941468/full#supplementary-material

References

1. Wynne-Davies, R. Congenital vertebral anomalies: aetiology and relationship to spina bifida cystica. *J Med Genet.* (1975) 12:280–8. doi: 10.1136/jmg.12.3.280

2. Brand MC. Examination of the newborn with congenital scoliosis: focus on the physical. *Adv Neonatal Care.* (2008) 8:265–73.

3. McMaster MJ, Ohtsuka K. The natural history of congenital scoliosis. a study of two hundred and fifty-one patients. *J Bone Joint Surg Am Vol.* (1982) 64:1128–47.

4. Mortier GR, Cohn DH, Cormier-Daire V, Hall C, Krakow D, Mundlos S, et al. Nosology and classification of genetic skeletal disorders: 2019 revision. *Am J Med Genet Part A.* (2019) 179:2393–419. doi: 10.1002/ajmg.a.61366

5. Wittler L, Shin EH, Grote P, Kispert A, Beckers A, Gossler A, et al. Expression of Msgn1 in the presomitic mesoderm is controlled by synergism of Wnt signalling and Tbx6. *EMBO Rep.* (2007) 8:784–9. doi: 10.1038/sj.embor.7401030

6. Oginuma M, Niwa Y, Chapman DL, Saga Y. Mesp2 and Tbx6 cooperatively create periodic patterns coupled with the clock machinery during mouse somitogenesis. *Development.* (2008) 135:2555–62. doi: 10.1242/dev.019877

7. Zhao W, Ajima R, Ninomiya Y, Saga Y. Segmental border is defined by ripply2-mediated Tbx6 repression independent of Mesp2. *Dev Biol.* (2015) 400:105–17. doi: 10.1016/j.ydbio.2015.01.020

8. Yasuhiko Y, Haraguchi S, Kitajima S, Takahashi Y, Kanno J, Saga Y. Tbx6-mediated notch signaling controls somite-specific Mesp2 expression. *Proc Nat Acad Sci USA*. (2006) 103:3651–6. doi: 10.1073/pnas.0508238103

9. Yasuhiko Y, Kitajima S, Takahashi Y, Oginuma M, Kagiwada H, Kanno J, et al. Functional importance of evolutionally conserved Tbx6 binding sites in the presomitic mesoderm-specific enhancer of Mesp2. *Development.* (2008) 135:3511–9. doi: 10.1242/dev.027144

10. Takemoto T, Uchikawa M, Yoshida M, Bell DM, Lovell-Badge R, Papaioannou VE, et al. Tbx6-dependent Sox2 regulation determines neural or mesodermal fate in axial stem cells. *Nature.* (2011) 470:394–8. doi: 10.1038/nature09729

11. Chen W, Liu J, Yuan D, Zuo Y, Liu Z, Liu S, et al. Progress and perspective of Tbx6 gene in congenital vertebral malformations. *Oncotarget.* (2016) 7:57430–41. doi: 10.18632/oncotarget.10619

12. Sparrow DB, McInerney-Leo A, Gucev ZS, Gardiner B, Marshall M, Leo PJ, et al. Autosomal dominant spondylocostal dysostosis is caused by mutation in Tbx6. *Hum Mol Genet.* (2013) 22:1625–31. doi: 10.1093/hmg/ddt012

13. Lefebvre M, Duffourd Y, Jouan T, Poe C, Jean-Marçais N, Verloes A, et al. Autosomal recessive variations of Tbx6, from congenital scoliosis to spondylocostal dysostosis. *Clin Genet.* (2017) 91:908–12. doi: 10.1111/cge.12918

14. Otomo N, Takeda K, Kawai S, Kou I, Guo L, Osawa M, et al. Bi-allelic loss of function variants of Tbx6 causes a spectrum of malformation of spine and rib including congenital scoliosis and spondylocostal dysostosis. *J Med Genet.* (2019) 56:622–8. doi: 10.1136/jmedgenet-2018-105920

15. Wu N, Ming X, Xiao J, Wu Z, Chen X, Shinawi M, et al. Tbx6 null variants and a common hypomorphic allele in congenital scoliosis. *N Engl J Med.* (2015) 372:341–50. doi: 10.1056/NEJMoa1406829

16. Liu J, Wu N, Yang N, Takeda K, Chen W, Li W, et al. Tbx6-associated congenital scoliosis (Tacs) as a clinically distinguishable subtype of congenital scoliosis: further evidence supporting the compound inheritance and Tbx6 gene dosage model. *Genet Med.* (2019) 21:1548–58. doi: 10.1038/s41436-018-0377-x

17. Takeda K, Kou I, Kawakami N, Iida A, Nakajima M, Ogura Y, et al. Compound heterozygosity for null mutations and a common hypomorphic risk haplotype in Tbx6 causes congenital scoliosis. *Hum Mutat.* (2017) 38:317–23. doi: 10.1002/humu.23168

18. Chen W, Lin J, Wang L, Li X, Zhao S, Liu J, et al. Tbx6 missense variants expand the mutational spectrum in a non-mendelian inheritance disease. *Hum Mutat.* (2020) 41:182–95. doi: 10.1002/humu.23907

19. Feng X, Cheung JPY, Je JSH, Cheung PWH, Chen S, Yue M, et al. Genetic variants of Tbx6 and Tbxt identified in patients with congenital scoliosis in Southern China. *J Orthop Res.* (2020) 39:971–88. doi: 10.1002/jor.24805

20. Li J, Shi L, Zhang K, Zhang Y, Hu S, Zhao T, et al. Varcards: an integrated genetic and clinical database for coding variants in the human genome. *Nucleic Acids Res.* (2018) 46:D1039–48. doi: 10.1093/nar/gkx1039

21. Richards S, Aziz N, Bale S, Bick D, Das S, Gastier-Foster J, et al. Standards and guidelines for the interpretation of sequence variants: a joint consensus recommendation of the American College of medical genetics and genomics and the association for molecular pathology. *Genet Med.* (2015) 17:405–24. doi: 10.1038/gim.2015.30

22. Fromer M, Purcell SM. Using Xhmm software to detect copy number variation in whole-exome sequencing data. *Curr Protocols Hum Genet.* (2014) 81:7.23.1–21. doi: 10.1002/0471142905.hg0723s81.

23. Riggs ER, Andersen EF, Cherry AM, Kantarci S, Kearney H, Patel A, et al. Technical standards for the interpretation and reporting of constitutional copy-number variants: a joint consensus recommendation of the American college of medical genetics and genomics (Acmg) and the clinical genome resource (Clingen). *Genet Med.* (2020) 22:245–57. doi: 10.1038/s41436-019-0686-8

24. Riggs ER, Church DM, Hanson K, Horner VL, Kaminsky EB, Kuhn RM, et al. Towards an evidence-based process for the clinical interpretation of copy number variation. *Clin Genet.* (2012) 81:403–12. doi: 10.1111/j.1399-0004.2011.01818.x

25. Chen Z, Yan Z, Yu C, Liu J, Zhang Y, Zhao S, et al. Cost-effectiveness analysis of using the Tbx6-associated congenital scoliosis risk score (Tacscore) in genetic diagnosis of congenital scoliosis. *Orphanet J Rare Dis.* (2020) 15:250. doi: 10.1186/s13023-020-01537-y

26. Barik S, Mishra D, Gupta T, Yadav G, Kandwal P. Surgical outcomes following hemivertebrectomy in congenital scoliosis: a systematic review and observational meta-analysis. *Eur Spine J.* (2021) 30:1835–47. doi: 10.1007/s00586-021-06812-5

27. Bixby EC, Skaggs K, Marciano GF, Simhon ME, Menger RP, Anderson RCE, et al. Resection of congenital hemivertebra in pediatric scoliosis: the experience of a two-specialty surgical team. *J Neurosurg Pediatr.* (2021) [Online ahead of print]. doi: 10.3171/2020.12.PEDS20783.

28. Bao BX, Yan H, Tang JG, Qiu DJ, Wu YX, Cheng XK. An analysis of the risk factors for adding-on phenomena after posterior hemivertebral resection and pedicle screw fixation for the treatment of congenital scoliosis caused by hemivertebral malformation. *Therapeut Clin Risk Manage.* (2022) 18:409–19. doi: 10.2147/tcrm.s352793

29. Mladenov K, Kunkel P, Stuecker R. Hemivertebra resection in children, results after single posterior approach and after combined anterior and posterior approach: a comparative study. *Eur Spine J.* (2012) 21:506–13. doi: 10.1007/s00586-011-2010-4

30. Li Y, Wang G, Jiang Z, Cui X, Li T, Liu X, et al. One-stage posterior excision of lumbosacral hemivertebrae: retrospective study of case series and literature review. *Medicine.* (2017) 96:e8393. doi: 10.1097/md.0000000000008393

31. Crostelli M, Mazza O, Mariani M. Posterior approach lumbar and thoracolumbar hemivertebra resection in congenital scoliosis in children under 10 years of age: results with 3 years mean follow up. *Eur Spine J.* (2014) 23:209–15. doi: 10.1007/s00586-013-2933-z

32. Zhang J, Shengru W, Qiu G, Yu B, Yipeng W, Luk KD. The efficacy and complications of posterior hemivertebra resection. *Eur Spine J.* (2011) 20:1692–702. doi: 10.1007/s00586-011-1710-0

33. Ruf M, Harms J. Hemivertebra resection by a posterior approach: innovative operative technique and first results. *Spine.* (2002) 27:1116–23. doi: 10.1097/00007632-200205150-00020

34. Hedequist DJ, Hall JE, Emans JB. Hemivertebra excision in children via simultaneous anterior and posterior exposures. *J Pediatr Orthop*. (2005) 25:60–3. doi: 10.1097/00004694-200501000-00014

35. Guo J, Zhang J, Wang S, Zhang Y, Yang Y, Yang X, et al. Surgical outcomes and complications of posterior hemivertebra resection in children younger than 5 years old. *J Orthop Surg Res.* (2016) 11(1):48. doi: 10.1186/s13018-016-0381-2

36. Erturer RE, Kilinc BE, Gokcen B, Erdogan S, Kara K, Ozturk C. The results of hemivertebra resection by the posterior approach in children with a mean follow-up of five years. *Adv Orthop.* (2017) 2017:4213413. doi: 10.1155/2017/4213413

37. Zhou C, Liu L, Song Y, Liu H, Li T, Gong Q, et al. Hemivertebrae resection for unbalanced multiple hemivertebrae: is it worth It? *Eur Spine J.* (2014) 23:536–42. doi: 10.1007/s00586-013-3065-1

38. Zhuang Q, Zhang J, Li S, Wang S, Guo J, Qiu G. One-stage posterior-only lumbosacral hemivertebra resection with short segmental fusion: a more than 2-year follow-up. *Eur Spine J.* (2016) 25:1567–74. doi: 10.1007/s00586-015-3995-x

39. Ruf M, Jensen R, Letko L, Harms J. Hemivertebra resection and osteotomies in congenital spine deformity. *Spine.* (2009) 34:1791–9. doi: 10.1097/BRS.0b013e3181ab6290

40. Huang Y, Feng G, Song Y, Liu L, Zhou C, Wang L, et al. Efficacy and safety of one-stage posterior hemivertebral resection for unbalanced multiple hemivertebrae: a more than 2-year follow-up. *Clin Neurol Neurosurg.* (2017) 160:130–6. doi: 10.1016/j.clineuro.2017.07.009

41. Yaszay B, O'Brien M, Shufflebarger HL, Betz RR, Lonner B, Shah SA, et al. Efficacy of hemivertebra resection for congenital scoliosis: a multicenter retrospective comparison of three surgical techniques. *Spine.* (2011) 36:2052–60. doi: 10.1097/BRS.0b013e318233f4bb

42. Wang S, Zhang J, Qiu G, Li S, Yu B, Weng X. Posterior hemivertebra resection with bisegmental fusion for congenital scoliosis: more than 3 year outcomes and analysis of unanticipated surgeries. *Eur Spine J.* (2013) 22:387–93. doi: 10.1007/s00586-012-2577-4

43. Guo D, Yao Z, Qi X, Li C, Zhang X. Short fixation with a 3-rod technique for posterior hemivertebra resection in children younger than 5 years old. *Pediatr Investig.* (2020) 4:104–8. doi: 10.1002/ped4.12206

44. Weiss LA, Shen Y, Korn JM, Arking DE, Miller DT, Fossdal R, et al. Association between microdeletion and microduplication at 16p11.2 and autism. *N Engl J Med.* (2008) 358:667–75. doi: 10.1056/NEJMoa075974

45. Walters RG, Jacquemont S, Valsesia A, de Smith AJ, Martinet D, Andersson J, et al. A new highly penetrant form of obesity due to deletions on chromosome 16p11.2. *Nature.* (2010) 463:671–5. doi: 10.1038/nature08727

46. Jacquemont S, Reymond A, Zufferey F, Harewood L, Walters RG, Kutalik Z, et al. Mirror extreme bmi phenotypes associated with gene dosage at the chromosome 16p11.2 Locus. *Nature.* (2011) 478:97–102. doi: 10.1038/nature10406

47. Zhang YB, Zhang JG. Treatment of early-onset scoliosis: techniques, indications, and complications. *Chin Med J.* (2020) 133:351–7. doi: 10.1097/CM9.0000000000000614

frontiers | Frontiers in Medicine

TYPE Original Research
PUBLISHED 16 August 2022
DOI 10.3389/fmed.2022.963883

OPEN ACCESS

EDITED BY
Jian Gao,
Shanghai Children's Medical Center, China

REVIEWED BY
Zhougui Ling,
The Fourth Affiliated Hospital of Guangxi Medical University, China
Yi Zuo,
Wuhan University of Science and Technology, China
Yanling Wu,
Yanbian University, China

*CORRESPONDENCE
Tao Huang
24867509@qq.com

SPECIALTY SECTION
This article was submitted to Precision Medicine, a section of the journal Frontiers in Medicine

RECEIVED 08 June 2022
ACCEPTED 25 July 2022
PUBLISHED 16 August 2022

CITATION
Li Y, Shu J, Cheng Y, Zhou X and Huang T (2022) Identification of key biomarkers in Angelman syndrome by a multi-cohort analysis. *Front. Med.* 9:963883. doi: 10.3389/fmed.2022.963883

Identification of key biomarkers in Angelman syndrome by a multi-cohort analysis

Yong Li[2], Junhua Shu[1], Ying Cheng[1], Xiaoqing Zhou[1] and Tao Huang[1]*

[1]Department of Pediatrics, Maternal and Child Health Hospital of Hubei Province, Tongji Medical College, Huazhong University of Science and Technology, Wuhan, China, [2]Department of Pediatric Intensive Care Unit, Maternal and Child Health Hospital of Hubei Province, Tongji Medical College, Huazhong University of Science and Technology, Wuhan, China

The Angelman Syndrome (AS) is an extreme neurodevelopmental disorder without effective treatments. While most patients with this disease can be diagnosed by genetic testing, there are still a handful of patients have an unrecognized genetic cause for their illness. Thus, novel approaches to clinical diagnosis and treatment are urgently needed. The aim of this study was to identify and characterize differentially expressed genes involved in AS and built potential diagnostic panel for AS by NGS sequencing. A multi-cohort analysis framework was used to analyze stem cell-derived neurons from AS patients in GSE160747 dataset. We identified three differentially expressed genes (ACTN1, ADAMTS2, SLC30A8) differentiates AS patients from controls. Moreover, we validated the expression patterns of these genes in GSE146640, GSE120225. Receiver operating characteristic (ROC) curves analysis demonstrated that these genes could function as potential diagnostic biomarkers [AUC = 1 (95% CI 1–1)]. This study may provide new approach for diagnosing patients with AS and helping to develop novel therapies in treating AS patients.

KEYWORDS

Angelman syndrome, diagnosis, biomarkers, RNA-seq, pediatrics

Introduction

A rare neurodevelopment disorder called Angelman syndrome (AS) was first described in 1965 by Dr. Harry Angelman, an English pediatrician, who described three severely children with it (1). Symptoms of AS include delayed development, lack of speech, ataxia, and, occasionally, attacks. There is an estimated incidence of AS between 1/10,000 and 1/20,000 (2). Mutations of the maternal UBE3A (ubiquitin protein ligase E3A) gene cause AS in 8% of the cases (3, 4). UBE3A affects protein levels and function through ubiquitination. The UBE3A gene in neurons is imprinted: predominantly maternal alleles are expressed with little or no expression of paternal alleles (5). Unlike gene deletions, the UBE3A gene has a strong relationship with autism when duplicated or triple copied. AS is diagnosed if the patient meets the consensus clinical diagnosis

criteria and/or demonstrates maternally inherited UBE3 allele expression or functional deficits. Since an estimated 90% of individuals with typical AS phenotypes can be identified through molecular genetics testing, The remaining 10% of AS patients have an as yet unknown genetic cause for the disease (6). Although rapid progress has been made in understanding the disease-causing process in AS, the gene-specific treatment is still limited (7).

Due to the rarity of AS in children, there is almost little research on the disease, let alone drugs. Finding new diagnostic modalities and potential therapeutic targets becomes more challenging. In this study, we analyzed samples from transcriptomics cohorts and identified novel biomarkers for AS diagnosis. Moreover, as a result of these differentially expressed genes, we can find potential therapeutic targets and gain a deeper understanding pathogenesis of AS.

Materials and methods

Data sources

We identified 3 prospective AS studies (GSE160747, GSE146640, GSE120225) that were potentially eligible for inclusion in the study. We downloaded datasets from the GEO database.[1] We identified 3 datasets and divided them into two "training" and one "validation" dataset (**Table 1**).

Gene expression data and statistics analyses

All transcriptomic data were normalized using the GC-Robust Multi-array Average. A log2 transformation was applied to all gene expression before analysis. To underestimates the between-trial variance, we used the DerSimonian-Laird random-effects combine gene expression effect sizes *via* Hedges' g effect size. Moreover, based on gene effect size (ES > 1.3), and Fisher's method false discovery rate (FDR < 0.9), we identified a subset of genes as the AS score.

Creation of Angelman syndrome score

As a starting point, we ran a forward search using the MetaIntegrator R package to identify the parsimonious gene set best suited for diagnostic ability (8). A forward search begins with the gene that has the best discriminative ability, and then at each step adds the gene with the greatest weighted AUC. Once the weighted AUC reaches some threshold, no further additions can raise it further. Every time a new gene was added to the forward search, we determined the AS score in the following: Mean (upregulated genes)-Mean (downregulated genes).

Results

The three diagnostic biomarkers of Angelman syndrome in two training datasets

We achieved a systematic search for data on transcriptome-wide expression between normal and AS tissue. According to the previously described method (ES > 1.3, FDR < 0.9), 12 genes were significantly upregulated, while 22 genes were significantly downregulated (**Figure 1A**). After forward search, we identified a set of 3 differentially expressed genes (ACTN1, ADAMTS2, SLC30A8) in AS/Normal that was optimized for diagnostic ability (**Figures 1B–D**). The AS signature (three diagnostic biomarkers) distinguished AS from normal subjects with a summary area under the curve (AUC) = 0.98 (95% CI 0.92–1) in the training dataset (**Figure 1E**).

Validation of the three diagnostic biomarkers in two external datasets of Angelman syndrome

We further verified the AS signature in the two-validation set. For each dataset, we computed the effect size and meta-score by the previously described method (**Figures 2A–C**). **Figures 2D,E** violin plot showing the Meta-score of the 3-gene signature for separating AS from control group GSE120225 and GSE146640. The AUC = 1 (95% CI 1–1) differential AS from normal subjects by the AS signature in two validation datasets (**Figures 2F,G**). Meanwhile, we also compared with the well-known AS diagnostic marker UBE3A, which distinguished AS from normal subjects with a summary AUC = 0.76 (95% CI 0.45–0.93) (**Figure 2H**).

Discussion

Families and individuals suffering from AS carry a heavy burden, due to the disease is so rare, treatment and medication

TABLE 1 Demographic of the study in training and validation dataset.

GEO ID	Sample size	Sample type	Annotation
GSE160747	36	iPSC-derived neurons	Training
GSE146640	12	iPSC-derived neurons	Training
GSE120225	6	H9 human embryonic stem cell lines	Validation

1 http://www.ncbi.nlm.nih.gov/geo/

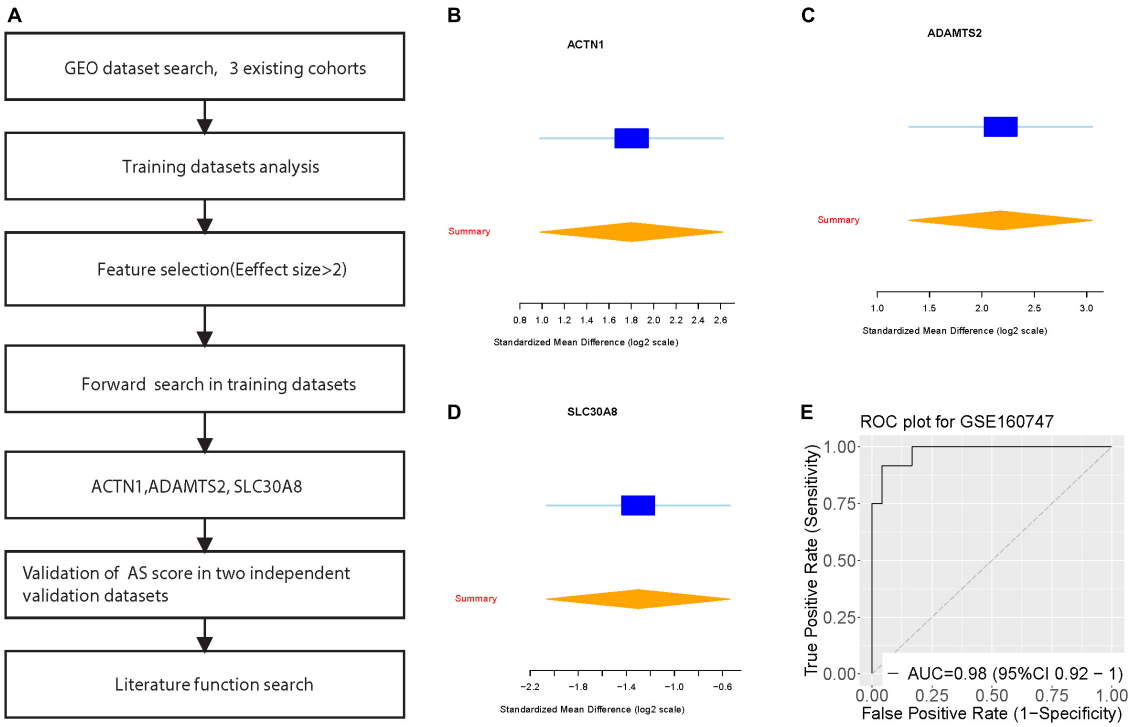

FIGURE 1
Discovery of three differentially expressed genes in diagnosis of Angelman syndrome. **(A)** Multi-cohort analysis workflow for identifying and validating the three differentially expressed genes. **(B–D)** The up-regulated gene (ACTN1) and down-regulated genes (ADAMTS2, and SLC30A8) from the forward searches in GSE160747. The x axis represents standardized mean difference between AS and dengue control. **(D,E)** ROC curves of patients with AS vs. controls in GSE160747.

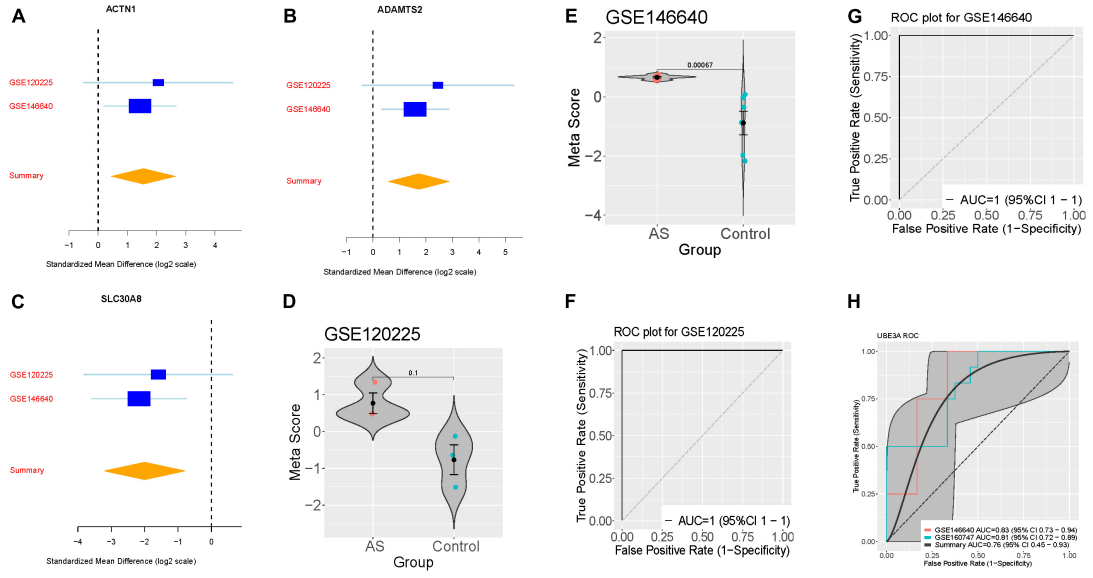

FIGURE 2
Validation of three differentially expressed genes diagnosis of AS. **(A–C)** The up-regulated gene (ACTN1) and down-regulated genes (ADAMTS2, and SLC30A8) searches in GSE120225 and GSE146640. The x axis represents standardized mean difference between AS and dengue control. **(D,E)** violin plot illustrating the meta-score of the three differentially expressed genes for differentiate AS from Control in GSE120225 and GSE146640. **(F,G)** ROC curves of patients with AS vs. controls in GSE120225 and GSE146640. **(H)** ROC curves of UBE3A diagnostic power in the training and validation dataset.

are difficult to obtain. Currently, three treatment approaches for AS are in preclinical and clinical effect. The reintroduction of the UBE3A protein into the neurons through gene replacement therapies is one approach. It is also possible to "unsilence" paternal copies of the UBE3A gene. Thirdly, drugs that target proteins and effector mRNAs known to be affected in the pathophysiology of AS are being investigated (9).

In the current study, we identified three genes that are differentially expressed under UBE3A mutation in stem cell-derived neurons by mRNAs. As a result, we developed a model for AS scores using these three genes at the same time. Specifically, ACTN1, ADAMTS2, and SLC30A8 could serve as a biomarker to distinguish AS from normal patients. Alpha-actinin (ACTN) is an actin crosslinking protein. There are four varieties of ACTN, including two isoforms not found in muscles, ACTN1 and ACTN4.12. The non-muscle cytoskeletal protein, Alpha-actinin-1, is located at microfilament bundles and adherens-type junctions where it functions to bind actin to the cell membrane (10). To our knowledge, this is the first report of the ACTN1 have differential expression in in AS.

Studies suggest patients with missense mutation in the ACTN1 usually have an decreased number of large platelets and anisocytosis, but no *in vivo* changes to platelets (11). ADAMTS2 is an enzyme that clips a short chain of amino acids from the end of procollagens, which allows them to assemble into structural collagen molecules. The metalloproteinase ADAMTS-2 is responsible for processing fibrillar procollagen precursors to mature collagen molecules (12, 13). The Protein encoded by SLC30A8 (Solute Carrier Family 30 Member 8) is a zinc efflux transporter that impact the collection of zinc in intracellular vesicles (14). Interestingly, SNPs in SLC30A8 are extremely associated with Type 2 diabetes and gender-specific schizophrenia (15–17). It is likely that Zinc transporters or insulin secretion play a direct role in AS.

In spite of the extensive research, we have done on AS, there are still many limitations. Due to AS's rarity, there are still a limited number of samples we can obtain. Meanwhile, the functions of these significantly expressed genes needs to be verified *in vitro* and *in vivo*. Developing and finding drugs that target these genes is also necessary.

Data availability statement

The original contributions presented in this study are included in the article/supplementary material, further inquiries can be directed to the corresponding author.

Ethics statement

The studies involving human participants were reviewed and approved by the Tongji Medical College. The patients/participants provided their written informed consent to participate in this study.

Author contributions

TH and YL had the idea and launched the investigation. YL analyzed the results and drafted the manuscript. All authors contributed to the article and approved the submitted version.

Conflict of interest

The authors declare that the research was conducted in the absence of any commercial or financial relationships that could be construed as a potential conflict of interest.

Publisher's note

References

1. Van Buggenhout G, Fryns J-P. Angelman syndrome (as, mim 105830). *Eur J Hum Genet.* (2009) 17:1367–73.

2. Williams CA. Neurological aspects of the Angelman syndrome. *Brain Dev.* (2005) 27:88–94.

3. Fang M, Li Y, Ren J, Hu R, Gao X, Chen L. Epilepsy-associated ube3a deficiency downregulates retinoic acid signalling pathway. *Front Genet.* (2021) 12:681295. doi: 10.3389/fgene.2021.681295

4. Dagli A, Buiting K, Williams C. Molecular and clinical aspects of Angelman syndrome. *Mol Syndromol.* (2011) 2:100–12.

5. Wang J, Lou SS, Wang T, Wu RJ, Li G, Zhao M, et al. UBE3A-mediated PTPA ubiquitination and degradation regulate PP2A activity and dendritic spine morphology. *Proc Natl Acad Sci USA.* (2019) 116:12500–5. doi: 10.1073/pnas.1820131116

6. Margolis SS, Sell GL, Zbinden MA, Bird LM. Angelman syndrome. *Neurotherapeutics.* (2015) 12:641–50.

7. Williams CA, Driscoll DJ, Dagli AI. Clinical and genetic aspects of Angelman syndrome. *Genet Med.* (2010) 12:385–95.

8. Haynes WA, Vallania F, Liu C, Bongen E, Tomczak A, Andres-Terrè M, et al. Empowering multi-cohort gene expression analysis to increase reproducibility. *Pac Symp Biocomput.* (2017) 22:144–53. doi: 10.1142/9789813207813_0015

9. Markati T, Duis J, Servais L. Therapies in preclinical and clinical development for Angelman syndrome. *Expert Opin Invest Drugs.* (2021) 30:709–20.

10. Kunishima S, Okuno Y, Yoshida K, Shiraishi Y, Sanada M, Muramatsu H, et al. ACTN1 mutations cause congenital macrothrombocytopenia. *Am J Hum Genet.* (2013) 92:431–8.

11. Guéguen P, Rouault K, Chen JM, Raguénès O, Fichou Y, Hardy E, et al. A missense mutation in the alpha-actinin 1 gene (ACTN1) is the cause of autosomal dominant macrothrombocytopenia in a large French family. *PLoS One.* (2013) 8:e74728. doi: 10.1371/journal.pone.0074728

12. Dubail J, Kesteloot F, Deroanne C, Motte P, Lambert V, Rakic JM, et al. ADAMTS-2 functions as anti-angiogenic and anti-tumoral molecule independently of its catalytic activity. *Cell Mol Life Sci.* (2010) 67:4213–32. doi: 10.1007/s00018-010-0431-6

13. Wang W-M, Lee S, Steiglitz BM, Scott IC, Lebares CC, Allen ML, et al. Transforming growth factor-β induces secretion of activated ADAMTS-2: a procollagen III N-proteinase. *J Biol Chem.* (2003) 278:19549–57. doi: 10.1074/jbc.M300767200

14. Pound LD, Sarkar SA, Benninger RK, Wang Y, Suwanichkul A, Shadoan MK, et al. Deletion of the mouse Slc30a8 gene encoding zinc transporter-8 results in impaired insulin secretion. *Biochem J.* (2009) 421:371–6.

15. Fukue K, Itsumura N, Tsuji N, Nishino K, Nagao M, Narita H, et al. Evaluation of the roles of the cytosolic N-terminus and His-rich loop of ZNT proteins using ZNT2 and ZNT3 chimeric mutants. *Sci Rep.* (2018) 8:14084. doi: 10.1038/s41598-018-32372-8

16. Rutter GA, Chimienti F. SLC30A8 mutations in type 2 diabetes. *Diabetologia.* (2015) 58:31–6.

17. Tamaki M, Fujitani Y, Hara A, Uchida T, Tamura Y, Takeno K, et al. The diabetes-susceptible gene SLC30A8/ZnT8 regulates hepatic insulin clearance. *J Clin Invest.* (2013) 123:4513–24. doi: 10.1172/JCI68807

frontiers | Frontiers in Medicine

TYPE Brief Research Report
PUBLISHED 30 August 2022
DOI 10.3389/fmed.2022.944950

OPEN ACCESS

EDITED BY
Jian Gao,
Shanghai Children's Medical Center, China

REVIEWED BY
Dora Janeth Fonseca,
Rosario University, Colombia
Muhammad Umair,
University of Management and Technology, Pakistan

*CORRESPONDENCE
Jun Guo
guojunbjmu@163.com

†These authors have contributed equally to this work

SPECIALTY SECTION
This article was submitted to Precision Medicine, a section of the journal Frontiers in Medicine

RECEIVED 16 May 2022
ACCEPTED 08 August 2022
PUBLISHED 30 August 2022

CITATION
Chen Y, Sun Q, Hao C, Guo R, Wang C, Yang W, Zhang Y, Wang F, Li W and Guo J (2022) Identification of a novel variant in N-cadherin associated with dilated cardiomyopathy. *Front. Med.* 9:944950. doi: 10.3389/fmed.2022.944950

Identification of a novel variant in N-cadherin associated with dilated cardiomyopathy

Yuanying Chen[1,2†], Qiqing Sun[3†], Chanjuan Hao[1,2], Ruolan Guo[1,2], Chentong Wang[1,2], Weili Yang[2], Yaodong Zhang[2], Fangjie Wang[3], Wei Li[1,2] and Jun Guo[1,2*]

[1]Beijing Key Laboratory for Genetics of Birth Defects, Beijing Pediatric Research Institute, MOE Key Laboratory of Major Diseases in Children, Capital Medical University, Center of Rare Diseases, National Center for Children's Health, Beijing Children's Hospital, Capital Medical University, Beijing, China, [2]Henan Key Laboratory of Pediatric Inherited and Metabolic Diseases, Children's Hospital Affiliated to Zhengzhou University, Zhengzhou Hospital of Beijing Children's Hospital, Zhengzhou, China, [3]Department of Cardiology, Children's Hospital Affiliated to Zhengzhou University, Zhengzhou Hospital of Beijing Children's Hospital, Zhengzhou, China

Background: Dilated cardiomyopathy (DCM), which is a major cause of heart failure, is a primary cardiac muscle disease with high morbidity and mortality rates. DCM is a genetically heritable disease and more than 10 gene ontologies have been implicated in DCM. *CDH2* encodes N-cadherin and belongs to a superfamily of transmembrane proteins that mediate cell–cell adhesion in a calcium-dependent manner. Deficiency of *CDH2* is associated with arrhythmogenic right ventricular cardiomyopathy (OMIM: 618920) and agenesis of the corpus callosum, cardiac, ocular, and genital syndrome (OMIM: 618929). However, there have been no reports of isolated DCM associated with *CDH2* deficiency.

Methods: We performed whole exome sequencing in a 12-year-old girl with non-syndromic DCM and her unaffected parents. Variants in both known DCM-related genes and novel candidate genes were analyzed and pathogenicity confirmation experiments were performed.

Results: No pathogenic/likely pathogenic variant in known DCM-related genes was identified in the patient. We found a *de novo* variant in a candidate gene *CDH2* in the patient, namely, c.474G>C/p.Lys158Asn (NM_001792.5). This variant has not been reported in the ClinVar or Human Gene Mutation Database (HGMD). CDH2 p.Lys158Asn was found in the conserved domain of N-cadherin, which is associated with the hydrolysis of the precursor segment and interference with adhesiveness. Furthermore, we tested the expression and efficiency of cell–cell adhesion while overexpressing the CDH2 Lys158Asn mutant and two previously reported variants in *CDH2* as positive controls. The adhesion efficiency was considerably reduced in the presence of the mutated CDH2 protein compared with wild-type CDH2 protein, which suggested that the mutated CDH2 protein's adhesion capacity was impaired. The variant was probably pathogenic after integrating clinical manifestations, genetic analysis, and functional tests.

Conclusion: We identified a *CDH2* variant in DCM. We observed a new clinical symptom associated with N-cadherin deficiency and broadened the genetic spectra of DCM.

KEYWORDS

N-cadherin, dilated cardiomyopathy, cell-cell adhesion, *de novo* variant, whole exome sequencing

Introduction

Dilated cardiomyopathy (DCM), which is a major cause of heart disorders, is a primary cardiac muscle disease with high morbidity and mortality rates (1). The estimated incidence and prevalence of DCM is 1:2,500–3,000 (2). However, DCM might be much more common, and the frequency could be 1 in 250 individuals (3). The genetic basis of DCM is highly complex and diverse. Gene mutations contributing to DCM affect the function of proteins, including sarcomere, cytoskeleton, nuclear envelope, γ-secretase activity, ion channel, mitochondrial, spliceosomal, sarcoplasmic reticulum, and desmosomal proteins (3). There are more than 50 DCM-associated genes, but only 12 genes (*BAG3*, *DES*, *DSP*, *FLNC*, *LMNA*, *MYH7*, *PLN*, *RBM20*, *SCN5A*, *TNNC1*, *TNNT2*, and *TTN*) are classified as having a definitive or strong relationship with DCM (4, 5).

The *CDH2* gene encodes N-cadherin, which is a classical type I cadherin that plays a critical role in cell–cell adhesion in the nervous system and the heart (6–8). Rare heterozygous *CDH2* variants are associated with the occurrence of human diseases. Accogli et al. reported nine individuals with variants in *CDH2* who showed agenesis of the corpus callosum, cardiac, ocular, and genital (ACOG) syndrome (9). Variants of *CDH2* also cause arrhythmogenic right ventricular cardiomyopathy (ARVC) (10–12), Peters anomaly (13), and brain arteriovenous malformation (14) in a few cases. Besides the biological relevance of N-cadherin in human illnesses, animals lacking N-cadherin in certain tissues show impaired internal cortex structures (15) and cardiac function (16–18).

In this study, we identified a *de novo* heterozygous *CDH2* variant, c.474G>C/p.Lys158Asn (NM_001792.5), in a non-syndromic patient who had DCM without other abnormalities using trio whole exome sequencing. To explain the pathogenicity, we ectopically overexpressed wild-type CDH2 protein and its variants in HeLa cells. We found that the adhesion efficiency was considerably lower when carrying the mutated CDH2 proteins than that with the wild-type protein, which indicated that the adhesive ability of mutated N-cadherin was impaired. To the best of our knowledge, there have been no reports of *CDH2* deficiency in isolated DCM. We identified a novel *CDH2* variant and extended the genotype–phenotype spectrum of DCM.

Materials and methods

Participants

The proband was a girl aged 12 years who was admitted to the Department of Cardiology, Zhengzhou Hospital of Beijing Children's Hospital because of edema in both lower limbs without obvious inducement. This study was approved by the Institutional Review Board (IRB) of Beijing Children's Hospital, Capital Medical University (Ethics Approval Number 2015-26). Informed consent was obtained from the subject and her parents. The use of patient-specific information and images was granted by her parents.

Whole exome sequencing, bioinformatics analysis, and Sanger sequencing

Genomic DNA of peripheral blood was extracted, purified, and broken into random segments. The genomic DNA was then captured using the Agilent SureSelect Human All Exome V6 Kit (Agilent Technologies, Santa Clara, CA, USA), and a sequencing library was prepared. Using the Illumina Hiseq X Ten sequencer (Illumina, San Diego, CA, USA), we carried out whole exome sequencing with a reading length of 150 bp. The data obtained from sequencing (raw data) were subject to quality control, basic data analysis, and filtering to remove joint sequences and repeat sequences. Sequence alignment was performed according to the GRCh37/hg19 human reference genome sequence, and the single-nucleotide polymorphisms and insertion–deletion polymorphisms of samples were annotated. Sequencing depth, coverage, and homogeneity were counted. Variants were filtered according to the analytical workflow (Figure 1A). We analyzed the variant frequency and filtered out the common variants with an allele population variation >0.5%, or >2% if the variant was homozygous or if there was a second variant in the gene using 1000 Genome, dbSNP, gnomAD, and in-house databases. Variants were classified into two categories: variants in DCM-related genes and variants in novel candidate DCM genes. Fifty-one genes curated by a DCM Gene Curation Expert Panel that proposed to have a monogenic role in isolated, idiopathic DCM in humans were considered as DCM-related genes (Supplementary Table S1) (5).

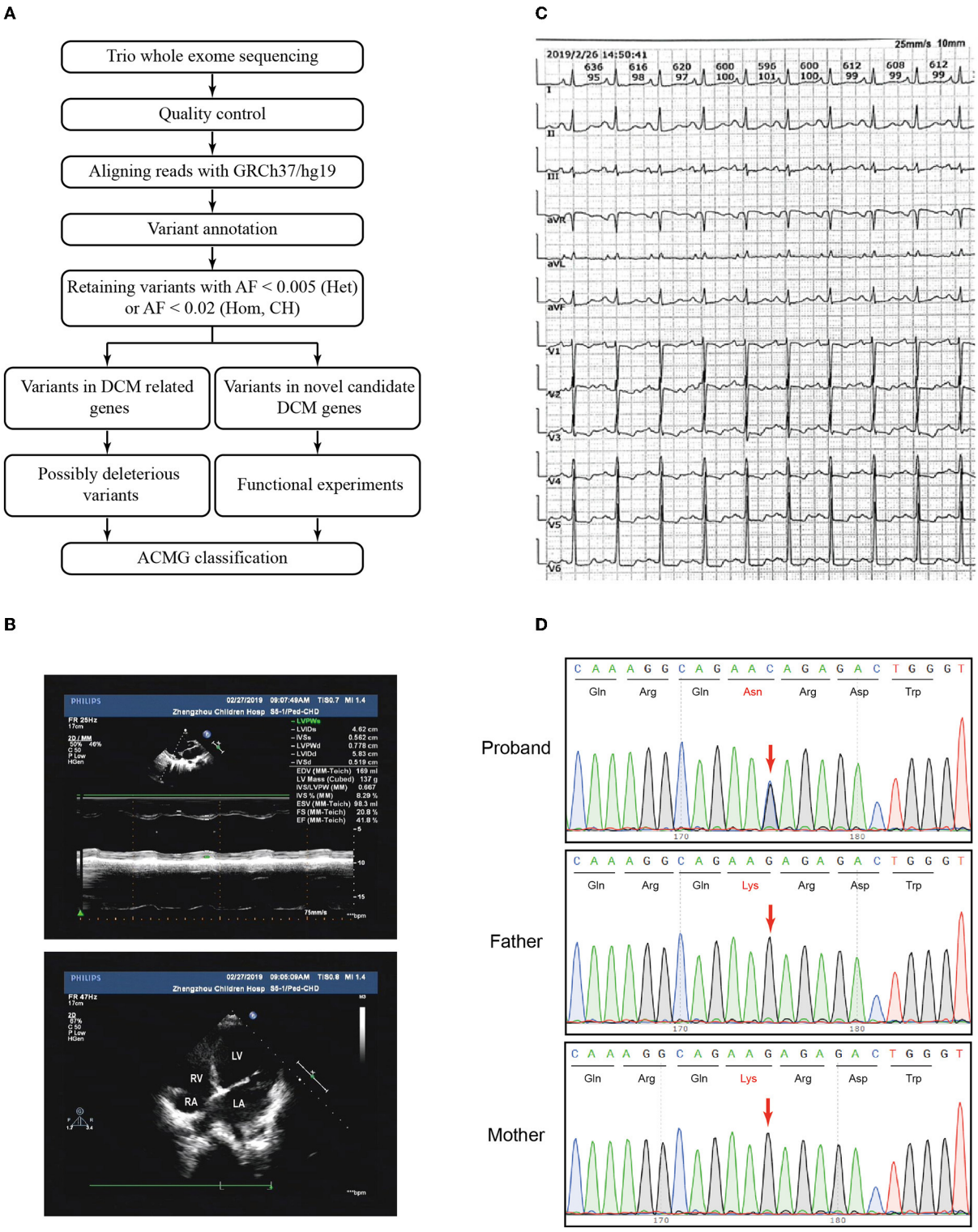

FIGURE 1
Variant filtration workflow and the phenotype of the patient. **(A)** Variant filtration workflow employed in this study. AF: allele frequency; Het, heterozygous; Hom, homozygous; CH, compound heterozygous; DCM, dilated cardiomyopathy; ACMG, American College of Medical Genetics and Genomics. **(B)** The echocardiography showed an apical four-chamber view of the proband's indicating dilation of the right ventricle. RV, right ventricle; RA, right atrium; LV, left ventricle; LA, left atrium. **(C)** Electrocardiogram (ECG) showed sinus rhythm, P wave changes, and ST-T changes. **(D)** Sanger sequencing confirmed that the variant *CDH2* c.474G>C was heterozygous in the proband and not inherited from her parents. The arrows indicated the mutated nucleotides.

Prediction software, such as Polyphen-2 (http://genetics.bwh.harvard.edu/pph2/), SIFT (http://sift.jcvi.org), Mutation Taster (http://www.mutationtaster.org), and CADD (http://cadd.gs.washington.edu/), was used to evaluate the harmfulness of the variants. Loss-of-function (LoF) variants, such as stop gain, stop loss, frameshift indels, and splice site variants (2 nt plus/minus the exon boundary), as well as missense variants predicted to be deleterious by at least two prediction tools were defined as possibly deleterious variants. The pathogenicity of variants was classified in accordance with the American College of Medical Genetics and Genomics (ACMG) Standards and Guidelines (19). Sanger sequencing was performed using the ABI 3730xl DNA Analyzer (Applied Biosystems, MA, USA). The used oligonucleotides are chr18-25591882-Forward 5'-GGCTTTCTACAACACTACAGAAAT-3' and chr18-25591882-Reverse 5'-ACTGTGATTCCTATGCTTTCAGGT-3'.

Constructs and site-directed mutagenesis

The *CDH2* cDNA library for the human N-cadherin cloning template was purchased from OriGene (China). Using the site-directed mutagenesis strategy, wild-type CDH2 (pCMV6-CDH2-Flag) and mutation constructs (pCMV6-CDH2 Lys158Asn-Flag, pCMV6-CDH2 Asp407Asn-Flag, and pCMV6-CDH2 Asp597Asn-Flag) were successfully established using KOD-Plus Neo (TOYOBO, Japan) and Dpn I (Thermo Fisher Scientific, USA). The primers used to generate amplicons of *CDH2*-specific variation sites are shown in Supplementary Table S2. Positive clones were verified by sequencing.

Western blot

HeLa cells (Zhejiang Meisen Cell Technology Co., Ltd. Catalog number: CTCC-001-0006) were transfected, collected, and lysed using cell lysis buffer (Beyotime Biotechnology, China). Sodium dodecyl sulfate-polyacrylamide gel electrophoresis (SDS-PAGE) was performed using a 4–15% gradient gel (Applygen Technologies, China). Proteins were electrophoretically transferred onto a polyvinylidene fluoride (PVDF) membrane and subjected to immunoblotting. Flag and β-actin antibodies were purchased from Sigma (Merck, Germany) with a dilution of 1:1000 in Western blot.

Cell–cell adhesion assay

The cell–cell adhesion assay was conducted following the protocol as described by Accogli et al. with slight modifications (9). HeLa cells were transfected with a pCMV6-Flag vector (Control), pCMV6-CDH2-Flag (CDH2), pCMV6-CDH2 Lys158Asn-Flag (CDH2 Lys158Asn), pCMV6-CDH2 Asp407Asn-Flag (CDH2 Asp407Asn), and pCMV6-CDH2 Asp597Asn-Flag (CDH2 Asp597Asn) constructs for 24 h. Transfected cells were trypsinized and seeded in triplicate (1×10^5/well) into a 24-well plate with extracellular buffer (140 mM NaCl, 5 mM KCl, 10 mM glucose, and 10 mM HEPES) containing 2 mM Ca^{2+} and 1% bovine serum albumin. The cells were then incubated for 1 h at 37°C for aggregate formation. An aggregate was defined as >4 cells. The aggregated cell number (A1) and the total cell number (A0) were counted. The fraction of cell adhesion was defined as A1/A0.

Statistical analysis

Data are shown as mean ± standard deviation of three independent experiments. One-way analysis of variance was used to conduct statistical analysis, and Bonferroni's correction was used to perform multiple comparisons. The significance value was set at $p < 0.05$.

Results

Clinical description

The proband had intermittent edema of both lower limbs for 14 days. She was born full-term with a birth weight of 3.15 kg and had normal physical and mental development. While growing up, she had poor physical condition. She usually had difficulty in movement, easily sweated after activities, easily vomited, and had abdominal discomfort. According to her history, the patient appeared to have chronic cardiac insufficiency. The patient's parents were non-consanguineous and reported no family history of cardiomyopathy.

Echocardiography and diagnosis

The patient and her parents had echocardiography performed. The patient showed an enlarged left atrium and left ventricle, mild to moderate mitral regurgitation, mild tricuspid regurgitation, and slightly decreased left ventricular systolic function (Figure 1B, Table 1). Electrocardiogram (ECG) showed sinus rhythm, P wave changes, and ST-T changes (Figure 1C). Combined with her previous medical history, a diagnosis of DCM was considered (1). Echocardiography showed that the left ventricular end diastolic dimension (LVDd) of the patient was 58.3 mm, which is much larger (>117%) than normal left ventricular diastolic dysfunction values. The patient's left ventricular ejection fraction was 42%, and fractional shortening

TABLE 1 Measurement data of echocardiography.

Name	Measurement	Name	Measurement	Name	Measurement
LAD	51.6 mm	RAD	34.3 mm	RVOT	20.1 mm
MPA	21.5 mm	Vmax	0.59 m/s	LPA	9.4 mm
RPA	10.1 mm	AoD	18.1 mm	Vmax	0.84 m/s
MVE	0.79 m/s	MVA	0.47 m/s	TVE	0.49 m/s
TVA	0.31 m/s	RVDd	13.9 mm	IVSTd	5.2 mm
LVDd	58.3 mm	LVPWd	6.5 mm	LVDs	46.2 mm
EDV	169 ml	ESV	98.3 ml	SV	70.7 ml
EF	42%	FS	21%	DAO	0.98 m/s

LAD, left atrium dimension; MPA, main pulmonary artery; RPA, right pulmonary artery; MVE, mitral valve inflow E wave velocity; TVA, tricuspid valve inflow A wave velocity; LVDd, left ventricular end diastolic dimension; EDV, end diastolic volume; EF, ejection fraction; RAD, right atrium dimension; Vmax, maximum velocity; AoD, ascending aorta dimension; MVA, mitral valve inflow A wave velocity; RVDd, right ventricular end diastolic dimension; LVPWd, left ventricular posterior wall dimension; ESV, end-systolic volume; FS, fractional shortening; RVOT, right ventricular outflow tract; LPA, left pulmonary artery; TVE, tricuspid valve inflow E wave velocity; IVSTd, interventricular septum time dimension; LVDs, left ventricular end-systolic dimension; SV, stroke volume; DAO, descending aorta.

(FS) was 21%, which met the diagnostic criteria of DCM. The patient's parents had no symptoms of heart failure, and their echocardiographic findings were normal. The proband and her parents were enrolled in this study. Blood samples were obtained to conduct whole exome sequencing because gene mutations that contribute to DCM are highly diverse and complex.

Genetic analysis

Trio whole exome sequencing was performed using peripheral blood DNA from the patient with DCM and her unaffected parents. A total of 354 rare variants in the proband (Supplementary Table S3) were detected. Five rare heterozygous variants in DCM-related genes were identified and 3 of which were possibly deleterious variants in this patient (Supplementary Table S4), including a variant in *MYH6* inherited from the patient's father and 2 variants in *TTN* inherited from the patient's father and mother, respectively. No pathogenic/likely pathogenic variant in DCM-related genes was identified in the proband according to the ACMG guidelines. To identify variants in novel candidate DCM genes, we evaluated the homozygous, compound heterozygous, and *de novo* variants after variant filtration, and found a *de novo* *CDH2* variant, NC_000018.9(NM_001792.5):c.474G>C, NP_001783.2:p.(Lys158Asn), in the patient. Subsequent Sanger sequencing confirmed that the variant was heterozygous in the proband and not inherited from her parents (Figure 1D).

This variant has not been reported in the Human Gene Mutation Database (HGMD) or ClinVar database and is not present in population databases. Multiple *in silico* prediction tools supported a pathogenic effect (Table 2) of this variant. Sequence alignment indicated that the variant was conserved among most species (Figure 2A). CDH2 is structurally divided into a signal peptide, a cadherin propeptide, five extracellular cadherin repeats, a transmembrane region, and a cytoplasmic tail. Recently, several rare heterozygous *CDH2* variants encoding extracellular cadherin repeats and the cytosolic region were associated with ARVC, ACOG syndrome, Peters anomaly, and arteriovenous malformation in the brain (Figure 2B). The CDH2 Lys158Asn variant in our proband is located at the propeptide domain, which is responsible for endoproteolytic cleavage. Amino acid mutations in the propeptide (Arg-X_1-Lys-Arg-X_2-Trp, i.e., R-X_1-K-R-X_2-W polypeptide) lead to the inability of

TABLE 2 Population Allele frequency and predicted pathogenicity score of the *CDH2* variant.

	NC_000018.9(NM_001792.5):c.474G>C, NP_001783.2:p.(Lys158Asn)
Gene	*CDH2*
Chromosome location	chr18:25591882
Transcript	NM_001792.5
Amino acid change	p.Lys158Asn
Zygosity	Heterozygous
Allele frequency in population	
gnomAD_exome East Asian	-
1000 genomes	-
dbSNP	-
ExAc	-
***In silico* prediction**	
SIFT	Damaging (score: 0.002)
Polyphen-2_HVAR	Probably damaging (score: 0.998)
MutationTaster	Disease causing (score: 1.0)
CADD	Damaging (score: 33)

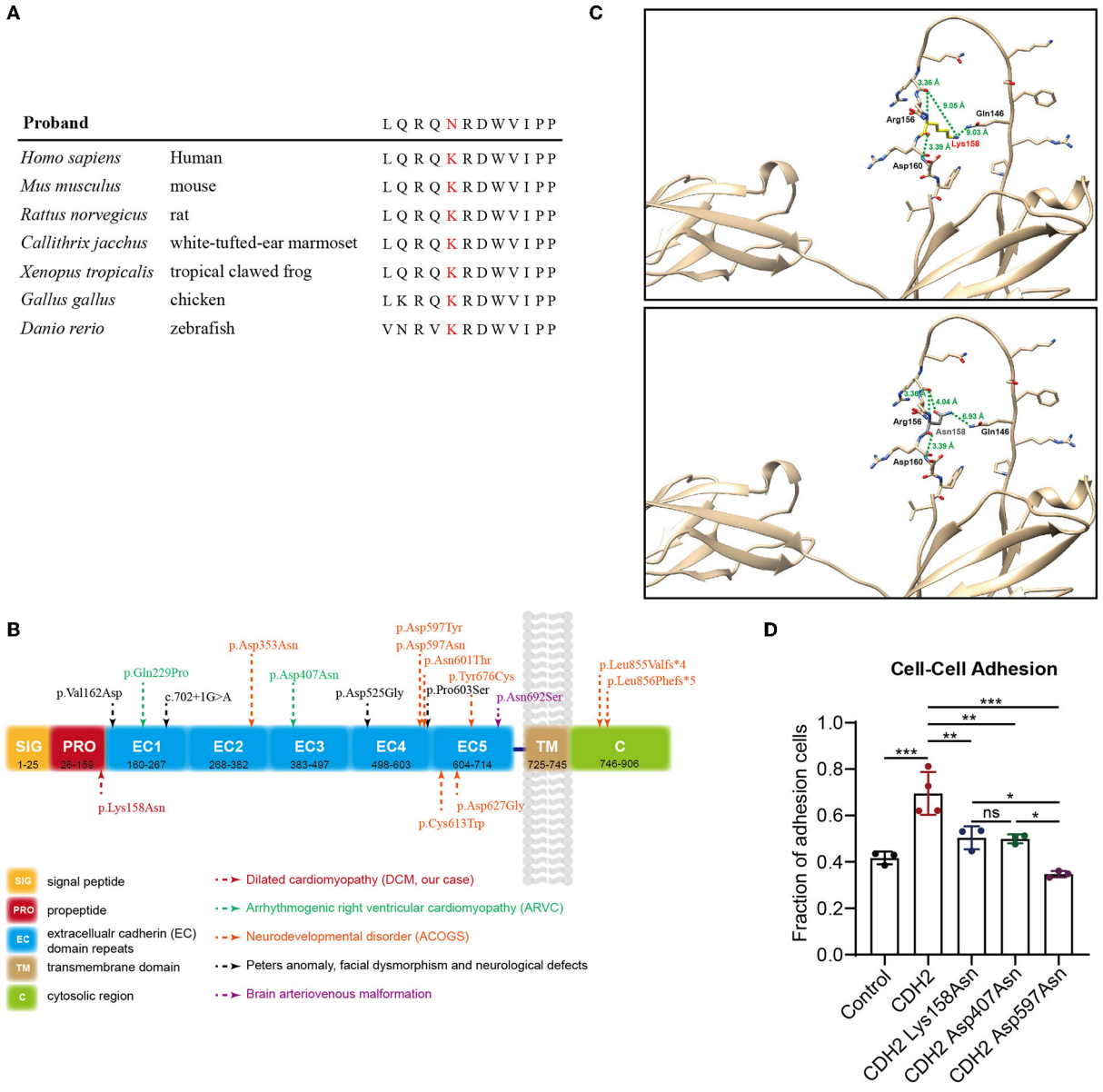

FIGURE 2
Genetic analysis and functional tests of the *de novo* variant (c.474G>C/p.Lys158Asn) in *CDH2*. **(A)** Sequence alignment of human CDH2 and other species shows the conservation of the affected residue (p.Lys158Asn). **(B)** Schematic representation of the topological domains of CDH2 protein. Rare heterozygous *CDH2* variants linked to ARVC, ACOGs, Peters anomaly, and brain arteriovenous malformation were annotated. **(C)** The structure of CDH2 and Lys158Asn mutant. The human CDH2 protein structure was modeled from the "AlphaFold Protein Structure Database" (AlphaFoldDB: P19022, https://alphafold.com/). The structure was aligned with the solution structure of neural cadherin prodomain (PDB: 1OP4) and analyzed using UCSF chimera. **(D)** The cell-cell adhesion efficiency of the wild-type and CDH2 variations. The significance value was set as $p < 0.05$ (*), $p < 0.01$ (**), and $p < 0.001$ (***).

hydrolysis of the precursor segment and might interfere with adhesiveness.

Functional experiments

In the first place, we analyze the structure of CDH2 and Lys158Asn mutant. The human CDH2 protein structure was modeled from the "AlphaFold Protein Structure Database" (AlphaFoldDB: P19022, https://alphafold.com/). The structure was aligned with the solution structure of neural cadherin prodomain (PDB: 1OP4) and analyzed using UCSF chimera (20). The CDH2 Lys158Asn mutant was located in a long unstructured loop. We evaluated the hydrogen bond forming, the distances between amino acids, the structural clashes, and the molecule contacts. We found that the backbone of the 158

lysine (Lys158) residue can form polar interactions between nearby 156 Arginine (Arg156) and 160 aspartic acid (Asp160). The lysine residue changed into asparagine (Asn158) did not affect backbone polar interaction. Whereas the side chain has a violent change of conformation, thus the remote distances (9.05 Å and 9.03 Å) from 146 glutamine (Gln146) changed into 4.04 Å and 6.93 Å and may impair the endoproteolytic cleavage (Figure 2C). Then, functional experiments were performed to further evaluate the pathogenicity of the *CDH2* variant. We cloned *CDH2* and its variants into a flag-tagged pCMV6-Entry vector using site-directed mutagenesis. Two additional *CDH2* variants, p.Asp407Asn and p.Asp597Asn, were used as positive controls, because they have been proved to be pathogenic or experimentally demonstrate to impair cell–cell adhesion. An empty flag-tagged pCMV6-Entry vector was used as a negative control. Control plasmids, the wild-type, and constructs carrying *CDH2* variations were transfected into HeLa cells and seeded for Western blot and cell–cell adhesion assays. There were no significant differences in protein concentrations between the wild-type and CDH2 Lys158Asn and CDH2 Asp407Asn. The protein expression level of CDH2 Asp597Asn was 40% higher than that of the wild-type (Supplementary Figures S1A,B), which may be an artifact of overexpression. We then normalized protein expression levels and conducted a cell–cell adhesion assay. The cell–cell adhesion efficiency of CDH2 Lys158Asn was approximately 30% lower compared with the wild-type CDH2 (Figure 2D). Additionally, the cell–cell adhesion efficiency of CDH2 Asp597Asn was 20% lower than that of CDH2 Lys158Asn and CDH2 Asp407Asn. This finding indicated a relationship between the loss of mediating the cell–cell adhesion ability and pathogenicity. According to the ACMG guidelines, the *CDH2* variant, NC_000018.9(NM_001792.5):c.474G>C and NP_001783.2:p.(Lys158Asn), was classified as pathogenic (PS2+PS3+PM2+PP3) after integrating genetic analysis and functional tests.

Discussion

In this study, no pathogenic/likely pathogenic variant in 51 DCM-related genes based on previous reports (Supplementary Table S1) was identified in the proband. However, we identified a *de novo CDH2* heterozygous missense variant, c.474G>C/p.Lys158Asn.

Classical cadherin proteins are involved in the cell–cell adhesion process (21, 22). The classical cadherins are subdivided into types I and II and are comprised of five repeated extracellular (EC1–5) regions. The extracellular domain of cadherins provides three calcium-binding pockets and interacts with other cadherins in *cis* and *trans*. The cytoplasmic tail of cadherins binds with adaptor proteins, such as catenins, which connect cadherins to the actomyosin cytoskeleton (21, 23). *CDH2* encodes N-cadherin, which is a transmembrane protein and a critical calcium-dependent factor that mediates cell–cell adhesion (24). N-cadherin is highly expressed in the heart and other tissues, such as neurons. In heart tissues, N-cadherin is expressed in a structure called the intercalated disc, through which cardiomyocytes are extensively interconnected (25). The intercalated disc ensures tight electromechanical coupling of cardiomyocytes, thus protecting the integrity and function of the myocardium. This highly organized structure comprises three junction complexes of gap junctions, desmosomes, and adherens junctions. The gap junction is essential for intercellular communications, especially rapid electrical transmission between cells (26). The desmosomes provide structural support *via* interactions of desmosomal cadherins with the filament system desmin (27). Adherens junctions are composed of a classic cadherin in the heart, N-cadherin, and mediate calcium-dependent cell adhesion (28). The junction complexes of the intercalated disc must be organized properly to maintain the normal function of myocytes. The two desmosomal cadherins desmocollin-2 (*DSC2*) and desmoglein-2 (*DSG2*) mediate cell–cell adhesion of cardiomyocytes. Heterozygous or homozygous variants of *DSC2* and *DSG2* have been described in patients with arrhythmogenic cardiomyopathy (29–31).

Limited data have implicated the involvement of N-cadherin in the pathogenesis of arrhythmogenic cardiomyopathy in humans. A previous study identified a *CDH2* missense variant (c.686A>C, p.Gln229Pro) in a three-generation family with ARVC by whole exome sequencing. Subsequently, the authors examined 73 ARVC probands with negative mutations in known ARVC genes and found another likely pathogenic variant in *CDH2* (c.1219G>A, p.Asp407Asn) (10). Another study performed whole exome sequencing and genomic triangulation in a pedigree, as well as in a 14-year-old female proband with arrhythmogenic cardiomyopathy, her affected mother and sister, and her unaffected father. The authors found that *CDH2* c.1219G>A (p.Asp407Asn) was likely a pathogenic variant and concluded that *CDH2* was a novel autosomal dominant susceptibility gene for arrhythmogenic cardiomyopathy (11). Reevaluation cohort of genetic variants associated with ARVC confirmed these *CDH2* variants (12). Recently, *CDH2* variants were reported to be associated with a Mendelian neural developmental disorder. Nine individuals with a syndromic neural developmental disorder were characterized by ACOG syndrome (9). This study also showed that the variants in *CDH2* impaired the adhesive activity of N-cadherin. Therefore, *CDH2* appears to cause human genetic diseases, such as ARVC and ACOG syndrome.

Several animal models have been used to determine the essential role of N-cadherin in the structural integrity of the heart and the relationship between N-cadherin and cardiac development and function. Ferreira-Cornwell et al. established a transgenic mouse model using the mouse myosin heavy chain (MHC) promoter, which can specifically express chicken N-cadherin in the heart (αMHC/Ncad). They found that the size

of αMHC/Ncad hearts was larger than that in non-transgenic mice. Histological analysis showed a dilated left ventricle and thinner ventricular wall in αMHC/Ncad hearts, which suggested that the modulation of cadherin-mediated adhesion contributed to DCM (32). Another study generated N-cadherin conditional knockout mice using a cardiac-specific tamoxifen-inducible Cre transgene, which resulted in N-cadherin deletion in the myocardium. The authors from this previous study showed that intercalated discs, adherens junctions, and desmosomes disappeared. The mutant mice displayed moderate DCM and died because of arrhythmia (16). Another similar mouse model showed that the expression of the gap junction proteins connexin-43 and connexin-40 was significantly decreased in N-cadherin cardiac-restricted knockout mice, which led to a ventricular conduction defect (17). *CDH2* mutant zebrafish also showed an enlarged pericardial cavity and disorganized atrium and ventricle, which suggests a vital role of N-cadherin in cardiac development in zebrafish (18). Studies in animal models have suggested that N-cadherin produces the phenotype of DCM whereby it may be one of the pathogenic genes of DCM.

In our study, the patient has a large left ventricle without arrhythmia. Typical ARVC, balanced ARVC, and right ventricular dominant ARVC were not considered. There was no low voltage of QRS wave complex in limb lead and T-wave inversion in inferior wall lead in ECG, which did not support a phenotype of left ventricular dominant ARVC. So, we considered a diagnosis of idiopathic DCM. Then, we found the *de novo CDH2* variant c.474G>C (p.Lys158Asn) in the patient. This variant has not been reported in the ClinVar or HGMD. Sanger sequencing confirmed that the missense variant was heterozygous in the proband and absent in her unaffected parents. There were no facial or neurodevelopmental abnormalities in the proband. During hospitalization, digoxin, hydrochlorothiazide, spironolactone, aspirin tablets, and potassium citrate granules were used for the treatment. The proband improved and was discharged from the hospital. A follow-up study was conducted for 1 year. Initially, the proband's condition was stable. The proband's edema then became more serious, and she was hospitalized in Beijing Children's Hospital and the local hospital three times intermittently, where maintenance treatment was carried out. The edema and arrhythmia of the proband became aggravated. Her left ventricular ejection fraction was 33% at the last hospitalization. An electrocardiogram showed frequent ventricular premature beats. The patient then developed arrhythmia and died at age 13. All of the phenotypes were consistent with the manifestation of DCM.

Subsequent studies showed that the *CDH2* variant p.Lys158Asn was located in the N-cadherin prodomain and was conserved in most species. The adhesive capacity of cadherins relies on the removal of the prodomain because cleavage of the precursor peptide is required for the maturation of N-cadherin. The endogenous cleavage site mutation may not affect the N-cadherin targeting the plasma membrane but may disturb the interaction between N-cadherins to form homodimers (33, 34). Previous studies have shown that endogenous protease digestion depends on the recognition site (Arg-X_1-Lys-Arg-X_2-Trp, i.e., R-X_1-K-R-X_2-W polypeptide) (35). After the original recognition sites changed to specific digestion sites of trypsin and factor Xa, they cannot be recognized by the endogenous protease. Mutations in the endogenous recognition sites interfere with adhesive activities. Therefore, the N-cadherin mutation p.Lys158Asn in endogenous protease digestion sites may affect the proteolysis of the prodomain and subsequently affect the function of N-cadherin (35, 36). Our experiment using transfected HeLa cells with the *CDH2* Lys158Asn mutant showed unchanged protein expression levels and lower adhesion efficiency compared with those in the wild-type. This finding suggests that the N-cadherin prodomain also plays a vital role in mediating cell adhesion. Moreover, the differences in adhesion efficiency in HeLa cells between CDH2 Asp597Asn and CDH2 Lys158Asn may explain the various phenotypes. In conclusion, we identified a novel *CDH2* variant, c.474G>C (p.Lys158Asn), in a patient with nonsyndromic DCM by exome sequencing. We discovered a new clinical phenotype of this *CDH2* variant and extended the currently known genetic variety of DCM.

Data availability statement

The original contributions presented in the study are included in the article/Supplementary material, further inquiries can be directed to the corresponding author/s. Whole exome sequencing data were not deposited because of the low number of patients described in this manuscript, to protect patient privacy and confidentiality.

Ethics statement

The studies involving human participants were reviewed and approved by the Ethics Committee of Beijing Children's Hospital, Capital Medical University. Written informed consent to participate in this study was provided by the participants' legal guardian/next of kin. Written informed consent was obtained from the individual(s), and minor(s)' legal guardian/next of kin, for the publication of any potentially identifiable images or data included in this article.

Author contributions

YC and JG designed and performed most of the experiments, analyzed the data, and wrote the manuscript. QS collected clinical data of the proband. CH and RG helped to validate the data. CW and WY helped with plasmids construction. YZ, FW, and WL helped to organize the clinical data. JG were

responsible for forming the hypothesis, project development, data coordination, writing, finalizing, and submitting the manuscript. All authors have read and approved the manuscript.

Funding

This research was supported by the Ministry of Science and Technology of China (2016YFC1000306), the National Natural Science Foundation of China (81770234 and 31830054), the Beijing Municipal Science and Technology Commission Foundation (Z181100001918003), and the Beijing Municipal Commission of Health and Family Planning Foundation (ShouFa 2018-2-1141).

Acknowledgments

We greatly appreciate Dr. Yingjun Feng for the help with participant recruitments and sample collections. We thank all the people who have been involved in our study. We also thank Ellen Knapp, Ph.D., from Liwen Bianji (Edanz) (www.liwenbianji.cn/), for editing the English text of a draft of this manuscript.

Conflict of interest

The authors declare that the research was conducted in the absence of any commercial or financial relationships that could be construed as a potential conflict of interest.

Publisher's note

Supplementary material

The Supplementary Material for this article can be found online at: https://www.frontiersin.org/articles/10.3389/fmed.2022.944950/full#supplementary-material

References

1. Maron BJ, Towbin JA, Thiene G, Antzelevitch C, Corrado D, Arnett D, et al. Contemporary definitions and classification of the cardiomyopathies: an American Heart Association Scientific Statement from the Council on Clinical Cardiology, Heart Failure and Transplantation Committee; Quality of Care and Outcomes Research and Functional Genomics and Translational Biology Interdisciplinary Working Groups; and Council on Epidemiology and Prevention. *Circulation.* (2006) 113:1807–16. doi: 10.1161/CIRCULATIONAHA.106.174287

2. Miura K, Nakagawa H, Morikawa Y, Sasayama S, Matsumori A, Hasegawa K, et al. Epidemiology of idiopathic cardiomyopathy in Japan: results from a nationwide survey. *Heart.* (2002) 87:126–30. doi: 10.1136/heart.87.2.126

3. Hershberger RE, Hedges DJ, Morales A. Dilated cardiomyopathy: the complexity of a diverse genetic architecture. *Nat Rev Cardiol.* (2013) 10:531–47. doi: 10.1038/nrcardio.2013.105

4. Gerull, B., Klaassen, S. and Brodehl, A. The genetic landscape of cardiomyopathies. *Cell Metab.* (2019) 21:174–182. doi: 10.1007/978-3-030-27371-2_2

5. Jordan E, Peterson L, Ai T, Asatryan B, Bronicki L, Brown E, et al. Evidence-Based assessment of genes in dilated cardiomyopathy. *Circulation.* (2021) 144:7–19. doi: 10.1161/CIRCULATIONAHA.120.053033

6. Radice GL. N-cadherin-mediated adhesion and signaling from development to disease: lessons from mice. *Prog Mol Biol Transl Sci.* (2013) 116:263–89. doi: 10.1016/B978-0-12-394311-8.00012-1

7. Nguyen T, Mege RM. N-cadherin and fibroblast growth factor receptors crosstalk in the control of developmental and cancer cell migrations. *Eur J Cell Biol.* (2016) 95:415-26. doi: 10.1016/j.ejcb.2016.05.002

8. Cao ZQ, Wang Z, Leng, P. Aberrant N-cadherin expression in cancer. *Biomed Pharmacother.* (2019) 118:109320. doi: 10.1016/j.biopha.2019.109320

9. Accogli A, Calabretta S, St-Onge J, Boudrahem-Addour N, Dionne-Laporte A, Joset P, et al. De Novo pathogenic variants in n-cadherin cause a syndromic neurodevelopmental disorder with corpus collosum, axon, cardiac, ocular, and genital defects. *Am J Hum Genet.* (2019) 105:854–68. doi: 10.1016/j.ajhg.2019.09.005

10. Mayosi BM, Fish M, Shaboodien G, Mastantuono E, Kraus S, Wieland T, et al. Identification of Cadherin 2 (CDH2) Mutations in Arrhythmogenic Right Ventricular Cardiomyopathy. *Circ Cardiovasc Genet.* (2017) 10:1605. doi: 10.1161/CIRCGENETICS.116.001605

11. Turkowski KL, Tester DJ, Bos JM, Haugaa KH, Ackerman MJ. Whole exome sequencing with genomic triangulation implicates CDH2-encoded N-cadherin as a novel pathogenic substrate for arrhythmogenic cardiomyopathy. *Congenit Heart Dis.* (2017) 12:226–35. doi: 10.1111/chd.12462

12. Ye JZ, Delmar M, Lundby A, Olesen MS. Reevaluation of genetic variants previously associated with arrhythmogenic right ventricular cardiomyopathy integrating population-based cohorts and proteomics data. *Clin Genet.* (2019) 96:506–14. doi: 10.1111/cge.13621

13. Reis LM, Houssin NS, Zamora C, Abdul-Rahman O, Kalish JM, Zackai EH, et al. Novel variants in CDH2 are associated with a new syndrome including Peters anomaly. *Clin Genet.* (2020) 97:502–8. doi: 10.1111/cge.13660

14. Wang K, Zhao S, Liu B, Zhang Q, Li Y, Liu J, et al. Perturbations of BMP/TGF-beta and VEGF/VEGFR signalling pathways in non-syndromic sporadic brain arteriovenous malformations (BAVM). *J Med Genet.* (2018) 55:675–84. doi: 10.1136/jmedgenet-2017-105224

15. Kadowaki M, Nakamura S, Machon O, Krauss S, Radice GL. and Takeichi, M. N-cadherin mediates cortical organization in the mouse brain. *Dev Biol.* (2007) 304:22–33. doi: 10.1016/j.ydbio.2006.12.014

16. Kostetskii I, Li J, Xiong Y, Zhou R, Ferrari VA, Patel VV, et al. Induced deletion of the N-cadherin gene in the heart leads to dissolution of the intercalated disc structure. *Circ Res.* (2005) 96:346–54. doi: 10.1161/01.RES.0000156274.72390.2c

17. Li J, Patel VV, Kostetskii I, Xiong Y, Chu AF, Jacobson JT, et al. Cardiac-specific loss of N-cadherin leads to alteration in connexins with conduction slowing and arrhythmogenesis. *Circ Res.* (2005) 97:474–81. doi: 10.1161/01.RES.0000181132.11393.18

18. Bagatto B, Francl J, Liu B, Liu Q. Cadherin2 (N-cadherin) plays an essential role in zebrafish cardiovascular development. *BMC Dev Biol.* (2006) 6:23. doi: 10.1186/1471-213X-6-23

19. Richards S, Aziz N, Bale S, Bick D, Das S, Gastier-Foster J, et al. Standards and guidelines for the interpretation of sequence variants: a joint consensus recommendation of the American College of Medical Genetics and Genomics and the Association for Molecular Pathology. *Genet Med.* (2015) 17:405–24. doi: 10.1038/gim.2015.30

20. Pettersen EF, Goddard TD, Huang CC, Couch GS, Greenblatt DM, Meng EC, et al. UCSF Chimera–a visualization system for exploratory research and analysis. *J Comput Chem.* (2004) 25:1605–12. doi: 10.1002/jcc.20084

21. Wickström SA, Niessen CM. Cell adhesion and mechanics as drivers of tissue organization and differentiation: local cues for large scale organization. *Curr Opin Cell Biol.* (2018) 54:89–97. doi: 10.1016/j.ceb.2018.05.003

22. Priest AV, Shafraz O, Sivasankar S. Biophysical basis of cadherin mediated cell-cell adhesion. *Exp Cell Res.* (2017) 358:10–3. doi: 10.1016/j.yexcr.2017.03.015

23. Arslan FN, Eckert J, Schmidt T, Heisenberg CP. Holding it together: when cadherin meets cadherin. *Biophys J.* (2021) 120:4182–92. doi: 10.1016/j.bpj.2021.03.025

24. Hatta K, Nose A, Nagafuchi A, Takeichi M. Cloning and expression of cDNA encoding a neural calcium-dependent cell adhesion molecule: its identity in the cadherin gene family. *J Cell Biol.* (1988) 106:873–81. doi: 10.1083/jcb.106.3.873

25. Sheikh F, Ross RS, Chen, J. Cell-cell connection to cardiac disease. *Trends Cardiovasc Med.* (2009) 19:182–90. doi: 10.1016/j.tcm.2009.12.001

26. Severs NJ, Rothery S, Dupont E, Coppen SR, Yeh HI, Ko YS, et al. Immunocytochemical analysis of connexin expression in the healthy and diseased cardiovascular system. *Microsc Res Tech*. (2001) 52:301–22. doi: 10.1002/1097-0029(20010201)52:3<301::AID-JEMT1015>3.0.CO;2-Q

27. Green KJ, Gaudry CA. Are desmosomes more than tethers for intermediate filaments? *Nat Rev Mol Cell Biol.* (2000) 1:208–16. doi: 10.1038/35043032

28. Calore M, Lorenzon A, De Bortoli M, Poloni G, Rampazzo A. Arrhythmogenic cardiomyopathy: a disease of intercalated discs. *Cell Tissue Res.* (2015) 360:491–500. doi: 10.1007/s00441-014-2015-5

29. Marcus FI, McKenna WJ, Sherrill D, Basso C, Bauce B, Bluemke DA, et al. Diagnosis of arrhythmogenic right ventricular cardiomyopathy/dysplasia: proposed modification of the Task Force Criteria. *Eur Heart J.* (2010) 31:806–14. doi: 10.1093/eurheartj/ehq025

30. Brodehl A, Meshkov A, Myasnikov R, Kiseleva A, Kulikova O, Klauke B, et al. Hemi- and Homozygous Loss-of-Function Mutations in DSG2 (Desmoglein-2) Cause Recessive Arrhythmogenic Cardiomyopathy with an Early Onset. *Int J Mol Sci*. (2021) 22:3786. doi: 10.3390/ijms22073786

31. Brodehl A, Weiss J, Debus JD, Stanasiuk C, Klauke B, Deutsch MA, et al. A homozygous DSC2 deletion associated with arrhythmogenic cardiomyopathy is caused by uniparental isodisomy. *J Mol Cell Cardiol.* (2020) 141:17–29. doi: 10.1016/j.yjmcc.2020.03.006

32. Ferreira-Cornwell MC, Luo Y, Narula N, Lenox JM, Lieberman M, Radice GL. Remodeling the intercalated disc leads to cardiomyopathy in mice misexpressing cadherins in the heart. *J Cell Sci*. (2002) 115:1623–34. doi: 10.1242/jcs.115.8.1623

33. Koch AW, Farooq A, Shan W, Zeng L, Colman DR, Zhou MM. Structure of the neural (N-) cadherin prodomain reveals a cadherin extracellular domain-like fold without adhesive characteristics. *Structure*. (2004) 12:793–805. doi: 10.1016/j.str.2004.02.034

34. Ferrell PD, Oristian KM, Cockrell E, Pizzo SV. Pathologic proteolytic processing of N-cadherin as a marker of human fibrotic disease. *Cells*. (2022) 11:156. doi: 10.3390/cells11010156

35. Haussinger D, Ahrens T, Aberle T, Engel J, Stetefeld J, Grzesiek, S. Proteolytic E-cadherin activation followed by solution NMR and X-ray crystallography. *EMBO J.* (2004) 23:1699–708. doi: 10.1038/sj.emboj.7600192

36. Ozawa M, Kemler, R. Correct proteolytic cleavage is required for the cell adhesive function of uvomorulin. *J Cell Biol.* (1990) 111:1645–50. doi: 10.1083/jcb.111.4.1645

frontiers | Frontiers in Pediatrics

TYPE Original Research
PUBLISHED 26 September 2022
DOI 10.3389/fped.2022.1008996

OPEN ACCESS

EDITED BY
Jian Gao,
Shanghai Children's Medical Center, China

REVIEWED BY
Dong Rui,
Liuzhou Workers Hospital, China
Yi Zuo,
Wuhan University of Science and Technology, China

*CORRESPONDENCE
Zhaoxuan Huang
38688157@qq.com

SPECIALTY SECTION
This article was submitted to Obstetric and Pediatric Pharmacology, a section of the journal Frontiers in Pediatrics

RECEIVED 01 August 2022
ACCEPTED 12 August 2022
PUBLISHED 26 September 2022

CITATION
Hu K, Liu W, Gan Y and Huang Z (2022) Transcriptome analysis of childhood Guillain–Barré syndrome associated with supportive care.
Front. Pediatr. 10:1008996.
doi: 10.3389/fped.2022.1008996

Transcriptome analysis of childhood Guillain–Barré syndrome associated with supportive care

Ke Hu, Wanli Liu, Yi Gan and Zhaoxuan Huang*

Department of Pediatric, Maternal and Child Health Hospital of Hubei Province, Tongji Medical College, Huazhong University of Science and Technology, Wuhan, China

Childhood Guillain–Barré syndrome (GBS) is a rare neurological disease. Early diagnosis followed by precise treatment can reduce mortality. In this study, we collected two transcriptome data between GBS and controls from the publicly available databases (GEO dataset). We identified two distinct down-regulated genes (PTGDS and AR) in GBS by transcriptome analysis (n = 20). Based on the two distinct down-regulated genes in the GBS group, a two-gene diagnostic signature was developed. Moreover, gene expression analysis for the two-gene was performed on a patient with GBS before and after Supportive Care. RT–PCR results show that the expression of PTGDS increased after the patient was given supportive care. Therefore, PTGDS might be considered as a potential target for therapeutic target in GBS.

KEYWORDS

Guillain–Barré syndrome, pediatrics, transcriptome, nursing, biomarkers

Introduction

The Guillain–Barré syndrome is a common cause of acute flaccid paralysis in children. A small number of children will develop respiratory muscle weakness, which is a self-limiting disease with a good prognosis (1). There are approximately 2 in 100,000 new cases of the Guillain–Barré syndrome each year, and the disease has a global mortality rate of about 7.5% (2). It is typically accompanied by allodynia and muscle weakness, usually beginning with the hands and feet, and then moving to the arms and upper body (3). During the acute phase of the disease, 15% of patients will develop respiratory muscle attacks that may be life-threatening and require mechanical ventilation (4). Some may affect the autonomic nervous system, resulting in abnormal heart rate and blood pressure. There is no known cause of the Guillain–Barré syndrome, but research suggests that infection is often involved (5). As well as bacterial and viral infections, vaccines and surgery can trigger GBS. There have been reports of an unexpected rise in GBS cases in countries affected by Zika virus infection. On the

basis of the available evidence, there is a good possibility that Zika virus infection causes GBS (6). Currently, there is no known drug that can effectively treat GBS; however, supportive care can decrease symptoms and shorten its duration. Supportive care includes monitoring breathing, heartbeat, and blood pressure. The patient is usually placed on a ventilator if their breathing ability is impaired. Early diagnosis is the key to facilitating clinical decision making and treatment selection. Therefore, the aim of the present study was to identify mRNA signatures that may serve as early diagnostic biomarkers for GBS.

Materials and methods

Data sources

In total, two transcriptome datasets (GSE31014 and GSE72748) were downloaded from the GEO website[1] for the current relative transcriptome analysis. Additionally, we collected plasma samples of one patient with the Guillain–Barré syndrome before treatment (before), and at the end of treatments (After). Oral informed consent was obtained from the participant. Treatment and care were designed in accordance with the WHO criteria for the Guillain–Barré syndrome (1).

Bioinformatics and statistics analyses

Microarray data from GSE31014 was normalized by GC-Robust Multi-array Average (gcRMA) (7). Before analyzing gene expression, all the genes were transformed by a log2 coefficient. Differential gene expression analysis based on gene effect size (ES > 2), and false discovery rate (FDR < 0.05) (8, 9). RNA-Seq data from GSE72748 was processed by the nf-core/rnaseq pipeline (10). The ROC curve and forward search was performed with the R package "MetaIntegrator" (11). All the statistical analyses were performed with R (version 4.1.3). We imputed missing values using the MetImp (12). We obtained the meta-score by subtracting the mean expression of upregulated genes from the mean expression of downregulated genes.

RNA isolation and RT-PCR analysis

The RNA isolation was achieved by QIAamp RNA Blood Mini Kit according to the manufacturer's recommendations (Qiagen). cDNA was synthesized using the QuantiTect Reverse Transcription Kit (Qiagen). The qPCR methodology and primers were performed according to published articles (13, 14).

1 http://www.ncbi.nlm.nih.gov/geo/

Results

Differential gene expression analysis

In total, two transcriptome data between GBS and controls were collected from publicly available databases (GEO). Based on the criteria described in methods, we identified differentially expressed genes in **Figures 1A,B**. After a forward search in the training and validation dataset. In total, two significantly differentially expressed genes (PTGDS and AR), which were down-regulated in the GBS group in both cohorts (**Figures 1C,D**). **Figure 1E** shows the meta-scores of each sample in GSE31014. A statistically significant difference was observed between the GBS and control group ($P < 0.05$). Next, we used the two genes to build a GBS diagnostic signature.

Validation of the two-gene signature in two datasets of Guillain–Barré syndrome

To evaluate the diagnostic power of the 2-gene signature we performed an ROC analysis. The two-gene signature distinguishes GBS from normal with AUC = 0.96 [95% CI 0.85–1] in GSE31014 (**Figure 2A**). In GSE72748, the two-gene signature distinguishes GBS from normal with AUC = 0.67 (**Figure 2B**). To investigate the effect of supportive care on the two significant genes, we collected blood samples before supportive care and after supportive care in one patient with GBS. **Figure 2C** shows that the expression of PDGTS was increased after supportive care.

Immune cell fractions and immune checkpoint analysis

Figures 3A,B shows immune cell fractions from two transcriptome data. Both datasets have a significant difference in Endothelial cells. As shown in **Figure 3C**, PDCD1 immune checkpoint genes are down-regulated and expressed in the GBS group. **Figure 3D** shows the KEGG pathway classification (left panel), and the right panel shows the 20 most significantly enriched GO terms.

Discussion

The Guillain–Barré syndrome is a rare neurological disease for which there is no effective treatment. Thus, early diagnosis is a particularly meaningful issue that lets immediate measure toward treatment. The current cytoalbuminologic dissociation

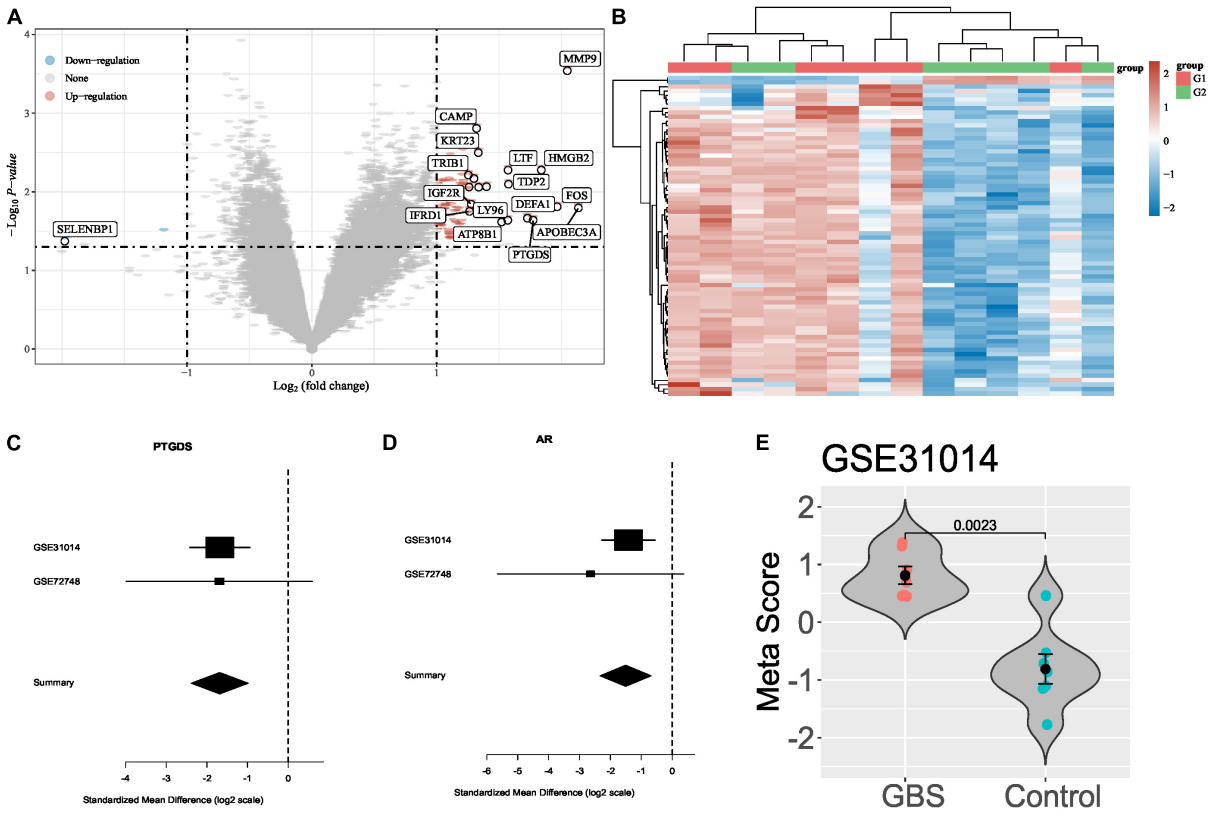

FIGURE 1
Differential gene expression analysis of GBS. **(A,B)** Differentially expressed genes between GBS and controls in GSE31014; **(C,D)** forest plots of PTGDS and AR gene in GSE31014 and GSE72748; **(E)** violin plot showing the performance of the 2-gene signature for separating GBS from control in GSE31014.

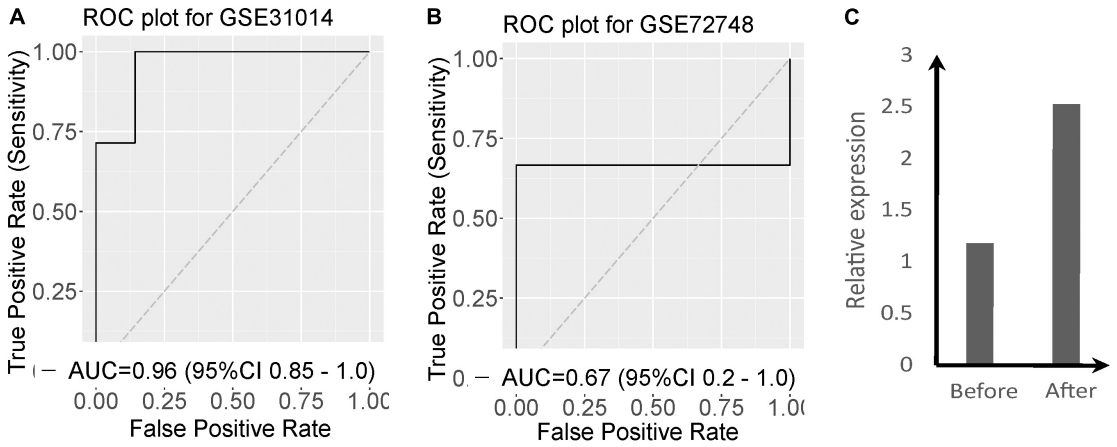

FIGURE 2
Validation of the two-gene signature in two datasets of GBS. **(A)** ROC curves and AUCs of the two-gene signature classification in GSE31014; **(B)** ROC curves and AUCs of the two-gene signature classification in GSE72748; **(C)** The expression of PTGDS of GBS patients before and after supportive care.

method for GBS detection requires an invasive biopsy (15). Therefore, the identification of novel non-invasive biomarkers for GBS diagnosis is preferred. By transcriptome analyses, we identified two new genes (PTGDS and AR) potentially related to GBS. Furthermore, the expression of PTGDS and AR was significantly decreased in the GBS group. Androgen receptor

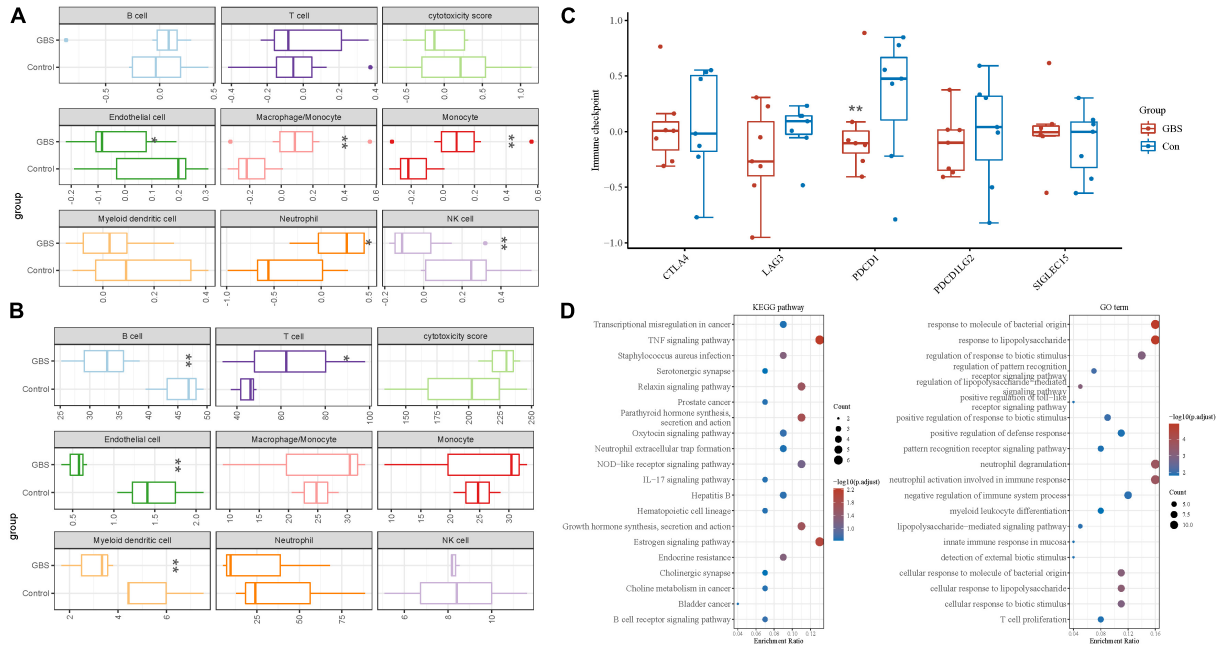

FIGURE 3
Immune cell fractions and immune checkpoint analysis. **(A,B)** Immune cell fractions in GSE31014 and GSE72748. **(C)** Immune-checkpoint-related genes in the discovery dataset. **(D)** The KEGG pathway and GO term analysis in the discovery dataset. $*p < 0.05$; $**p < 0.01$.

(AR) genes are responsible for constructing an androgen receptor protein. Androgen receptors function as DNA-binding transcription factors that control gene expression (16). During puberty and before birth, androgens play an important role in male sexual development. Prostaglandin-H2 D-isomerase (PTGDS) is an enzyme that converts prostaglandin H2 (PGH2) into prostaglandin D2 (PGD2). As a neuromodulator and trophic factor, PGD2 plays a key role in the central nervous system (17). Moreover, smooth muscle contraction and relaxation are also controlled by PGD2, and platelet aggregation is inhibited by it (18). Interestingly, the expression of this gene increased after the patient was given supportive care. This gene may be a potential target for treating GBS.

Data availability statement

The original contributions presented in this study are included in the article/supplementary material, further inquiries can be directed to the corresponding author.

Ethics statement

The studies involving human participants were reviewed and approved by Maternal and Child Health Hospital of Hubei Province. Written informed consent to participate in this study was provided by the participants' legal guardian/next of kin.

Author contributions

ZH: study conception. KH: data collection and analysis. KH and ZH: draft manuscript. All the authors reviewed the results and approved the final version of the manuscript.

Conflict of interest

The authors declare that the research was conducted in the absence of any commercial or financial relationships that could be construed as a potential conflict of interest.

Publisher's note

All claims expressed in this article are solely those of the authors and do not necessarily represent those of their affiliated organizations, or those of the publisher, the editors and the reviewers. Any product that may be evaluated in this article, or claim that may be made by its manufacturer, is not guaranteed or endorsed by the publisher.

References

1. Willison HJ, Jacobs BC, van Doorn PA. Guillain-barre syndrome. *Lancet.* (2016) 388:717–27. doi: 10.1016/S0140-6736(16)00339-1

2. Yuki N, Hartung H-P. Guillain–barré syndrome. *N Engl J Med.* (2012) 366:2294–304. doi: 10.1056/NEJMra1114525

3. Wijdicks EF, Klein CJ. Guillain-barre syndrome. *Mayo Clin Proc.* (2017) 92:467–79. doi: 10.1016/j.mayocp.2016.12.002

4. Hughes RA, Wijdicks EF, Benson E, Cornblath DR, Hahn AF, Meythaler JM, et al. Supportive care for patients with Guillain-Barré syndrome. *Arch Neurol.* (2005) 62:1194–8. doi: 10.1001/archneur.62.8.1194

5. Allos BM. Association between campylobacter infection and Guillain-Barré syndrome. *J Infect Dis.* (1997) 176:S125–8. doi: 10.1086/513783

6. Krauer F, Riesen M, Reveiz L, Oladapo OT, Martínez-Vega R, Porgo TV, et al. Zika virus infection as a cause of congenital brain abnormalities and Guillain–Barré syndrome: systematic review. *PLoS Med.* (2017) 14:e1002203. doi: 10.1371/journal.pmed.1002203

7. Wu Z, Irizarry RA. Preprocessing of oligonucleotide array data. *Nat Biotechnol.* (2004) 22:656–8. doi: 10.1038/nbt0604-656b

8. Henmi M, Copas JB. Confidence intervals for random effects meta-analysis and robustness to publication bias. *Stat Med.* (2010) 29:2969–83. doi: 10.1002/sim.4029

9. Enzmann DJJ. *Notes On Effect Size Measures For The Difference Of Means From Two Independent Groups: The Case Of Cohen'sd And Hedges'g January 12, 2015.* (2015).

10. Ewels PA, Peltzer A, Fillinger S, Patel H, Alneberg J, Wilm A, et al. The nf-core framework for community-curated bioinformatics pipelines. *Nat Biotechnol.* (2020) 38:276–8. doi: 10.1038/s41587-020-0439-x

11. Haynes WA, Vallania F, Liu C, Bongen E, Tomczak A, Andres-Terrè M, et al. Empowering multi-cohort gene expression analysis to increase reproducibility. *Proceedings of the Pacific Symposium on Biocomputing 2017.* Singapore: World Scientific (2017). p. 144–53. doi: 10.1142/9789813207813_0015

12. Wei R, Wang J, Su M, Jia E, Chen S, Chen T, et al. Missing value imputation approach for mass spectrometry-based metabolomics data. *Sci Rep.* (2018) 8:663. doi: 10.1038/s41598-017-19120-0

13. Ren Z, Gao M, Jiang W. Prognostic role of NLGN2 and PTGDS in medulloblastoma based on gene expression omnibus. *Am J Trans Res.* (2022) 14:3769.

14. Catteau-Jonard S, Jamin SP, Leclerc A, Gonzalès J, Dewailly D, Di Clemente N. Anti-Mullerian hormone, its receptor, FSH receptor, and androgen receptor genes are overexpressed by granulosa cells from stimulated follicles in women with polycystic ovary syndrome. *J Clin Endocrinol Metab.* (2008) 93:4456–61. doi: 10.1210/jc.2008-1231

15. Van der Meché F, Van Doorn P. Guillain-Barre syndrome and chronic inflammatory demyelinating polyneuropathy: immune mechanisms and update on current therapies. *Ann Neurol.* (1995) 37:14–31. doi: 10.1002/ana.410370704

16. Gelmann EP. Molecular biology of the androgen receptor. *J Clin Oncol.* (2002) 20:3001–15. doi: 10.1200/JCO.2002.10.018

17. Zhao W, Jiang B, Hu H, Zhang S, Lv S, Yuan J, et al. Lack of CUL4B leads to increased abundance of GFAP-positive cells that is mediated by PTGDS in mouse brain. *Hum Mol Genet.* (2015) 24:4686–97. doi: 10.1093/hmg/ddv200

18. Rezaee S, Kakavandi N, Shabani M, Khosravi M, Hosseini-Fard SR, Najafi M. COX and PTGDS gene expression levels in PGD2 synthesis pathway are correlated with miR-520 in patients with vessel restenosis. *Endocr Metab Immune Disord Drug Targets.* (2020) 20:1514–22. doi: 10.2174/1871530320666200511012142

frontiers | Frontiers in Pharmacology

TYPE Original Research
PUBLISHED 12 October 2022
DOI 10.3389/fphar.2022.988974

OPEN ACCESS

EDITED BY
Xue-Ning Li,
Fudan University, China

REVIEWED BY
Ravi Misra,
University of Rochester Medical Center, United States
Chintan K. Gandhi,
The Pennsylvania State University, United States
Elizabeth Susan Taglauer,
Boston University, United States
Evelyn Tsantikos,
Monash University, Australia

*CORRESPONDENCE
Jeffrey S. Barrett,
jbarrett@c-path.org

SPECIALTY SECTION
This article was submitted to Obstetric and Pediatric Pharmacology, a section of the journal Frontiers in Pharmacology

RECEIVED 07 July 2022
ACCEPTED 21 September 2022
PUBLISHED 12 October 2022

CITATION
Barrett JS, Cala Pane M, Knab T, Roddy W, Beusmans J, Jordie E, Singh K, Davis JM, Romero K, Padula M, Thebaud B and Turner M (2022), Landscape analysis for a neonatal disease progression model of bronchopulmonary dysplasia: Leveraging clinical trial experience and real-world data.
Front. Pharmacol. 13:988974.
doi: 10.3389/fphar.2022.988974

Landscape analysis for a neonatal disease progression model of bronchopulmonary dysplasia: Leveraging clinical trial experience and real-world data

Jeffrey S. Barrett[1]*, Megan Cala Pane[1], Timothy Knab[2], William Roddy[1], Jack Beusmans[2], Eric Jordie[2], Kanwaljit Singh[1], Jonathan Michael Davis[3], Klaus Romero[1], Michael Padula[4], Bernard Thebaud[5] and Mark Turner[6]

[1]Critical Path Institute, Tucson, AZ, United States, [2]Metrum Research Group, Tariffville, CT, United States, [3]Tufts Medical Center and the Tufts Clinical and Translational Science Institute, Boston, MA, United States, [4]Division of Neonatology, Children's Hospital of Philadelphia, Philadelphia, PA, United States, [5]Department of Pediatrics, Ottawa Hospital Research Institute, Ottawa, ON, Canada, [6]Department of Women's and Children's Health Institute of Translational Medicine, University of Liverpool, Liverpool, United Kingdom

The 21st Century Cures Act requires FDA to expand its use of real-world evidence (RWE) to support approval of previously approved drugs for new disease indications and post-marketing study requirements. To address this need in neonates, the FDA and the Critical Path Institute (C-Path) established the International Neonatal Consortium (INC) to advance regulatory science and expedite neonatal drug development. FDA recently provided funding for INC to generate RWE to support regulatory decision making in neonatal drug development. One study is focused on developing a validated definition of bronchopulmonary dysplasia (BPD) in neonates. BPD is difficult to diagnose with diverse disease trajectories and few viable treatment options. Despite intense research efforts, limited understanding of the underlying disease pathobiology and disease projection continues in the context of a computable phenotype. It will be important to determine if: 1) a large, multisource aggregation of real-world data (RWD) will allow identification of validated risk factors and surrogate endpoints for BPD, and 2) the inclusion of these simulations will identify risk factors and surrogate endpoints for studies to prevent or treat BPD and its related long-term complications. The overall goal is to develop qualified, fit-for-purpose disease progression models which facilitate credible trial simulations while quantitatively capturing mechanistic relationships relevant for disease progression and the development of future treatments. The extent to which neonatal RWD can inform these models is unknown and its appropriateness cannot be guaranteed. A component of this approach is the critical evaluation of the various RWD sources for context-of use (COU)-driven models. The present manuscript defines a landscape of the data including targeted literature searches and solicitation of neonatal RWD sources from international stakeholders; analysis plans to develop a family of

models of BPD in neonates, leveraging previous clinical trial experience and real-world patient data is also described.

KEYWORDS

bronchopulmonar dysplasia, neonates, disease progression, real world data (RWD), rare disease

Introduction

Bronchopulmonary dysplasia (BPD) is a chronic inflammatory lung disease that affects thousands of neonates and infants every year (Steinhorn et al., 2021). The pathophysiology and severity are characterized by the need for supplemental oxygenation or ventilatory support at 36 or 40 weeks post-menstrual age (PMA). BPD represents disruption of normal lung development before the saccular stage (before 32 weeks PMA), corresponding to a crucial time in the formation and architectural development of alveoli. Risk factors are numerous including: internal factors (prematurity, gender, genetics, *in utero* tobacco exposure/growth), iatrogenic factors (mechanical ventilation or/and oxygen supplementation, blood transfusions), or external factors (antenatal or/and postnatal infection, intra-uterine growth restriction). Although it is largely accepted that BPD results from lung damage and inflammation/oxidation triggered by mechanical ventilation and hyperoxia, the specific molecular mechanisms that result in compromised lung function and arrested development remain unknown. BPD likely represents several heterogeneous endotypes, with multi-hit processes likely (Niedermaier and Hilgendorff, 2015; Thébaud et al., 2019). Chest radiographs, blood tests, and echocardiograms (to assess the presence of pulmonary hypertension) may also be helpful to evaluate prognosis but can be non-specific. Preferred endpoints have varied significantly over decades (Cuevas Guaman et al., 2021) and there has been very little work on intermediate timepoints needed to recognize disease progression. While recent advances in neonatal care have improved the survival of very low-birthweight infants, the rates of BPD have not improved accordingly. This is mainly due to our limited understanding of the pathogenesis and the lack of effective therapeutic options currently available.

The definition of BPD has been constantly evolving over the past 30 years, with up to 18 separate definitions reported in the literature (Steinhorn et al., 2021). Some of the evolution in the definition of BPD is tied to changes in etiology that have resulted from advances in neonatal care, such as antenatal corticosteroid administration and postnatal surfactant therapy, which have improved the survival of extremely premature infants. What has been described as "old" BPD, often linked to lung damage and fibrosis from injury induced by oxygen toxicity and barotrauma from prolonged mechanical ventilation, has become less common than the concept of "new" BPD focused more on grow arrest and disordered lung development. Much of the discussion also involves establishing a definition that correlates with pulmonary outcome later in infancy and childhood. Of course, all definitions need to be put in the context of the current standard of care and treatment strategies which have changed considerably over time.

In response to a recent grant award from FDA, the International Neonatal Consortium (INC) has an opportunity to collate and evaluate real world data (RWD) sources to assess their value in informing various aspects of neonatal drug development. There is a greater recognition that such data may provide an important key to assess the heterogeneity of neonatal populations as well as the significant variability in respect to the current standard of care (Horton et al., 2021). While this report provides a broad landscape of the available data sources to inform a family of models to assess BPD disease progression, it is the RWD that represents the new Frontier in this effort. A key deliverable from the INC RWD grant (1 U01 FD007220-01) is the development of a universal definition of BPD that will serve as the anchor and baseline for models that capture the relevant disease biology and quantify disease progression over time.

The current state of clinical and biological resources that would facilitate a bridge to better understand BPD is conceptualized in Figure 1. Biological events and processes underpin the short- and long-term clinical manifestations of BPD. Techniques to measure biological events and mechanisms have not been delineated or deployed at sufficient scale to provide a comprehensive "map" of the condition. Similarly, clinical events have not been defined other than a variety of short- and long-term endpoints. Clinical observations are not informed by the timing or nature of biological processes or mechanisms. In other conditions, information about the stages of pathophysiology (biological processes) and clinical events inform the development of therapeutic options. Data from biological and clinical sources, summarized in Figure 2, can be combined in "disease progression models" (DPM) that capture the stages of disease development, the timing of the stages, and the extent of variation between individuals in the pathway to disease. DPM are a key tool in drug development allowing rational targeting of interventions and evidence-based planning of clinical trials (Fouarge et al., 2021; Barrett et al., 2022). Here we review the DPM concept

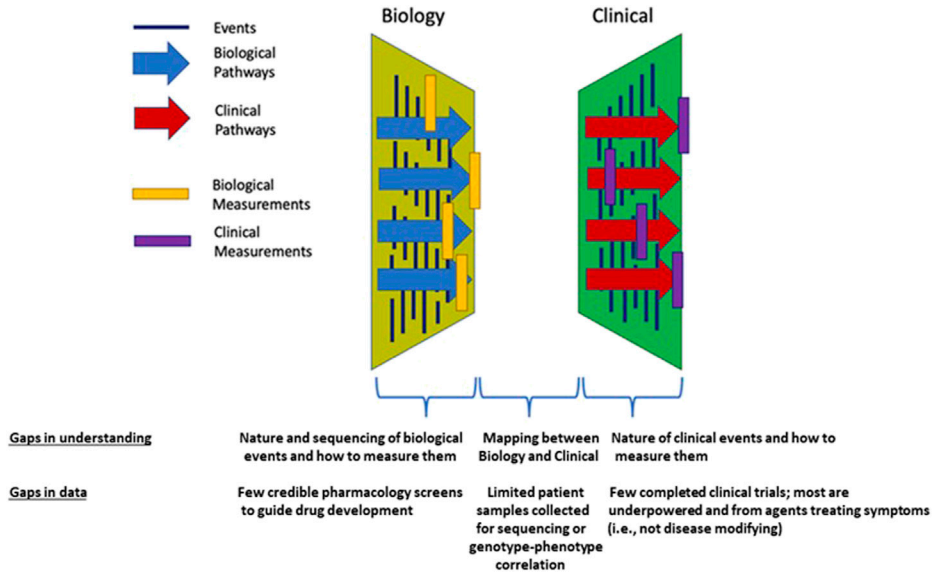

FIGURE 1
Conceptual framework for the necessary connections and current knowledge gaps between biologic and clinical data which exist for BPD.

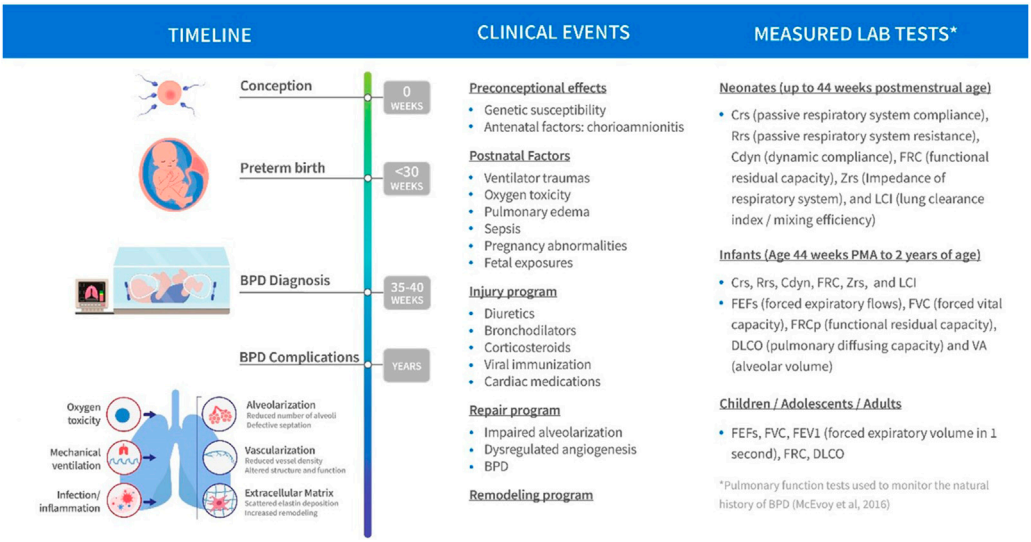

FIGURE 2
Schematic of BPD disease progression with variables of clinical interest linked to stage of progression.

applied to strategies for the development of a BPD DPM. This manuscript seeks to both prospectively assess the potential of the clinical real-world data to inform BPD (and therefore, other complications of extreme prematurity) definition and also the potential of utilizing such data to construct models that would inform BPD drug development as a context of use.

Methods—literature review

Underpinning this landscape data analysis is a narrative review of BPD DPM. The search for 1990–2021 peer-reviewed articles via the National Library of Medicine's PubMed site included Academic OneFile, JSTOR, Sage Journals, and related

databases [including Scopus and the Directory of Open Access Journals (DOAJ)]. Google Scholar was also utilized to locate open access articles. MeSH terms included the following: Animals; Animals, Newborn; Bronchopulmonary Dysplasia/metabolism*; Bronchopulmonary Dysplasia/pathology*; Disease Models, Animal*; Humans; Infant, Newborn; Infant, Premature/growth and development; Infant, Premature/metabolism*; Lung/growth and development Lung/metabolism*; Lung/pathology*; Rabbits. Selected references identified by this search were supplemented by papers from the authors' collections and identification of additional resources among subject matter experts from the INC. The INC BPD working group and modeling and simulation sub-team filtered the literature search results into categories that would include one of the following: relevant data from which model priors could be abstracted, published models of various types (e.g., predictive, descriptive, mechanistic, etc.), descriptive and/or quantitative definitions of BPD to be used as comparators for a future definition.

Baseline animal model evaluation

There have been numerous efforts to develop appropriate animal models of BPD to improve our understanding of the disease origin, progression, treatment, and prevention. These animal models have been explored in a broad range of species (Salaets et al., 2017; van der Merwe et al., 2021). Mice and rats are commonly used for models of BPD (e.g., chronic hyperoxia) due to ready availability, low cost, short gestational durations, and large litter sizes. Full-term mouse and rat pups are born during the saccular stage, which aligns with lung development in preterm neonates. However, despite term mouse and rat lungs being structurally underdeveloped, they are functionally mature and do not require respiratory support similar to preterm neonates at risk for the development of BPD, thereby limiting the translatability of these models. A well-constructed quantitative systems pharmacology (QSP) model often relies on animal models to help define relationships with key moieties of interest. This contributes to disease progression or is involved in the cascade of events that define a target molecule's interaction with physiologic organs, tissues, and cells of interest. Rate constants involved in the various reaction kinetics are often scalable across species and can be approximated in humans with appropriate allometric scaling techniques.

Several mouse and rat studies have contributed to much of the current understanding of the pathogenesis of BPD and identified important signaling molecules that can be used to inform semi-mechanistic mathematical models of disease progression (Tawhai and Burrowes, 2003; Zhou et al., 2019). These signaling molecules are relevant biomarkers that are used as indicators of inflammatory changes and immune events and include neutrophils, monocytes, inflammatory cytokines/chemokines, matrix proteins, growth factors, etc. These biomarkers can be found in various biofluids such as blood, urine, and bronchoalveolar lavage.

Following hyperoxic exposure, many species develop inflammation and alveolar simplification like that observed in rats and mice. Increased concentrations of pro-inflammatory cytokines and chemokines are likely central mediators of the response to many noxious stimuli. These studies can be used to calibrate mathematical models of the pro- and anti-inflammatory response dynamics and support the translation of these models across species. The rodent experiments have also been useful for the design of large animal trials including non-human primates.

Non-human primates are the most translationally relevant models of BPD, but account for the fewest studies available due to steep costs and ethical concerns (Nardiello et al., 2017). Rabbits, pigs, and sheep fill the gap between rodents and primates (D'Angio et al., 2016). The baboon experience has been beneficial for studying short-term BPD disease progression including providing clinically credible lung function and histology data (Coalson et al., 1982; Yoder and Coalson, 2014). The preterm baboon model does permit investigation of molecular pathways and genetic regulation of inflammatory processes in the developing lung (Yoder and Coalson, 2014) though there is likely less interest in keeping these colonies viable recently given the cost of maintaining.

Despite the number of animal models, no clinically relevant and standardized model exists, leaving several gaps that must be addressed to optimize the pathophysiology and treatment of BPD (Wickramasinghe et al., 2021a). The vast majority of preclinical models of BPD aim to achieve a simplified alveolar structure with disordered surrounding vasculature in order to study relevant mechanisms of malformation. A consequence of focusing on disease onset is that these preclinical models have yet to expand into longitudinal frameworks that connect to long-term outcomes. Few studies continue experimental observation beyond the well-controlled period of pathogenic insults due to the extreme financial and time commitments (Yoder and Coalson, 2014; Wickramasinghe et al., 2021a). The introduction of an intermittent insult methodology that combines injury and repair phases to align with clinical protocols more closely has expanded some study durations, but not enough to capture long-term sequelae of the disease (Ratner et al., 2009). Additionally, there is a lack of standardized approaches to introducing noxious stimuli across the range of investigated species, which highlights the broad spectrum of insults that have been explored but simultaneously restricts translational comparability. Establishing standardized protocols could facilitate a more systematic review of the direct impact that various insults have on lung development. While many studies report structural and histological findings that demonstrate alveolar simplification, few are accompanied by physiological metrics of gas exchange (Reynolds et al., 2010; Wickramasinghe et al., 2021a). Including any functional metrics would add a quantitative layer to these studies and help elucidate

structure-function relationships throughout lung development, which would be useful from a longitudinal mathematical modeling standpoint. Lastly, although pulmonary dysfunction is the primary outcome explored in many animal models of BPD, the downstream complications involving other organ systems is not well-defined. Neurodevelopmental impairment and retinopathy are known comorbidities likely linked to a dysregulated immune response and should be considered along with changes in other organ systems in future animal models of BPD (Wickramasinghe et al., 2021b). An examination of the extrapulmonary organs in these animals will facilitate a more complete picture and facilitate an improved understanding of BPD pathophysiology and progression.

Further complicating the feasibility of developing a QSP-type model of disease progression in BPD is the classification of BPD as a syndrome rather than a disease. Without clearly defined endotypes and phenotypes, establishing a link between the two using mechanistic and quantitative terms is not possible. The complex mechanistic interactions induced by the various noxious stimuli contribute to the heterogeneity of disease trajectories and complicate the classification into clinical subtypes or phenotypes (Wu et al., 2020). The fields of genomics and metabolomics hold promise for identifying unique signatures of specific interactions or patterns that could be used for classification. Two recent studies have explored the complex intracellular dynamics that occur during the transition to air breathing by using single-cell RNA-sequencing (scRNA-seq) to generate cellular composition maps and identify biologically plausible pathological pathways (Hurskainen et al., 2021; Zepp et al., 2021).

Several of the animal models aim to identify the basic mechanisms of late lung development by inducing alveolar simplification and vascular irregularities, hallmarks of the new BPD. These studies have uncovered a multitude of new mechanisms of normal and dysregulated lung development. One recent example in the area of lung cellular and molecular physiology is a study that probed the role of oxygen and steroids (e.g., dexamethasone) in the regulation of surfactant secretion by alveolar epithelial type II cells (AEC2s). Htun et al. (Htun et al., 2021) proposed a mechanism in support of the observed effect of glucocorticoids in increasing surfactant secretion through suppression of components within the natriuretic peptide system of AEC2s. Still, the interplay of these molecular and cellular pathways involved in lung development, injury, and repair remains complex and the influence on arresting proper lung maturation is not fully understood.

To date, the existing preclinical model data has not been collectively assembled in a meaningful way. This is an essential step for the initiation of a multi-scale QSP model that would provide a more clinically structured disease progression model for BPD. This initial landscaping effort has incorporated a preclinical data coordination plan to support the family of models that will support efforts to evaluate RWD sources that support regulatory decision making.

Results

Current development of therapeutic options to treat BPD

Current therapeutics for BPD and RDS involve ventilatory management, steroids, and administration of various agents such as pulmonary surfactant, caffeine, vitamin A, nitric oxide, diuretics, and stem cells (Michael et al., 2018). Some are only at early stages of evaluation and only steroids, vitamin A and caffeine are the only interventions that have shown to reduce BPD based on RCTs. The efficacy of these agents in preventing and ameliorating BPD varies depending on the populations studied and the timing of the intervention(s). Some of these agents have been developed opportunistically rather than through a planned application of insights from preclinical work. Since there are few pharmaceutical sponsors who would conduct and store such data, the typical preclinical safety, pharmacology, and PK/PD data for these agents is sparse or nonexistent. Published preclinical investigations suggests multiple therapeutic targets are relevant (Bhandari, 2014). Planned application of preclinical work is also hampered by the lack of an accurate quantitative description of the current and evolving standard of care, which can be defined and codified in a DPM. This could be the starting point for an RWD-informed clinically focused standard of care baseline model from which drug treatment models could be compared. A non-mechanistic trajectory of disease progression from time of diagnosis could be constructed to complement future clinical trial simulations.

BPD disease progression

It is unclear when BPD begins, but many believe its origins occur *in-utero* (Taglauer et al., 2018). It would seem to depend on perinatal history as severe documented chorio or preeclampsia with associated IUGR do initiate BPD before birth. Detailed assessment of neonatal pulmonary function after a preterm delivery is difficult but would offer great value to understand the evolution of disease and identify potential windows of vulnerability and intervention. In preterm neonates, lung development that would normally occur *in-utero* happens postnatally under altered mechanical and environmental conditions. This includes active tidal breathing with strain/stretch of immature intrathoracic structures and a state of relative hyperoxia (even in room air). Lung development is also affected by conditions precipitating preterm delivery, including inflammation and infections. While preterm delivery impacts normal alveolarization and pulmonary vascularization, it can also affect mechanical processes in the lung (McEvoy and Aschner, 2015). As they mature, individuals manifest with ongoing respiratory symptoms and reduced lung function, with pulmonary function tests (PFTs) showing expiratory flow

TABLE 1 Previously published BPD prognostic and quantitative models to be utilized for qualification of future BPD disease progression model.

Model (Reference)	Category	Data Sources	Purpose
Review of 23 clinical prediction models (Onland et al., 2013)	Regression-based models; multivariate analyses; retrospective and prospective	A variety of data sources including the PreVILIG database	• Review the quality and validity of models that predict BPD in preterm infants using clinical information from the first week of life • Attempted to externally validate models and compare predictors identified
BPD severity prediction model (Valenzuela-Stutman et al., 2019)	Binary logistic regression models to evaluate the predictive value of different variables, using respiratory hospitalization as the primary outcome	• Primary cohort included 188 premature infants (≤32 weeks PMA) admitted to the NICU at Children's National Health System (CNHS) in Washington, D.C. • The validation cohort included 130 premature infants (≤36 weeks PMA) admitted to the NICU at The Hospital Militar Central and the Hospital Universitario Clinica San Rafael in Bogota, Colombia.	• Approach improved BPD risk assessment, particularly in extremely premature infants. • Internal validation included lung X-ray imaging and phenotypical characterization of BPD severity levels. • External validation conducted in an independent longitudinal cohort of premature infants (≤36 weeks PMA, n = 130; Bogota).
BPD risk prediction model (Alvarez-Fuente et al., 2019)	Multivariate logistic regression model to identify risk factors for BPD development by determining the odds ratio of both groups, no-BPD versus BPD, in relation to clinical, echocardiographic and analytic factors	• 5 Spanish hospitals: 50 patients with a median gestational age of 26 weeks and weight of 871 g (range 590-1200g).	• Study and model aimed to explore the ability of clinical, echocardiographic and analytical variables to predict moderate or severe BPD in a cohort of extremely preterm infants.
BPD severity prediction (Taglauer et al., 2018)	Forward logistic regression models with predictive values evaluated using a ROC curve	Multicenter study including 16,407 infants weighing 500-1500 g (2001-2015) from the Neocosur Network	• Predictive power models for moderate/severe BPD and BPD/death at four postnatal ages. • Birth weight contributed the most in explaining BPD, followed by GA and 1-min Apgar score
BPD Risk factors in preterm infants (Alvarez-Fuente et al., 2019)	Multiple logistic regression analysis: sensitivity and specificity of the model assessed by ROC curve	Seventy-two preterm infants (30 with BPD and 42 non-BPD controls) admitted in the NICU of the Children's Hospital of Soochow University during 2017 enrolled; prospective longitudinal study	• To identify postnatal risk factors for bronchopulmonary dysplasia (BPD) development in preterm infants with gestational age ≤32 weeks • Perinatal data, a neonatal critical illness score (NCIS), different soluble B7-H3(sB7-H3), and interleukin-18 (IL-18) levels by days after birth collected; early predictive model for BPD development established
Mechanistic model of gas exchange and ventilation under a broad range of local and systemic inflammatory stimuli (Reynolds et al., 2010)	Diffusion of oxygen and carbon dioxide, hemoglobin uptake of oxygen, and enzymatic reactions governing carbon dioxide and bicarbonate levels.	ODE-based multi-scale model based on literature priors	• Simulation model of pulmonary function under inflammatory stress and of interventions aimed at improving gas exchange in this broadly relevant context. • Generically multiscale model to be improved in its physiologic accuracy and computational load.
Integrative anatomically-based model - incorporates descriptions of material properties and anatomical structure at a range of levels of interest (Tawhai and Burrowes, 2003)	Finite element meshes of the lung lobes, airways, blood vessels, parenchyma, and microcirculation.	Database of publications, models, and data related to the pulmonary circulation	• Provides a framework for quantitative description of a system's geometry, behavior, or interactions. Laboratory observations are incorporated into the models as, for example, geometric data or rate constants, and experimentation is also used to validate the model's performance. • "Lung Atlas" is currently being developed based on structural and functional computed tomography (CT) imaging (Alvarez-Fuente et al., 2019)

limitation at school age (which may respond to bronchodilators) and into adulthood. There is concern that BPD will predispose to chronic obstructive pulmonary disease (COPD) since infants are beginning life with reduced lung function and longitudinal cohorts indicate that individuals track along their predetermined PFT percentiles throughout life.

Due to advances in neonatal care, increased numbers of preterm neonates are surviving at lower gestational ages. Up to half of extremely low birth weight infants may develop BPD. Owing to paucity of evidence and absence of comprehensive guidelines for outpatient management, there is significant variation in management. Additionally, the only validated phenotypes for preterm respiratory disease are at a single timepoint (36 weeks corrected gestational age). Work is needed to define the respiratory outcomes for individuals born preterm over their lifetime.

Models for BPD

Quantitative models fall in many categories and offer value to drug development in a variety of ways. In the context of a model-informed drug development (MIDD) approach, models can be developed to de-risk decision making at various stages of drug development. These include quantitative system pharmacology (QSP), pharmacokinetic (PK), pharmacokinetic-pharmacodynamic (PK/PD), physiologically based pharmacokinetic (PBPK), pharmacometric (PMX), clinical trial simulation (CTS) and pharmacoeconomic models. Several of these foundational models may be incorporated into a clinical trial simulation paradigm used to project the probability of technical success (PTOS) for a proposed trial design. A range of models have already been developed and published to support BPD research and clinical disease management (Table 1).

Several predictive models are available for BPD. Most predictive models include several BPD risk factors, such as birth weight, GA, chorioamnionitis, preeclampsia, respiratory parameters, etc. (Ding et al., 2020; Valenzuela-Stutman et al., 2019; Nino et al., 2020). These known risk factors increase neonatologists' awareness of the potential risk of BPD in selected patients but are still not able to universally identify patients with a high risk of developing moderate to severe BPD and tend to overestimate this risk. This makes it difficult to implement early interventions for selected patients who will, with high probability, develop the most severe disease.

Disease progression models

In general, modeling progression of chronic diseases enables better understanding of disease prognosis and provides insights into staging systems. This approach could assist early diagnosis and personalized care and facilitate the development and evaluation of interventions. Other types of models, including disease progression and quantitative systems pharmacology models, have the potential to provide more mechanistic understanding of disease biology in the context of development, maturation, and other time dependencies. This assumes that the data supporting these relationships is of sufficient quantity, diversity, and quality. To date, there are few quantitative models other than the predictive models shown in Table 1 and no disease progression models for BPD.

To characterize the natural progression of disease, these models generally incorporate longitudinal data for biomarker(s) of disease severity or can incorporate more direct measures of disease severity. Although such data are unlikely to be collected during routine clinical care, there is some hope that laboratory measures currently monitored in BPD may be suitable for that purpose. Disease models are also often linked to PK–PD models so the influence of drug treatment on disease progression can be quantified and evaluated. Once again, it is important to note that there are no well-established and effective agents for the prevention and/or treatment of BPD reflected in the current standard of care. However, there may be an opportunity to optimize dosing of current treatment options that shift or mitigate BPD progression.

Semi-mechanistic models are a particular class of disease progression models with great potential to impact BPD. These models are both data-driven (e.g., fully empirical models) and grounded in biological and pathophysiological processes similar to traditional systems models. To effectively combine both approaches and to achieve the optimum balance between parsimony and goodness-of-fit, the model is limited to the most critical processes that are necessary to explain the relevant data. In the case of a well-developed model of BPD disease progression, the key processes to consider are the complex inflammatory pathways that result from both genetic and environmental triggers and the processes involved with the structural and functional changes that occur in the lungs of the preterm neonate. In BPD, oxidation and inflammation are the common denominators that link genetic and environmental factors associated with disease severity. From this etiological perspective, a semi-mechanistic model could provide an avenue to interrogate the interplay of infection, hyperoxia, and barotrauma/volutrauma with the structural and functional changes observed in the lungs of individuals with BPD. The stages of lung development are well-delineated, but the relationship between the development of the immune response and resolution at the various stages of lung development is not fully understood (Kolls, 2017). From a drug development context much of this knowledge is focused on adult lung disease and related conditions where financial incentives are easier to define which is also a motivation herein to provide a context and framework from which BPD can be better defined and acted upon.

Relevant biomarkers can be used to calibrate a model that incorporates inflammatory pathways and to probe for the presence of links between the pro- and anti-inflammatory imbalance and the emergent phenotype of alveolar simplification and dysregulated vascularization observed in BPD (Bhandari, 2014; Balany and Bhandari, 2015). Some inflammation-related biomarkers that could support this future study include cytokines/chemokines, reactive oxygen and nitrogen species, as well as growth factors and other mediators. It is possible that disease endotypes exist that are defined by different drivers of inflammation and different response profiles, but still give way to the same disease phenotype. If true, modeling could be used to classify the endotypes and to subsequently explore potential therapeutic regimens unique to the identified endotypes. It may also be possible to link such a model to clinical outcomes like PFTs or a more discrete outcome like the probability of developing moderate to severe BPD. Yet, developing another predictive model without a mechanistic link to BPD disease progression is not enough.

The INC RWD project will develop a variety of models that facilitate a quantitative description of BPD. This reflects the underlying pathophysiology and disease biology, not only in the context of the available data, but also future data types that could be collected during routine clinical care as well as in the conduct of future clinical trials. Well-curated RWD from neonates can contribute to the validation of quantitative models of symptom progression and facilitate the development of useful insights and the generation of RWE. The workplan is summarized in Table 2. Figure 3 includes a data flow diagram describing the process from data acquisition through development of a dataset used for model development.

Data requirements

Outcomes

Well-defined outcomes are essential for the development of DPM. DPMs need to progress towards an outcome to select and weigh variables included in the model. The definitions of clinical endpoints have been "definitions of convenience" that are used to inform clinical practice, benchmarking, and epidemiology. Extant endpoints are based on time points and assessments that have clinical validity. These clinical definitions have not been validated for reproducibility or prediction of long-term outcomes and do not reflect biological mechanisms or key events in disease progression. The lack of uniform definitions for clinical endpoints has prevented effective meta-analyses among existing therapeutic studies of BPD (Cole et al., 2010). In addition, the lack of a consistent, well-founded definition also hinders the development of new therapies. From a modeling perspective, one consideration is that clinical SMEs can be used to define credible patient profiles from a combination of existing RWD observations and plausible/credible models so these model-based virtual patients can be used to qualify components of the model as its being assembled.

Data sources: RWD and clinical trials

In one sense neonatology is a data-rich specialty since neonates are monitored closely in the NICU. This fact informs the belief that RWD can inform the development of DPM and important outcomes despite the lack of adequately powered, neonatal clinical trials. The availability of RWD reflecting the diversity in populations and disease stage can also contribute to the generalizability of the model. To date, neonatal RWD has not been collated from multiple sources.

Randomized clinical trial data can be used to drive the development of empirical models of BPD disease progression that rely more heavily on statistical methods rather than the mechanistic underpinnings of systems-based approaches. Data can be pooled across multiple studies and population-based methods can be utilized to explain the observed interindividual subject variability on the baseline severity and rate of disease progression. These methods incorporate covariates and patient characteristics from the available data to describe the variability and to identify sub-types of the disease that may respond differentially to a given treatment. Mathematical models that account for the diversity in a disease population can be used to generate powerful clinical trial simulation tools for trial design optimization (Barrett et al., 2022).

Unfortunately, the portfolio of new drugs or other modalities to treat BPD is small and legacy trials with historical agents have been largely underpowered and have focused on symptomatic relief. This is primarily due to the lack of phenotypic discrimination and uncertain disease progression. A variety of agents have been developed or re-purposed to target different points in the pathways that lead to BPD, including anti-inflammatories, diuretics, steroids, pulmonary vasodilators, antioxidants, and molecules involved in the cell signaling cascade thought to be involved in the pathogenesis of BPD. IL1RA, glyburide, and inhaled budesonide are currently the most promising anti-inflammatory therapies that have the potential to prevent BPD in preterm infants. However, more studies will have to investigate the safety and potential long-term effects in human neonates. Another aspirational emphasis of this work is to leverage the relevant knowledge from adult lung disease and drug development tools to facilitate the BPD data, model and drug development tools landscape so that an easier and perhaps less costly roadmap to development can be defined.

Data collection

Data will be collected from clinical trials and real-world data sources including Electronic Health Records, clinical registries, observational studies (Table 3). Contributing organizations

TABLE 2 Proposed workplan—critical requirements of the BPD disease progression model effort based on initial scoping from INC working group.

Task	Details
Modeling strategy plan	• Identify family of models that would facilitate clinical decision making and the design of clinical trials in neonatal BPD patients (likely to include QSP, disease progression, clinical utility, and clinical trial simulation models)
Develop quantitative clinical attributes that can be used to define BPD patient phenotypes	• Using a "reverse engineering" approach applied to published clinical prediction models (see Table 3), identify clinical variables form various RWD sources and values / ranges identified with BPD severity. Explore boundaries and patient selection via sensitivity analysis.
Identify data sources and elements that would be utilized in each target model type	• From the varied RWD sources (See Table 3), identify presence of data used to develop and validate the various model types.
Verify data quality concerns based on "fit-for-purpose" approach	• Assess data quality metrics for each of the identified sources likely to contribute to uncertainty in the model development and the fidelity of the final model and model predictions.
Conduct simulations to verify model operating characteristics	• Explore boundary conditions of key variables, model parameters and response predictions.

TABLE 3 RWD available to construct BPD Disease Progression Model from committed sources to the recent INC / C-Path Grant with FDA.

Contribution Organization—Dataset Type
Dataset Name
Tufts Medical Center—Electronic Health Records
Nagano Children's Hospital—Electronic Health Records
Kyorin University—Electronic Health Records
Driscoll Children's Hospital—Electronic Health Records
Prisma Health Children's Hospital—Electronic Health Records
Children's Hospital of Philadelphia—Electronic Health Records
University of New Mexico Health Sciences Center—Electronic Health Records
University of Texas Health San Antonio—Electronic Health Records
Anne & Robert H. Lurie Children's Hospital of Chicago—Electronic Health Records
Prentice Women's Hospital/Northwestern—Electronic Health Records
University of Utah Health Science Center—Electronic Health Records
UPMC Children's Hospital of Pittsburgh—Electronic Health Records
Mount Sinai Hospital (Canada)—Electronic Health Records
University of Minnesota: Masonic Children's Hospital—Electronic Health Records
Children's Mercy Hospital Kansas City—Electronic Health Records
Tufts Medical Center—Clinical Trial
Efficacy of Recombinant Human Clara Cell 10 Protein (rhCC10) Administered to Premature Neonates with Respiratory Distress Syndrome
Tufts Medical Center—Observational Study
Improving Bronchopulmonary Dysplasia (BPD) Predictors and Outcomes for Clinical Trials (STOP-BPD)
NICHD DASH / NRN—Clinical Trial
Surfactant Positive Airway Pressure and Pulse Oximetry Trial (SUPPORT)
Children's Hospital Colorado—Observational Study
Genetic Basis for Impaired Angiogenic Signaling in BPD
Chiesi Pharmaceuticals—Clinical Trial
A Study to Investigate the Safety, Tolerability and Efficacy Of Nebulized Curosurf In Preterm Neonates With Respiratory Distress Syndrome (RDS)
Chiesi Pharmaceuticals—Clinical Trial
A Double Blind, Randomized, Controlled Study to Evaluate CHF 5633 (Synthetic Surfactant) and Poractant Alfa in Neonates with Respiratory Distress Syndrome (RDS)
Chiesi Pharmaceuticals—Clinical Trial
European Non-Interventional Post-Authorization Study to Assess Drug Utilization and Safety Of Caffeine Citrate (Peyona) In Treatment Of Premature Infants
NICHD DASH / NRN—Clinical Trial
Inhaled Nitric Oxide for Preterm Infants with Severe Respiratory Failure (Preemie iNO)

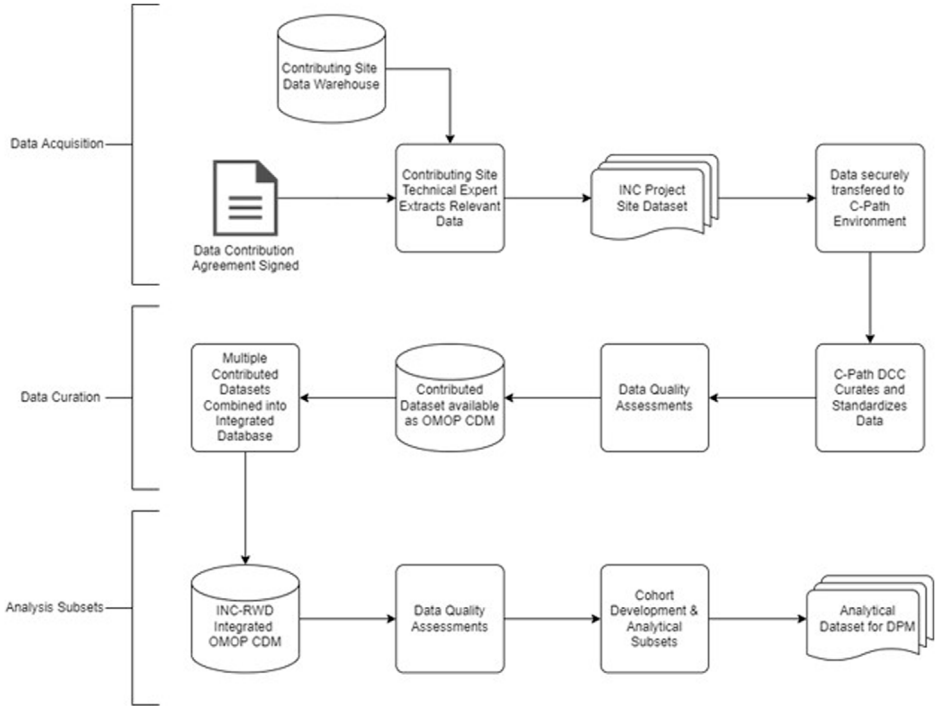

FIGURE 3
Data flow diagram to generate analytical subset from contributed real world data.

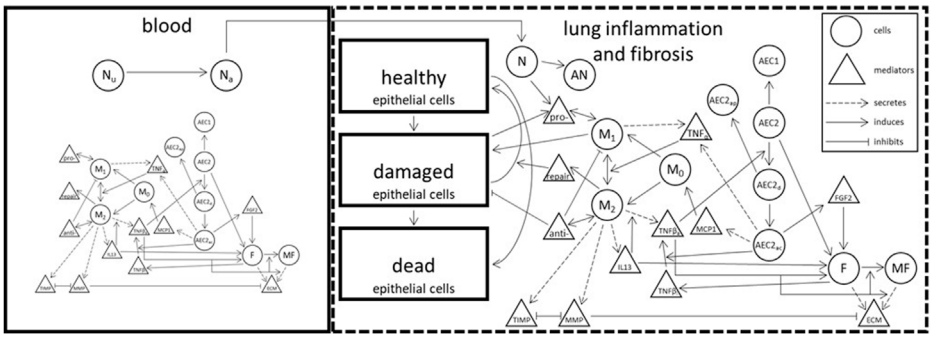

FIGURE 4
Abstract representation of model including all interactions [modified from (Cogo et al., 2007; Minucci et al., 2020).

include members of the International Neonatal Consortium and I-ACT. Working in partnership with C-Path's Data Collaboration Center (DCC), the contributing organizations will develop and execute queries to extract data from the EHR, clinical data warehouse, or other research databases and registries as appropriate. Data elements that will be included in the data extracted were identified by subject matter experts as being relevant to the clinical presentation of BPD. For data from electronic health records, contributing organizations have been asked to develop cohorts that included records from neonates and their mothers who were admitted to the neonatal intensive care unit between 22- and 42-week gestational age. As a component of the data extraction process contributing organizations have been asked to remove identifiable information from their datasets and apply de-identification methods to the source data to protect the privacy of the patients. Data will be securely transferred to the DCC where an integrated database will be assembled, and data validation will

occur. The DCC will store the data in secure environments with appropriate access-based controls to minimize the risk of data breach and conduct additional assessment of the data to ensure identifiable data elements have been removed to protect patient privacy.

Data integration

Given the breadth and variation of source data structure and data element representation, there are technical challenges with developing a DPM due to the lack of interoperability of source data. In order to ease these challenges, we will standardize the structure, content, and semantics of the data to make it possible to modeling of all data sources with a uniform approach. The INC project will use the Observational Health Data Sciences and Informatics (OHDSI) program's Observation Medical Outcomes Partnership (OMOP) Common Data Model (CDM) (Stang et al., 2010) as the data model used to integrate datasets for this project. The OMOP CDM provides a consistent and reliable data model to represent all observational data and has an extensive set of vocabulary mappings to a hierarchical vocabulary of concept sets. In cases where a contributing organization has an existing mapping to a common data model, these will be requested and the DCC will work with local experts to confirm these mappings contain the variables identified by the working group. In the scenario that a site does not have a mapping to a CDM the DCC will request the data in the current format and then conduct all data transformation activities locally. After validating transformation of the data to a CDM the data will be loaded into a common database. Data validation will occur on both the source data and the data transformations.

Data quality assessment

In addition to the technical challenges surrounding the integration and interoperability, data generated from real-world settings are intended for operational use and not optimized for research. The lack of systematic data collection, errors introduced by system bugs or human mistakes, and ambiguous data definitions raise concerns about the utility and reliability of the real-world data. A critical piece of a generating evidence from RWD will assessing the quality of the data and ensuring "fitness for use" within the context of the disease.

The INC project will leverage previous work and lessons learned from data quality frameworks available in the literature (Kahn et al., 2012; Kahn et al., 2016; Khare et al., 2017; Khare et al., 2019; Liaw et al., 2021) and existing software packages to guide our assessment. Standardizing the data into the OMOP CDM has an additional benefit of a data model that lends itself to assessing data quality and the availability of robust open-source projects supported by the community to evaluate data quality such as the Data Quality Dashboard which includes over 3,300 data quality checks (Blacketer et al., 2021; Liaw et al., 2021). The assessment will focus on verifying and validating the conformance, completeness, and plausibility of the data. Using these assessments will help identify erroneous records and provide an overall assessment of the reliability of both each dataset prior to combining multiple datasets into a single integrated data model and after the integration has occurred. The assessments will include data quality checks that cover a range of factors that could contribute to the overall "fitness for use". Because the multitude of sources of errors, the assessments will evaluate multiple dimensions of the data from multiple perspectives. One key feature is ensuring the integrity of data types. For example, evaluating that the numeric data fields include only numeric values and that the values themselves are plausible given biological or temporal restraints on the range of values that could exist. A related data quality check will need to assess the range of values given the measurement unit for a given observation. Additional data checks will test the temporal reliability and plausibility of the data and the related records within the data. For example, these checks will evaluate if records reporting the use of respiratory support devices have dates that occur after the date of birth.

Another important aspect of these assessments includes evaluating the completeness of data both in the level of value missingness but also in the coverage of key data elements. For example, ensuring that the data provided by a contributing institution includes data elements which are relevant to developing a disease progression model and accurately describing the patient's engagement with the health care facility. In cases where the completeness of data is lacking it will be important to contextually understand if these data are missing due to errors in the extraction process or the lack of availability in source systems and to incorporate appropriate statistical error estimation in the disease progression model.

One unique challenge of the INC project is the integration of multisite data. The process of combining multiple data sources poses unique challenges especially from a data quality perspective. It is possible for each individual sites dataset to pass the data quality assessments but when compared to datasets from other sites there are discrepancies that result in it not being reasonable to combine the dataset. These discrepancies may occur due to the characteristics and statistical distributions of the data being significantly different and explainable by understanding local site clinical practices or they may be due to semantic irregularities in the data. In the case of variation introduced by site specific protocols these instances will need to be reviewed to determine if it is appropriate to still combine the data. In instances of semantic irregularities these may be able to be resolved by further data curation of the data elements. Previous work has described the implications of research networks and combining multisite datasets that will guide the development of key assessments (Kahn et al., 2012). To assess variations in data characteristics across multisite datasets we will calculate and evaluate comparative descriptive statistics for data elements

that are important for the fitness of use to identify anomalies in data patterns.

Analytical dataset and cohort subsets

After combining the source datasets into an integrated database an analytical subset will be generated for use in generating the disease progression model. The development of this analytical subset requires identifying similar patient cohorts for comparison and selecting covariates that are appropriate for the model. Identifying patient cohorts will rely on defining computable phenotypes that can be applied to the patient population. A computable phenotype includes clinical characteristics defined by a set of data elements and logical expressions that can be understood by a machine and electronically queried to identify similar patients within a population (Richesson et al., 2013). In addition to phenotypical relationships, details such as observation periods, time-at-risk, completeness of data, and density of data will play important roles in identifying a subset of patients into a cohort. Groups of patients will be identified to comprise of comparator and outcome cohorts that will compromise the patients and observations to be used during data analysis.

Initial modeling efforts

A multidisciplinary team comprised of clinical subject matter experts including clinical care givers, clinical trialists, researchers, and quantitative scientists including experienced modelers, data scientists and engineers have participated in monthly meetings to develop the workplan, assemble and advise on the relevant datasets and assess the data availability, suitability, and quality for the proposed DPM context of use. With the focus of constructing a BPD QSP model that can represent a mechanistic anchor from which a future BPD DPM can be assembled, a multiscale approach was proposed with the following goals: 1) describe the relevant physiologic landscape involved with BPD disease progression (e.g., lung, GI tract, and immune system), 2) define states/conditions which define the "healthy" versus "disease" states, and 3) describe maturation and developmental considerations which include different patient phenotypes and disease roadmaps.

At the lowest level of model granularity, compartments and their associated cellular-molecular interactions and distributions describing inflammation and fibrosis present in BPD (in both blood and lung tissue) are described. Figure 4 represents an idealized schematic from which the lowest level of model granularity is defined. Elements of the model consistent with the 3 goals described above are being codified and challenged by both preclinical and clinical SMEs. The working group plans to provide these early efforts to the broader BPD stakeholder community consistent with an Open Science framework. This will likely involve the creation of a secure Git Hub environment from which others can contribute in the future.

Discussion

This is the first effort to review the landscape of BPD data, models, and other resources that could facilitate a strategy for the development of a family of quantitative models of BPD. While much of the emphasis is on RWD sources, the effort also includes the consolidation of preclinical data sources from relevant *in vitro* and animal experiments that would represent an anchor for mechanistic models including a QSP model. Complimentary models focused on the clinical value of current disease management practices more reliant on RWD are also a significant part of this effort. While interest is high for investigating the utility of RWD and real-world evidence (RWE) to inform drug development, we cannot assume that such data will fulfill its potential in all cases. A critical step in the context of use (COU) process is the definition of requirements and expectations regarding the performance of tools brought to regulators to support decision making. The ability of RWD sources and RWE derived from such sources to support such tools and the corresponding COU remains a work in progress reliant on the critical evaluation of data quality. Likewise, models constructed from or validated by such data must be of adequate quality to meet "fit-for-purpose" requirements as well. While there may be reasons to relax such requirements in situations where data is sparse and difficult to obtain, such decisions must be risk-based with adequate and well-informed justification from a diverse group of stakeholders.

Many knowledge gaps exist for BPD. While some may be addressed by accumulated and high-quality data, others will require more targeted investigation with attention to biomarkers both established and exploratory. In addition to the data, a multidisciplinary team of quantitative and clinical scientists must continue to challenge what has been evaluated thus far (preclinically and clinically), proposing experiments and analyses which help better define the disease progression as week as identify treatment options including a variety of modalities and disease progression in the context of distinct clinical phenotypes. Quantitative models serve the purpose of informing such prospective investigations based on scenario testing that evaluates and designs sampling times and frequency and sample size considerations (Mould, 2007; Cook and Bies, 2016). A disease progression model can also describe patient phenotypes and inform enrollment criteria as well as the timing of proposed interventions and treatments relative to the current standard of care (Cook and Bies, 2016; Gruneau et al., 2021). Hence, they have tremendous value for both the sponsors of such proposed interventions and regulators who must evaluate their safety and efficacy.

An important component of the disease progression model is the availability of credible longitudinal data in each patient. Such data would in theory capture the natural history of the disease and discriminate patient disease trajectories while examining response to treatment. Some examples of measure lab tests of

clinical interest that could facilitate tracking of disease progression are summarized in Figure 2. In this respect the availability of RWD in BPD patients is theoretically of great value. Part of the challenge herein is to evaluate utility of the RWD based both on its quality, credibility and clinical information value and not assume that it is useful for this purpose based on its availability in the target population. Much of these data are still based on an opportunistic sampling approach given the fragility of the population. A plan to propose a DPM framework is still useful to identify both data and knowledge gaps as well as propose prospective study designs potentially incorporating more informative markers of disease progression at appropriate sampling times (Cook and Bies, 2016).

A key determinant for the overall success of this effort is the commitment for data sharing, collaboration, and transparency. The INC community is extremely knowledgeable and committed to the cause but relies on an extended group of stakeholders to deliver these high-quality data. It is also incumbent on pharmaceutical and academic researchers to promote the science, consider new biomarkers, use more innovative clinical trial designs, and remain unsatisfied with the status quo. Success for this effort demands this level of participation and investment. The proposed approach to consider RWD to guide models that inform BPD drug development is sound and rigorous. It will surely experience challenges and there can be no declared victories except continuing to fill gaps in our knowledge and understanding.

Our intention with this initial modeling effort is to build upon the data landscaping to produce a mechanistic QSP model as the starting point for a collaborative effort that eventually informs a BPD DPM. Measures of success (early and late) will be described further in an open-source format as the intention is to extend the initial FDA/INC-led effort to a broader community of BPD stakeholders including academic, regulatory, and industrial scientists.

Data availability statement

The original contributions presented in the study are included in the article/Supplementary Materials, further inquiries can be directed to the corresponding author.

Author contributions

JB was the primary architect of the manuscript but all authors contributed to the writing, editing and creative input. WR added the data science and quality components, MC, TK, JB, and EJ added the modeling strategy and scoping and KS, JD, KR, MT, MP, and BT added the clinical perspective and criteria for clinical assessments.

Funding

Federal funding was received from FDA grant, 1 U01 FD007220-01.

Conflict of interest

TK, JB, and EJ were employed by the Metrum Research Group.

The remaining authors declare that the research was conducted in the absence of any commercial or financial relationships that could be construed as a potential conflict of interest.

Publisher's note

Supplementary material

The Supplementary Material for this article can be found online at: https://www.frontiersin.org/articles/10.3389/fphar.2022.988974/full#supplementary-material

References

Alvarez-Fuente, M., Moreno, L., LopezOrtego, P., Arruza, L., Avila-Alvarez, A., Muro, M., et al. (2019). Exploring clinical, echocardiographic and molecular biomarkers to predict bronchopulmonary dysplasia. *PLoS ONE* 14 (3), e0213210. doi:10.1371/journal.pone.0213210

Balany, J., and Bhandari, V. (2015). Understanding the impact of infection, inflammation, and their persistence in the pathogenesis of bronchopulmonary dysplasia. *Front. Med.* 2, 90. doi:10.3389/fmed.2015.00090

Barrett, J. S., Nicholas, T., Azer, K., and Corrigan, B. W. (2022). Role of disease progression models in drug development. *Pharm. Res.* 39, 1803–1815. doi:10.1007/s11095-022-03257-3

Bhandari, V. (2014). Postnatal inflammation in the pathogenesis of bronchopulmonary dysplasia. *Birth Defects Res. A Clin. Mol. Teratol.* 100 (3), 189–201. doi:10.1002/bdra.23220

Blacketer, C., Defalco, F. J., Ryan, P. B., and Rijnbeek, P. R. (2021). Increasing trust in real-world evidence through evaluation of observational data quality. *J. Am. Med. Inf. Assoc.* 28 (10), 2251–2257. doi:10.1093/jamia/ocab132

Coalson, J. J., Kuehl, T. J., Escobedo, M. B., Hilliard, J. L., Smith, F., Meredith, K., et al. (1982). A baboon model of bronchopulmonary dysplasia. II. Pathologic features. *Exp. Mol. Pathol.* 37, 335–350. doi:10.1016/0014-4800(82)90046-6

Cogo, P. E., Toffolo, G. M., Ori, C., Vianello, A., Chierici, M., Gucciardi, A., et al. (2007). Surfactant disaturated-phosphatidylcholine kinetics in acute respiratory distress syndrome by stable isotopes and a two compartment model. *Respir. Res.* 8, 13. doi:10.1186/1465-9921-8-13

Cole, F. S., Alleyne, C., Barks, J. D., Boyle, R. J., Carroll, J. L., Dokken, D., et al. (2010). NIH consensus development conference: Inhaled nitric oxide therapy for premature infants. *NIH Consens. State. Sci. Statements* 27 (5), 1–34.

Cook, S. F., and Bies, R. R. (2016). Disease progression modeling: Key concepts and recent developments. *Curr. Pharmacol. Rep.* 2 (5), 221–230. doi:10.1007/s40495-016-0066-x

Cuevas Guaman, M., Dahm, P. H., and Welty, S. E. (2021). The challenge of accurately describing the epidemiology of bronchopulmonary dysplasia (BPD) based on the various current definitions of BPD. *Pediatr. Pulmonol.* 56, 3527–3532. doi:10.1002/ppul.25434

D'Angio, C. T., Ambalavanan, N., Carlo, W. A., McDonald, S. A., Skogstrand, K., Hougaard, D. M., et al. (2016). Blood cytokine profiles associated with distinct patterns of bronchopulmonary dysplasia among extremely low birth weight infants. *J. Pediatr.* 174, 45–51.e5. doi:10.1016/j.jpeds.2016.03.058

Ding, L., Wang, H., Geng, H., Cui, N., Huang, F., Zhu, X., et al. (2020). Prediction of bronchopulmonary dysplasia in preterm infants using postnatal risk factors. *Front. Pediatr.* 8, 349. doi:10.3389/fped.2020.00349

Fouarge, E., Monseur, A., Boulanger, B., Annoussamy, M., Seferian, A. M., De Lucia, S., et al. (2021). Hierarchical Bayesian modelling of disease progression to inform clinical trial design in centronuclear myopathy. *Orphanet J. Rare Dis.* 16, 3. doi:10.1186/s13023-020-01663-7

Gruneau, L., Ekstedt, M., Kechagias, S., and Henriksson, M. (2021). Disease progression modeling for economic evaluation in nonalcoholic fatty liver disease—a systematic review. *Clin. Gastroenterology Hepatology* S1542-3565 (21), 01153–01158. doi:10.1016/j.cgh.2021.10.040

Horton, D. B., Blum, M. D., and Burcu, M. (2021). Real-world evidence for assessing treatment effectiveness and safety in pediatric populations. *J. Pediatr.* S0022-3476 (21), 312–316. doi:10.1016/j.jpeds.2021.06.062

Htun, Z. T., Schulz, E. V., Desai, R. K., Marasch, J. L., McPherson, C. C., Mastrandrea, L. D., et al. (2021). Postnatal steroid management in preterm infants with evolving bronchopulmonary dysplasia. *J. Perinatol.* 41 (8), 1783–1796. doi:10.1038/s41372-021-01083-w

Hurskainen, M., Mižíková, I., Cook, D. P., Andersson, N., Cyr-Depauw, C., Lesage, F., et al. (2021). Single cell transcriptomic analysis of murine lung development on hyperoxia-induced damage. *Nat. Commun.* 12 (1), 1565–1619. doi:10.1038/s41467-021-21865-2

Kahn, M. G., Callahan, T. J., Barnard, J., Bauck, A. E., Brown, J., Davidson, B. N., et al. (2016). A harmonized data quality assessment terminology and framework for the secondary use of electronic health record data. *EGEMS (Wash DC)* 4 (1), 1244. doi:10.13063/2327-9214.1244

Kahn, M. G., Raebel, M. A., Glanz, J. M., Riedlinger, K., and Steiner, J. F. (2012). A pragmatic framework for single-site and multisite data quality assessment in electronic health record-based clinical research. *Med. Care* 50, S21–S29. doi:10.1097/MLR.0b013e318257dd67

Khare, R., Utidjian, L., Ruth, B. J., Kahn, M. G., Burrows, E., Marsolo, K., et al. (2017). A longitudinal analysis of data quality in a large pediatric data research network. *J. Am. Med. Inf. Assoc.* 24 (6), 1072–1079. doi:10.1093/jamia/ocx033

Khare, R., Utidjian, L. H., Razzaghi, H., Soucek, V., Burrows, E., Eckrich, D., et al. (2019). Design and refinement of a data quality assessment workflow for a large pediatric research network. *EGEMS (Wash DC)* 7 (1), 36. doi:10.5334/egems.294

Kolls, J. K. (2017). Commentary: Understanding the impact of infection, inflammation and their persistence in the pathogenesis of bronchopulmonary dysplasia. *Front. Med.* 4, 24. doi:10.3389/fmed.2017.00024

Liaw, S. T., Guo, J. G. N., Ansari, S., Jonnagaddala, J., Godinho, M. A., Borelli, A. J., et al. (2021). Quality assessment of real-world data repositories across the data life cycle: A literature review. *J. Am. Med. Inf. Assoc.* 28 (7), 1591–1599. doi:10.1093/jamia/ocaa340

McEvoy, C. T., and Aschner, J. L. (2015). The natural history of bronchopulmonary dysplasia: The case for primary prevention. *Clin. Perinatol.* 42 (4), 911–931. doi:10.1016/j.clp.2015.08.014

Michael, Z., Spyropoulos, F., Ghanta, S., and Christou, H. (2018). Bronchopulmonary dysplasia: An update of current pharmacologic therapies and new approaches. *Clin. Med. Insights. Pediatr.* 12, 1179556518817322. doi:10.1177/1179556518817322

Minucci, S. B., Heise, R. L., and Reynolds, A. M. (2020). Review of mathematical modeling of the inflammatory response in lung infections and injuries. *Front. Appl. Math. Stat.* 36. doi:10.3389/fams.2020.00036

Mould, D. R. (2007). *Pharmacometrics*. John Wiley & Sons, 547–581. Developing models of disease progression.

Nardiello, C., Mižíková, I., and Morty, R. E. (2017). Looking ahead: Where to next for animal models of bronchopulmonary dysplasia? *Cell Tissue Res.* 367, 457–468. doi:10.1007/s00441-016-2534-3

Niedermaier, S., and Hilgendorff, A. (2015). Bronchopulmonary dysplasia - an overview about pathophysiologic concepts. *Mol. Cell. Pediatr.* 2, 2. doi:10.1186/s40348-015-0013-7

Nino, G., Mansoor, A., Perez, G. F., Arroyo, M., Xuchen, X., Weinstock, J., et al. (2020). Validation of a new predictive model to improve risk stratification in bronchopulmonary dysplasia. *Sci. Rep.* 10, 613. doi:10.1038/s41598-019-56355-5

Onland, W., Debray, T. P., Laughon, M. M., Miedema, M., Cools, F., Askie, L. M., et al. (2013). Clinical prediction models for bronchopulmonary dysplasia: A systematic review and external validation study. *BMC Pediatr.* 13, 207. doi:10.1186/1471-2431-13-207

Ratner, V., Slinko, S., Utkina-Sosunova, I., Starkov, A., Polin, R. A., and Ten, V. S. (2009). Hypoxic stress exacerbates hyperoxia-induced lung injury in a neonatal mouse model of bronchopulmonary dysplasia. *Neonatology* 95 (4), 299–305. doi:10.1159/000178798

Reynolds, A., Bard Ermentrout, G., and Clermont, G. (2010). A mathematical model of pulmonary gas exchange under inflammatory stress. *J. Theor. Biol.* 264 (2), 161–173. doi:10.1016/j.jtbi.2010.01.011

Richesson, R. L., Hammond, W. E., Nahm, M., Wixted, D., Simon, G. E., Robinson, J. G., et al. (2013). Electronic health records based phenotyping in next-generation clinical trials: A perspective from the NIH health care systems collaboratory. *J. Am. Med. Inf. Assoc.* 20 (2), e226–e231. doi:10.1136/amiajnl-2013-001926

Salaets, T., Gie, A., Tack, B., Deprest, J., and Toelen, J. (2017). Modelling bronchopulmonary dysplasia in animals: Arguments for the preterm rabbit model. *Curr. Pharm. Des.* 23 (38), 5887–5901. doi:10.2174/1381612823666170926123550

Stang, P. E., Ryan, P. B., Racoosin, J. A., Overhage, J. M., Hartzema, A. G., Reich, C., et al. (2010). Advancing the science for active surveillance: Rationale and design for the observational medical outcomes partnership. *Ann. Intern. Med.* 153 (9), 600–606. doi:10.7326/0003-4819-153-9-201011020-00010

Steinhorn, R. H., and Davis, J. M. (2021). "Bronchopulmonary dysplasia," in *Avery and MacDonald's neonatology, pathophysiology, and management of the Newborn*. Editors J. P. Boardman, A. Groves, and J. Ramasethu. 8th edition (Philadelphia, PA: J. B. Lippincott).

Taglauer, E., Abman, S. H., and Keller, R. L. (2018). Recent Advances in antenatal factors predisposing to bronchopulmonary dysplasia. *Semin. Perinatol.* 42 (7), 413–424. doi:10.1053/j.semperi.2018.09.002

Tawhai, M. H., and Burrowes, K. S. (2003). Developing integrative computational models of pulmonary structure. *Anat. Rec. B New Anat.* 275 (1), 207–218. doi:10.1002/ar.b.10034

Thébaud, B., Goss, K. N., Laughon, M., Whitsett, J. A., Abman, S. H., Steinhorn, R. H., et al. (2019). Bronchopulmonary dysplasia. *Nat. Rev. Dis. Prim.* 5, 78. doi:10.1038/s41572-019-0127-7

Valenzuela-Stutman, D., Marshall, G., Tapia, J. L., Mariani, G., Bancalari, A., and Gonzalez, Á.Neocosur Neonatal Network (2019). Bronchopulmonary dysplasia: Risk prediction models for very-low- birth-weight infants. *J. Perinatol.* 39 (9), 1275–1281. doi:10.1038/s41372-019-0430-x

van der Merwe, J., van der Veeken, L., Inversetti, A., Galgano, A., Toelen, J., and Deprest, J. (2021). Earlier preterm birth is associated with a worse neurocognitive outcome in a rabbit model. *PLoS One* 16 (1), e0246008. doi:10.1371/journal.pone.0246008

Wickramasinghe, L. C., van Wijngaarden, P., Johnson, C., Tsantikos, E., and Hibbs, M. L. (2021). An experimental model of bronchopulmonary dysplasia features long-term retinal and pulmonary defects but not sustained lung inflammation. *Front. Pediatr.* 9, 689699. doi:10.3389/fped.2021.689699

Wickramasinghe, L. C., van Wijngaarden, P., Johnson, C., Tsantikos, E., and Hibbs, M. L. (2021). The immunological link between neonatal lung and eye disease. *Clin. Transl. Immunol.* 10 (8), e1322. doi:10.1002/cti2.1322

Wu, K. Y., Jensen, E. A., White, A. M., Wang, Y., Biko, D. M., Nilan, K., et al. (2020). Characterization of disease phenotype in very preterm infants with severe bronchopulmonary dysplasia. *Am. J. Respir. Crit. Care Med.* 201 (11), 1398–1406. doi:10.1164/rccm.201907-1342OC

Yoder, B. A., and Coalson, J. J. (2014). Animal models of bronchopulmonary dysplasia. The preterm baboon models. *Am. J. Physiol. Lung Cell. Mol. Physiol.* 307 (12), L970–L977. doi:10.1152/ajplung.00171.2014

Zepp, J. A., Morley, M. P., Loebel, C., Kremp, M. M., Chaudhry, F. N., Basil, M. C., et al. (2021). Genomic, epigenomic, and biophysical cues controlling the emergence of the lung alveolus. *Science* 371, aebc3172. doi:10.1126/science.abc3172

Zhou, W., Shao, F., and Li, J. (2019). Bioinformatic analysis of the molecular mechanism underlying bronchial pulmonary dysplasia using a text mining approach. *Medicine* 98, e18493. doi:10.1097/MD.0000000000018493

frontiers | Frontiers in Medicine

TYPE Original Research
PUBLISHED 10 November 2022
DOI 10.3389/fmed.2022.1040747

OPEN ACCESS

EDITED BY
Jian Wang,
Shanghai Children's Medical Center, China

REVIEWED BY
Abdul Nasir,
The Second Affiliated Hospital of Zhengzhou University, China
Maria Monticelli,
University of Campania Luigi Vanvitelli, Italy

*CORRESPONDENCE
Zhe Xu
zhexu_cmu@163.com
Huan Xing
xinghuan63@126.com

†These authors have contributed equally to this work and share first authorship

SPECIALTY SECTION
This article was submitted to Precision Medicine, a section of the journal Frontiers in Medicine

RECEIVED 09 September 2022
ACCEPTED 17 October 2022
PUBLISHED 10 November 2022

CITATION
Wang C, Zhang Y, Hu X, Wang L, Xu Z and Xing H (2022) Novel pathogenic variants in *KIT* gene in three Chinese piebaldism patients.
Front. Med. 9:1040747.
doi: 10.3389/fmed.2022.1040747

Novel pathogenic variants in *KIT* gene in three Chinese piebaldism patients

Chen Wang[1†], Yingzi Zhang[2†], Xuyun Hu[3], Lijuan Wang[1], Zhe Xu[1*] and Huan Xing[1*]

[1]Department of Dermatology, National Center for Children's Health, Beijing Children's Hospital, Capital Medical University, Beijing, China, [2]Department of Dermatology, Shunyi Maternal and Children's Hospital of Beijing Children's Hospital, Beijing, China, [3]Beijing Key Laboratory for Genetics of Birth Defects, MOE Key Laboratory of Major Diseases in Children, Genetics and Birth Defects Control Center, National Center for Children's Health, Beijing Children's Hospital, Beijing Pediatric Research Institute, Capital Medical University, Beijing, China

Background: Piebaldism is a rare autosomal dominant disease, and roughly 75% patients had *KIT* gene mutations. Up to date, approximately 90 *KIT* mutations causing piebaldism were reported.

Methods: To identify *KIT* gene mutations in three pediatric piebaldism patients from different families and explore the genotype-phenotype correlation, peripheral blood DNA were collected from probands and their parents. Whole-exome sequencing was performed to detect potential disease-causing variants in the three probands. Putative variants were validated by Sanger sequencing.

Results: Heterozygous variants of c.2469_2484del (p.Tyr823*), c.1994G > C (p.Pro665Leu), and c.1982_1983insCAT (p.662_663insIle) in *KIT* gene were detected in three probands. These variants were all novel and classified as pathogenic/likely pathogenic variants according to the interpretation guidelines of American College of Medical Genetics and Genomics and the Association for Molecular Pathology. The probands carrying variants located in tyrosine kinase domain exhibited a more severe phenotype.

Conclusion: The piebaldism in three families was caused by novel heterozygous *KIT* variants. The severity of phenotypes is related with the types and locations of different mutations. Our results further provided evidence for genetic counseling for the three families.

KEYWORDS

piebaldism, *KIT* gene, whole-exome sequencing, café-au-lait macule, genotype-phenotype correlation

Introduction

Piebaldism (OMIM 172800) is a rare autosomal dominant disorder of congenital depigmentation characterized by patches of white skin and hair in a distinct ventral midline pattern (1). The white patches are involved in the areas of middle frontal, chest, abdomen, and limbs. The color and range remain stable throughout life. Some patients also have café-au-lait macules (CALMs) and intertriginous freckling, as well as extra-cutaneous manifestations such as, epitheliomas, occasional deafness and rare Hirschsprung disease. The incidence is unknown, yet it is estimated to be less than 1 in 20,000 (2). Both males and females are affected equally.

Piebaldism is caused by mutations in *KIT* or *SNAI2*. These two genes are involved in the development, survival, and migration of melanocyte precursors (3). Roughly 75% of piebaldism patients are caused by mutations in the *KIT* gene (OMIM 164920) located on chromosome 4q12 (4), while other patients may have mutations in alternative genes like the *SNAI2* gene (OMIM 172800) located on chromosome 8q11 (5). *KIT* encodes a transmembrane tyrosine kinase receptor KIT for stem cell factor, which is important in the melanogenesis pathway (6). The receptor KIT belongs to type III transmembrane receptor tyrosine kinase family. It is composed of an amino-terminal extracellular ligand-binding domain (EC), a single transmembrane domain (TB), and an intracellular tyrosine kinase (TK) domain. Mutations in *KIT* gene lead to abnormal melanocyte migration and the absence of melanocytes.

In order to identify underlying genetic etiology of piebaldism patients and further extend the phenotype and mutation spectra, we performed next-generation sequencing for three Chinese piebaldism families. In this study, we uncovered three novel pathogenic/likely pathogenic *KIT* variants (c.2469_2484del, c.1994G > C, and c.1982_1983insCAT). Our study provided the basis for genetic counseling of three piebaldism families. The results further elucidated the genotype-phenotype correlation that mutations in TK domain caused severe clinical manifestations.

Materials and methods

Patient recruitment

Three individuals clinically suspected as piebaldism were recruited from Beijing Children's Hospital. The age of these patients ranged from 5 months to 3 years. All the probands presented with varying degrees of skin pigmentation and poliosis. Written informed consents were obtained from the minors' legal guardian for the publication of any potentially identifiable images or data included in this article. This study was approved by the Institutional Medical Ethics Committee of Beijing Children's Hospital, Capital Medical University [(2022)-E-196-R] and conducted according to the Declaration of Helsinki.

Whole-exome sequencing

Peripheral blood of the probands and their parents were collected, and genomic DNA was extracted by Blood Genomic DNA Kit (TransGen, Beijing). Whole-exome sequencing (WES) was performed for three patients (mean depth > 100×). The library was sequenced on NovaSeq (Illumina, San Diego, America) and aligned to the GRCh38/hg38 human reference sequence using Burrows-Wheeler Aligner (BWA) with the MEM algorithm. BAM files were generated by Picard. Sequence reads were recalibrated by Realigner Target Creator in Genome Analysis Toolkit (GATK), and sequence variants were called by GATK Haplotype Caller. Copy Number Variants (CNVs) were called by read-depth strategy by CNVkit. Variants were annotated and filtered by software of Flash Analysis (fa.shanyint.com). Variants were classified following the American College of Medical Genetics and Genomics and the Association for Molecular Pathology (ACMG/AMP) interpretation standards and guidelines (7). Putative pathogenic variants detected by next-generation sequencing (NGS) were confirmed by Sanger sequencing. According to the WES results, Sanger sequencing was used to verify the gene mutation sites of the probands and their parents. Primer premier 5 software is used to design primers.

Histopathological examination

Skin biopsy was performed on a 1.0 cm × 0.5 cm fusiform skin tissue from the depigmented lesion on the right upper arm of Proband 1. The skin tissue was placed in normal saline and then fixed in 4% paraformaldehyde overnight. The fixed tissue was washed, dehydrated, and finally embedded with paraffin. Sections of 5-μm thickness were cut by a microtome (RIWARD, Shenzhen) and stained with hematoxylin and eosin (H&E). Skin tissue sections were observed under the light microscope (Keyence, China).

Results

Clinical manifestations

Clinical features of these three patients with piebaldism were summarized in **Table 1**. No other findings such as facial deformity, heterochromia iridis, deafness, or anemia were noticed. Patient 1 was a 2-year and 8-month-old boy with congenital leukodermal patches of the forehead, ventral abdomen, limbs, and a white forelock. The size of the patches

TABLE 1 Clinical manifestations of probands 1–3.

Proband	Age	Gender	Mutation	Origin	Involved area						
					Forehead	Forelock	Front chest	Abdomen	Back	Upper limbs	Lower limbs
1	2 years and 8 months	Male	c.2469_2484del(p.Tyr823*)	Paternal	+	+	+	+	–	+	+
2	9 months	Female	c.1994C > T(p.Pro665Leu)	*De Novo*	+	–	–	+	+	+	+
3	5 months	Male	c.1982_1983insCAT (p.662_663insIle)	Paternal	+	+	+	–	–	+	+

FIGURE 1
Main clinical manifestations of the three patients. Depigmented patches were involved in middle frontal, chest, abdomen, limbs of the patient 1 **(A)**, 2 **(B)** and 3 **(C)**. Normal pigment islands were scattered on trunk, and extremities. Café-au-lait macules were noticed on the right lower limb of Patient 1 and the front chest, left armpit, right lower limb of Patient 2.

increased proportionally with age. His father had a similar phenotype (Figure 1A). Patient 2 was a 9-month-old girl. She presented with poliosis and skin depigmentation patches on the forehead, trunk, limbs since birth. Both her parents had normal phenotype (Figure 1B). Patient 3, a 5-month-old boy, had a white forelock and unpigmented skin patches on the forehead,

trunk, bilateral arms, and legs since birth. His father had similar physical symptom, and other family members were not affected (Figure 1C).

Molecular genetic analysis

The results of WES showed that heterozygous variants of *KIT* gene (NM_000222.2) were detected in all three patients (Table 1 and Figure 2). Patient 1 had a paternal variant c.2469_2484del (p.Tyr823*) in exon 17, resulting in a termination codon at position 823. It is expected to lead to nonsense-mediated mRNA decay and lost the function. Patient 2 had a *de novo* variant c.1994C > T (p.Pro665Leu). Pro665 located on catalytic domain of tyrosine-protein kinase and was highly conserved according to predicting tools such as phyloP, GERP + + and REVEL. All SIFT, Polyphen-2, CADD and LRT had Damaging/Deleterious prediction of p.Pro665Leu. At the same site, p. Pro665Ser was already reported in another Chinese piebaldism family (8). Patient 3 had a paternal variant c.1982_1983insCAT (p.662_663insIle) which was also located on catalytic domain of tyrosine-protein kinase. All the three variants were absent in population databases including gnomAD, Exome Sequencing Project (ESP) and 1000G, and not reported in pervious literature. According to the ACMG/AMP interpretation standards and guidelines, c.2469_2484del (PVS1 + PM2 + PP4) and c.1994C > T (PS2 + PM1 + PM2 + PM5 + PP3 + PP4) were classified as pathogenic variants, c.1982_1983insCAT was classified as likely pathogenic variant (PM2 + PM4 + PP3 + PP4).

Pathological examination results

The skin biopsy specimen taken from Proband 1 revealed: atrophy of epidermis, vanishment of melanocytes and melanin pigment among basal cells, lymphocytes infiltration in the perivascular regions and elastic fiber degeneration (Figure 3). It is consistent with the pathological manifestations of piebaldism.

Discussion

In this study, we report three Chinese cases with pathogenic/likely pathogenic variants in *KIT*. All these variants were novel variants. These data expand the mutation spectrum of the *KIT* gene.

In 1991, Giebel and Spritz first reported that mutations in *KIT* gene could lead to piebaldism (4). To date, approximately 90 mutations in the *KIT* gene were reported in piebaldism according to the database of HGMD (professional 2022.3). For these mutations, 17 were identified in Chinese patients (Supplementary Table 1). The severity of clinical features in piebaldism patients correlate with the type and location

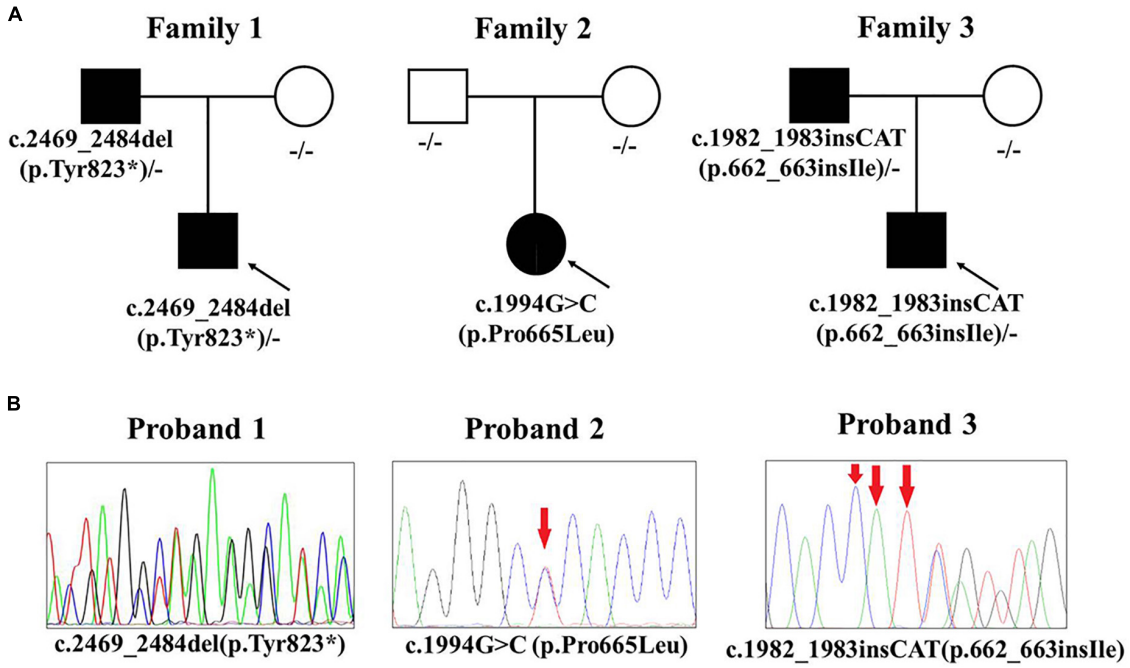

FIGURE 2
KIT mutations of the three piebaldism patients. **(A)** Pathogenic variants and their origin in the three families. **(B)** Sanger sequencing results of three pathogenic variants.

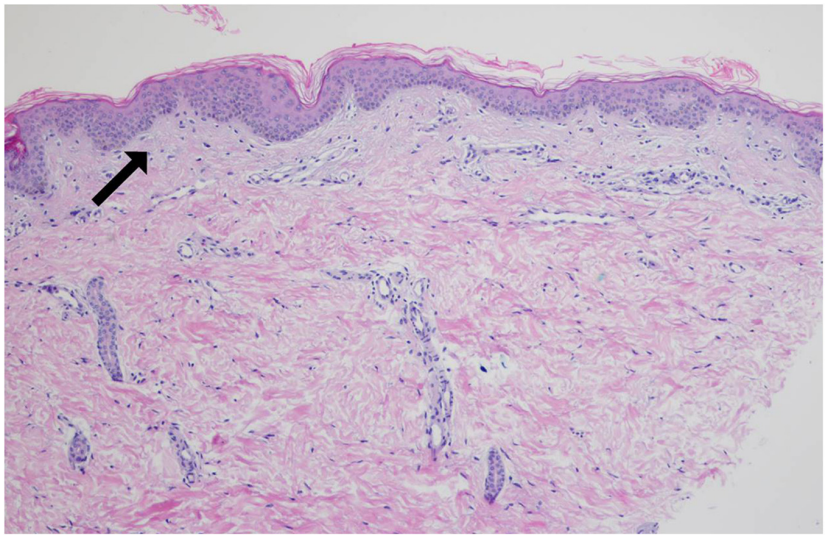

FIGURE 3
Pathological biopsy result of Patient 1. The arrow indicates that there is no melanocyte in stratum basal of the depigmented area (hematoxylin-eosin staining, ×200).

of *KIT* gene mutations (9, 10). Dominant-negative inhibition caused by missense mutations in the TK domain could lead to most severe phenotype. The mild piebaldism phenotype is associated with frameshift variants and missense variants occur in the N-terminal EC domain with haploinsufficiency, and some patients do not even develop any clinical manifestations. Truncating mutations located in the intracellular TK domain or any mutations at or near the TB domain result in intermediate severe phenotype, and different patients in a same family may have different phenotypes. The variants of these three probands were all located in TK domain. Compared with patients who carried the variants in EC domain reported in previous literature (11), the clinical manifestations of three probands were more severe, and all of them showed typical white forelock on frontal scalp, relatively large leukoderma on the chest, abdomen, and extremities. The c. 2469_2484del mutation of Proband 1 located in exon 17 caused a termination codon at position 823 in TK domain. The expression product might lead to haploinsufficiency through nonsense-mediated decay (NMD), or dominant-negative by truncating protein. This type of mutation reduced the normal function of KIT by 50–75%, resulting in a more severe phenotype of this patient. The variants of Proband 2 and 3 were closed to ATP-binding sites (E671, C673, and D677) in TK domain. These two variants might decrease ATP-binding ability by changing motif topological structure according to SWISS-MODEL and AlphaFold. The mutated protein partially retained kinase function and caused milder phenotype of Probands 2 and 3 than Proband 1. This milder phenotype was also reported in a Chinese piebaldism patient with *KIT* missense mutation P665S previously (8). However, proving the precise effect of these mutations requires biochemistry, bioinformatics analysis, and *in vitro* experiment. Meanwhile, the influence of modifying genes or environmental factors on penetrance cannot be ruled out, and further studies are needed.

Significantly, in addition to typical dermatology manifestations of piebaldism, two probands (Probands 1 and 2) in this study also had CALMs. CALMs may present at birth or childhood, and are association with several genetic disorders, such as Neurofibromatosis type 1 (NF1), Legius syndrome (12). NF1 is an autosomal dominant disease characterized by CALM, freckling, neurofibroma, and Lisch nodule (13). It is caused by heterozygous mutation in *NF1* gene. Legius syndrome is also an autosomal dominant disorder due to inactivating mutations in *SPRED1* (14). Individuals with Legius syndrome typically have multiple CALMs, intertriginous freckling without neurofibroma or other tumor. In our study, more than six CALMs > 5 mm in size were found on the trunk or limbs of Proband 2, and less than six in Proband 1. No freckling or neurofibroma was found in three probands, and no *NF1* or *SPRED1* mutation was detected by genetic analysis. Among all the affected family members, none of them had CALMs or freckling. Patients with similar skin manifestations have also been reported in the previous literature (15–17). In the reported cases, all piebaldism patients with CALMs had missense *KIT* mutations located in the TK domain. Therefore, some researchers suggested that CALMs might be related to the location and type of *KIT* gene mutation (17–22). In our study, two variants of Probands 1 and 2 were also located in the TK domain. The p.Tyr823* variant identified in Proband 1 was the first truncating variant in piebaldism patient with CALMs. These two variants could lead to the loss of KIT tyrosine kinase function, inadequate

phosphorylation of *SPRED1*, and eventually result in the loss of inhibition of Ras/MAPK pathway (23). More cases are needed to determine whether CALM or freckling is an uncommon phenotypic variation in the piebaldism spectrum.

In conclusion, we uncovered genetic etiology of three Chinese piebaldism patients and reported three novel pathogenic/likely pathogenic variants. We found novel variants next to ATP-binding site might cause less severe phenotypes. We also reported the first truncating variant in piebaldism patient causing CALMs. Our results further expanded clinical and variants spectra and provided more evidence to elaborate genotype-phenotype correlation of *KIT* mutation.

Data availability statement

The datasets presented in this article are not readily available to protect patient privacy and confidentiality. Requests to access the datasets should be directed to the corresponding author/s.

Ethics statement

This study was approved by the Institutional Medical Ethics Committee of Beijing Children's Hospital, Capital Medical University [(2022)-E-196-R]. Written informed consent to participate in this study was provided by the participants' legal guardian/next of kin. Written informed consent were obtained from the minors' legal guardian for the publication of any potentially identifiable images or data included in this article.

Author contributions

HX and ZX designed the research and supervised the study. CW collected cases and followed up patients. YZ analyzed the data and wrote the manuscript. XH revised the manuscript. LW collected cases. All authors contributed to the article and approved the final version.

Funding

The authors were funded by grants from the National Natural Science Foundation of China (grant no. 82000745) and the Maternal and Child Health Fund of Shunyi Maternal and Children's Hospital of Beijing Children's Hospital (grant no. Y-FYJK-202209).

Acknowledgments

We thank all patients who participated in this study.

Conflict of interest

The authors declare that the research was conducted in the absence of any commercial or financial relationships that could be construed as a potential conflict of interest.

Publisher's note

Supplementary material

The Supplementary Material for this article can be found online at: https://www.frontiersin.org/articles/10.3389/fmed.2022.1040747/full#supplementary-material

References

1. Shah M, Patton E, Zedek D. *Piebaldism*. Treasure Island, FL: StatPearls (2022).

2. Agarwal S, Ojha A. Piebaldism: a brief report and review of the literature. *Indian Dermatol Online J.* (2012) 3:144–7. doi: 10.4103/2229-5178.96722

3. Saleem MD. Biology of human melanocyte development, Piebaldism, and Waardenburg syndrome. *Pediatr Dermatol.* (2019) 36:72–84. doi: 10.1111/pde.13713

4. Giebel LB, Spritz RA. Mutation of the KIT (mast/stem cell growth factor receptor) protooncogene in human piebaldism. *Proc Natl Acad Sci U.S.A.* (1991) 88:8696–9. doi: 10.1073/pnas.88.19.8696

5. Sanchez-Martin M, Perez-Losada J, Rodriguez-Garcia A, Gonzalez-Sanchez B, Korf BR, Kuster W, et al. Deletion of the SLUG (SNAI2) gene results in human piebaldism. *Am J Med Genet Part A.* (2003) 122A:125–32. doi: 10.1002/ajmg.a.20345

6. Pham DDM, Guhan S, Tsao H. KIT and melanoma: biological insights and clinical implications. *Yonsei Med J.* (2020) 61:562–71.

7. Richards S, Aziz N, Bale S, Bick D, Das S, Gastier-Foster J, et al. Standards and guidelines for the interpretation of sequence variants: a joint consensus recommendation of the American college of medical genetics and genomics and the association for molecular pathology. *Genet Med.* (2015) 17:405–24. doi: 10.1038/gim.2015.30

8. Zheng Y, Liu F, Yang Y, Liang Y. Novel KIT missense mutation p665s in a Chinese Piebaldism family. *Ann Dermatol.* (2017) 29:801–3. doi: 10.5021/ad.2017.29.6.801

9. Spritz RA, Holmes SA, Ramesar R, Greenberg J, Curtis D, Beighton P. Mutations of the KIT (mast/stem cell growth factor receptor) proto-oncogene account for a continuous range of phenotypes in human piebaldism. *Am J Hum Genet.* (1992) 51:1058–65.

10. Ward KA, Moss C, Sanders DS. Human piebaldism: relationship between phenotype and site of kit gene mutation. *Br J Dermatol.* (1995) 132:929–35. doi: 10.1111/j.1365-2133.1995.tb16951.x

11. Yin XY, Ren YQ, Yang S, Xu SX, Zhou FS, Du WH, et al. A novel KIT missense mutation in one Chinese family with piebaldism. *Arch Dermatol Res.* (2009) 301:387–9. doi: 10.1007/s00403-009-0955-5

12. Lalor L, Davies OMT, Basel D, Siegel DH. Cafe au lait spots: when and how to pursue their genetic origins. *Clin Dermatol.* (2020) 38:421–31. doi: 10.1016/j.clindermatol.2020.03.005

13. Cimino PJ, Gutmann DH. Neurofibromatosis type 1. *Handb Clin Neurol.* (2018) 148:799–811. doi: 10.1016/B978-0-444-64076-5.00051-X

14. Brems H, Legius E. Legius syndrome, an update. molecular pathology of mutations in SPRED1. *Keio J Med.* (2013) 62:107–12. doi: 10.2302/kjm.2013-0002-RE

15. Chang T, McGrae JD Jr, Hashimoto K. Ultrastructural study of two patients with both piebaldism and neurofibromatosis 1. *Pediatr Dermatol.* (1993) 10:224–34; discussion 88. doi: 10.1111/j.1525-1470.1993.tb00366.x

16. Angelo C, Cianchini G, Grosso MG, Zambruno G, Cavalieri R, Paradisi M. Association of piebaldism and neurofibromatosis type 1 in a girl. *Pediatr Dermatol.* (2001) 18:490–3. doi: 10.1046/j.1525-1470.2001.1862005.x

17. Duarte AF, Mota A, Baudrier T, Morais P, Santos A, Cerqueira R, et al. Piebaldism and neurofibromatosis type 1: family report. *Dermatol Online J.* (2010) 16:11. doi: 10.5070/D38PG2D4SZ

18. Chiu YE, Dugan S, Basel D, Siegel DH. Association of Piebaldism, multiple cafe-au-lait macules, and intertriginous freckling: clinical evidence of a common pathway between KIT and sprouty-related, ena/vasodilator-stimulated phosphoprotein homology-1 domain containing protein 1 (SPRED1). *Pediatr Dermatol.* (2013) 30:379–82. doi: 10.1111/j.1525-1470.2012.01858.x

19. Stevens CA, Chiang PW, Messiaen LM. Cafe-au-lait macules and intertriginous freckling in piebaldism: clinical overlap with neurofibromatosis type 1 and Legius syndrome. *Am J Med Genet Part A.* (2012) 158A:1195–9. doi: 10.1002/ajmg.a.35297

20. Oiso N, Kishida K, Fukai K, Motokawa T, Hosomi N, Suzuki T, et al. A Japanese piebald patient with auburn hair colour associated with a novel mutation p.P832L in the KIT gene and a homozygous variant p.I120T in the MC1R gene. *Br J Dermatol.* (2009) 161:468–9. doi: 10.1111/j.1365-2133.2009.09138.x

21. Spritz RA, Itin PH, Gutmann DH. Piebaldism and neurofibromatosis type 1: horses of very different colors. *J Investig Dermatol.* (2004) 122:xxxiv–v. doi: 10.1046/j.0022-202X.2004.22235.x

22. Spritz RA, Holmes SA, Itin P, Kuster W. Novel mutations of the KIT (mast/stem cell growth factor receptor) proto-oncogene in human piebaldism. *J Investig Dermatol.* (1993) 101:22–5. doi: 10.1111/1523-1747.ep12358440

23. Saito H, Yoshida T, Yamazaki H, Suzuki N. Conditional N-rasG12V expression promotes manifestations of neurofibromatosis in a mouse model. *Oncogene.* (2007) 26:4714–9. doi: 10.1038/sj.onc.1210250

frontiers | Frontiers in Pharmacology

TYPE Case Report
PUBLISHED 15 December 2022
DOI 10.3389/fphar.2022.1038090

OPEN ACCESS

EDITED BY
Jian Gao,
Shanghai Children's Medical Center, China

REVIEWED BY
Wei-Zen Sun,
National Taiwan University Hospital, Taiwan
Katrin Õunap,
University of Tartu, Estonia

*CORRESPONDENCE
Chih-Shung Wong,
w82556@gmail.com
Min-Jia Li,
minjiali@livemail.tw

†These authors have contributed equally to this work

SPECIALTY SECTION
This article was submitted to Obstetric and Pediatric Pharmacology, a section of the journal Frontiers in Pharmacology

RECEIVED 06 September 2022
ACCEPTED 25 November 2022
PUBLISHED 15 December 2022

CITATION
Chang E-C, Chang Y-H, Tsai Y-S, Hung Y-L, Li M-J and Wong C-S (2022), Case report: The art of anesthesiology—Approaching a minor procedure in a child with MPI-CDG. *Front. Pharmacol.* 13:1038090. doi: 10.3389/fphar.2022.1038090

Case report: The art of anesthesiology—Approaching a minor procedure in a child with MPI-CDG

En-Che Chang[1], Yu-Hsuan Chang[1], Yu-Shiun Tsai[1], Yi-Li Hung[2], Min-Jia Li[3*†] and Chih-Shung Wong[1,3,4*†]

[1]School of Medicine, Fu-Jen Catholic University, New Taipei, Taiwan, [2]Department of Pediatrics, Cathay General Hospital, Taipei, Taiwan, [3]Department of Anesthesiology, Cathay General Hospital, Taipei, Taiwan, [4]Graduate Institute of Medical Science, National Defense Medical, Taipei, Taiwan

Background: Protein glycosylation plays an important role in post-translational modification, which defines a broad spectrum of protein functions. Accordingly, infants with a congenital disorder of glycosylation (CDG) can have N-glycosylation, O-glycosylation, or combined N- and O-glycosylation defects, resulting in similar but different multisystem involvement. CDGs can present notable gastrointestinal and neurologic symptoms. Both protein-losing enteropathy and hypotonia affect the decision of using anesthetics. We reported a case of MPI-CDG with protein-losing enteropathy and muscular hypotonia that underwent different anesthesia approach strategies of vascular access. Here, we highlight why intubation with sevoflurane anesthesia and sparing use of muscle relaxants is the optimal strategy for such a condition.

Case presentation: A 25-month-old girl, weighing 6.6 kg and 64 cm tall, suffered chronic diarrhea, hypoalbuminemia, and hypotonia since birth. Protein-losing enteropathy due to MPI-CDG was documented by whole-exome sequencing. She underwent three sedated surgical procedures in our hospital. The sedation was administered twice by pediatricians with oral chloral hydrate, intravenous midazolam, and ketamine, to which the patient showed moderate to late recovery from sedation and irritability the following night. The most recent one was administered by an anesthesiologist, where endotracheal intubation was performed with sevoflurane as the main anesthetic. The patient regained consciousness immediately after the operation. She had no complications after all three sedation/anesthesia interventions and was discharged 7 days later, uneventful after the third general anesthesia procedure.

Conclusion: We performed safe anesthetic management in a 25-month-old girl with MPI-CDG using sevoflurane under controlled ventilation. She awoke immediately after the procedure. Due to the disease entity, we suggested bypassing the intravenous route to avoid excess volume for drug administration and that muscle relaxant may not be necessary for endotracheal intubation and patient immobilization when performing procedures under general anesthesia in CDG patients.

KEYWORDS

CDG, ketamine, sevoflurane, hypoalbuminemia, neuromuscular blocking agents, hypotonia, intravenous flushing

1 Introduction

The provision of safe anesthesia for pediatric patients depends on a clear understanding of the physiologic, pharmacologic, and psychological differences between children and adults (Miller et al., 2009). Practitioners should evaluate several critical pre-operational conditions when planning for pediatric anesthesia. These medical conditions include but are not limited to a patient's developmental status, the aim of the surgery, preoperative preparation, pharmacology of the candidate drugs, and the possible side effects after administration (Miller et al., 2009). Every step matters; the more information collected, the better the plan can be made. This is particularly important when it comes to dealing with rare diseases. Infants with CDGs present varying levels of involvement of the central nervous system (most often hypotonia and ataxia), dysmorphology, gastrointestinal symptoms including protein-losing enteropathy, and other signs (Kliegman et al., 2016). Some symptoms affect the choice of anesthesia management, while facial dysmorphism/preterm birth raises worries of airway insecurity; both protein-losing enteropathy and hypotonia can affect the decisions made during anesthesia management. To date, the literature on this subject lacks reports on anesthesia management in children with CDGs. To date, only three reports have been published, each regarding CDG types, namely, PMM2-CDG, ALG6-CDG, and STT3B-CDG (Sakai et al., 2017) (Meaudre et al., 2005) (Lehavi et al., 2011). Sakai et al. (2017) suggested the use of neuromuscular monitoring when using rocuronium on CDG patients with hepatic dysfunction and hypotonia. Meaudre et al. (2005) highlighted the complexity of coagulopathy in CDG patients and the perioperative assessment of clotting factors, as part of which practitioners use fresh frozen plasma or a prothrombin complex concentrate to lower hemorrhagic risk during surgery (Altassan et al., 2019). Lehavi et al. (2011) described a nitrous oxide–remifentanil-based anesthesia on a 6-year-old boy (16.2 kg), taking into account concerns about the CDG patient's hemodynamic status and hepatic function. At present, there are no specific guidelines for managing anesthesia in CDG patients, and more data is required. In response, the present study reports on the anesthesia practices used for a 25-month-old girl suffering from MPI-CDG with protein-losing enteropathy and muscular hypotonia. In our case, we present three approaches to anesthesia management during vascular access for regular albumin infusion, performed by different specialists. We also discuss the particular concerns of the approaches and propose an overall strategy.

2 Case presentation

The patient was a 25-month-old girl, who weighed 6.6 kg (< 0.1 percentile) and was 64 cm (< 0.1 percentile) tall. She was diagnosed with MPI-CDG with protein-losing enteropathy, hypoalbuminemia, hypogammaglobulinemia (IgG = 118.0 mg/dl), muscular hypotonia, and some dysmorphic features, including a wide prominent forehead, flat nose, large anterior fontanelle, web neck, and skeletal dysplasia (Figure 1). Her liver transaminase levels were within normal limits (AST = 17 IU/L; ALT = 14 IU/L). She underwent three sedated vascular access surgeries for regular albumin infusion in our hospital. The sedation was administered twice by pediatricians to place a peripherally inserted central catheter (PICC), and the most recent one was administered by anesthesiologists for a port-a-cath exchange. The pediatricians gave oral chloral hydrate, intravenous midazolam, and ketamine while monitoring vital signs including body temperature (BT), blood pressure (BP), heart rate (HR), arterial oxyhemoglobin saturation (SaO_2), and respiratory rate (RR). On the other hand, the anesthesiologist performed endotracheal intubation and gave sevoflurane inhalation with oxygen while monitoring similar vital signs including end-tidal carbon dioxide ($ETCO_2$) for airway and respiratory function monitoring.

The first sedation was administered by pediatricians in the pediatric intensive care unit (PICU) for the purpose of placing a PICC. Routine non-invasive monitoring was established, including BT, BP, HR, SaO_2, and RR. Before anesthesia, her vital signs were stable: BT: 36.4°C, BP: 95/74 mmHg, HR: 114/min, SaO_2: 100%, and RR: 34/min. The sedation was induced orally using a 3.5 ml 10% chloral hydrate solution (0.5 cc· kg^{-1}), intravenous 0.7 mg midazolam (0.1 mg · kg^{-1}), and continued on 6 mg ketamine (0.9 mg · kg^{-1}) seven times, with a total dosage of 42 mg within 169 min. The surgery lasted 215 min; however, we failed to insert the PICC. During the procedure, the addition of ketamine was adjusted according to restlessness to ensure that the patient did not wake up. The patient's vital signs remained stable, with no bradycardia, hypotension, apnea, or arterial desaturation, during the whole procedure. After awakening from the procedure, there were no other symptoms or discomfort for the patient, except for appearing irritable the following night.

The second sedation was also administered by pediatricians in the PICU to place a PICC. The procedure was performed by a plastic surgeon, who asked for a completely stable patient during the operation. Routine monitoring was established, including BT, BP, HR, SaO_2, and RR. Before the anesthesia, her vital signs were stable: BT: 36.2°C, BP: 91/57 mmHg, HR: 120/min, SaO_2: 99%, and RR: 30/min. Prior to the procedure, she was induced using

3.4 ml 10% chloral hydrate solution (0.5 cc· kg^{-1}), 0.7 mg midazolam (0.1 mg · kg^{-1}), and continued on 6 mg ketamine (0.9 mg · kg^{-1}) five times, with a total dosage of 30 mg within 147 min. The surgery lasted 90 min, anesthesia time was 170 min, and a heart rate over 150/min was used as a sign of awakening and for additional drug dosage supplements. The patient remained stable, and a PICC was successfully placed. During the operation, her vital signs were also stable, with no bradycardia, hypotension, apnea, or arterial desaturation. There were no other complications or discomfort from the patient except for appearing irritable the night after the administration of anesthesia.

The latest anesthesia was administered by anesthesiologists for a port-a-cath exchange in the operating room. At the pre-anesthesia assessment, her anesthesia status was graded as American Society of Anesthesiologists (ASA) Class III for CDG disease entity and possible difficulty in airway establishment. The laboratory examination showed hypoalbuminemia and anemia, and her chest X-ray showed increased non-specific infiltrate in the bilateral lower lungs. Electrocardiography showed normal sinus rhythm. Before the anesthesia, her vital signs were stable with BT: 36.2°C, BP: 89/47 mmHg, HR: 119/min, SaO_2: 99%, and RR: 50/min. In order to minimize complications from endotracheal intubation, GlideScope® was used, and the patient was brought to a sniffing position with neck protection. After successful airway establishment, sevoflurane was used as the main anesthesia. After evaluating the patient's muscle tone, muscle relaxants were not administered. A total of 0.1 mg atropine was given to maintain the heart rate (150–160/min) for an adequate cardiac output. The surgery lasted 60 min, and the anesthesia time lasted 120 min. The patient's vital signs remained stable and under secured ventilation control, with no bradycardia, hypotension, apnea, or arterial desaturation. After completion of the operation, the patient regained consciousness and was sent back to the PICU, where the ET tube was removed and a nasal cannula was placed for 4 h. No complication or discomfort was observed, and the patient was discharged uneventfully 7 days later.

FIGURE 1
Photo of the patient before the port-a-cath exchange. Her dysmorphic features were wide prominent forehead, flat nose, large anterior fontanelle, web neck, and skeletal dysplasia.

3 Discussion

3.1 Overview

Three anesthetic interventions were performed in our reported MPI-CDG case. When facing rare diseases, the common obstacles for healthcare professionals include diagnostic delays and lack of information and treatment options. A comprehensive evaluation is particularly critical in situations like this. In this case, the anesthesiologists routinely and thoroughly evaluated the patient's condition, especially included assessing the patient's airway condition. While each of the patients' experiences under anesthetic were fine, it is important to remember that the aim of using anesthesia is to ease the patient for an unbothered surgery.

3.2 Airway management

When managing children under anesthesia, it is important to constantly maintain a secured airway with satisfactory ventilation and oxygenation. A failed airway can cause hypoxia, potentially leading to brain damage and death within minutes (Cook and MacDougall-Davis, 2012). It is currently reported that more than half of critical perioperative events in children are respiratory complications (Habre et al., 2017). Any improvement in preparation (mainly preoxygenation and patient positioning), intubation techniques, and removal of airway devices can minimize perioperative complications. Additionally, capnography monitoring for critical information on ventilation, perfusion, and metabolism is a standard tool that ensures the establishment of a secured endotracheal tube (Soto et al., 2004). In cases in which difficulties with the airway might be expected, it is recommended that intravenous access be prepared beforehand for instant management of potential

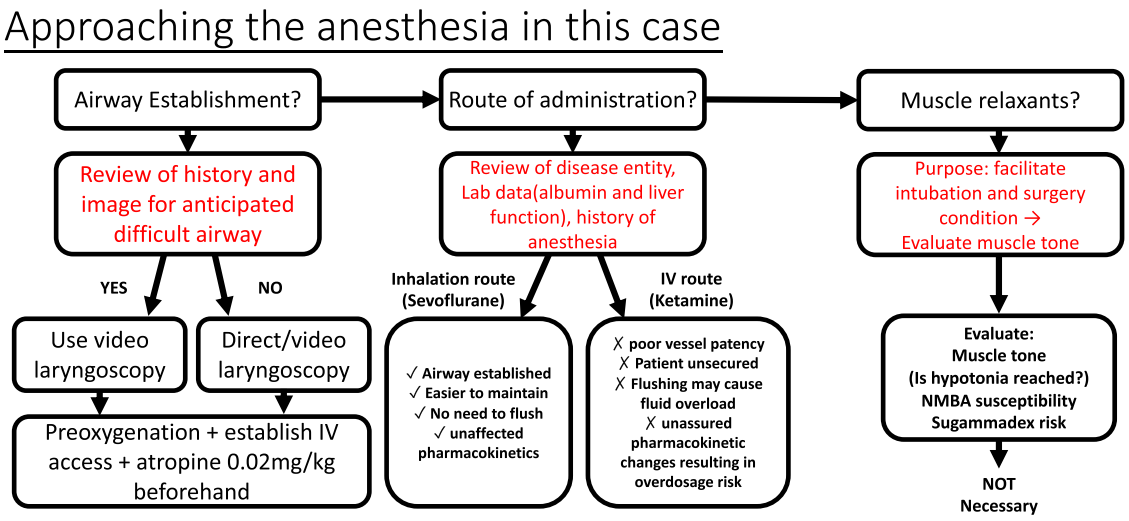

FIGURE 2
Approach to the anesthesia in the case. Secured airway prevents respiratory complications and brain hypoxia in children's anesthesia. After the review of X-ray and evaluating child appearance, video larnygoscopy was chosen for expected difficult airway intubation. Decision of the route of administration depends on the pros and cons. Hypoalbuminemia increases free active fraction of protein-bound drugs; at the same time, elevated liver transaminases/liver pathology may also interfere with drug metabolism, in this case, ketamine. On the other hand, anesthetic sevoflurane was eliminated directly *via* lung exhalation, bypassing the liver metabolism. Therefore, the inhalation route outweighed the IV route with its convenience and safety. Muscle relaxants act to facilitate endotracheal intubation and operation; in this case, with hypotonia and the muscle relaxation effect of sevoflurane, NMBAs were not necessary. Sugammadex is a good choice for immediately reversing non-depolarizing muscle relaxants (rocuronium or vecuronium). However, it has not been approved by the USFDA for use in children under two years of age.

emergencies, e.g., laryngospasm and bradycardia, where the latter is usually prevented by administering 0.02 mg/kg atropine (Karsli, 2015). In addition, experts recently recommended the use of video laryngoscopy as the first option for patients in which intubation is anticipated to be difficult (Dadure et al., 2019).

The concerns mentioned above were addressed in the third operation. In this case, we anticipated difficult airway management because of dysmorphism (low-set ears, wide eye distance, and some retrognathia) (Roth et al., 2021) and a narrow airway evidenced by X-rays. Preoxygenation and a neutral airway position were established, atropine 0.1 mg was administered through pre-established PICC, and video laryngoscopy (GlideScope®) was used for tracheal intubation. The successful airway establishment and monitoring of $ETCO_2$ not only secured the patient's status for surgery but also suited the chosen anesthesia route, which is discussed in the next section.

3.3 Anesthetic administration

The induction of general anesthesia for children occurs either by inhalation or intravenously (IV). While inhalation induction is the most common technique in young children, there are several conditions for which IV induction is preferred. Whatever the route, it is always necessary to evaluate the children's history and laboratory findings before planning the anesthetic to be used. We discussed the concerns in three dimensions: patients' laboratory status, ketamine experience and pharmacokinetics, and IV route drawbacks.

First of all, Saad et al. (2020) strongly highlighted the importance of preoperative malnutrition screening and management for the risk of anesthetic overdose. In our case, the girl has hypoalbuminemia with underlying protein-losing enteropathy. Although supported by intravascular nutrient support, her preoperative albumin levels were all low. The high prevalence of hepatic dysfunction in CDG patients is also noticeable (da Silva et al., 2017) (Schollen et al., 2004), with her transaminases within normal limits but prothrombin time shortened. These laboratory findings affect the pharmacokinetics of anesthetics, in this case, ketamine.

In children, ketamine plays an anesthetic role in short-term procedures. Well-known for its psychodysleptic effects, ketamine is a rapid-acting N-methyl-D-aspartic acid (NMDA) receptor non-competitive antagonist (Kurdi et al., 2014). It also interacts with opioid receptors, monoamine, cholinergic, purinergic, and adrenoreceptor systems, providing both positive and negative modulation in sedation and analgesia (Nowacka and Borczyk, 2019). The benefits include preserving children's cardio-respiratory stability by enhancing or maintaining a normal skeletal muscle tone (Rosenbaum et al., 2021). However, this does not ensure a secured airway and there may be transient

TABLE 1 Comparison of the three anesthetic practices. Notice the durations of both ketamine-induced anesthesia and hypoalbuminemia status, which raise overdose and fluid overload concerns.

	Anesthesia by pediatrics for CVC (9/22)	Anesthesia by pediatrics for PICC (10/08)	Anesthesia by anesthesiologist for port-a-cath (10/11)
Duration of anesthesia	215 min (14:50–18:25) BW:6577 g	170 min (15:30–18:20) BW:6692 g	120 min (8:10–10:10) BW:6600 g
Anesthetics and dose			
General	Chloral hydrate soln. 10% dose 3.5 ml at 0 min, midazolam 15 mg/3 ml dose 0.7 mg at 20 min, ketamine 500 mg/10 ml dose 6 mg at 36 min, 100 min, 128 min, 154 min, 178 min, 192 min, and 205 min, respectively (seven times totally)	Chloral hydrate soln. 10% dose 3.4 ml at 0 min, midazolam 15 mg/3 ml dose 0.7 mg at 45 min, ketamine 500 mg/10 ml dose 6 mg at 55 min, 57 min, 89 min, 134 min, and 202 min, respectively (five times totally)	Sevoflurane 4L/min from 0 min to 5 min (5 min, Induction), sevoflurane 2L/min from 5 min to 90 min (85 min, maintain) O_2 2L/min from 0 min to 120 min
Local	Lidocaine HCl 2% dose 20 ml at 15 min	None	None
Muscle relaxants	None	None	None
Others	None	None	Atropine 0.1 mg
Vital sign			
Before anesthesia	BT: 36.4, HR: 114, SaO_2: 100, and RR: 34	BT: 36.2, HR: 120, SaO_2: 99, and RR: 30	BT: 36, HR: 119, SaO_2: 99, and RR: 50
During anesthesia	Vital signs stable, BT: 36.7, HR: 124 ~128, SaO2: 98 ~100%, and RR: 43 ~53	Vital signs stable, BT: 36.2 ~37.0, HR: 120 ~135, SaO2: 99 ~100%, and RR: 30 ~54	Vital sign stable, BT: 36.5 ~37.0, HR: 145 ~150 ET intubation with control ventilation: $ETCO_2$: 41 ~52, SaO_2: 100%
After anesthesia	BP: 84/54 mmHg, BT: 36.7 ~37.9, HR: 154, SaO_2: 100, RR: 39, and emotional irritation for one night	HR: 150, SaO_2: 100%, RR: 42, and emotional irritation for one night	One vomiting episode after arriving from the PICU while on an ET tube, fair spirit after removal of the ET tube intermittently asleep/awake, nasal cannula flow rate: 0.5L/min, BT: 36.9, HR: 146, BP: 81/66, SaO_2: 100, and RR: 29 ~51
Lab	Albumin: 2.3 g/dl (L, 9/20) and albumin: 2.4 g/dl (L, 9/27)	Albumin: 1.4 g/dl (L, 10/04) and albumin: 1.8 g/dl (L, 10/09)	Albumin: 1.8 g/dl (L, 10/09) and albumin: 3.2 g/dl (L, 10/09)
Comments	Not suggested due to 1) overdose and flushing concerns. 2) Ketamine: pharmacokinetics and side effect. 3) IV drug supplement when the child shows signs of awakening, interrupting the surgery. 4) Not intubated		Suggested: 1) intubated with secured airway. 2) Secured anesthesia with an inhalation route

minimal respiratory depression if ketamine is administered too rapidly or in too high a dose. Therefore, pharmacokinetics should always be evaluated on a case-by-case basis. According to the literature (Trevor et al., 2019) (Miller et al., 2009), ketamine onset occurs rapidly due to high lipid solubility and ceases its effect by redistribution to inactive sites at a half-life of 11–16 min. Two aspects of ketamine properties were the foci in our case. For one, it is metabolized in the liver through N-demethylation by the cytochrome CYP3A4 (Dinis-Oliveira, 2017). Second, ketamine is the only intravenous anesthetic that has low protein binding (approximately 12%). In our experience, pediatricians empirically chose IV ketamine with midazolam adjuvant for two sedation episodes. Propofol was not used for her age, under 3, according to the Food and Drug Administration (FDA) of the United States. Although both single and accumulative ketamine dosage were within normal limits (induction 0.5–2 mg/kg, lethal dose 600 mg/kg (Orhurhu1 et al., 2021)), the supplement interval (mean 25 min) indicated a mildly prolonged sedation. We tried to explain this outcome despite the lack of literature on the two foci, liver metabolism and protein binding mentioned above. Given that the girl showed normal transaminase levels, we considered there to be a low risk of hepatic-derived complications in the anesthesia outcome. On the other hand, hypoalbuminemia has a great effect on high protein-binding agents; since ketamine is one of the low protein-binding anesthetics, ketamine pharmacokinetics are rarely studied in hypoalbuminemia. However, as hypoalbuminemia more or less reduces protein-binding and increases the free active fraction of drugs (Pino, 2019), we considered this as the cause of her two prolonged ketamine sedations. Last, ketamine-induced dissociation is a major side effect causing concern in pediatric anesthesia. Although midazolam was used as an adjuvant to reduce ketamine induction dosage, the child showed irritability after both interventions. Therefore, the decision to use ketamine should be made carefully, especially when the child shows abnormal susceptibility.

Residual drugs can remain in the dead space of intravenous lines, which is especially crucial when giving small-volume infusions (< 250 ml), according to the National Infusion and Vascular Access Society (NIVAS, 2021). However, there are debates about whether it is necessary to flush, due to there being a lack of evidence. The current guidance (NIVAS, 2019) provides three options, including discarding the infusion set, flushing manually with 50 ml sodium chloride (0.9%), and flushing with a closed system using an additional fixed needle free connector at the top of the given set. Heparin is also used to prevent intraluminal clot formation and/or catheter colonization (Goossens, 2015). Recently, experts (Rout et al., 2020) (Cousins, 2018) have raised concerns about underdosing, claiming that most healthcare organizations chose option one rather than flushing to cut costs. This is supported by Harding et al. (2020) who found out that up to 35% of medication may not be administered due to residual volume, with the greatest percentage associated with 50-ml solutions. In our case, the girl received seven and five ketamine IV bolus at 0.12 ml per dose (Ketalar®500mg/10 ml, 6 mg per dose) in her first two operations, which fits the definition of small-volume infusion. According to NIVAS, in this case, the best practice that minimizes medication loss would be to flush the cannula before and after the drug administration, which in our general practice will be twice the catheter dead space volume. When planning her third anesthesia, we considered not using the intravenous route for two reasons. For one, she had undergone numerous intravenous procedures since her birth, which brought concerns about her peripheral vessel patency. Second, given the dead space (2 ml) in her PICC and the small volume of her dosage (0.12 ml), flushing for complete administration was necessary. Unfortunately, this may have brought about fluid overload when repeated doses were needed in such a small baby (6.6 kg) with hypoalbuminemia. According to Holliday and Segar (1957), the fluid rate for full maintenance of a 6.6-kg child is approximately 26.4 ml/h. If we applied the practice mentioned previously, we would have flushed an estimated 30 ml, an amount beyond full maintenance, which meant that the calculated fluid overload percentage, using the definition developed by Goldstein et al. (2001) or the Goldstein method, would have increased by 1.8%, with every 1% increase in the odds ratio by 1.04 (Selewski et al., 2011). On the other hand, the induction of inhalation agents depends primarily on gas flow or controlled ventilation in children. Taking advantage of the secured intubation we established beforehand and preserving her heart rate with atropine, we chose sevoflurane as the anesthetic for our third operation, in addition to the common benefits of the drug. Finally, the inhalation route also strongly supports the maintenance of sedation for the entire duration of the operation and avoiding intravenous flushing with its realted concerns.

3.4 Hypotonia and muscle relaxants

Muscle relaxants, or neuromuscular blocking agents (NMBAs), are commonly used in anesthesia under the indication to facilitate intubation and surgery condition. However, the use of NMBAs should be determined individually (Gueret et al., 2004). NMBAs can have an unexpectedly prolonged effect in patients with hypotonia, and the susceptibility of patients with CDG to non-depolarizing NMBAs remains unclear (Sakai et al., 2017). Although it is not well understood, to the best of our knowledge, trans-synaptic signaling is reduced in CDGs (Frappaolo et al., 2018), the expression of postsynaptic nicotinic acetylcholine receptors with normal function is also reduced (Freeze et al., 2014). This supports our assumption in treating CDG as myasthenia gravis when it comes to NMBAs. For most surgical procedures, administration of NMBAs is not necessary for patients with myasthenia. Adequate relaxation is often reached using inhalation agents alone (Nitahara et al., 2007) (Rocca et al., 2003), in our case, sevoflurane. Even if NMBAs are needed, due to susceptibility concerns (Eisenkraft et al., 1988), it has been suggested that non-depolarizing NMBAs should be used, namely rocuronium or vecuronium with a reversal with sugammadex (Tsukada et al., 2021) (de Boer et al., 2014). However, sugammadex has not received FDA approval for use in children, and to date, there are limited data regarding its administration to pediatric patients (Tobias, 2017). Therefore, due to the patient's hypotonia and adequate relaxation after administering sevoflurane, additional muscle relaxants were not required to achieve the degree of immobilization required for the surgeon to proceed with the port-a-cath replacement.

3.5 Summary and strategy

The pharmacological characteristics of good sedation and analgesia include ease of application, rapid action, short duration of action, and lack of significant adverse reactions (Norambuena et al., 2013). An experienced and professional practitioner can be a valuable asset when approaching unclear situations (Schulz et al., 2013). The cases presented here raise three crucial concerns of anesthesia, including airway management, choice of drug, and the decision to use a muscle relaxant. Although there is a lack of precise guidelines for anesthesia in CDGs, decisions can still be made by a comprehensive strategy (Figure 2) including evaluating the patient, understanding the underlying mechanisms, and weighing the medical risks and benefits, all to achieve the final purpose—to assure the surgeon and secure the patient.

4 Conclusion

This study reports rare clinical experiences in MPI-CDG children's anesthesia management. Comparing the three anesthetic experiences, we have reviewed the decisions made by two specialists (Table 1). Based on our review of the literature and discussion of recent studies, we suggest that when anesthesia is needed for CDG patients practitioners use inhaled anesthetics instead of the intravenous route and consider not using NMBAs if patients show hypotonia. These findings will help in administering an anesthetic to CDG children in the future and we encourage further research on this subject.

Data availability statement

The original contributions presented in the study are included in the article/Supplementary Material; further inquiries can be directed to the corresponding authors.

Ethics statement

The studies involving human participants were reviewed and approved by Cathay General Hospital IRB (CGH-IRB No. P111017). Written informed consent to participate in this study was provided by the participants' legal guardians/next of kin. Written informed consent was obtained from the minor(s)' legal guardian/next of kin for the publication of any potentially identifiable images or data included in this article.

Author contributions

E-CC contributed to the design, writing, review, and revision of this manuscript. Y-HC and Y-ST contributed to collecting data and drafting the manuscript. C-SW guided E-CC in design, writing and final reviewing the case report. Y-LH and M-JL contributed to the anesthesia management of the case and proofread the final manuscript.

Conflict of interest

The authors declare that the research was conducted in the absence of any commercial or financial relationships that could be construed as a potential conflict of interest.

Publisher's note

All claims expressed in this article are solely those of the authors and do not necessarily represent those of their affiliated organizations, or those of the publisher, the editors, and the reviewers. Any product that may be evaluated in this article, or claim that may be made by its manufacturer, is not guaranteed or endorsed by the publisher.

References

Altassan, R., Péanne, R., Jaeken, J., Barone, R., Bidet, M., Borgel, D., et al. (2019). International clinical guidelines for the management of phosphomannomutase 2-congenital disorders of glycosylation: Diagnosis, treatment and follow up. *J. Inherit. Metab. Dis.* 42, 5–28. doi:10.1002/jimd.12024

Cook, T. M., and MacDougall-Davis, S. R. (2012). Complications and failure of airway management. *Br. J. Anaesth.* 109, i68-i85. doi:10.1093/bja/aes393

Cousins, D. (2018). Patients are being underdosed: We need new guidance on small-volume drug infusions. *Clin. Pharm.* 10. doi:10.1211/CP.2018.20205779

da Silva, D. M., Ferreira, V. D. R., Monticelli, M., Janeiro, P., Videira, P. A., da Silva, P. W., et al. (2017). Liver involvement in congenital disorders of glycosylation (CDG). a systematic review of the literature. *J. Inherit. Metab. Dis.* 40, 195–207. doi:10.1007/s10545-016-0012-4

Dadure, C., Sabourdin, N., Veyckemans, F., Babre, F., Bourdaud, N., et al. (2019). Management of the child's airway under anaesthesia: The French guidelines. *Anaesth. Crit. Care Pain Med.* 38, 681–693. doi:10.1016/j.accpm.2019.02.004

de Boer, H. D., Shields, M. O., and Booij, L. H. D. J. (2014). Reversal of neuromuscular blockade with sugammadex in patients with myasthenia gravis: A case series of 21 patients and review of the literature. *Eur. J. Anaesthesiol.* 31, 715–721. doi:10.1097/EJA.0000000000000153

Dinis-Oliveira, R. J. (2017). Metabolism and metabolomics of ketamine: A toxicological approach. *Forensic Sci. Res.* 2, 2–10. doi:10.1080/20961790.2017.1285219

Eisenkraft, J. B., Book, W. J., Mann, S. M., Papatestas, A. E., and Hubbard, M. (1988). Resistance to succinylcholine in myasthenia gravis: A dose-response study. *Anesthesiology* 69, 760–763. doi:10.1097/00000542-198811000-00021

Frappaolo, A., Sechi, S., Kumagai, T., Karimpour-Ghahnavieh, A., Tiemeyer, M., and Giansanti, M. G. (2018). Modeling congenital disorders of n-linked glycoprotein glycosylation in drosophila melanogaster. *Front. Genet.* 9, 436. doi:10.3389/fgene.2018.00436

Freeze, H. H., Chong, J. X., Bamshad, M. J., and Ng, B. G. (2014). Solving glycosylation disorders: Fundamental approaches reveal complicated pathways. *Am. J. Hum. Genet.* 94, 161–175. doi:10.1016/j.ajhg.2013.10.024

Goldstein, S. L., Currier, H., Cd, G., Cosio, C. C., Brewer, E. D., and Sachdeva, R. (2001). Outcome in children receiving continuous venovenous hemofiltration. *Pediatrics* 107, 1309–1312. doi:10.1542/peds.107.6.1309

Goossens, G. A. (2015). Flushing and locking of venous catheters: Available evidence and evidence deficit. *Nurs. Res. Pract.* 2015, 1–12. doi:10.1155/2015/985686

Gueret, G., Rossignol, B., Kiss, G., Wargnier, J. P., Miossec, A., Spielman, S., et al. (2004).,Is muscle relaxant necessary for cardiac surgery? *Anesth. Analg.* 99.(5), FF, 1330–1333. doi:10.1213/01.ANE.0000132984.56312-FF

Habre, W., Disma, N., Virag, K., Becke, K., Hansen, T. G., Habre, M. J., et al. (2017). Incidence of severe critical events in paediatric anaesthesia (apricot): A prospective multicentre observational study in 261 hospitals in Europe. *Lancet. Respir. Med.* 05, 412–425. doi:10.1016/S2213-2600(17)30116-9

Harding, M., Stefka, S., Bailey, M., Morgan, D., and Anderson, A. (2020). Best practice for delivering small-volume intermittent intravenous infusions. *J. Infus. Nurs.* 43, 47–52. doi:10.1097/NAN.0000000000000355

Holliday, M. A., and Segar, W. E. (1957). The maintenance need for water in parenteral fluid therapy. *Pediatrics* 19, 823–832. doi:10.1542/peds.19.5.823

Karsli, C. (2015). Managing the challenging pediatric airway: Continuing professional development. *Can. J. Anaesth.* 62, 1000–1016. doi:10.1007/s12630-015-0423-y

Kliegman, R., Stanton, B., Geme, J., Schor, N., and Behrman, R. (2016). *Nelson textbook of pediatrics*. Philadelphia: Elsevier.

Kurdi, M. S., Theerth, K. A., and Deva, R. S. (2014). Ketamine: Current applications in anesthesia, pain, and critical care. *Anesth. Essays Res.* 08, 283–290. doi:10.4103/0259-1162.143110

Lehavi, A., Mandel, H., and Katz, Y. S. (2011). Anesthetic management of a boy with congenital disorder of glycosylation (CDG) i-x. *Int. J. Clin. Med.* 02, 325–327. doi:10.4236/ijcm.2011.23056

Meaudre, E., Meyrieux, V., Suprano, I., Camboulives, J., and Paut, O. (2005). Anesthesia considerations in carbohydrate-deficient glycoprotein syndrome type i. *Paediatr. Anaesth.* 15, 905–906. doi:10.1111/j.1460-9592.2005.01671.x

Miller, R. D., Eriksson, L. I., Fleisher, L. A., Wiener-Kronish, J. P., and Young, W. L. (2009). *Miller's anesthesia*. Philadelphia: Elsevier Health Sciences.

Nitahara, K., Sugi, Y., Higa, K., Shono, S., and Hamada, T. (2007). Neuromuscular effects of sevoflurane in myasthenia gravis patients. *Br. J. Anaesth.* 98, 337–341. doi:10.1093/bja/ael368

Norambuena, C., Yañez, J., Flores, V., Puentes, P., Carrasco, P., and Villena, R. (2013). Oral ketamine and midazolam for pediatric burn patients: A prospective, randomized, double-blind study. *J. Pediatr. Surg.* 48, 629–634. doi:10.1016/j.jpedsurg.2012.08.018

Nowacka, A., and Borczyk, M. (2019). Ketamine applications beyond anesthesia – A literature review. *Eur. J. Pharmacol.* 860, 172547. doi:10.1016/j.ejphar.2019.172547

Orhurhu1, V. J., Vashisht, R., Claus2, L. E., and Cohen, S. P. (2021). "Ketamine toxicity," in *StatPearls* (Tampa, FL, United States: StatPearls Publishing).

Pino, R. M. (2019). "Specific considerations with liver disease - metabolism of anesthetic," in *Clinical anesthesia procedures of the Massachusetts general hospital*. Editors R. M. Pino and Wolters Kluwer. Ninth Edition.

Rocca, G. D., Coccia, C., Diana, L., Pompei, L., Costa, M. G., Rocca, E. T., et al. (2003). Propofol or sevoflurane anesthesia without muscle relaxants allow the early extubation of myasthenic patients. *Can. J. Anaesth.* 50, 547–552. doi:10.1007/BF03018638

Rosenbaum, S. B., Gupta, V., and Palacios, J. L. (2021). "Ketamine," in *StatPearls* (Tampa, FL, United States: StatPearls Publishing).

Roth, D. M., Bayona, F., Baddam, P., and Graf, D. (2021). Craniofacial development: Neural crest in molecular embryology. *Head. Neck Pathol.* 15, 01–15. doi:10.1007/s12105-021-01301-z

Rout, J., Essack, S., and Brysiewicz, P. (2020). Residual fluid after IV infusion drug administration: Risk of suboptimal dosing. *Br. J. Nurs.* 29, S6-S8. doi:10.12968/bjon.2020.29.2.S6

Saad, M., Clec'h, B. L., and Dhonneur, G. (2020). Hypoalbuminemia-related prolonged sedation after general anesthesia: A case report. *A. A. Pract.* 14, e01180. doi:10.1213/XAA.0000000000001180

Sakai, W., Yoshikawa, Y., Tokinaga, Y., and Yamakage, M. (2017). Anesthetic management of a child with phosphomannomutase-2 congenital disorder of glycosylation (pmm2-cdg). *JA Clin. Rep.* 3, 8. doi:10.1186/s40981-017-0080-y

Schollen, E., Frank, C. G., Keldermans, L., Reyntjens, R., Grubenmann, C. E., Clayton, P. T., et al. (2004). Clinical and molecular features of three patients with congenital disorders of glycosylation type ih (CDG-Ih) (ALG8 deficiency). *J. Med. Genet.* 41, 550–556. doi:10.1136/jmg.2003.016923

Schulz, C. M., Endsley, M. R., Kochs, E. F., Gelb, A. W., and Wagne, K. J. (2013). Situation awareness in anesthesia: Concept and research. *Anesthesiology* 118, 729–742. doi:10.1097/ALN.0b013e318280a40f

Selewski, D. T., Cornell, T. T., Lombel, R. M., Blatt, N. B., Han, Y. Y., Mottes, T., et al. (2011). Weight-based determination of fluid overload status and mortality in pediatric intensive care unit patients requiring continuous renal replacement therapy. *Intensive Care Med.* 37, 1166–1173. doi:10.1007/s00134-011-2231-3

Soto, R. G., Fu, E. S., Jr, H. V., and Miguel, R. V. (2004). Capnography accurately detects apnea during monitored anesthesia care. *Anesth. Analg.* 379, 379–382. doi:10.1213/01.ANE.0000131964.67524.E7

Tobias, J. D. (2017). Current evidence for the use of sugammadex in children. *Paediatr. Anaesth.* 27, 118–125. doi:10.1111/pan.13050

Trevor, A., Katzung, B., and Knuidering-Hall, M. (2019). *Katzung & trevor's pharmacology examination and board review*. New York: McGraw-Hill Education.

Tsukada, S., Shimizu, S., and Fushimi, K. (2021). Rocuronium reversed with sugammadex for thymectomy in myasthenia gravis: A retrospective analysis of complications from Japan. *Eur. J. Anaesthesiol.* 38, 850–855. doi:10.1097/EJA.0000000000001500

frontiers | Frontiers in Medicine

TYPE Original Research
PUBLISHED 03 May 2023
DOI 10.3389/fmed.2023.1099470

OPEN ACCESS

EDITED BY
Yang Zhou,
Brown University, United States

REVIEWED BY
Soroush Seifirad,
Harvard Medical School, United States
Padmaja Mummaneni,
United States Food and Drug Administration, United States

*CORRESPONDENCE
Britta Steffens
✉ britta.steffens@ukbb.ch

†These authors have contributed equally to this work and share first authorship
‡These authors have contributed equally to this work and share last authorship

SPECIALTY SECTION
This article was submitted to Precision Medicine, a section of the journal Frontiers in Medicine

RECEIVED 15 November 2022
ACCEPTED 14 March 2023
PUBLISHED 03 May 2023

CITATION
Steffens B, Koch G, Gächter P, Claude F, Gotta V, Bachmann F, Schropp J, Janner M, l'Allemand D, Konrad D, Welzel T, Szinnai G and Pfister M (2023) Clinically practical pharmacometrics computer model to evaluate and personalize pharmacotherapy in pediatric rare diseases: application to Graves' disease. *Front. Med.* 10:1099470. doi: 10.3389/fmed.2023.1099470

Clinically practical pharmacometrics computer model to evaluate and personalize pharmacotherapy in pediatric rare diseases: application to Graves' disease

Britta Steffens[1*†], Gilbert Koch[1†], Pascal Gächter[2], Fabien Claude[2], Verena Gotta[1], Freya Bachmann[3], Johannes Schropp[3], Marco Janner[4], Dagmar l'Allemand[5], Daniel Konrad[6], Tatjana Welzel[1], Gabor Szinnai[2,7‡] and Marc Pfister[1,7‡]

[1]Pediatric Pharmacology and Pharmacometrics, University Children's Hospital Basel UKBB, University of Basel, Basel, Switzerland, [2]Pediatric Endocrinology and Diabetology, University Children's Hospital Basel UKBB, University of Basel, Basel, Switzerland, [3]Department of Mathematics and Statistics, University of Konstanz, Konstanz, Germany, [4]Division of Pediatric Endocrinology, Diabetology and Metabolism, Department of Pediatrics, Inselspital, Bern University Hospital, University of Bern, Bern, Switzerland, [5]Department of Pediatric Endocrinology and Diabetology, Children's Hospital of Eastern Switzerland, St. Gallen, Switzerland, [6]Division of Pediatric Endocrinology and Diabetology and Children's Research Centre, University Children's Hospital Zurich, University of Zurich, Zurich, Switzerland, [7]Department of Clinical Research, University of Basel and University Hospital Basel, Basel, Switzerland

Objectives: Graves' disease (GD) with onset in childhood or adolescence is a rare disease (ORPHA:525731). Current pharmacotherapeutic approaches use antithyroid drugs, such as carbimazole, as monotherapy or in combination with thyroxine hormone substitutes, such as levothyroxine, as block-and-replace therapy to normalize thyroid function and improve patients' quality of life. However, in the context of fluctuating disease activity, especially during puberty, a considerable proportion of pediatric patients with GD is suffering from thyroid hormone concentrations outside the therapeutic reference ranges. Our main goal was to develop a clinically practical pharmacometrics computer model that characterizes and predicts individual disease activity in children with various severity of GD under pharmacotherapy.

Methods: Retrospectively collected clinical data from children and adolescents with GD under up to two years of treatment at four different pediatric hospitals in Switzerland were analyzed. Development of the pharmacometrics computer model is based on the non-linear mixed effects approach accounting for inter-individual variability and incorporating individual patient characteristics. Disease severity groups were defined based on free thyroxine (FT4) measurements at diagnosis.

Results: Data from 44 children with GD (75% female, median age 11 years, 62% receiving monotherapy) were analyzed. FT4 measurements were collected in 13, 15, and 16 pediatric patients with mild, moderate, or severe GD, with a median FT4 at diagnosis of 59.9 pmol/l (IQR 48.4, 76.8), and a total of 494 FT4 measurements during a median follow-up of 1.89 years (IQR 1.69, 1.97). We observed no notable difference between severity groups in terms of patient characteristics, daily carbimazole starting doses, and patient years. The final pharmacometrics computer model was developed based on FT4 measurements and on carbimazole or on carbimazole and levothyroxine doses involving two clinically relevant covariate effects: age at diagnosis and disease severity.

Discussion: We present a tailored pharmacometrics computer model that is able to describe individual FT4 dynamics under both, carbimazole monotherapy

and carbimazole/levothyroxine block-and-replace therapy accounting for inter-individual disease progression and treatment response in children and adolescents with GD. Such clinically practical and predictive computer model has the potential to facilitate and enhance personalized pharmacotherapy in pediatric GD, reducing over- and underdosing and avoiding negative short- and long-term consequences. Prospective randomized validation trials are warranted to further validate and fine-tune computer-supported personalized dosing in pediatric GD and other rare pediatric diseases.

KEYWORDS

Graves' disease (GD), pediatric rare diseases, hyperthyroidism, thyrotoxicosis, carbimazole monotherapy, block-and-replace therapy, mathematical model, pharmacometrics model

Introduction

Graves' disease (GD) is an autoimmune form of acquired hyperthyroidism (1–5). GD with onset in childhood or adolescence is a rare pediatric disease (ORPHA:525731) in contrast to the adult age group (6, 7). Incidence in children ranges from 0.1 to 3.4/100,000 in Europe and is increasing over decades (Denmark 1982–1988 vs. 1998–2012, 0.79 to 1.58/100,000; Sweden 1990–1999 vs. 2000–2009, 1.6 to 2.8/100,000) (8–11). In three pediatric studies, 71–83% of patients were diagnosed at the age of 10 years or later, 15–20% between 5 and 9 years, and 2–9% were younger than 5 years (8, 12, 13). Children with GD suffer from weight loss, goiter, tachycardia, and tremor at diagnosis, while endocrine orbitopathy is present in ≈ 30% of affected patients in contrast to a higher frequency of 60–70% in the adult population (4, 5, 9, 13, 14). Anxiety, depression, fatigue, and impaired cognitive function may be associated symptoms and lead to a decline in academic and athletic performance (15–17). Thus, children with GD require adequate, personalized therapy to normalize thyroid function, improve quality of life, and avoid negative long-term consequences as in adults (18, 19).

Antithyroid drugs are the first-line treatment in children with GD (3–5, 20, 21). A definitive cure by thyroidectomy or radioiodine ablation is recommended in patients whose hyperthyroidism is not controlled despite the highest doses of antithyroid drugs or who suffer severe adverse events related to pharmacotherapy (3). Long-term pharmacotherapy with carbimazole (CMZ) is safe before thyroidectomy or radioiodine ablation in children and adolescents (22–24). Pharmacotherapy with propylthiouracil is no longer recommended in pediatric GD due to the increased risk of liver failure (3, 20, 21, 25, 26).

The main goal of pharmacotherapy is normalization of free thyroxine (FT4) levels within 4–8 weeks, depending on disease severity (3, 21, 26, 27). In pediatric GD, two treatment approaches currently exist. The first approach is a complete blocking of thyroid hormone production with CMZ combined with a thyroid hormone substitution with levothyroxine (LT4), also called CMZ/LT4 block-and-replace therapy (3, 20, 21, 26, 28). However, with this treatment approach, up to 25% of pediatric patients show dose-related side effects such as rash and pruritus, and rarely agranulocytosis, hepatitis, and/or vasculitis. For this reason, current international guidelines recommend another treatment approach, a carefully titrating CMZ monotherapy (20, 26, 29, 30). A first recent randomized controlled trial in children with GD showed that there is no evidence for better biochemical control when administering a mean CMZ dose of 0.61 mg/kg/day for CMZ/LT4 block-and-replace vs. 0.3 mg/kg/day for CMZ monotherapy (28). In our retrospective cohort, data show that both treatment approaches were still applied in clinical practice.

Both treatment approaches require frequent outpatient visits and blood sample collections to monitor safety, including clinical and laboratory adverse events of CMZ, and efficacy, to avoid both overdosing associated with iatrogenic hypothyroidism and underdosing resulting in persistent hyperthyroidism (3, 20, 21, 26). Once thyroid hormones are normalized, continuous CMZ adjustments, taking into account the patient's age and weight, disease severity at diagnosis, and disease activity during treatment, are mandatory (3, 20, 21, 26). Disease severity may be extremely variable in patients with newly diagnosed GD. Prepubertal children may, in particular, have severe forms of GD and an increased risk of disease recurrence despite adequate CMZ treatment and appropriate drug adherence (3, 12, 26).

To mitigate the risk of somatic, metabolic, and cognitive impairment, aforementioned aspects should be taken into account for optimized individual CMZ dosing in pediatric GD. To this end, a tailored pharmacometrics (PMX) computer model was developed to characterize FT4 dynamics under both current treatment approaches, CMZ monotherapy and CMZ/LT4 block-and-replace therapy, with the ultimate goal of personalizing CMZ dosing in pediatric GD, (i) reducing the time needed to restore thyroid homeostasis after diagnosis, (ii) increasing the time within reference ranges of thyroid hormones during follow-up, (iii) reducing the number of outpatient visits and blood draws, (iv) enhancing the quality of life, and academic and athletic performance in pediatric patients, and (v) avoiding negative long-term consequences.

For successful implementation in clinical practice, such a tailored PMX computer model (i) has to be in a reasonable balance between complexity to account for physiological

mechanisms and simplicity to utilize sparse clinical and laboratory data, and a small number of input parameters (31), (ii) has to follow pharmacokinetics/pharmacodynamics (PK/PD) modeling principles (32–35), and (iii) has to be developed in the context of non-linear mixed effects (NLME) modeling (36).

This research article has two main objectives: first, to perform a descriptive analysis of a retrospective dataset with clinical and laboratory data from children and adolescents with GD up to 2 years of treatment; and second, to develop a clinically practical PMX computer model that can characterize and predict individual FT4 dynamics under CMZ monotherapy and CMZ/LT4 block-and-replace therapy in pediatric GD.

Methods

This section consists of six paragraphs describing (i) study design and retrospective data collection procedure, (ii) descriptive data analysis of retrospective data of the whole patients' cohort and per disease severity group, (iii) PK and PD components of the PMX computer model for CMZ monotherapy and CMZ/LT4 block-and-replace therapy, (iv) the NLME approach to characterize each individual in a patient population, (v) covariate testing in the PMX modeling process, and (vi) statistical data presentation and applied software packages.

Study design and retrospective data collection procedure

In this retrospective multicenter longitudinal cohort study of pediatric patients, patient data were included, if (i) children had a confirmed GD [based on elevated FT4 and/or triiodothyronine (T3) and positive antithyroid stimulating hormone receptor antibodies (TRABs)], (ii) children were treated for GD between 1990 and (a) 12/2020 at each of University Children's Hospital Basel, University Hospital Bern, and University Children's Hospital Zurich or (b) 12/2013 at Children's Hospital Eastern Switzerland in St. Gallen, (iii) a complete set of data that includes documented CMZ, clinical baseline characteristics, relevant laboratory parameters at diagnosis and/or start of CMZ treatment, and, in case of CMZ/LT4 block-and-replace therapy, LT4 dose history during the complete follow-up period was available, and (iv) at least two follow-up visits after CMZ treatment start were documented. Pediatric patients were excluded from the study if CMZ and/or LT4 doses were missing at the first visit or any follow-up visit, or if there was documented, inappropriate drug adherence.

Ethical approval for this study (2018-01770) was obtained and amended (01/2021) by the lead local ethics committee (Ethikkommission Nordwest- und Zentralschweiz EKNZ) and all locally responsible ethics committees (Kantonale Ethikkommission Bern, Ethikkommission Zürich, Ethikkommission Ostschweiz EKOS). Data were captured and standardized for each study visit in the designated electronic database secuTrial®. Data from patients were pseudonymized. The study was performed in compliance with the tenets of the Declaration of Helsinki and Good Clinical Practice.

Descriptive analysis of retrospective data

Relevant disease-related clinical and laboratory data, such as age (years), body weight (kilogram, kg), FT4 (pmol/l), and thyroid stimulating hormone (TSH, mU/l), from the start of CMZ treatment ($t_0 = 0$ day) were included in the analysis. Disease severity was defined based on FT4 measurement at the time of diagnosis [or, if missing, based on TSH and/or thyroxine (T4) measurements]. Patients were categorized as severe (FT4 $>$ 70 pmol/l), moderate (FT4 50–70 pmol/l), and mild (FT4 $<$ 50 pmol/l) according to Léger et al. (26).

Total daily CMZ dose (mg/day) and total daily dose per kg body weight (mg/kg/day) were compared between patients receiving CMZ monotherapy and those receiving CMZ/LT4 block-and-replace therapy at the start of LT4 replacement treatment.

Missing daily body weight values were calculated by linear interpolation.

PK and PD components of the PMX computer model

The prodrug CMZ has a high bioavailability (90–100%) and is quickly absorbed (within 15–30 min) from the gastrointestinal tract (37). After oral administration, CMZ (molecular weight, MW_{CMZ} = 186.23 g/mol) is rapidly metabolized into the pharmacologically active metabolite methimazole (MMZ) (MW_{MMZ} = 114.17 g/mol) (37). Since $MW_{MMZ}/MW_{CMZ} = 0.61$, a dose of 1 mg CMZ corresponds to 0.61 mg MMZ. By blocking the thyroid peroxidase enzyme, and hence preventing iodination and coupling of thyroglobulin residues, MMZ reduces the production of the thyroid hormones T3 and T4. The time of maximum MMZ plasma concentration t_{max} is reported to be 1–2 h after oral administration of CMZ (37). The elimination half-life t_{half} of MMZ has been described as variable, ranging from 4 to 12 h, depending on the individual patient, but not related to thyroid status or disease severity (37–40). In addition, in adults, weight dependence of the volume of distribution V is referred to as 0.5 l/kg (37), and a bi-exponential profile of MMZ concentration was observed (39).

A general PMX computer model consists of two components: a PK and a PD component. PMX approaches are increasingly utilized to inform key decisions such as dose selection in drug research and development (41, 42). During the last years, PMX models have also been applied to evaluate and optimize dosing strategies in clinical practice, particularly in pediatrics (43–46).

In the context of GD, the PK component characterizes MMZ concentration caused by the administered CMZ doses (Component I), and the PD component characterizes the inhibitory effect of MMZ on the increased endogenous T4 production (Component II). For patients receiving CMZ/LT4 block-and-replace therapy, the

administration of LT4 substitutes is included in Component II. Due to this structure, the PMX computer model is explicitly controlled by the doses and is based on pharmacological, physiological, and biological principles.

Component I: PK computer model for CMZ and its active metabolite

The PK of CMZ and its active metabolite, MMZ, is characterized by a linear multi-compartment model including absorption, metabolism, and peripheral distribution. A schematic of the PK model is shown in Figure 1A, and model equations are presented in the following:

CMZ absorption is characterized by

$$\frac{d}{dt}A_b^C(t) = In^C\left(t_j^C, d_j^C\right) - k_a^C \cdot A_b^C(t), \quad A_b^C(0) = 0 \tag{1}$$

where k_a^C (1/day) is the absorption rate and In^C is the dosing input function with a dose of CMZ d_j^C (mg) and dosing time point t_j^C (day). The amount of CMZ A^C (mg) in the central compartment is described by

$$\frac{d}{dt}A^C(t) = k_a^C \cdot A_b^C(t) - k_t \cdot A^C(t), \quad A^C(0) = 0 \tag{2}$$

where k_t (1/day) is the metabolic transit rate, and the amount of MMZ A^M (mg) in the central compartment is given by

$$\begin{aligned}\frac{d}{dt}A^M(t) &= f^M \cdot k_t \cdot A^C(t) - k_{el}^M \cdot A^M(t) - k_{12} \cdot A^M(t) \\ &\quad + k_{21} \cdot P(t), \quad A^M(0) = 0 \end{aligned} \tag{3}$$

$$\frac{d}{dt}P(t) = k_{12} \cdot A^M(t) - k_{21} \cdot P(t), \quad P(0) = 0 \tag{4}$$

where f^M (unit-less) is the metabolic conversion factor, k_{el}^M (1/day) is the elimination rate, and k_{12} (1/day) and k_{21} (1/day) are the distribution rates for the peripheral compartment P.

Finally, the concentration of MMZ is obtained by

$$C^M(t) = \frac{A^M(t)}{V^M\left(W(t)\right)} \quad \text{with } V^M\left(W(t)\right) = f_V^M \cdot W(t) \tag{5}$$

where $W(t)$ (kg) is the body weight over time and f_V^M (l/kg) is a proportionality factor relating current body weight with volume of distribution of MMZ.

Component II: PD computer model characterizing FT4 dynamics under treatment

The structural PMX computer model for endogenous T4 production and exogenous LT4 treatment is similar to the one-compartment PK model for congenital hypothyroidism presented by Koch et al. (31), but with one difference in interpretation: in the case of CMZ/LT4 block-and-replace therapy, k_{endo}^{T4} (nmol/day) denotes the (GD-induced) increased endogenous T4 production rate. Under CMZ monotherapy, this endogenous T4 production will be inhibited. This means that the proposed PMX computer model extends the model presented by Koch et al. (31) by including the inhibitory effect of CMZ treatment on the endogenous T4 production rate *via* the MMZ concentration.

To be precise, utilizing a commonly used inhibitory effect term (32, 34, 47) on k_{endo}^{T4} (nmol/day) with respect to $C^M(t)$ (mg/l) results in

$$\frac{d}{dt}A_b^{T4}(t) = In^{T4}\left(t_j^{T4}, d_j^{T4}, F^{T4}\right) - k_a^{T4} \cdot A_b^{T4}(t), \quad A_b^{T4}(0) = 0 \tag{6}$$

$$\begin{aligned}\frac{d}{dt}T4(t) &= k_a^{T4} \cdot A_b^{T4}(t) + k_{endo}^{T4} \cdot \left(1 - \frac{I_{\max} \cdot C^M(t)}{IC_{50} + C^M(t)}\right) \\ &\quad - k_{el}^{T4} \cdot T4(t), \; T4(0) = \frac{k_{endo}^{T4}}{k_{el}^{T4}}\end{aligned} \tag{7}$$

$$C^{FT4}(t) = \frac{0.3 \cdot T4(t)}{V^{T4}\left(W(t)\right)} \quad \text{with } V^{T4}\left(W(t)\right) = f_V^{T4} \cdot \left(\frac{W(t)}{W_{Ref}}\right)^{\beta} \tag{8}$$

where $I_{\max} \leq 1$ (unit-less) is the maximal inhibitory drug effect, IC_{50} (mg/l) is the MMZ concentration causing the half-maximal inhibitory effect, In^{T4} is the dosing input function, d_j^{T4} (mcg/day) is the dose of LT4 at the time point t_j^{T4} (day) converted with factor 1.29 to nmol/day ($MW_{T4} = 776.9$ g/mol), $F^{T4} \leq 1$ (unit-less) is the bioavailability of LT4, and k_a^{T4} (1/day) is the respective absorption rate. The initial condition for T4 in Equation (7) ensures that the endogenous T4 production is in equilibrium before treatment, as per Koch et al. (31). Finally, FT4 concentration was obtained by converting the T4 unit nmol/l into the FT4 unit pmol/l, and assuming that the FT4 concentration corresponds to 0.03% of T4, as per Koch et al. (31). Weight dependence of the volume of distribution V^{T4} (l) was included in an analogous manner as in Koch et al. (31). This means that V^{T4} is assumed to be proportional to a power of the quotient of current weight and reference weight W_{Ref} (corresponding to this GD population) with multiplicative factor f_V^{T4} (l) and power exponent β (unit-less). A schematic of Equations (6)–(8) is presented in Figure 1B.

The final PMX computer model consists of Equations (1)–(8), and the entire schematic is displayed in Figure 1. It should be noted, in the case of CMZ monotherapy, that In^{T4} is equal to zero for all t. Hence, A_b^{T4} is also zero.

Time-varying covariates were tested as additional regressors and directly implemented in the PMX computer model (Equations 1–8) as proposed in the Monolix Suite 2021R1 (Lixoft, Orsay, France). All time-constant covariates were tested with the Monolix Suite 2021R1's default settings.

NLME approach to characterize each individual in a patient population

NLME modeling (36) is the gold standard to simultaneously characterize individual patients stemming from the same cohort/population. The basic idea is that, on the one hand, each patient shares some similar properties, e.g., physiology and disease, but on the other hand, has individual distinctive characteristics, e.g., response to treatment. Hence, the final

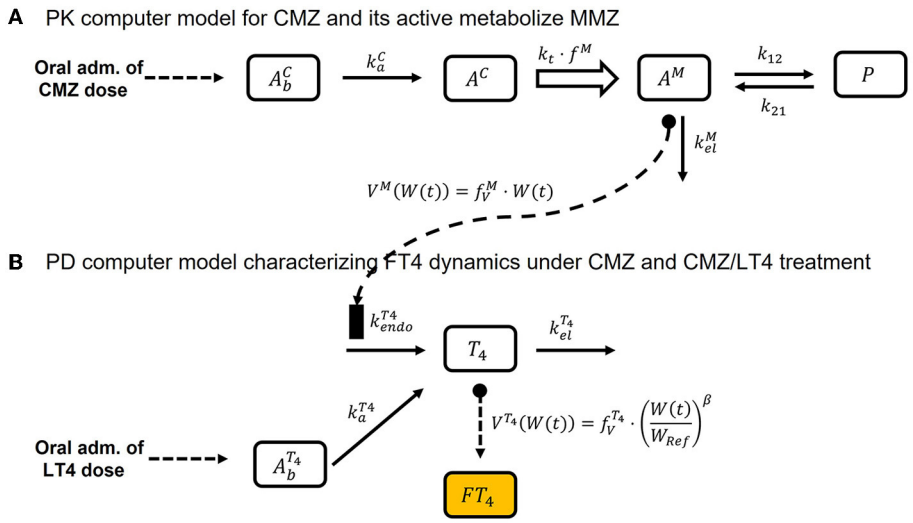

FIGURE 1
Schematic of the final PMX computer model, Equations (1)–(8). **(A)** Illustrates the schematic of the PK computer model, Equations (1)–(5), and **(B)** shows the schematic of the PD computer model, Equations (6)–(8).

PMX computer model (Equations 1–8) is structurally valid for all patients in the population, but each patient has their own individual model parameters. The result of the NLME analysis consists of (i) population model parameters (fixed effects) characterizing the average patient in the population, (ii) standard deviations (random effects) characterizing the distributions of the individual model parameters, and (iii) effects of covariates on model parameters. Application of the NLME analysis is of major importance to developing a predictive PMX computer model that, in clinical practice, can be reliably applied to a newly diagnosed patient since this patient will not only be classified based on its available FT4 measurements and its covariates but also on the knowledge learned from the previously analyzed patients' cohort/population represented by fixed and random effects.

Covariate testing in the PMX modeling process

Covariates to be tested in the PMX computer model were selected based on completeness, possible correlations among each other, and clinical plausibility. We included age at diagnosis, sex, and disease severity in the covariate testing. In addition, the type of treatment in terms of CMZ monotherapy or CMZ/LT4 block-and-replace therapy was included as a possible categorical covariate.

The continuous covariates TSH, weight, and body mass index at diagnosis were not available for all patients and were therefore not tested. Body weight over time, with interpolated measurements for missing values, was already included in the model for scaling volume of distribution, comparing Equations (5) and (8).

We also tested the effect of changing the type of treatment on the endogenous T4 production rate k_{endo}^{T4} by implementing an on/off switch depending on whether the patient received CMZ only or both CMZ and LT4.

TSH effects over time were not tested for two reasons. First, based on the available data, TSH did not provide more information about the observed FT4 variability than was already described by the model. Second, regular TRAB measurements are not required during follow-up and thus were not tested as a possible covariate.

Statistical data presentation and applied software packages

All laboratory and demographic values are reported as median together with the interquartile range (IQR) (25%-percentile, 75%-percentile). Descriptive statistical analysis and simulations were performed in R 4.1.0 (R core team, Vienna, Austria), and hypothesis testing was executed with the Student's *t*-test for normally distributed values and with the Wilcoxon rank sum test for non-normally distributed values. We consider a *p*-value smaller than 0.05 to be significant. NLME modeling was performed in the Monolix Suite 2021R1. A-posteriori data visualization was implemented in R or MATLAB 2020a (MathWorks, Natick, MA, USA).

Results

The Results section consists of three paragraphs, describing: (i) retrospective data, (ii) parameter setup of the PK and PD components of the final PMX computer model and covariate effects, and (iii) additional sensitivity analyses.

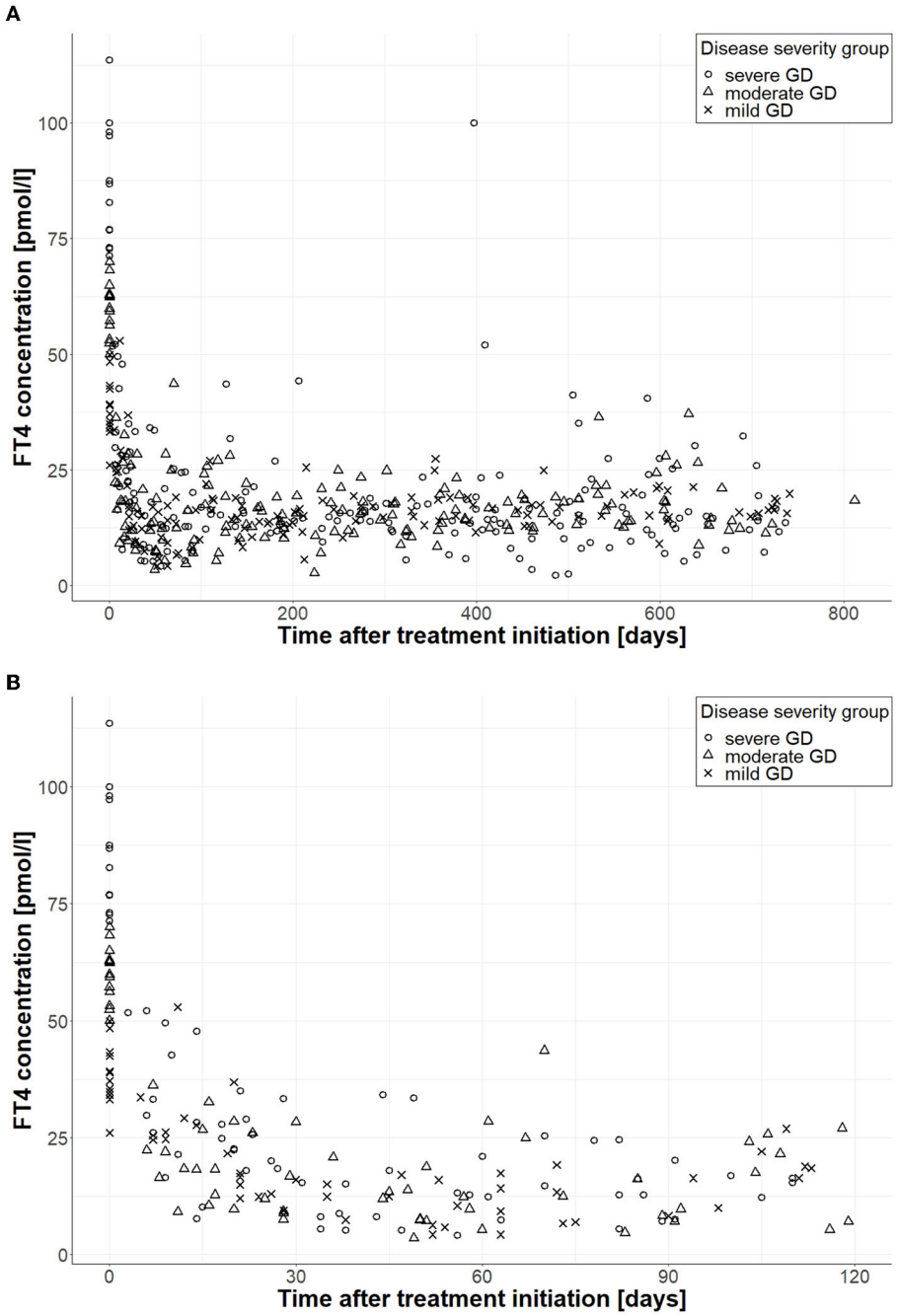

FIGURE 2
FT4 measurements according to disease severity during follow-up. **(A)** Shows FT4 measurements during the whole follow-up ($n = 494$), and **(B)** displays FT4 measurements during the first 120 days ($n = 129$); circles correspond to FT4 measurements of patients with severe GD, triangles belong to patients with moderate GD, and crosses correspond to patients with mild GD.

Descriptive analysis of retrospective data

A total of 58 pediatric patients with GD were found to be eligible. After screening for inclusion and exclusion criteria, 44 patients (75% female) were included for modeling and further analysis. All these patients had more than two FT4 measurements, and body weight information ($n = 455$) was available from at least 30% of clinical visits during follow-up. According to the severity grading defined by Léger et al. (26), 13 patients were categorized as mild, 15 patients as moderate, and 16 patients as severe.

Patient characteristics at diagnosis such as age (years), weight (kg), FT4 (pmol/l), and TSH (mU/l), in addition to total daily CMZ starting dose (mg/day) and total daily CMZ starting dose per kg body weight (mg/kg/day) per disease severity group, were compared. We observed no significant difference among the three

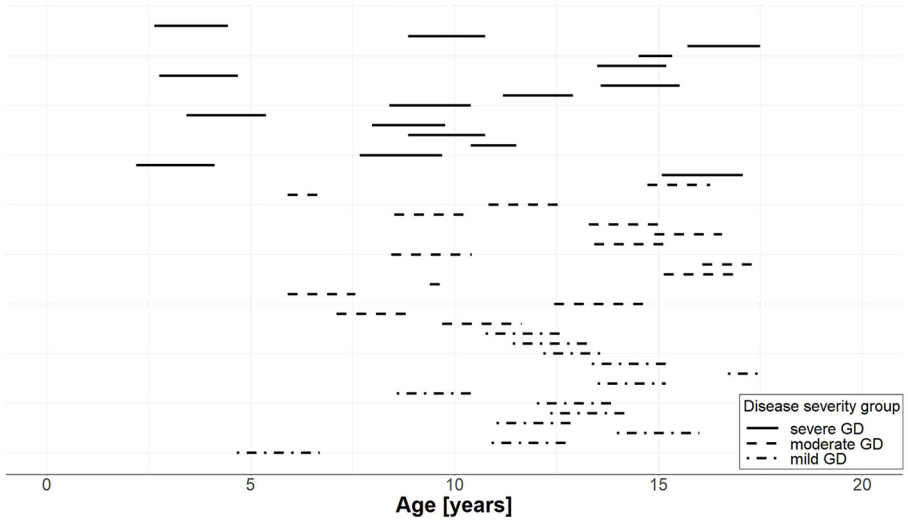

FIGURE 3
Years of follow-up for each of the 44 individual patients with GD per severity group. The start of the line represents the age at the start of pharmacotherapy and the length of the line represents the duration of follow-up; solid lines correspond to patients with severe GD, dashed lines to patients with moderate GD, and dash-dotted lines to patients with mild GD.

groups in terms of patient characteristics, total daily CMZ doses, and patient years and follow-up years.

On average, 11 FT4 measurements were available per patient with a minimum of 3 and a maximum of 36 measurements. The median end of monitoring was at day 688.5 (617.8, 719.0) with a range of 126 to 812 days. FT4 measurements ($n = 494$) of the final patient cohort divided by severity group during the whole follow-up (Panel A) and during the first 120 days (Panel B) are shown in Figure 2, and the years of follow-up for each patient are displayed in Figure 3.

A total of $n = 27$ patients (61%) received CMZ monotherapy. For $n = 17$ patients receiving CMZ/LT4 block-and-replace therapy, the median start of LT4 treatment, and thus the median start of CMZ/LT4 block-and-replace therapy, was at day 75 (52, 183) ranging from 28 to 364 days.

Regarding the two current pharmacotherapy approaches, we observed no significant difference in patient characteristics at diagnosis, total daily CMZ starting doses, and total daily CMZ starting doses per kg body weight. The median total daily CMZ starting dose per kg body weight was 0.70 (0.60, 0.77) mg/kg/day with a range of [0.36, 1.35] mg/kg/day for patients receiving CMZ monotherapy, and for CMZ/LT4 block-and-replace therapy, 0.76 (0.60, 0.87) mg/kg/day with a range of [0.37, 1.40] mg/kg/day.

Detailed information on patient characteristics at the time of diagnosis is presented in Table 1, and information regarding treatment during follow-up is presented in Table 2.

PK and PD components of the PMX computer model

Component I: Computer PK model for CMZ and its active metabolite

The PK model parameters of CMZ and its active metabolite MMZ (Equations 1–5) were based on values reported in the literature (39, 40) and product labels (37). To realize a peak time of $t_{max} = 2$ (h) for MMZ concentration after oral CMZ administration, k_a^C was set to 144 (1/day) and k_t to 28.8 (1/day). The half-life of MMZ was assumed to be 6 h, and therefore k_{el}^M was set to 2.77 (1/day). The metabolic conversion factor was set to $f^M = 0.61$ (unit-less), and the distribution rates k_{12} and k_{21} for the peripheral compartment were both set to 2.4 (1/day). The proportionality factor relating body weight to the volume of distribution was reported as $f_V^M = 0.5$ (l/kg). In our population, CMZ was administered three times a day and was implemented accordingly for data fitting and parameter estimation.

To demonstrate the predictive capability of the developed PK model (Equations 1–5) for CMZ and its active metabolite MMZ, average MMZ concentrations of hyperthyroid patients were digitized from Cooper et al. (48) and Okamura et al. (39) for a single oral MMZ administration of 10, 30, and 60 mg. To apply our PK model, MMZ doses were converted to CMZ doses, resulting in 16.4, 49.2, and 96.4 mg. In Cooper et al. (48), MMZ was measured after oral MMZ administration of 30 and 60 mg in five hyperthyroid GD patients for up to 8 h. Since weight was not reported, we assumed an average value of 60 kg. In Okamura et al. (39), MMZ was measured after oral MMZ administration of 10 mg in 15 hyperthyroid patients for up to 48 h with an average weight of 46.8 kg. Please compare Figure 4 for measurements and simulation of the CMZ PK model Equations (1)–(5) (the figure was reduced to 1 day for clarity). Overall, the developed PK model (Equations 1–5) characterized the digitized data from the literature well with the chosen parameter values.

Component II: PD computer model characterizing FT4 dynamics under treatment

FT4 measurements were fitted with the NLME approach (36, 49). In brief, each individual has the same structural model (Equations 1–8); however, individual covariate effects on model parameters are implemented, and most model parameters follow

TABLE 1 Patient characteristics at baseline for all patients and by disease severity, expressed as n (%) for categorical variables or as median (IQR) for continuous variables.

	All patients	Patients with severe GD[a]	Patients with moderate GD[a]	Patients with mild GD[a]	Stats severe moderate mild
		FT4 > 70 pmol/l	FT4 50–70 pmol/l	FT4 < 50 pmol/l	
Patients (*n*)[b]	44	16 (36%)	15 (34%)	13 (30%)	
Female patients (*n*)	33 (75%)	15 (94%)	10 (67%)	8 (62%)	
Age (yrs)	11.0 (8.4, 13.5)	8.9 (6.6, 13.5)	10.8 (8.5, 14.1)	12.0 (10.9, 13.4)	n.s.[f]
Weight (kg)[c]	31.4 (27.8, 50.0)	31.9 (28.6, 50.0)	30.5 (25.7, 39.1)	41.5 (27.9, 46.2)	n.s.[f]
FT4 (pmol/l)[d]	59.9 (48.4, 76.8)	84.8 (76.9, 97.9)	59.6 (53.9, 62.9)	38.9 (34.8, 43.2)	
TSH (mU/l)[e]	0.002 (0.002, 0.004)	0.002 (0.004, 0.006)	0.002 (0.002, 0.002)	0.002 (0.002, 0.003)	

[a]Disease severity defined according to guidelines (13).
[b]Three missing values for FT4 at diagnosis, severity groups determined by TSH and/or T4 measurements.
[c]Six missing values.
[d]Three missing values.
[e]One missing value.
[f]Not significant if p-value $\geq$ 0.05.

a (usually log-normal) distribution to realize inter-individual variability (IIV).

The bioavailability of LT4 was set to $F^{T4} = 0.6$ in Equation (6), and the reference weight value W_{Ref} was chosen as the median for all patients in this GD population over the entire treatment duration, resulting in $W_{Ref} = 42.7$ kg. The T4 absorption rate k_a^{T4} in Equations (6)–(7) was set to $k_a^{T4} = 20$ (1/day) and the T4 elimination rate k_{el}^{T4} was set to $k_{el}^{T4} = 0.1$ (1/day), both without IIV, as per Koch et al. (31) for rationale. In our population, LT4 was administered once per day. The endogenous T4 production rate k_{endo}^{T4} (nmol/day) and the MMZ concentration causing the half-maximal inhibitory effect IC_{50} (mg/l) in Equation (7) were estimated with IIV. With regard to Equation (8), both the factor f_V^{T4} (l) relating body weight with the volume of distribution of T4 and the power exponent β (unit-less) were estimated with a fixed standard deviation for the IIV. Interestingly, the estimated population value of β was close to the value obtained in neonates and infants with congenital hypothyroidism, compared to Koch et al. (31). Finally, the maximum inhibitory drug effect parameter in Equation (7) was set to $I_{\max} = 0.9$ without IIV. A log-normal distribution was applied to all parameters equipped with IIV.

Significant covariate effects of disease severity and age at diagnosis on the endogenous production rate k_{endo}^{T4} (nmol/day) were found and included in the final PMX computer model. Almost all of the IIV could be explained by these covariate effects.

The final covariate effect model for an individual's endogenous T4 production rate $k_{endo,i}^{T4}$ is

$$\log\left(k_{endo,i}^{T4}\right) = \log\left(k_{endo}^{T4}\right) + \beta_{k_{endo}^{T4}}^{AGE} \cdot \log\left(\frac{AGE}{AGE_{Ref}}\right) + \begin{cases} 0 & \text{for mild GD} \\ \beta_{k_{endo}^{T4}}^{Cat\ 2} & \text{for moderate GD} \\ \beta_{k_{endo}^{T4}}^{Cat\ 1} & \text{for severe GD} \end{cases}$$

where $AGE_{Ref} = 8.98$ (yrs) corresponds to the weighted mean, the default setting in the Monolix Suite.

All model parameter estimates and values are shown in Table 3. Goodness-of-fit plots and a selection of individual profiles are presented in the Supplementary material.

Additional sensitivity analyses

In the following, additional sensitivity analyses are reported for completeness. We explicitly emphasize that these results are not part of the final PMX computer model and solely serve as additional information.

Evaluation of the potential effect of CMZ/LT4 block-and-replace therapy on the endogenous T4 production

We tested whether the type of treatment, i.e., receiving CMZ monotherapy vs. receiving CMZ/LT4 block-and-replace therapy, has an impact on thyroid function and inhibition during follow-up. In the case of CMZ/LT4 block-and-replace therapy, a reduced endogenous thyroid function, represented by a smaller value for k_{endo}^{T4} (nmol/day) and a reduced half-maximal inhibitory effect, represented by a smaller value for IC_{50} (mg/l), were observed. As there is no obvious clinically reasonable interpretation for these potential effects, further investigation is warranted.

Application of a simplified PK computer model for CMZ treatment and its active metabolite

The applied PK computer model for CMZ treatment and its active metabolite MMZ (Equations 1–5) is a very detailed and mechanism-based representation. However, due to several numerical and technical reasons, such a detailed representation can be computationally extremely elaborate. Hence, we tested whether

10.3389/fmed.2023.1099470

TABLE 2 Patient information on treatment at baseline and during follow-up for all patients and by disease severity, expressed as n (%) for categorical variables or as median (IQR) for continuous variables.

	All patients	Patients with severe GD[a]	Patients with moderate GD[a]	Patients with mild GD[a]	Stats severe moderate mild
		FT4 >70 pmol/l	FT4 50–70 pmol/l	FT4 < 50 pmol/l	
Patient years (yrs)	76.44	28.27	24.43	23.74	
Follow-up (yrs)	1.89 (1.69, 1.97)	1.89 (1.77, 1.94)	1.79 (1.59, 1.91)	1.97 (1.88, 1.99)	n.s.[c]
CMZ starting dose (mg/day)	19.28 (19.28, 38.56)	20.18 (19.28, 38.56)	19.28 (19.28, 32.13)	19.28 (19.28, 32.13)	
CMZ starting dose per kg of body weight (mg/kg/day)[b]	0.72 (0.6, 0.81)	0.73 (0.65, 0.81)	0.67 (0.55, 0.83)	0.7 (0.45, 0.77)	n.s.[c]
Patients receiving CMZ monotherapy (*n*)	27 (61%)	11 (69%)	10 (67%)	6 (46%)	
Time point of switch to block-and-replace therapy (days after treatment initiation)	75 (52, 183)	85 (43, 89)	119 (60, 254)	73 (52, 75)	n.s.[c]
LT4 starting dose for block-and-replace therapy (mcg/kg/day)[b]	1.86 (1.57, 2.20)	1.78 (1.69, 2.17)	2.12 (1.57, 2.20)	1.86 (1.34, 2.22)	n.s.[c]
CMZ dose at switch to block-and-replace therapy (mg/kg/day)[b]	0.42 (0.32, 0.44)	0.43 (0.33, 0.53)	0.43 (0.32, 0.44)	0.38 (0.30, 0.42)	n.s.[c]

[a]Disease severity defined according to guidelines (13).
[b]Computed based on calculated values for missing weight measurements.
[c]Not significant if p-value $\geq$ 0.05.

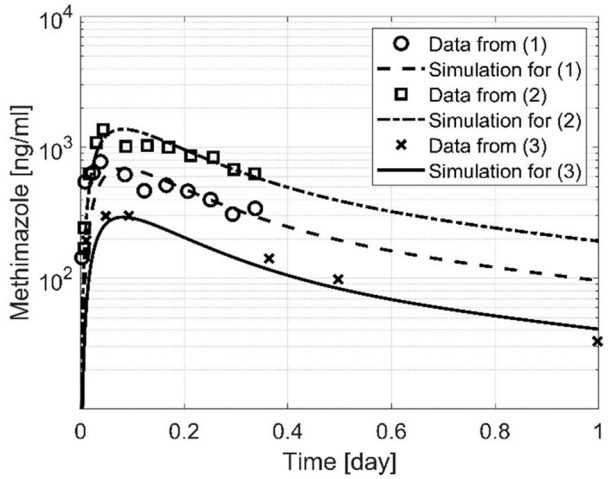

FIGURE 4
Three simulations based on the developed PK computer model, Equations (1)–(5). MMZ measurements for (1) and (2) were obtained from Cooper et al. (48) with an oral dose of 30 and 60 mg, and MMZ measurements for (3) were obtained from Okamura et al. (39) with an oral dose of 10 mg.

a simplified PK computer model leads to similar results regarding data fitting, parameter estimates, and goodness-of-fit plots.

Due to the fast absorption of CMZ, the quick metabolism after CMZ administration, and the three times daily drug administration, it is possible to replace Equations (1)–(5) by a simplified one-compartment intravenous (IV) model with a single total dose per day:

$$\frac{d}{dt}\overline{A^M}(t) = In^C(\overline{t_k^C}, \overline{d_k^C}, F^C) - k_{el}^M \cdot \overline{A^M}(t), \quad \overline{A^M}(0) = 0 \qquad (9)$$

$$\overline{C^M}(t) = \frac{\overline{A^M}(t)}{V^M(W(t))} \qquad with \quad V^M(W(t)) = f_V^M \cdot W(t) \qquad (10)$$

where $\overline{d_k^C}$ (mg) is the total dose per day at the time point $\overline{t_k^C}$ (day) and the value of the metabolic conversion factor is now incorporated in the input function In^C *via* the scaling factor F^C. The remaining parameters k_{el}^M and f_V^M have been chosen as before.

The profile of $\overline{C^M}(t)$ Equations (9) and (10) has higher but daily peak concentrations and therefore impacts the value of the half-maximal inhibitory effect caused by the MMZ concentration IC_{50}. As expected, the simplified PK model Equations (9) and (10) produced a lower IC_{50} value of 0.016 (mg/l). All other parameters, the objective function value, and the goodness-of-fit plots showed no significant difference.

A major advantage of the simplified PK model Equations (9) and (10) is the reduction of computational costs, not only during data fitting but also for potential application in a clinical setting. The PMX computer model with the simplified CMZ PK Equations (6)–(10) is approximately six times faster than the PMX computer model with the detailed CMZ PK Equations (1)–(8). Hence, if

TABLE 3 Population estimates (fixed effects), standard deviation of random effects, covariate effect parameters, and additional parameters obtained from data fitting using the final PMX computer model, Equations (1)–(8).

Parameter	Description	Unit	Estimate (r.s.e.[a])
Population estimates (fixed effects)			
k_a^C	CMZ absorption rate	1/day	144 fix
k_t	Metabolism transit rate	1/day	28.8 fix
f^M	Metabolic conversion factor	unit-less	0.61 fix
k_{el}^M	MMZ elimination rate	1/day	2.77 fix
k_{12}	Peripheral compartment distribution rate	1/day	2.4 fix
k_{21}	Peripheral compartment distribution rate	1/day	2.4 fix
f_V^M	Proportionality factor	l/kg	0.5 fix
k_a^{T4}	T4 absorption rate	1/day	20 fix
k_{endo}^{T4}	Endogenous T4 production rate	nmol/day	261 (7)
k_{el}^{T4}	T4 elimination rate	1/day	0.1 fix
$I_{\max}$	Maximal inhibitory effect of MMZ	unit-less	0.9 fix
IC_{50}	MMZ concentration for half-maximal inhibitory effect	mg/l	0.024 (18)
f_V^{T4}	Multiplicative factor	l	20.3 (9)
β	Power exponent	unit-less	0.7 (18)
Standard deviation of the random effects			
$\omega_{k_{endo}^{T4}}$			0.04 (58)
$\omega_{IC_{50}}$			0.77 (15)
$\omega_{f_V^{T4}}$			0.1 fix
ω_{beta}			0.25 fix
Covariate effect parameters			
$\beta_{k_{endo}^{T4}}^{AGE}$	Age effect on k_{endo}^{T4}		0.464 (13)
$\beta_{k_{endo}^{T4}}^{Cat\ 1}$	Disease severity (severe GD) effect on k_{endo}^{T4}		0.52 (14)
$\beta_{k_{endo}^{T4}}^{Cat\ 2}$	Disease severity (moderate GD) effect on k_{endo}^{T4}		0.16 (49)
Additional parameters			
Prop. res. error			0.344 (4)
−2LL value			3,333

[a] Relative standard error.
The rationale for the fixed population parameters is found in the Results section.

no PK measurements are available for data fitting, and a large difference exists in the time scales of CMZ treatment (hours) and FT4 measurements (weeks, months), a simplified PK model performs equally well.

Discussion

In this section, we discuss the main results in the context of our two research objectives: (i) descriptive analysis of retrospective clinical data from 44 pediatric patients with mild, moderate, or severe GD, and (ii) development of a clinically practical PMX computer model that can characterize and predict individual FT4 dynamics under both current treatment approaches in pediatric GD (20, 21, 26, 29).

The first objective was a descriptive analysis of this retrospectively collected multicenter data of pediatric patients diagnosed with GD. We included 44 pediatric patients with equal numbers per severity group. In this GD cohort, two treatment approaches were observed. The majority (61%) received CMZ monotherapy, whereas all other patients (39%) received CMZ/LT4 block-and-replace therapy with a median start of LT4 administration at day 75 (IQR 52, 183). Although hepatic insufficiency is known as a contraindication for the continuing administration of CMZ, in this retrospective study, hepatic values were not documented systematically. However, in the case of moderate hepatitis, treatment would be stopped, and, as reported in a recent systematic review (50), mild elevation of transaminases is rare in children (1% of treated pediatric patients).

The general challenges of collecting patient records with a rare disease and the limitations of retrospective multicenter

studies were discussed in Koch et al. (31). In addition, the challenges and opportunities of developing a clinically relevant PMX computer model for congenital hypothyroidism (CH) based on retrospectively collected multicenter data are explained (31). To harmonize the data, we introduced a time-dependent normalizing method. However, in this study, compared to the CH-study (31), we observed two decisive distinctions: (i) age-specific laboratory FT4 reference ranges showed only slight and negligible differences, and (ii) information about laboratory reference ranges was incomplete for a few patients. Since, as already discussed in Koch et al. (31), normalization should be considered *"the last resort"* (51), we did not apply a normalizing method for potential laboratory differences in this analysis.

The second objective was to develop a practical and predictive PMX computer model to characterize FT4 dynamics under CMZ monotherapy and CMZ/LT4 block-and-replace therapy for clinical application. Since the 1950s, several mathematical models describing the hypothalamic–pituitary–thyroid axis have been developed, offering detailed insights into the complexity of the underlying physiological mechanisms. However, most of these publications focus on a specific research question and not on applicability and feasibility in clinical practice (31, 52–62). Our final, tailored PMX computer model (Equations 1–8, 6–10) requires minimal data, which are typically measured during outpatient visits. In addition, it was developed in the NLME framework, accounts for the typical pharmacological, physiological, and biological principles, and allows for individualized therapy. In this NLME context, not only the FT4 measurements and covariates of a newly diagnosed patient are utilized for prediction but also all the learned knowledge from the already analyzed representative population.

The presented clinically practical PMX computer model consists of a detailed PK model for CMZ treatment and its active metabolite MMZ based on information from the literature. We demonstrated that this detailed PK model well-describes the MMZ concentration digitized from the literature. However, since MMZ concentration is not measured in clinical practice, we showed that the complex PK computer model (Equations 1–5) can be replaced by a simpler PK computer model (Equations 9–10) which may be of great advantage in clinical application by reducing the required input parameters and computational cost. In addition, we have shown that the use of the simplified PK computer model only affects the IC_{50} value but does not affect the quality of the data fitting.

Moreover, we observed two clinically relevant covariate effects on the endogenous T4 production rate. On the one hand, we observed a positive effect of age at diagnosis. From a clinical perspective, this effect can be explained by the size of the thyroid. The older the patients at diagnosis, the larger the volume of the thyroid, and consequently, the larger the endogenous T4 production rate. On the other hand, we observed an effect of disease severity on the endogenous production rate. The three disease severity levels, mild, moderate, and severe GD, were defined based on FT4 at diagnosis, and increased FT4 values correspond to a larger endogenous T4 production rate. Using the patients with mild GD as the reference group, the severity effect is positive, resulting in an increased endogenous production rate for more severely diseased patients. In detail, this means, for patients with moderate GD, the endogenous production rate is, with respect to the production rate of mild diseased patients, increased by <20%, and for patients with severe GD by more than 65%.

In Figure 5, we illustrate both covariate effects by plotting the endogenous T4 production rate (*y*-axis) as a function of age at

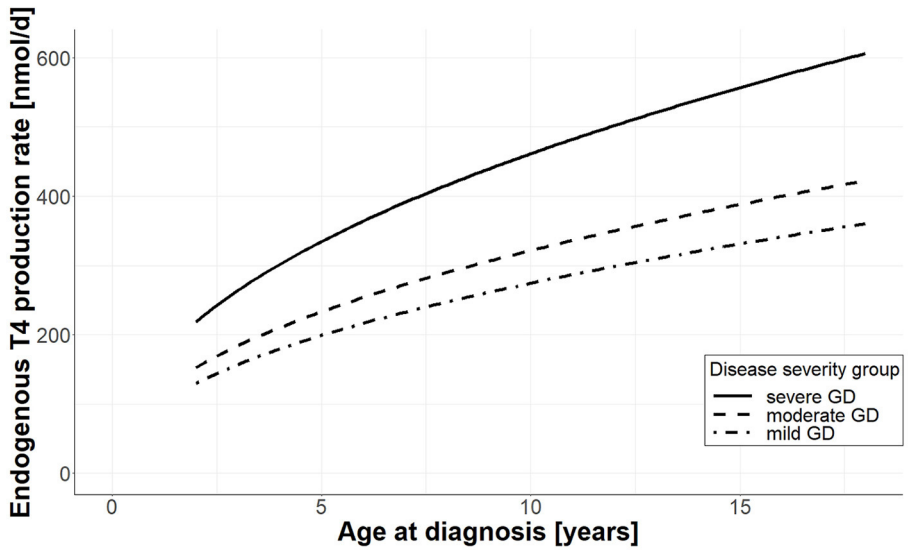

FIGURE 5
Effect of age and disease severity on endogenous T4 production rate. For each disease severity group, the endogenous production rate (*y*-axis) is plotted as a function of age at diagnosis (*x*-axis); the solid line shows the production rate for patients with severe GD, the dashed line corresponds to patients with moderate GD, and the dashed-dotted line corresponds to patients with mild GD.

diagnosis (x-axis) for each of the three different disease severity groups, namely severe GD (solid line), moderate GD (dashed line), and mild GD (dashed-dotted line).

Two further aspects are of interest for translation and application in clinical practice. On the one hand, due to the NLME modeling framework, our practical PMX computer model allows for personalized individual dose optimization (63) for pharmacotherapy in pediatric GD and facilitates the implementation of PMX-based clinical decision support tools (64).

On the other hand, as heart rate (HR) is a useful clinical marker to monitor thyroid activity in children with GD under treatment, it would be interesting to test for possible effects when including heart rate values in the model as a covariate. Due to a considerable number of missing values (23%) on tachycardia and heart function at diagnosis in our retrospective dataset, this could not be realized in this PMX model development. We aim to extend our developed PMX computer model by adding an FT4-HR component that describes the relationship between FT4 kinetics and the development of tachycardia.

Recent case reports indicate that wearable devices that continuously measure heart rate may facilitate the diagnosis and monitoring of adolescents with GD during the COVID-19 pandemic (65, 66). Furthermore, a recent prospective longitudinal study demonstrates the feasibility of monitoring heart rate in adults with hyperthyroidism using wearable technology. The combination of heart rate as a clinical marker in addition to FT4 dynamics has the potential to further facilitate the implementation of our predictive PMX computer model in clinical practice (67). As such, the application of our PMX modeling approach to heart rate monitoring at on-site consultation and at home with wearable devices is the obvious next step toward the implementation of computer-assisted, enhanced individualized monitoring and treatment of children and adolescents with GD in clinical practice.

In conclusion, the developed clinically practical PMX computer model with PK and PD components that account for inter-individual disease progression and treatment response is a promising approach to evaluate and improve individualized pharmacotherapy in children with GD with the potential to reduce over- and underdosing and avoid negative short- and long-term consequences. Prospective randomized validation trials are warranted to further validate and fine-tune computer-assisted, personalized pharmacotherapy in pediatric GD and other rare pediatric diseases.

Data availability statement

The original contributions presented in the study are included in the article/Supplementary material, further inquiries can be directed to the corresponding author.

Ethics statement

The studies involving human participants were reviewed and approved by Lead local Ethics Committee (Ethikkommission Nordwest- und Zentralschweiz EKNZ) and all local responsible Ethics Committees (Kantonale Ethikkommission Bern, Ethikkommission Zürich, Ethikkommission Ostschweiz EKOS). Written informed consent to participate in this study was provided by the participants' legal guardian/next of kin.

Author contributions

GK, TW, and GS designed the study protocol. PG, FC, MJ, Dl'A, DK, and GS were responsible for patient recruitment and data collection. BS, GK, GS, and MP analyzed the data. BS, GK, VG, FB, JS, and MP were responsible for or contributed to model development. BS, GK, FC, GS, and MP wrote the manuscript. All authors provided critical feedback on the manuscript and read and approved the submitted version.

Funding

This study was supported by a grant awarded to GK from the Swiss National Science Foundation; grant No. 179510. This work was supported by the DFG, project No. SCHR 692/3-1 (Germany).

Conflict of interest

The authors declare that the research was conducted in the absence of any commercial or financial relationships that could be construed as a potential conflict of interest.

Publisher's note

All claims expressed in this article are solely those of the authors and do not necessarily represent those of their affiliated organizations, or those of the publisher, the editors and the reviewers. Any product that may be evaluated in this article, or claim that may be made by its manufacturer, is not guaranteed or endorsed by the publisher.

Supplementary material

The Supplementary Material for this article can be found online at: https://www.frontiersin.org/articles/10.3389/fmed.2023.1099470/full#supplementary-material

References

1. Davies TF, Andersen S, Latif R, Nagayama Y, Barbesino G, Brito M, et al. Graves' disease. *Nat Rev Dis Primer*. (2020) 6:1–23. doi: 10.1038/s41572-020-0184-y

2. Smith TJ, Hegedüs L. Graves' disease. *N Engl J Med*. (2016) 375:1552–65. doi: 10.1056/NEJMra1510030

3. Mooij CF, Cheetham TD, Verburg FA, Eckstein A, Pearce SH, Léger J, et al. 2022 European Thyroid Association Guideline for the management of pediatric Graves' disease. *Eur Thyroid J*. (2022) 11. doi: 10.1530/ETJ-21-0073

4. Polak M, Refetoff S, Szinnai G, Vliet GV. Disorders of the thyroid gland. In: Sarafoglou K, Hoffmann GF, Roth KS, editors. *Pediatric Endocrinology and Inborn*

Errors of Metabolism. New York, NY: McGraw-Hill Education (2017). Available online at: https://accesspediatrics.mhmedical.com/content.aspx?aid=1140319020 (accessed October 28, 2021).

5. Polak M, Szinnai G. Chapter 83: thyroid disorders. In: Rimoin DL, Pyeritz RE, editors. *Emery and Rimoin's Essential Medical Genetics*. Amsterdam; Boston, MA: Academic Press (2013).

6. INSERM. *Orphanet: Pediatric Onset Graves Disease*. Available online at: https://www.orpha.net/consor/cgi-bin/OC_Exp.php?lng=en&Expert=525731 (accessed November 1, 2022).

7. Abraham-Nordling M, Wallin G, Träisk F, Berg G, Calissendorff J, Hallengren B, et al. Thyroid-associated ophthalmopathy; quality of life follow-up of patients randomized to treatment with antithyroid drugs or radioiodine. *Eur J Endocrinol.* (2010) 163:651–7. doi: 10.1530/EJE-10-0475

8. Kjær RH, Andersen MS, Hansen D. Increasing incidence of juvenile thyrotoxicosis in Denmark: a nationwide study, 1998-2012. *Horm Res Paediatr.* (2015) 84:102–7. doi: 10.1159/000430985

9. Rodanaki M, Lodefalk M, Forssell K, Arvidsson C-G, Forssberg M, Åman J. The incidence of childhood thyrotoxicosis is increasing in both girls and boys in Sweden. *Horm Res Paediatr.* (2019) 91:195–202. doi: 10.1159/000500265

10. Le Moal J, Chesneau J, Goria S, Boizeau P, Haigneré J, Kaguelidou F, et al. Spatiotemporal variation of childhood hyperthyroidism: a 10-year nationwide study. *Eur J Endocrinol.* (2022) 187:675–83. doi: 10.1530/EJE-22-0355

11. Taylor PN, Albrecht D, Scholz A, Gutierrez-Buey G, Lazarus JH, Dayan CM, et al. Global epidemiology of hyperthyroidism and hypothyroidism. *Nat Rev Endocrinol.* (2018) 14:301–16. doi: 10.1038/nrendo.2018.18

12. Kaguelidou F, Alberti C, Castanet M, Guitteny M-A, Czernichow P, Léger J. Predictors of autoimmune hyperthyroidism relapse in children after discontinuation of antithyroid drug treatment. *J Clin Endocrinol Metab.* (2008) 93:3817–26. doi: 10.1210/jc.2008-0842

13. Williamson S, Greene SA. Incidence of thyrotoxicosis in childhood: a national population based study in the UK and Ireland. *Clin Endocrinol.* (2010) 72:358–63. doi: 10.1111/j.1365-2265.2009.03717.x

14. Boelaert K, Torlinska B, Holder RL, Franklyn JA. Older subjects with hyperthyroidism present with a paucity of symptoms and signs: a large cross-sectional study. *J Clin Endocrinol Metab.* (2010) 95:2715–26. doi: 10.1210/jc.2009-2495

15. Wu T, Flowers JW, Tudiver F, Wilson JL, Punyasavatsut N. Subclinical thyroid disorders and cognitive performance among adolescents in the United States. *BMC Pediatr.* (2006) 6:12. doi: 10.1186/1471-2431-6-12

16. Hamed SA, Attiah FA, Abdulhamid SK, Fawzy M. Behavioral assessment of children and adolescents with Graves' disease: a prospective study. *PLoS ONE.* (2021) 16:e0248937. doi: 10.1371/journal.pone.0248937

17. Xie H, Chen D, Zhang J, Yang R, Gu W, Wang X. Characteristics of Graves' disease in children and adolescents in Nanjing: a retrospective investigation study. *Front Public Health.* (2022) 10:993733. doi: 10.3389/fpubh.2022.993733

18. Cramon P, Winther KH, Watt T, Bonnema SJ, Bjorner JB, Ekholm O, et al. Quality-of-life impairments persist six months after treatment of Graves' hyperthyroidism and toxic nodular goiter: a prospective cohort study. *Thyroid.* (2016) 26:1010–8. doi: 10.1089/thy.2016.0044

19. Lane LC, Cheetham TD, Perros P, Pearce SHS. New therapeutic horizons for graves' hyperthyroidism. *Endocr Rev.* (2020) 41:873–84. doi: 10.1210/endrev/bnaa022

20. Ross DS, Burch HB, Cooper DS, Greenlee MC, Laurberg P, Maia AL, et al. 2016 American Thyroid Association Guidelines for diagnosis and management of hyperthyroidism and other causes of thyrotoxicosis. *Thyroid.* (2016) 26:1343–421. doi: 10.1089/thy.2016.0229

21. Minamitani K, Sato H, Ohye H, Harada S, Arisaka O. Guidelines for the treatment of childhood-onset Graves' disease in Japan, 2016. *Clin Pediatr Endocrinol Case Rep Clin Investig.* (2017) 26:29–62. doi: 10.1297/cpe.26.29

22. Ohye H, Minagawa A, Noh JY, Mukasa K, Kunii Y, Watanabe N, et al. Antithyroid drug treatment for graves' disease in children: a long-term retrospective study at a single institution. *Thyroid.* (2014) 24:200–7. doi: 10.1089/thy.2012.0612

23. Kourime M, McGowan S, Al Towati M, Ahmed SF, Stewart G, Williamson S, et al. Long-term outcome of thyrotoxicosis in childhood and adolescence in the west of Scotland: the case for long-term antithyroid treatment and the importance of initial counselling. *Arch Dis Child.* (2018) 103:637–42. doi: 10.1136/archdischild-2017-313454

24. Song A, Kim SJ, Kim M-S, Kim J, Kim I, Bae GY, et al. Long-term antithyroid drug treatment of graves' disease in children and adolescents: a 20-year single-center experience. *Front Endocrinol.* (2021) 12:687834. doi: 10.3389/fendo.2021.687834

25. Rivkees SA, Szarfman A. Dissimilar hepatotoxicity profiles of propylthiouracil and methimazole in children. *J Clin Endocrinol Metab.* (2010) 95:3260–7. doi: 10.1210/jc.2009-2546

26. Léger J, Oliver I, Rodrigue D, Lambert A-S, Coutant R. Graves' disease in children. *Ann Endocrinol.* (2018) 79:647–55. doi: 10.1016/j.ando.2018.08.001

27. Sato H, Minagawa M, Sasaki N, Sugihara S, Kazukawa I, Minamitani K, et al. Comparison of methimazole and propylthiouracil in the management of children and adolescents with Graves' disease: efficacy and adverse reactions during initial treatment and long-term outcome. *J Pediatr Endocrinol Metab.* (2011) 24:257–63. doi: 10.1515/jpem.2011.194

28. Wood CL, Cole M, Donaldson M, Dunger DB, Wood R, Morrison N, et al. Randomised trial of block and replace vs dose titration thionamide in young people with thyrotoxicosis. *Eur J Endocrinol.* (2020) 183:637–45. doi: 10.1530/EJE-20-0617

29. Cheetham T, Bliss R. Treatment options in the young patient with Graves' disease. *Clin Endocrinol.* (2016) 85:161–4. doi: 10.1111/cen.12871

30. Rivkees SA. Controversies in the management of Graves' disease in children. *J Endocrinol Invest.* (2016) 39:1247–57. doi: 10.1007/s40618-016-0477-x

31. Koch G, Steffens B, Leroux S, Gotta V, Schropp J, Gächter P, et al. Modeling of levothyroxine in newborns and infants with congenital hypothyroidism: challenges and opportunities of a rare disease multi-center study. *J Pharmacokinet Pharmacodyn.* (2021) 48:711–23. doi: 10.1007/s10928-021-09765-w

32. Dayneka NL, Garg V, Jusko WJ. Comparison of four basic models of indirect pharmacodynamic responses. *J Pharmacokinet Biopharm.* (1993) 21:457–78. doi: 10.1007/BF01061691

33. Bonate PL (editors) *Pharmacokinetic-Pharmacodynamic Modeling and Simulation*. 1st ed. Boston, MA: Springer (2006).

34. Koch G, Schropp J. Mathematical concepts in pharmacokinetics and pharmacodynamics with application to tumor growth. In: Kloeden PE, Pötzsche C, editors. *Nonautonomous Dynamical Systems in the Life Sciences. Lecture Notes in Mathematics*. Cham: Springer International Publishing (2013). p. 225–50

35. Gabrielsson J, Weiner D. *Pharmacokinetic and Pharmacodynamic Data Analysis: Concepts and Applications*. CRC press (2001).

36. Lavielle M. *Mixed Effects Models for the Population Approach: Models, Tasks, Methods and Tools*. Chapman and Hall/CRC (2014). Available online at: https://hal.archives-ouvertes.fr/hal-01122873 (accessed July 23, 2021).

37. Neo-Mercazoletab. *Medsafe NZ*. Available online at: https://www.medsafe.govt.nz/Profs/Datasheet/n/Neo-Mercazoletab.pdf (accessed October 28, 2021).

38. Skellern GG, Knight BI, Low CK, Alexander WD, McLarty DG, Kalk WJ. The pharmacokinetics of methimazole after oral administration of carbimazole and methimazole, in hyperthyroid patients. *Br J Clin Pharmacol.* (1980) 9:137–43. doi: 10.1111/j.1365-2125.1980.tb05823.x

39. Okamura Y, Shigemasa C, Tatsuhara T. Pharmacokinetics of methimazole in normal subjects and hyperthyroid patients. *Endocrinol Jpn.* (1986) 33:605–15. doi: 10.1507/endocrj1954.33.605

40. Methimazole. *Drugbank*. Available online at: https://go.drugbank.com/drugs/DB00763 (accessed October 28, 2021).

41. Wetherington JD, Pfister M, Banfield C, Stone JA, Krishna R, Allerheiligen S, et al. Model-based drug development: strengths, weaknesses, opportunities, and threats for broad application of pharmacometrics in drug development. *J Clin Pharmacol.* (2010) 50:31S—46S. doi: 10.1177/0091270010377629

42. Stone JA, Banfield C, Pfister M, Tannenbaum S, Allerheiligen S, Wetherington JD, et al. Model-based drug development survey finds pharmacometrics impacting decision making in the pharmaceutical industry. *J Clin Pharmacol.* (2010) 50:20S—30S. doi: 10.1177/0091270010377628

43. Koch G, Datta AN, Jost K, Schulzke SM, van den Anker J, Pfister M. Caffeine citrate dosing adjustments to assure stable caffeine concentrations in preterm neonates. *J Pediatr.* (2017) 191:50–6.e1. doi: 10.1016/j.jpeds.2017.08.064

44. Wilbaux M, Fuchs A, Samardzic J, Rodieux F, Csajka C, Allegaert K, et al. Pharmacometric approaches to personalize use of primarily renally eliminated antibiotics in preterm and term neonates. *J Clin Pharmacol.* (2016) 56:909–35. doi: 10.1002/jcph.705

45. Koch G, Schropp J, Pfister M. Facilitate treatment adjustment after overdosing: another step toward 21st-century medicine. *J Clin Pharmacol.* (2017) 57:704–11. doi: 10.1002/jcph.852

46. Brussee JM, Schulz JD, Coulibaly JT, Keiser J, Pfister M. Ivermectin dosing strategy to achieve equivalent exposure coverage in children and adults. *Clin Pharmacol Ther.* (2019) 106:661–7. doi: 10.1002/cpt.1456

47. Koch G, Schropp J, Jusko WJ. Assessment of non-linear combination effect terms for drug-drug interactions. *J Pharmacokinet Pharmacodyn.* (2016) 43:461–79. doi: 10.1007/s10928-016-9490-0

48. Cooper DS, Bode HH, Nath B, Saxe V, Maloof F, Ridgway EC. Methimazole pharmacology in man: studies using a newly developed radioimmunoassay for methimazole. *J Clin Endocrinol Metab.* (1984) 58:473–9. doi: 10.1210/jcem-58-3-473

49. Owen JS, Friedler-Kelly J. *Introduction to Population Pharmacokinetic / Pharmacodynamic Analysis with Nonlinear Mixed Effects Models | Wiley*. J. Wiley & Sons (2014). Available online at: https://www.wiley.com/en-us/Introduction$+$to$+$Population$+$Pharmacokinetic$+$Pharmacodynamic$+$Analysis$+$with$+$Nonlinear$+$Mixed$+$Effects$+$Models-p-9780470582299 (accessed July 23, 2021).

50. van Lieshout JM, Mooij CF, van Trotsenburg ASP, Zwaveling-Soonawala N. Methimazole-induced remission rates in pediatric Graves' disease: a systematic review. *Eur J Endocrinol.* (2021) 185:219–29. doi: 10.1530/EJE-21-0077

51. Chuang-Stein C. Some issues concerning the normalization of laboratory data based on reference ranges. *Drug Inf J DIJ Drug Inf Assoc.* (2001) 35:153–6. doi: 10.1177/009286150103500117

52. Riggs DS. Quantitative aspects of iodine metabolism in man. *Pharmacol Rev.* (1952) 4:284–370.

53. Danziger L, Elmergreen GL. The thyroid-pituitary homeostatic mechanism. *Bull Math Biophys.* (1956) 18:1–13. doi: 10.1007/BF02477840

54. Mak PH, DiStefano JJ. Optimal control policies for the prescription of thyroid hormones. *Math Biosci.* (1978) 42:159–86. doi: 10.1016/0025-5564(78)90094-9

55. Degon M, Chipkin SR, Hollot CV, Zoeller RT, Chait Y, A. computational model of the human thyroid. *Math Biosci.* (2008) 212:22–53. doi: 10.1016/j.mbs.2007.10.009

56. Mukhopadhyay B, Bhattacharyya R. A mathematical model describing the thyroid-pituitary axis with time delays in hormone transportation. *Appl Math.* (2006) 51:549–64. doi: 10.1007/s10492-006-0020-z

57. Leow MK-S. A mathematical model of pituitary–thyroid interaction to provide an insight into the nature of the thyrotropin–thyroid hormone relationship. *J Theor Biol.* (2007) 248:275–87. doi: 10.1016/j.jtbi.2007.05.016

58. Eisenberg M, Samuels M, DiStefano JJ. Extensions, validation, and clinical applications of a feedback control system simulator of the hypothalamo-pituitary-thyroid axis. *Thyroid.* (2008) 18:1071–85. doi: 10.1089/thy.2007.0388

59. Ekerot P, Ferguson D, Glämsta E-L, Nilsson LB, Andersson H, Rosqvist S, et al. Systems pharmacology modeling of drug-induced modulation of thyroid hormones in dogs and translation to human. *Pharm Res.* (2013) 30:1513–24. doi: 10.1007/s11095-013-0989-4

60. Langenstein C, Schork D, Badenhoop K, Herrmann E. Relapse prediction in Graves' disease: towards mathematical modeling of clinical, immune and genetic markers. *Rev Endocr Metab Disord.* (2016) 17:571–81. doi: 10.1007/s11154-016-9386-8

61. Berberich J, Dietrich JW, Hoermann R, Müller MA. Mathematical modeling of the pituitary–thyroid feedback loop: role of a TSH-T3-shunt and sensitivity analysis. *Front Endocrinol.* (2018) 9:91. doi: 10.3389/fendo.2018.00091

62. Pandiyan B, Merrill SJ, Di Bari F, Antonelli A, Benvenga S. A patient-specific treatment model for Graves' hyperthyroidism. *Theor Biol Med Model.* (2018) 15:1. doi: 10.1186/s12976-017-0073-6

63. Bachmann F, Koch G, Pfister M, Szinnai G, Schropp J. OptiDose: computing the individualized optimal drug dosing regimen using optimal control. *J Optim Theory Appl.* (2021) 189:46–65. doi: 10.1007/s10957-021-01819-w

64. Nekka F, Csajka C, Wilbaux M, Sanduja S, Li J, Pfister M. Pharmacometrics-based decision tools facilitate mHealth implementation. *Expert Rev Clin Pharmacol.* (2017) 10:39–46. doi: 10.1080/17512433.2017.1251837

65. Griffith ML, Bischoff LA, Baum HBA. Approach to the patient with thyrotoxicosis using telemedicine. *J Clin Endocrinol Metab.* (2020) 105:2812–8. doi: 10.1210/clinem/dgaa373

66. Shanefield SC, Kelly MN, Posa M. Wearable technology leads to initial workup of Graves' Disease in an adolescent female. *J Adolesc Health.* (2022) 71:370–2. doi: 10.1016/j.jadohealth.2022.03.021

67. Lee J-E, Lee DH, Oh TJ, Kim KM, Choi SH, Lim S, et al. Clinical feasibility of monitoring resting heart rate using a wearable activity tracker in patients with thyrotoxicosis: prospective longitudinal observational study. *JMIR MHealth UHealth.* (2018) 6:e159. doi: 10.2196/mhealth.9884

frontiers | Frontiers in Medicine

TYPE Original Research
PUBLISHED 14 July 2023
DOI 10.3389/fmed.2023.1113460

OPEN ACCESS

EDITED BY
Jian Gao,
Shanghai Children's Medical Center, China

REVIEWED BY
Padmaja Mummaneni,
United States Food and Drug Administration, United States
Jürgen Föll,
Children's University Hospital of Regensburg, Germany

*CORRESPONDENCE
Adriana Ceci
✉ adriceci.uni@gmail.com

†These authors have contributed equally to this work and share first authorship

RECEIVED 01 December 2022
ACCEPTED 16 June 2023
PUBLISHED 14 July 2023

CITATION
Ceci A, Conte R, Didio A, Landi A, Ruggieri L, Giannuzzi V and Bonifazi F (2023) Target therapy for high-risk neuroblastoma treatment: integration of regulatory and scientific tools is needed. *Front. Med.* 10:1113460. doi: 10.3389/fmed.2023.1113460

Target therapy for high-risk neuroblastoma treatment: integration of regulatory and scientific tools is needed

Adriana Ceci*, Rosa Conte†, Antonella Didio†, Annalisa Landi, Lucia Ruggieri, Viviana Giannuzzi and Fedele Bonifazi

Research Department, Fondazione per la Ricerca Farmacologica Gianni Benzi Onlus, Bari, Italy

Introduction: Several new active substances (ASs) targeting neuroblastoma (NBL) are under study. We aim to describe the developmental and regulatory status of a sample of ASs targeting NBL to underline the existing regulatory gaps in product development and to discuss possible improvements.

Methods: The developmental and regulatory statuses of the identified ASs targeting NBL were investigated by searching for preclinical studies, clinical trials (CTs), marketing authorizations, pediatric investigation plans (PIPs), waivers, orphan designations, and other regulatory procedures.

Results: A total of 188 ASs were identified. Of these, 55 were considered 'not under development' without preclinical or clinical studies. Preclinical studies were found for 115 ASs, of which 54 were associated with a medicinal product. A total of 283 CTs (as monotherapy or in combination) were identified for 70 ASs. Of these, 52% were at phases 1, 1/2, and 2 aimed at PK/PD/dosing activity. The remaining ones also included efficacy. Phase 3 studies were limited. Studies were completed for 14 ASs and suspended for 11. The highest rate of ASs involved in CTs was observed in the RAS-MAPK-MEK and VEGF groups. A total of 37 ASs were granted with a PIP, of which 14 involved NBL, 41 ASs with a waiver, and 18 ASs with both PIPs and waivers, with the PIP covering pediatric indications different from the adult ones. In almost all the PIPs, preclinical studies were required, together with early-phase CTs often including efficacy evaluation. Two PIPs were terminated because of negative study results, and eight PIPs are in progress. Variations in the SmPC were made for larotrectinib sulfate/Vitrakvi® and entrectinib/Rozlytrek® with the inclusion of a new indication. For both, the related PIPs are still ongoing. The orphan designation has been largely adopted, while PRIME designation has been less implemented.

Discussion: Several ASs entered early phase CTs but less than one out of four were included in a regulatory process, and only two were granted a pediatric indication extension. Our results confirm that it is necessary to identify a more efficient, less costly, and time-consuming "pediatric developmental model" integrating predictive preclinical study and innovative clinical study designs. Furthermore, stricter integration between scientific and regulatory efforts should be promoted.

KEYWORDS

neuroblastoma, rare diseases, drug development, target therapy, pediatric regulation

Introduction

Neuroblastoma (NBL) is the commonest pediatric extracranial solid tumor (1). While local low-risk NBL can be controlled with a high rate of cure (2), there is an urgent need to develop new treatment options for the high-risk NBL that still represents a leading cause of death from cancer in children (3) due to chemoresistance and frequent metastatic relapse. Optimized regimens incorporating emerging new molecules targeting NBL and other pediatric cancers are under development (4). By the end of 2020, the number of pediatric oncology medicinal products (MPs) increased; however, this increase was lower than what was observed for adult products. In fact, a total of 174 oncology medicinal products have been approved by the European Medicine Agency (EMA) in the period 2007–2020, but only 35 (20%) have been approved for use in children in the same period (5).

The scarcity of pediatric medicinal products is not surprising. In fact, the experience accumulated in the recent years demonstrates that the process of approval for a "pediatric" or a "rare diseases" product is particularly long and complex and affected by several research barriers and gaps (5, 6). Moreover, commercial and financial issues represent possible obstacles for the complete and timely development of such products (7).

The lack of novel pediatric oncology MPs appears in huge contrast with the numerous ASs identified in recent years targeting tumor-specific genomic abnormalities with the greatest potential to be developed as effective cancer therapies (8, 9). In some cases, genomic abnormalities identified in pediatric cancer are different from those correlated to adult cancers; in other cases, they are similar. However, while several new cancer agents are emerging worldwide, only rarely, pediatric indications were included in the adult drug or in pediatric-specific development programs (i.e., dinutuximab, representing the only product approved for NBL).

Focusing on NBL, the number of novel ASs targeting genetic mutations and molecular pathway aberrations, such as MYCN, BIRC5, PHOX2B, as well as epigenetic factors, tyrosine receptor kinase (TRK) inhibitors, and other targets, is impressive, as summarized in relevant studies (10–16). However, the number of ASs that has reached the patients (i.e., included in frontline therapies or granted with a marketing authorization—MA) is very low. Indeed, the extensively very high number of potentially druggable targets has been considered a relevant barrier to successfully developing new MPs (17). The project ACCELERATE, faced with these issues, started a prioritization initiative to identify more promising ASs to be advanced in the developmental process (18). Clarification on preclinical aspects, such as the availability of reliable "pediatric cancer model" and "proof of concept" for pediatric indication, emerges as a relevant premise, and a proposal to define a "preclinical package", shared with regulators, is under discussion (19). In line with these initiatives, the Neuroblastoma New Drug Development Strategy (NDDS) activated a prioritization process within ASs targeting NBL that ended in 2020 (20) with 40 genetic targets evaluated and 23 ASs prioritized for further development.

To bring a pediatric MP onto the market, both in the European Union (EU)[1] and the United States of America (USA) (21), there is the obligation for the sponsors of a new AS or of a still in-patent MP to complete a detailed plan of pediatric studies [i.e., the Pediatric Investigation Plan, PIP in the EU (22), and the Pediatric Study Plans—PsPs in the USA (23)], as agreed with the concerned regulatory agencies. This obligation may only be waived for one of the legally accepted reasons (24), such as (1) a product intended for a disease or condition not existing in a specified age subset; (2) an expected lack of safety or efficacy; or (3) a lack of significant therapeutic benefit in the pediatric population (23).

Among these, the waivers agreed to on the grounds that the proposed drug is intended for the treatment of adult cancers, not to be used in children, have been largely granted in the EU, but in July 2015, the Pediatric Committee (PDCO) adopted a review of the class waiver list (25) aimed at limiting these types of waiver applications.

In the USA, the RACE for Children Act (FDA Reauthorization Act) (26) provides that pediatric studies must be conducted if the mechanism of action (MoA) of the AS may be relevant for a pediatric cancer indication independent of the adult indication. Currently, the transition to a similar MoA-based regulatory approach is being favorably considered within the European Commission (EC) proposal for revision of the Pediatric and Orphan Regulation (6).

In addition, a number of regulatory tools, procedures, and incentives [i.e., the orphan designation (27), Scientific Advice/Protocols Assistance, research funds, conditional approval, and PRIME designation] were included in the EU legislative framework to support and accelerate the development of MP particularly relevant for patients, especially in case of innovative products. All these tools are fully applicable to NBL.

Similar to the USA, the EU legislation[1] was introduced with the aim to provide children with medicines appropriately assessed for pediatric use on the basis of a full developmental plan that includes preclinical and clinical investigations. Compliance with the current legislation may be challenging in the pediatric oncology field since some regulatory processes and procedures may be too rigid to address the rapid evolution of scientific advancements. This issue is particularly relevant at the academic level: The results from a recent survey showed that researchers face several difficulties in collaborating with regulators, including poor availability and flexibility from ethics committees/regulators for clarification and support (5).

The aim of this study was to analyze, in parallel, the developmental status and the regulatory status of ASs targeting NBL suitable for entering into frontline therapies and for being authorized for pediatric use in the EU, by considering (a) availability of preclinical and clinical studies relevant to a pediatric

1 Regulation (EC) No 1901/2006 of the European Parliament and of the Council of 12 December 2006 on medicinal products for pediatric use and amending Regulation (EEC) No 1768/92, Directive 2001/20/EC, Directive 2001/83/EC and Regulation (EC) No 726/2004 (Text with EEA relevance). Official Journal of the European Union L 378/.2. 27.12.2006. Available online at: https://eur-lex.europa.eu/legal-content/EN/TXT/PDF/?uri=CELEX:32006R1901&from=EN (accessed November 14, 2022).

marketing authorization (MA); (b) availability of an agreed PIP (or of a waiver) and its advancements; and (c) other regulatory procedures applied to the concerned ASs.

Emerging gaps from this analysis and suggestions for improvement were considered and have been discussed also in light of the next revision of the EU Pediatric and Orphan Regulations,[1] (21).

Materials and methods

Study sample

ASs targeting NBL were searched by consulting PubMed (28). The following search terms were adopted: (All field < target therapy > AND All field < neuroblastoma >). Specific filters were applied such as follows: child (birth, 18 years); language (English); article type (review and systematic review); and publication date (January 2018–June 2022). The resulting articles were first screened by the title and abstract to eliminate non-relevant articles (i.e., not focused on NBL or not reporting ASs targeting NBL). The selected articles were processed to derive a list of the ASs for which the following information was available: name of the AS; type of the substance (chemical or biological); and type and description of molecular pathways/genetic aberration targeting NBL. If details were not available, the article was excluded. Immunotherapy and other therapeutic agents were also excluded from the study sample.

Developmental status

For each AS, the following information was collected from both literature and the available clinical trials database (https://clinicaltrials.gov/) (29): (1) preclinical toxicity/safety and other studies that are considered necessary to support pediatric studies and marketing authorization of products (30); (2) clinical trials (CTs) and their phases and aims (pharmacokinetic—PK/pharmacodynamics—PD, studies and dose rationale, efficacy-safety trials); (3) other studies, including extrapolation, modeling, and simulation. When available, information about the status of the study (e.g., recruiting, not recruiting, completed, suspended, terminated, and withdrawn) and the availability of study results was collected. For preclinical studies, in addition to literature, we also consulted the European Public Assessment Reports (EPARs, as available on EMA website) to capture studies already submitted to the regulatory authority during previous MA procedures. Preclinical studies aimed to test the pediatric oncology model and "proof of concept" studies were not considered in this study.

Regulatory information

For each AS, it was investigated for its inclusion in (1) an MP, approved up to 2022 and their adult and/or pediatric indications; (2) a waiver (i.e., class or product-specific waiver) and the waiver indication; (3) an agreed PIP including indication and advancement status (expected and current time to completion, and compliance check), an age range of the experimental population(s), and also the number and type of studies required (i.e., quality, preclinical, clinical, and other studies); and (4) other regulatory procedures (such as orphan designation and PRIME eligibility, conditional approvals, protocol assistance, or other scientific advices).

All data were collected by consulting the EMA publicly available sources, including EPARs (31), orphan designation list (32), opinions and decisions on PIPs and product-specific waivers (33), a list of products granted eligibility to PRIME (34), and EMA annual reports (35).

Two authors performed the literature search as well as the extraction of information from the selected articles independently. Possible inconsistencies were solved by discussion or by appeal to another researcher.

Figure 1 represents the pediatric drug developmental process for easy understanding.

Analysis

A descriptive analysis of the results was performed. A comparative analysis was also made among groups of ASs. Indeed, the ASs in the NDDS priority list, based on a high-level scientific process aimed to identify the more promising ASs, are compared with ASs granted with a PIP under the request of a commercial sponsor during a regulatory-based procedure. In addition, the comparison included all the substances that did not receive a PIP and the substances already receiving a MA.

According to the aims of the study, the comparison considered the number of ASs for which the preclinical and clinical studies are available or ongoing, the number and type of regulatory procedures, i.e., PIPs, and the studies' results submitted to the regulatory authorities to be included in the product SmPC.

Results

Active substances targeting neuroblastoma: study sample identification and classification

A total of 182 publications resulted from the literature search. Of them, 144 studies were excluded: 32 were not focused on NBL; 44 did not report sufficient details on the molecular NBL target; and 68 were dealing with other therapeutic approaches such as immunotherapy, radiotherapy, and nanomedicine. Therefore, 39 studies (10–17, 20, 36–66) were considered for the analysis. The selection process is shown in Supplementary Figure 1.

A total of 557 ASs targeting NBL were derived by these studies: 369 were present in more than one study and thus counted only once. The remaining 188 represent the final sample of the study: 185 (98.4%) are chemical agents (small molecules) and three are biologicals. Figure 2 reports the ASs classified by the molecular target. In detail, the ASs targeting N-MYC oncogene are the most represented (67, 35.6%), followed by agents targeting epigenetic factors (22, 11.7%), TRK inhibitors (17, 9%), and the anaplastic lymphoma kinase (ALK) inhibitors (13, 6.9%). The whole list of

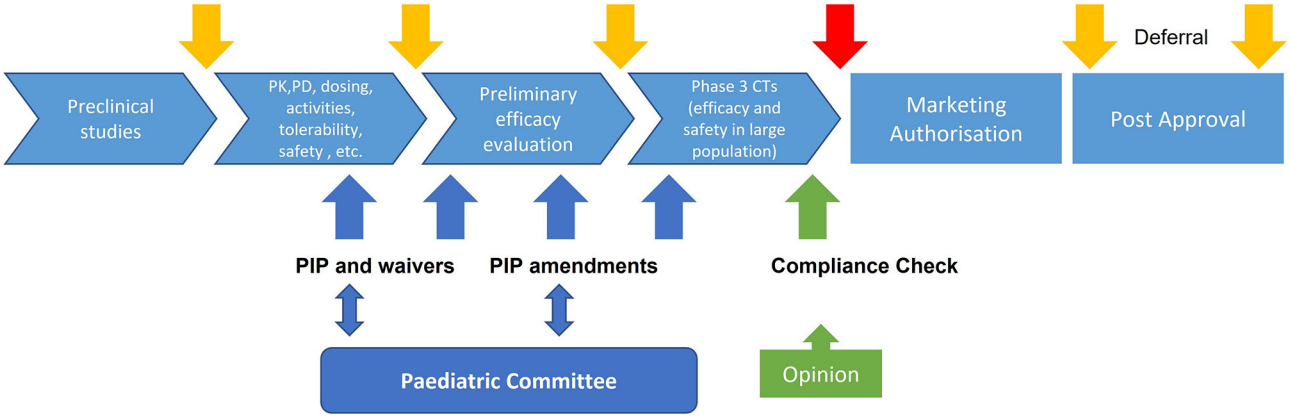

FIGURE 1
Pediatric drug developmental process.

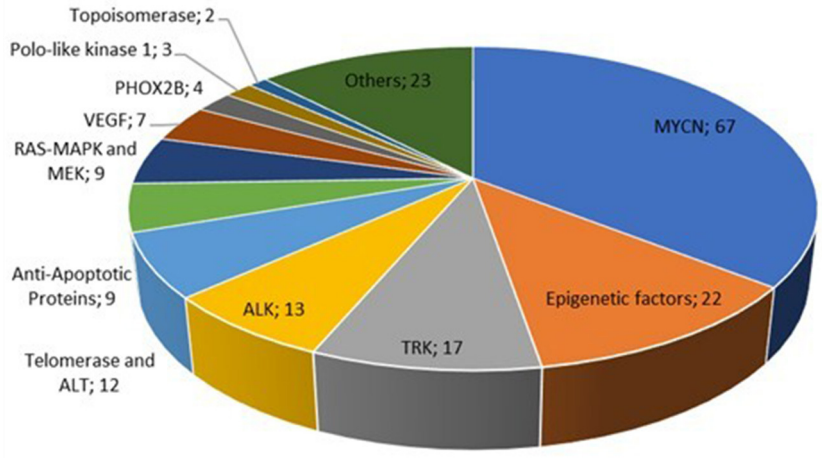

FIGURE 2
Number of active substances classified by molecular target.

the identified ASs and their molecular targets is included in the Supplementary material.

Developmental status

Preclinical studies

A total of 319 preclinical studies (i.e., toxicity, safety, and geno/carcinogenicity) were identified involving 115 ASs (Figure 3). Most of the studies were part of the MA dossiers of previously approved MPs. In contrast, 95 studies were not included in a MA and derived from the literature search. As shown in Figure 3, only 24 studies are pediatric-specific (i.e., juvenile animal studies). For 73 ASs, no preclinical studies were found.

Clinical studies

A total of 283 CTs conducted in NBL patients or in larger oncologic populations having NBL were found for 70 ASs both in monotherapy (60, 21.2%) and in combination (215, 76%). A total of 118 ASs were never included in a CT. In fact, of 118 ASs, 55 were tested neither with preclinical nor with clinical studies. Figure 4 details the type and number of CTs. Most of the CTs are phase 1 up to phase 2 trials (early trials) often covering preliminary efficacy evaluation.

As shown in Figure 4, out of the 283 studies, 52% were phase 1 and 1/2 studies aimed at PK/PD/dosing, activity, tolerability, and safety definition while the remaining CTs also included efficacy as primary or secondary outcomes. Phase 3, including randomized controlled trials (RCTs), were less represented, i.e., 22 RCTs related to 5 ASs, namely, *crizotinib, topotecan, doxorubicin, retinoic acid,* and *etoposide*.

A total of 154 studies were reported as active: recruiting, not yet recruiting, or active not recruiting; 88 (31.1%) were reported as completed; 41 (14.1%) reported as suspended, withdrawn, or no longer available. For 11 (*copanlisib, erlotinib, genistein, HDM201, imetelstat, pazopanib, panobinostat, SF1126, valproic*

acid, vandetanib, and *vistusertib*) out of 70 ASs, the development was interrupted.

Considering the type of AS and related target, further considerations were raised. The most represented Ass that entered into the clinical phase belong to the MYCN group (22 of 70, 31.4%). However, in the RAS-MAPK-MEK and VEGF groups, the highest rate of ASs in CTs including efficacy evaluation was observed (i.e., 77.8 and 71.4%, respectively) (Table 1). Supplementary Figure 2 summarizes the developmental status of the ASs in our sample.

Regulatory status

Active substances granted with pediatric investigation plans and waivers

A total of 37 ASs (out of 188) were granted a PIP, covering several indications, from the hematolymphoid system ($n = 13$), central nervous system (CNS) tumor ($n = 6$), solid tumor ($n = 14$), and other pediatric malignancies ($n = 10$). The NBL indication was included in 14 PIPs.

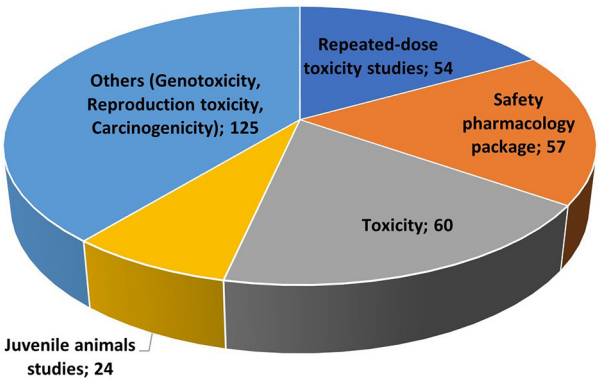

FIGURE 3
Preclinical studies: type and number.

A total of 29 PIPs were associated with an approved MP: 28 to an adult MP and 1 to a pediatric-only MP. The remaining eight were PIPs granted to a product under development.

A total of 41 ASs were linked to product-specific waivers or class waivers granted mainly for non-small cell lung cancer, melanoma, and breast cancer indications.

For 18 ASs (43.9%), both PIPs and waivers were granted: the PIPs covered one or more pediatric indications different from the adult ones, and the waivers covered the adult indication; however, seven included NBL.

Noticeably, *trametinib, dabrafenib*, and *binimetinib* have a PIP in the same adult indication (melanoma with BRAF mutation), but other indications targeted by the BRAF mutation of interest for pediatric tumors were also added. Details of ASs granted with both PIPs and waivers for different indications are shown in Table 2.

TABLE 1 Active substances entered in clinical trials.

Molecular target	*N* of ASs	ASs with clinical trials
MYCN	67 (35.6%)	22 (32.8%)
Epigenetic factors	22 (11.7%)	7 (31.8%)
TRK	17 (9%)	8 (47.1%)
ALK	13 (6.9%)	6 (46.1%)
Telomerase and ALT	12 (6.4%)	4 (33.3%)
Anti-apoptotic proteins	9 (4.8%)	2 (22.2%)
RAS-MAPK and MEK	9 (4.8%)	7 (77.8%)
VEGF	7 (3.7%)	5 (71.4%)
PHOX2B	4 (2.1%)	0
Polo-like kinase 1	3 (1.6%)	0
Topoisomerase	2 (1.1%)	2 (100%)
Others	23 (12.2%)	7 (30.4%)
Total	**188**	**70**

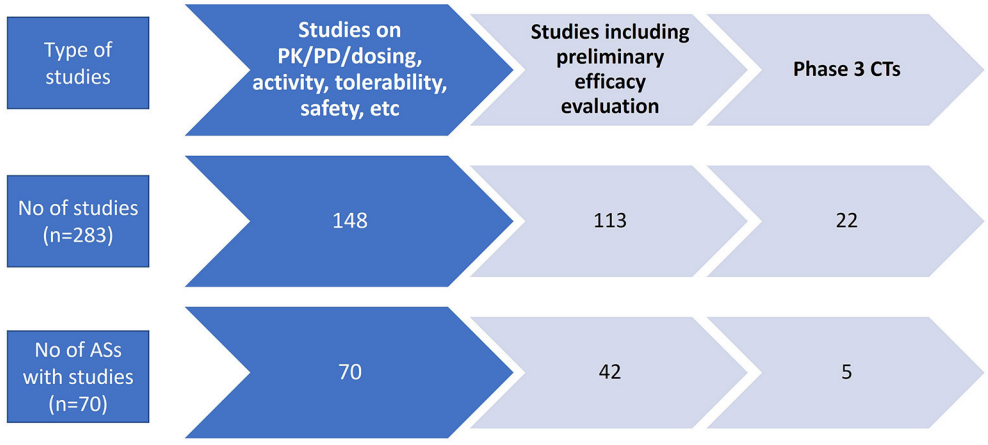

FIGURE 4
Number of clinical trials and active substances entered in clinical trials.

TABLE 2 Active substances granted with both pediatric investigation plans and waivers.

ASs	Approved adult indication	Waived condition	Agreed PIP indication
Abemaciclib	Breast cancer	Breast cancer	1. High-grade glioma, NBL; 2. Ewing's sarcoma
Afatinib	NSCLC	NSCLC	Malignant neoplasms (except hematopoietic and lymphoid tissues neoplasms); CNS malignant neoplasms
Binimetinib	Melanoma with a BRAF V600 mutation	Colorectal cancer	Melanoma with BRAF V600 mutations
Crizotinib	NSCLC	Lung malignant neoplasms	Anaplastic large cell lymphoma and inflammatory myofibroblastic tumors
Olaparib	Ovarian cancer, fallopian tube cancer, and peritoneal cancer	Ovarian cancer, fallopian tube cancer, and peritoneal cancer	Malignant neoplasms (except hematopoietic and lymphoid tissue neoplasms), HRR-mutated solid tumors
Trametinib	Melanoma and NSCLC with BRAF V600 mutation	NSCLC	1. Melanoma with BRAF V600 mutation; 2. Solid tumor with RAS, RAF, or MEK pathway activation; 3. Glioma with BRAF V600 mutation
Venetoclax	CLL and AML	CLL	NBL, acute lymphatic leukemia, acute myeloid leukemia, and non-Hodgkin lymphoma
Carfilzomib	Multiple myeloma	Multiple myeloma	T-cell or B-cell acute lymphoblastic leukemia
Dabrafenib	Melanoma and NSCLC with BRAF V600 mutation	NSCLC	1. Glioma with BRAF V600 mutation; 2. Melanoma with BRAF V600 mutation; 3. Solid tumors with BRAF V600 mutation
Talazoparib	Breast cancer	Breast cancer and prostate malignant neoplasms	Ewing's sarcoma
Imetelstat	Not applicable	Myelofibrosis	AML, myelodysplastic syndromes, and juvenile myelomonocytic leukemia
Erdafitinib	Not applicable	Urothelial carcinoma	Malignant neoplasms, locally advanced or metastatic solid tumors with FGFR alterations, and newly diagnosed solid tumors with FGFR alterations
Palbociclib	Breast neoplasms	Breast malignant neoplasm	Ewing's sarcoma
Ivosidenib	Not applicable	Malignant neoplasms (except CNS tumors, hematolymphoid);	Newly diagnosed or relapsed or refractory AML with an isocitrate dehydrogenase-1 mutation
Veliparib	Not applicable	1. Fallopian tube cancer, ovarian cancer, peritoneal carcinoma; 2. SCLC; 3. breast cancer	Newly diagnosed supratentorial high-grade glioma
Brigatinib	Anaplastic lymphoma kinase (ALK)-positive advanced NSCLC	NSCLC	Newly diagnosed ALK+ anaplastic large cell lymphoma; ALK+ unresectable or recurrent inflammatory myofibroblastic tumors
Ixazomib	Multiple myeloma	Systemic light chain amyloidosis and Multiple myeloma	Lymphoid malignancy (excluding multiple myeloma)
Ruxolitinib	Myelofibrosis, polycythemia vera, and graft-vs.-host disease	Thrombocythemia and polycythemia vera	1. Acute graft-vs.-host disease after allogeneic transplantation 2. Vitiligo 3. Chronic graft-vs.-host disease after allogeneic transplantation

NSCLC, non-small cell lung cancer; SCLC, small cell lung cancer; CLL, chronic lymphocytic leukemia; ALL, acute lymphocytic leukemia; AML, acute myeloid leukemia; NHL, non-Hodgkin lymphoma; CNS, central nervous system.

Most of these PIPs associated with a product covered by a waiver were granted after the EMA revision of the class waivers in 2015 (Figure 5).

Pediatric investigation plan contents

The contents of the 14 PIPs that include NBL indication are reported in Supplementary Table 1. In summary, five out of 14 (35.7%) NBL PIPs cover the whole pediatric population from birth, while nine out of 14 (64.3%) cover all ages except younger children (i.e., under 24, 12, 6, or 1 month of age). The PIP indication included NBL and other pediatric solid tumors or, more rarely, hematolymphoid or CNS malignancies.

The total number of (preclinical and clinical) studies required in each PIP varies from two (*afatinib*) to eight (*copanlisib*). In detail, non-clinical studies were required for all PIPs, except for *olaparib*,

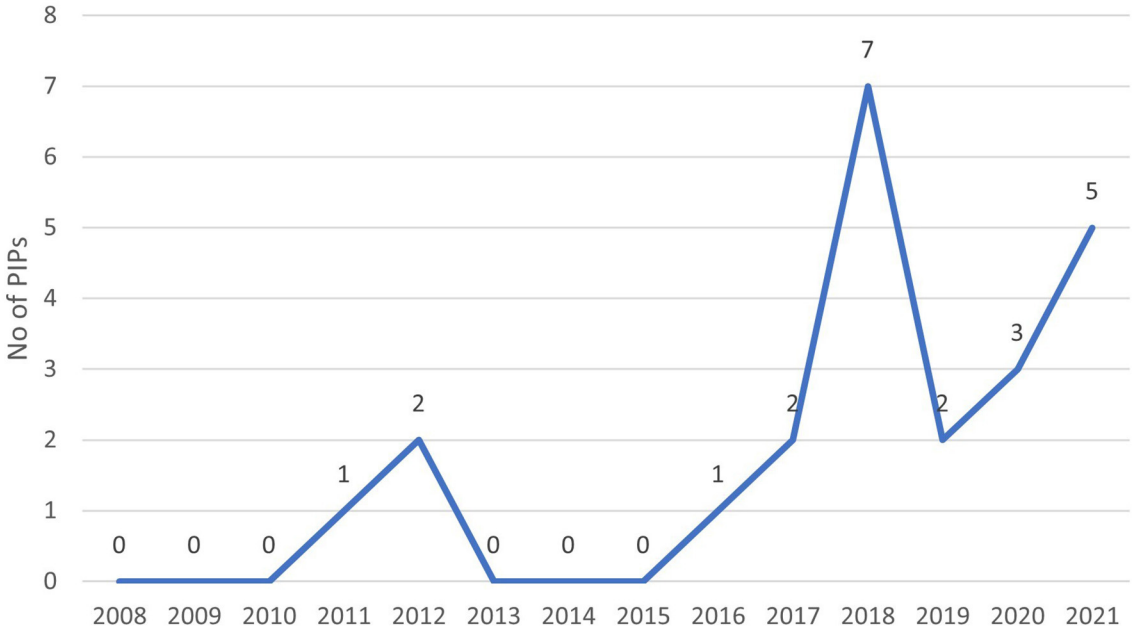

FIGURE 5
Active substances granted with both pediatric investigation plan and waiver by year.

an ASs already marketed for a different adult indication, and *erdafitinib*. Pediatric-specific studies (i.e., juvenile animal, and age-appropriated formulations) are the most required. The *in vivo/in vitro* pediatric disease model and biomarker studies were required in two PIPs, respectively.

All PIPs included early CTs (i.e., PK and dosing, activity, and safety), and seven of them also included efficacy studies. A phase 3 trial (RCT) was considered for *olaparib*. Extrapolation, modeling, and simulation studies, aimed to support the dosing regimen of the product, were required for six out of 14 PIPs. The expected duration for ongoing PIPs (i.e., the timing between the PIP decision date and the expected PIP completion date, as agreed with PDCO), varies from 2 to 17 years (mean value: 8.5 years). For five out of 14 PIPs (*abemaciclib, copanlisib, idasanutlin, olaparib, and venetoclax*), the expected duration is up to 2027 and, in the case of *olaparib*, it is up to 2035.

The current status of PIPs and their outcomes are described in Table 3: for two ASs (*cobimetinib and afatinib*), the PIP was concluded and received the compliance check after 7.4 and 2.6 years, respectively, while for the other two ASs (*trametinib and dabrafenib*), the studies were completed, but the PIP did not receive a compliance check.

Pediatric investigation plan outcomes

We investigated the status of non-clinical and clinical studies foreseen in the PIPs. Several completed preclinical studies, including juvenile animal toxicity studies, resulted in the MA dossiers of the approved MPs. For eight PIPs, clinical studies resulted in active, recruiting, or not recruiting. Development of *copanlisib* was terminated after a phase 1/2 study because of "no anticipated benefit respect to standard therapy". Negative outcomes were also reported for *cobimetinib* studies.

Modifications in the SmPC were made as follows: for *larotrectinib sulfate and entrectinib*, a new indication, including high-risk NBL, was included in SmPC, based on the preliminary results of the studies and efficacy data extrapolated by other adult studies, respectively; *entrectinib* is authorized for use in children older than 12 years. For *selpercatinib*, the preliminary results were included in the SmPC, without any change of the product indication. It should be noted that, for all these ASs, the related PIPs are still ongoing.

Other regulatory procedures

A total of 39 (20.7%) out of 188 ASs were included in the Community Register of designated Orphan Medicinal Products for a total of 59 orphan designations. Only two orphan designations cover the treatment of NBL. *Entrectinib* had an orphan designation, but it was withdrawn in 2018 after the product was designated within the PRIME scheme.

Developmental and regulatory status comparison

The results of comparison among different groups of ASs are shown in Table 4. The NDDS priority list group has the highest percentage of ASs with CTs and in particular of CTs, including efficacy preliminary data. No results from these NBL studies were included in SmPC. In the group of ASs associated with a PIP, we observed that all the ASs were entered into early CTs, but only a few included efficacy data. When considering the whole group of

10.3389/fmed.2023.1113460

TABLE 3 Pediatric investigation plans—clinical studies, status, and outcomes.

ASs	CC	Studies required in the PIPs	Studies available (completed or ongoing)	Status	SmPC variation
Abemaciclib	No	Dose escalation trial, in combination Study to evaluate safety and efficacy (recruiting)	Dose escalation trial, in combination	Recruiting	
Afatinib	Yes	Dose escalation trial to assess safety, PK, and anti-tumor activity (monotherapy)	Dose escalation trial to assess safety, PK, and anti-tumor activity (monotherapy)	Completed	No changes have been included in the SmPC.
Cobimetinib	Yes	Multiple dose 2-stage trial to evaluate PK, safety, and activity (monotherapy)	Multiple dose 2-stage trial to evaluate PK, safety, and activity (monotherapy)	Completed, negative outcome	No changes have been included in the SmPC.
Copanlisib	No	Dose escalating trial to PK, PD, safety, and activity; safety and efficacy trial (not planned)	Dose escalating trial to PK, PD, safety, and activity	Terminated no anticipated benefits	Product withdrawn
Entrectinib	No	Trial to evaluate PK, safety, and anti-tumor activity monotherapy	Trial to evaluate PK, safety, and anti-tumor activity monotherapy	Active not recruiting	*SmPC Variation:* Treatment of adult and pediatric patients 12 years of age and older
Idasanutlin	No	Trial to evaluate PK, toxicity, safety, and activity; trial to evaluate safety and efficacy	Trial to evaluate PK, toxicity, safety, and activity	Recruiting	
Larotrectinib sulfate	No	Trial to evaluate safety and efficacy still ongoing	Trial to evaluate PK, safety, and anti-cancer activity	Recruiting	*New indication:* Treatment of adult and pediatric patients with solid tumors that display an NTRK gene fusion
Olaparib	No	Study to evaluate safety, tolerability, PK, PD, and preliminary efficacy; multicenter study safety, tolerability, and efficacy (recruiting); randomized, controlled study (not started)	Study to evaluate safety, tolerability, PK, PD, and preliminary efficacy	Recruiting	
Trametinib	No	Dose escalation trial to evaluate safety, tolerability, PK, and PD in combination Bioavailability study in adults	Dose escalation trial to evaluate safety, tolerability, PK, and PD (in combination)	Recruiting	
Venetoclax	No	Dose determination and cohort expansion study; (in combination) Study to evaluate the efficacy	Dose determination and cohort expansion study (in combination)	Active not recruiting	
Dabrafenib	No	Dose escalation trial in combination Bioavailability study in adults	Dose escalation trial (in combination)	Completed	No changes have been included in the SmPC
Erdafitinib	No	Study to evaluate the safety, PK, and anti-tumor activity in pediatric patients Study to assess the safety, PK, and efficacy in pediatric patients and adults	Study to evaluate the safety, PK and anti-tumor activity in pediatric patients Study to assess the safety, PK, and efficacy in pediatric patients and adults	1. Suspended (accrual goal met) 2. Recruiting	
Regorafenib	No	Study to evaluate PK/PD, tolerability, safety, and tumor activity in the pediatric population PK model Study to evaluate the activity, safety, and efficacy	PK/PD, tolerability, safety, and tumor activity (in combination)	Active- not recruiting	
Selpercatinib	No	Studies to evaluate the MTD/recommended dose and dose-limiting toxicities (monotherapy)	Studies to evaluate the MTD/recommended dose and dose-limiting toxicities (monotherapy)	Both recruiting	Preliminary results included in the SmPC

ASs, active substance; CC, compliance check; SmPC, summary of product characteristics; PK, pharmacokinetic; PD, pharmacodynamics; MTD, maximum tolerated dose.

ASs with a MA, we observed a higher percentage of ASs already submitted to studies, both preclinical and clinical, including efficacy data. In addition, five ASs were granted a pediatric variation in the SmPC: three products, *entrectinib, larotrectinib sulfate,* and *selpercatinib*, are also part of the PIPs group. However, at the time of the SmPC variation, the PIPs were still ongoing. Thus,

TABLE 4 Comparison of the regulatory and developmental status.

	Preclinical (safety, toxicity)	Juvenile animal studies	Entered in CTs (PK/PD/dosing, activity, tolerability, safety)	Entered in CTs-preliminary efficacy	Pediatric variation or results in SmPC
ASs Associated to a NBL PIPs ($n = 14$)	13 (92.9%)	7 (50%)	14 (100%)	2 (14.3%)	3 (21.4%)
ASs not associated to a PIP ($n = 151$)	81 (53.6%)	9 (6%)	44 (29.1%)	31 (20.5%)	2 (8.7%)
ASs included in NDDS Priority list ($n = 23$)	14 (60.9%)	3 (13%)	22 (95.7%)	12 (52.2%)	0
ASs associated to a MA ($n = 54$)	54 (100%)	21 (38.9%)	40 (74.1%)	25 (46.3%)	5* (9.3%)
ASs not associated to a MA ($n = 134$)	61 (45.5%)	3 (2.2%)	15 (11.2%)	17 (12.7%)	0
ASs in total sample ($n = 188$)	115 (61.2%)	24 (12.8%)	70 (37.2%)	42 (22.3%)	5 (2.7%)

*Entrectinib; larotrectinib sulfate; temsirolimus; topotecan; selpercatinib.
ASs, active substances; CTs, clinical trials; PK, pharmacokinetic; PD, pharmacodynamics; SmPC, summary of product characteristics; NBL, neuroblastoma; PIP, pediatric investigation plans; NDDS, neuroblastoma new drug development strategy; MA, marketing authorization.

the variations seem to be independent of the PIP. The other two products *(etoposide* and *doxorubicin)* were approved for a pediatric oncology indication (including NBL) in several member states with national MAs not yet harmonized at the EU level.

Finally, there are 44 ASs, not granted a PIP, for which pediatric clinical studies were identified, including also efficacy preliminary data.

Discussion

There is a larger than expected number of ASs targeting NBL and other pediatric malignancies for which several preclinical and clinical studies have been conducted or are under development. In particular, this number is higher than what is described in the framework of the NDDS forum ended (2020), with 23 genetic targets prioritized out of 40 identified ASs targeting NBL. As a result of our research, 70 ASs entered into the clinical phase; indeed, these studies have been conducted without considering any priority. Owing to the challenges related to the small population and the rarity of the disease (67), it is unlikely that all these ASs, or almost a consistent part of them, will be able to complete a full developmental process up to the inclusion in the frontline or to the market.

Among the ASs included in the clinical phase, ASs targeting/acting on the N-MYC are the most represented and have preclinical and early clinical studies documented in the 46 and 31% of cases, respectively. However, for eight out of 22 ASs of the MYCN group that reached the clinical phase, development was suspended, confirming the several difficulties encountered in moving these drugs to the MA (20). A lower number but a higher percentage of ASs under study were demonstrated for ASs in RAS-MAPK-MEK and VEGF groups. A better outcome may be expected from these studies in the next years.

Our data showed that a large number of ASs (i.e., 115 of 188) have been investigated in preclinical studies, mainly as a part of adult product development, but pediatric-specific studies have been less represented.

On the contrary, it is imperative that the preclinical evaluation is tailored to pediatric specificities and needs, including the characterization of toxicology and safety aspects relevant to the children. Such specificities may have a huge impact on the development of pediatric medicines because it leads regulators to waive the pediatric clinical development for safety reasons, to include contraindications in the SmPC, and to modify/adjust dosing regimen, among others (68). To deal with this issue, an innovative approach is emerging in pediatric drug development, that is exploiting new models, i.e., cells, tissue, organoid, or *in silico* models (69), instead of animal models, under the paradigm that the utility of animal models in place of children for the evaluation of toxicology, efficacy, and safety parameters is very limited or uncertain (70). Moreover, it was suggested that the ability to predict PK and PD with the adoption of new toxicology models (71, 72) or the use of mechanistic simulations may reduce the need and the duration of pediatric clinical studies (73). In particular, preclinical studies on several ASs could help select more specific and efficacious agents on one or more pediatric tumors, facilitating their prioritization.

Improvement in the direction of reducing the number while increasing the efficiency of clinical studies is also expected by the adoption of an innovative clinical study design (more specifically, basket, umbrella, and platform trials) that is more responsive to the complexity of NBL trials (i.e., limited population, genetic and immune phenotypic traits common to other pediatric cancers, and different agents to be studied in combination) (74). Together with a larger application of pharmacometric models and, where possible, extrapolation of existing data, these CT designs may substantially facilitate the progress of more ASs for pediatric use.

As positive results from our regulatory evaluation of ASs targeting NBL, we underline the following:

1. There were more drugs included in a PIP application than in the previous scenario, which was characterized by a higher number of waivers than the agreed PIPs (5).
2. Several ASs for which a waiver was granted for adults indication were also granted with a PIP for a different pediatric oncologic indication, demonstrating that, even with the lack of a specific rule (as the RACE Act in the USA), a medicinal product can be granted both waivers for adult indications and PIP-covering indications of pediatric interest if justified by the MoA of the AS.
3. Through our analysis of the PIPs, we can derive that a combination of preclinical pediatric-specific studies (including formulation and juvenile animal studies) and early clinical studies with limited phase 3 trials is the approach most required by regulators. It may be useful to use this information as a guide for preparing future pediatric developmental plans.
4. Interestingly, out of 14 PIPs with NBL indication, six include extrapolation, modeling, and simulation studies. However, based on the preliminary results of a pilot study on pediatric and rare MPs approved by EMA (75), a significant increase in other computational and innovative statistical models, also including Real Word Data studies, is expected in the next future. This approach will reduce the total economic and resource costs with advantages for patients, avoiding clinical research with limited possibilities to be successful.

However, this analysis also clarifies that several unresolved issues remain, which are as follows:

1. The majority of PIPs and the pediatric variations in SmPC are associated with adult oncology products. This demonstrates that the development of pediatric oncology products is still driven by adult drugs and not by a pediatric-specific interest in the drug.
2. There are still several ASs, even having an MoA of interest for children granted with a waiver for which pediatric development is not required by the EMA. In the EU, it may be necessary to adopt an *ad hoc* rule, such as the RACE Act in the USA, to bridge this gap.
3. The current regulatory procedures seem to be unable to assure faster oncology drug development and its timely approval for the market. As an example, we can consider that *olaparib* received an adult MA in 2014; a PIP for a pediatric indication including NBL was only applied in 2018, with an expected duration for PIP completion of up to 2035. Thus, the pediatric product will (possibly) reach the market 21 years later than the product authorized for adults.
4. Other regulatory procedures applicable to rare and pediatric conditions have been little considered and may be poorly understood by sponsors and researchers (76). As an example, *entrectinib* was withdrawn by the Orphan Designation Registry, while it received the PRIME designation followed by an accelerated approval. This approval was obtained before completing the pediatric development plan and only covers their use in children older than 12 years, leading to high-risk NBL prevailing in younger children.

In conclusion, in pediatric oncology, the number of approved new medicines has not increased significantly during the recent years. With reference to NBL, some old ASs on the market are still used in current practice without including the NBL pediatric indication. Several new ASs have been proposed for development and included in early CTs, but only a few products have been registered for NBL. Considering the several ongoing initiatives,[2], [3],[4] some improvements may be implemented.

First of all, scientists, regulatory experts, and developers should work together to identify a more efficient, less costly, and time-consuming "pediatric developmental model" integrating predictive preclinical studies and innovative clinical study designs. This model should be proposed and adopted in the PIP application and then agreed by the regulators as fitting with regulatory standards.

Second, the current regulatory process should better support these new scientific paradigms. In particular, some measures proposed in the context of the revision of the European Pediatric and Orphan Regulations may greatly move forward in this direction (77), which are as follows: (a) a drug potentially useful for cancer should be excluded by the application of waiver based on "disease or condition not existing in the pediatric age" and (b) a PIP-staggered approach may be considered. With this approach, the approval of the PIPs will occur step by step and could be stopped or accelerated according to the preliminary results (i.e., predictive preclinical study results) avoiding the extremely long duration of some PIPs; and (c) new incentives specific for products addressing unmet needs for pediatric and rare diseases (i.e., a PRIME-adapted scheme or dedicated research funds) should be largely adopted.

Data availability statement

The raw data supporting the conclusions of this article will be made available by the authors, without undue reservation.

Author contributions

AC prepared the first draft of the manuscript, contributed to the design of the research and to set up the methodology, and participated in the analysis of results. RC and AD prepared the first draft of the manuscript and contributed to the design of the research, to perform the research, and to the analysis of the results. AL and LR contributed to the design of the research and provided a general review of the analyzed data. FB and VG provided the final review of the draft. All authors contributed to the article and approved the submitted version.

Conflict of interest

The authors declare that the research was conducted in the absence of any commercial or financial relationships

2 SIOP Europe-the European Society for Pediatric Oncology. Available online at: https://siope.eu/ (accessed November 14, 2022).

3 The Innovative Therapies for Children with Cancer (ITCC) Platform. Available online at: https://www.itccp4.eu/project/overview (accessed November 14, 2022).

4 European Pediatric Translational Research Infrastructure. Available online at: https://eptri.eu/ (accessed November 14, 2022).

that could be construed as a potential conflict of interest.

Publisher's note

All claims expressed in this article are solely those of the authors and do not necessarily represent those of their affiliated organizations, or those of the publisher, the editors and the reviewers. Any product that may be evaluated in this article, or claim that may be made by its manufacturer, is not guaranteed or endorsed by the publisher.

Supplementary material

The Supplementary Material for this article can be found online at: https://www.frontiersin.org/articles/10.3389/fmed.2023.1113460/full#supplementary-material

References

1. Chung C, Boterberg T, Lucas J, Panoff J, Valteau-Couanet D, Hero B, et al. Neuroblastoma. *Pediatr Blood Cancer.* (2021) 68(Suppl. 2):e28473. doi: 10.1002/pbc.28473

2. Brodeur GM, Maris JM. Neuroblastoma. In: Pizzo PA, Poplack DG, editors. *Principles and Practice of Pediatric Oncology*. Philadelphia, PA: Lippincott Williams & Wilkins (2015).

3. Gatta G, Botta L, Rossi S, Aareleid T, Bielska-Lasota M, Clavel J, et al. Childhood cancer survival in Europe 1999-2007: results of EUROCARE-5—a population-based study. *Lancet Oncol.* (2014) 15:35–47. doi: 10.1016/S1470-2045(13)70548-5

4. Ceci A, Felisi M, Baiardi P, Bonifazi F, Catapano M, Giaquinto C, et al. Medicines for children licensed by the European Medicines Agency (EMEA): the balance after 10 years. *Eur J Clin Pharmacol.* (2006) 62:947–52. doi: 10.1007/s00228-006-0193-0

5. Toma M, Felisi M, Bonifazi D, Bonifazi F, Giannuzzi V, Reggiardo G, et al. Paediatric medicines in Europe: the paediatric regulation-is it time for reform? *Front Med.* (2021) 8:593281. doi: 10.3389/fmed.2021.593281

6. Commission Staff Working Document Evaluation. *Joint Evaluation of Regulation (EC) No 1901/2006 of the European Parliament and of the Council of 12 December 2006 on Medicinal Products for Paediatric Use and Regulation (EC) No 141/2000 of the European Parliament and of the Council of 16 December 1999 on Orphan Medicinal Products.* (2020). Available online at: https://eur-lex.europa.eu/legal-content/EN/TXT/?uri=CELEX%3A52020SC0163 (accessed November 14, 2022).

7. Schoot RA, Otth MA, Frederix GWJ, Leufkens HGM, Vassal G. Market access to new anticancer medicines for children and adolescents with cancer in Europe. *Eur J Cancer.* (2022) 165:146–53. doi: 10.1016/j.ejca.2022.01.034

8. Notices from European Union Institutions, Bodies, Offices and Agencies. *Council Conclusions on Personalised Medicine for Patients (2015/C 421/03).* (2015). Available online at: https://eur-lex.europa.eu/legal-content/EN/TXT/PDF/?uri=CELEX:52015XG1217(01)&from=FR (accessed November 14, 2022).

9. Nishiwaki S, Ando Y. Gap between pediatric and adult approvals of molecular targeted drugs. *Sci Rep.* (2020) 10:17145. doi: 10.1038/s41598-020-73028-w

10. Zafar A, Wang W, Liu G, Wang X, Xian W, McKeon F, et al. Molecular targeting therapies for neuroblastoma: progress and challenges. *Med Res Rev.* (2021) 41:961–1021. doi: 10.1002/med.21750

11. Akter J, Kamijo T. How do telomere abnormalities regulate the biology of neuroblastoma? *Biomolecules.* (2021) 11:1112. doi: 10.3390/biom11081112

12. Greengard EG. Molecularly targeted therapy for neuroblastoma. *Children.* (2018) 5:142. doi: 10.3390/children5100142

13. Zanotti S, Decaesteker B, Vanhauwaert S, De Wilde B, De Vos WH, Speleman F. Cellular senescence in neuroblastoma. *Br J Cancer.* (2022) 126:1529–38. doi: 10.1038/s41416-022-01755-0

14. Li N, Spetz MR Li D, Ho M. Advances in immunotherapeutic targets for childhood cancers: a focus on glypican-2 and B7-H3. *Pharmacol Ther.* (2021) 223:107892. doi: 10.1016/j.pharmthera.2021.107892

15. Segura MF, Soriano A, Roma J, Piskareva O, Jiménez C, Boloix A, et al. Methodological advances in the discovery of novel neuroblastoma therapeutics. *Expert Opin Drug Discov.* (2022) 17:167–79. doi: 10.1080/17460441.2022.2002297

16. Wang J, Yao W, Li K. Applications and prospects of targeted therapy for neuroblastoma. *World J Pediatr Surg.* (2020) 3:e000164. doi: 10.1136/wjps-2020-000164

17. Fletcher JI, Ziegler DS, Trahair TN, Marshall GM, Haber M, Norris MD. Too many targets, not enough patients: rethinking neuroblastoma clinical trials. *Nat Rev Cancer.* (2018) 18:389–400. doi: 10.1038/s41568-018-0003-x

18. Vassal G, Rousseau R, Blanc P, Moreno L, Bode G, Schwoch S, et al. Creating a unique, multi-stakeholder Paediatric Oncology Platform to improve drug development for children and adolescents with cancer. *Eur J Cancer.* (2015) 51:218–24. doi: 10.1016/j.ejca.2014.10.029

19. Vassal G, Houghton PJ, Pfister SM, Smith MA, Caron HN Li XN, Shields DJ, et al. International Consensus on minimum preclinical testing requirements for the development of innovative therapies for children and adolescents with cancer. *Mol Cancer Ther.* (2021) 20:1462–8. doi: 10.1158/1535-7163.MCT-20-0394

20. Moreno L, Barone G, DuBois SG, Molenaar J, Fischer M, Schulte J, et al. Accelerating drug development for neuroblastoma: Summary of the Second Neuroblastoma Drug Development Strategy forum from Innovative Therapies for Children with Cancer and International Society of Paediatric Oncology Europe Neuroblastoma. *Eur J Cancer.* (2020) 136:52–68. doi: 10.1016/j.ejca.2020.05.010

21. FDA. *Best Pharmaceuticals for Children Act and Pediatric Research Equity Act Status Report to Congress July 1, 2015 – June 30, 2020.* Available online at: https://www.fda.gov/media/157840/download (accessed November 14, 2022).

22. EMA. *Paediatric Investigation Plans.* (2010). Available online at: https://www.ema.europa.eu/en/human-regulatory/research-development/paediatric-medicines/paediatric-investigation-plans (accessed November 20, 2022).

23. FDA. *Pediatric Study Plans: Content of and Process for Submitting Initial Pediatric Study Plans and Amended Initial Pediatric Study Plans.* (2020). Available online at: https://www.fda.gov/regulatory-information/search-fda-guidance-documents/pediatric-study-plans-content-and-process-submitting-initial-pediatric-study-plans-and-amended (accessed November 20, 2022).

24. European Commission. Guideline on the format and content of applications for agreement or modification of a paediatric investigation plan and requests for waivers or deferrals and concerning the operation of the compliance check and on criteria for assessing significant studies (Text with EEA relevance). *Off J Eur Union.* (2014) 279:C 338/1.

25. EMA. *List of Waived Classes of Medicines.* (2015). Available online at: https://www.ema.europa.eu/en/human-regulatory/research-development/paediatric-medicines/paediatric-investigation-plans/class-waivers (accessed November 20, 2022)

26. H.R.2430. *FDA Reauthorization Act (FDARA) of 2017.* (2017). Available online at: https://www.congress.gov/bill/115th-congress/house-bill/2430/text (accessed November 20, 2022).

27. European Commission. Regulation (EC) No 141/2000 of the European Parliament and of the council of 16 December 1999 on orphan medicinal products. *Off J Eur Commun.* (2000) 2201:L18/1.

28. National Center for Biotechnology Information. *National Library of Medicine.* Pubmed®. (2022). Available online at: https://pubmed.ncbi.nlm.nih.gov/ (accessed November 14, 2022).

29. National Institutes of Health (NIH). *U.S. National Library of Medicines.* Clinicaltrials.gov. (2022). Available online at: clinicaltrials.gov. (accessed July 30, 2022).

30. EMA. *EMA/CPMP/ICH/286/1995. ICH Guideline M3(R2) on Non-clinical Safety Studies for the Conduct of Human Clinical Trials and Marketing Authorisation For Pharmaceuticals.* (2009). Available online at: https://www.ema.europa.eu/en/documents/scientific-guideline/ich-guideline-m3r2-non-clinical-safety-studies-conduct-human-clinical-trials-marketing-authorisation_en.pdf (accessed November 14, 2022).

31. EMA. *Table of All European Public Assessment Reports (EPAR) for Human and Veterinary Medicines.* (2022). Available online at: https://www.ema.europa.eu/sites/default/files/Medicines_output_european_public_assessment_reports.xlsx (accessed October 30, 2022).

32. EMA. *Table of All Orphan Designations.* (2022). Available online at: https://www.ema.europa.eu/en/medicines/download-medicine-data#paediatric-investigation-plans-section (accessed October 30, 2022).

33. EMA. *Table of Opinions and Decisions on Paediatric Investigation Plans (PIPs)*. (2022). Available online at: https://www.ema.europa.eu/en/medicines/download-medicine-data#paediatric-investigation-plans-section (accessed October 30, 2022).

34. EMA. *List of Products Granted Eligibility*. (2022). Available online at: https://www.ema.europa.eu/en/human-regulatory/research-development/prime-priority-medicines (accessed October 30, 2022).

35. EMA. *Annual Reports and Work Programmes*. European Medicines Agency. (2022). Available online at: https://europa.eu (accessed October 15, 2022).

36. Aravindan N, Herman T, Aravindan S. Emerging therapeutic targets for neuroblastoma. *Expert Opin Ther Targets.* (2020) 24:899–914. doi: 10.1080/14728222.2020.1790528

37. Smith V, Foster J. High-risk neuroblastoma treatment review. *Children (Basel).* (2018) 5:114. doi: 10.3390/children5090114

38. Shimada H, Ikegaki N. Genetic and histopathological heterogeneity of neuroblastoma and precision therapeutic approaches for extremely unfavorable histology subgroups. *Biomolecules.* (2022) 12:79. doi: 10.3390/biom12010079

39. Ciaccio R, De Rosa P, Aloisi S, Viggiano M, Cimadom L, Zadran SK, et al. Targeting oncogenic transcriptional networks in neuroblastoma: from N-Myc to epigenetic drugs. *Int J Mol Sci.* (2021) 22:12883. doi: 10.3390/ijms222312883

40. Braoudaki M, Hatziagapiou K, Zaravinos A, Lambrou GI. MYCN in neuroblastoma: "old wine into new wineskins". *Diseases.* (2021) 9:78. doi: 10.3390/diseases9040078

41. Kaczmarska A, Sliwa P, Lejman M, Zawitkowska J. The use of inhibitors of tyrosine kinase in paediatric haemato-oncology-when and why? *Int J Mol Sci.* (2021) 22:12089. doi: 10.3390/ijms222112089

42. Brenner AK, Gunnes MW. Therapeutic targeting of the anaplastic lymphoma kinase (ALK) in neuroblastoma-A comprehensive update. *Pharmaceutics.* (2021) 13:1427. doi: 10.3390/pharmaceutics13091427

43. Pearson ADJ, Barry E, Mossé YP, Ligas F, Bird N, de Rojas T, et al. Second Paediatric Strategy Forum for anaplastic lymphoma kinase (ALK) inhibition in paediatric malignancies: ACCELERATE in collaboration with the European Medicines Agency with the participation of the Food and Drug Administration. *Eur J Cancer.* (2021) 157:198–213. doi: 10.1016/j.ejca.2021.08.022

44. Mlakar V, Morel E, Mlakar SJ, Ansari M, Gumy-Pause F. A review of the biological and clinical implications of RAS-MAPK pathway alterations in neuroblastoma. *J Exp Clin Cancer Res.* (2021) 40:189. doi: 10.1186/s13046-021-01967-x

45. Ando K, Nakagawara A. Acceleration or brakes: which is rational for cell cycle-targeting neuroblastoma therapy? *Biomolecules.* (2021) 11:750. doi: 10.3390/biom11050750

46. Zafar A, Wang W, Liu G, Xian W, McKeon F, Zhou J, et al. Targeting the p53-MDM2 pathway for neuroblastoma therapy: Rays of hope. *Cancer Lett.* (2021) 496:16–29. doi: 10.1016/j.canlet.2020.09.023

47. Jin Z, Lu Y, Wu Y, Che J, Dong X. Development of differentiation modulators and targeted agents for treating neuroblastoma. *Eur J Med Chem.* (2020) 207:112818. doi: 10.1016/j.ejmech.2020.112818

48. George SL, Parmar V, Lorenzi F, Marshall LV, Jamin Y, Poon E, et al. Novel therapeutic strategies targeting telomere maintenance mechanisms in high-risk neuroblastoma. *J Exp Clin Cancer Res.* (2020) 39:78. doi: 10.1186/s13046-020-01582-2

49. Southgate HED, Chen L, Curtin NJ, Tweddle DA. Targeting the DNA damage response for the treatment of high risk neuroblastoma. *Front Oncol.* (2020) 10:371. doi: 10.3389/fonc.2020.00371

50. Tucker ER, Poon E, Chesler L. Targeting MYCN and ALK in resistant and relapsing neuroblastoma. *Cancer Drug Resist.* (2019) 2:803–12. doi: 10.20517/cdr.2019.009

51. Lima L, de Melo TCT, Marques D, de Araújo JNG, Leite ISF, Alves CX, et al. Modulation of all-trans retinoic acid-induced MiRNA expression in neoplastic cell lines: a systematic review. *BMC Cancer.* (2019) 19:866. doi: 10.1186/s12885-019-6081-7

52. Kong X, Pan P, Sun H, Xia H, Wang X, Li Y, et al. Drug discovery targeting anaplastic lymphoma kinase (ALK). *J Med Chem.* (2019) 62:10927–54. doi: 10.1021/acs.jmedchem.9b00446

53. Pastor ER, Mousa SA. Current management of neuroblastoma and future direction. *Crit Rev Oncol Hematol.* (2019) 138:38–43. doi: 10.1016/j.critrevonc.2019.03.013

54. Aubry A, Galiacy S, Allouche M. Targeting ALK in cancer: therapeutic potential of proapoptotic peptides. *Cancers.* (2019) 11:275. doi: 10.3390/cancers11030275

55. Umapathy G, Mendoza-Garcia P, Hallberg B, Palmer RH. Targeting anaplastic lymphoma kinase in neuroblastoma. *APMIS.* (2019) 127:288–302. doi: 10.1111/apm.12940

56. Oh L, Hafsi H, Hainaut P, Ariffin H. p53, stem cell biology and childhood blastomas. *Curr Opin Oncol.* (2019) 31:84–91. doi: 10.1097/CCO.0000000000000504

57. MacFarland S, Bagatell R. Advances in neuroblastoma therapy. *Curr Opin Pediatr.* (2019) 31:14–20. doi: 10.1097/MOP.0000000000000711

58. Huang H. Anaplastic lymphoma kinase (ALK) receptor tyrosine kinase: a catalytic receptor with many faces. *Int J Mol Sci.* (2018) 19:3448. doi: 10.3390/ijms19113448

59. Zage PE. Novel therapies for relapsed and refractory neuroblastoma. *Children.* (2018) 5:148. doi: 10.3390/children5110148

60. Yuan J, Zhang S, Zhang Y. Nrf1 is paved as a new strategic avenue to prevent and treat cancer, neurodegenerative and other diseases. *Toxicol Appl Pharmacol.* (2018) 360:273–83. doi: 10.1016/j.taap.2018.09.037

61. Yoshida GJ. Emerging roles of Myc in stem cell biology and novel tumor therapies. *J Exp Clin Cancer Res.* (2018) 37:173. doi: 10.1186/s13046-018-0835-y

62. Jubierre L, Jiménez C, Rovira E, Soriano A, Sábado C, Gros L, et al. Targeting of epigenetic regulators in neuroblastoma. *Exp Mol Med.* (2018) 50:1–12. doi: 10.1038/s12276-018-0077-2

63. Tolbert VP, Matthay KK. Neuroblastoma: clinical and biological approach to risk stratification and treatment. *Cell Tissue Res.* (2018) 372:195–209. doi: 10.1007/s00441-018-2821-2

64. Della Corte CM, Viscardi G, Di Liello R, Fasano M, Martinelli E, Troiani T, et al. Role and targeting of anaplastic lymphoma kinase in cancer. *Mol Cancer.* (2018) 17:30. doi: 10.1186/s12943-018-0776-2

65. Janoueix-Lerosey I, Lopez-Delisle L, Delattre O, Rohrer H. The ALK receptor in sympathetic neuron development and neuroblastoma. *Cell Tissue Res.* (2018) 372:325–37. doi: 10.1007/s00441-017-2784-8

66. Valter K, Zhivotovsky B, Gogvadze V. Cell death-based treatment of neuroblastoma. *Cell Death Dis.* (2018) 9:113. doi: 10.1038/s41419-017-0060-1

67. Giannuzzi V, Conte R, Landi A, Ottomano SA, Bonifazi D, Baiardi P, et al. Orphan medicinal products in Europe and United States to cover needs of patients with rare diseases: an increased common effort is to be foreseen. *Orphanet J Rare Dis.* (2017) 12:64. doi: 10.1186/s13023-017-0617-1

68. EMA. *SME workshop: Focus on non-clinical aspects. Pre-clinical Requirements to Support Development of Paediatric Medicines.* (2016). Available online at: https://www.ema.europa.eu/en/documents/presentation/presentation-pre-clinical-requirements-support-development-paediatric-medicines-janina-karres_en.pdf (accessed November 20, 2022).

69. van Berlo D, Nguyen VV, Gkouzioti V, Leineweber K, Verhaar MC, van Balkom BW. Stem cells, organoids, and organ-on-a-chip models for personalized in vitro drug testing. *Curr Opin Toxicol.* (2021) 28:7–14. doi: 10.1016/j.cotox.2021.08.006

70. Bailey GP, Mariën D. The value of juvenile animal studies "What have we learned from preclinical juvenile toxicity studies? II" Birth Defects. *Res B Dev Reprod Toxicol.* (2011) 92:273–91. doi: 10.1002/bdrb.20328

71. EMA. *EMA/470807/2011 Veterinary Medicines and Product Data Management. Statement of the EMA Position on the Application of the 3Rs (Replacement, Reduction and Refinement) in the Regulatory Testing of Human and Veterinary Medicinal Products.* (2011). Available online at: https://www.ema.europa.eu/en/documents/other/statement-european-medicines-agency-position-application-3rs-replacement-reduction-refinement_en.pdf (accessed November 14, 2022).

72. Gorzalczany SB, Rodriguez Basso AG. Strategies to apply 3Rs in preclinical testing. *Pharmacol Res Perspect.* (2021) 9:e00863. doi: 10.1002/prp2.863

73. Zuang V, Dura A, Ahs Lopez E, Barroso J, Batista Leite S, Berggren E, et al. *Non-animal Methods in Science and Regulation, EUR 30960 EN.* Luxembourg: Publications Office of the European Union (2022).

74. Park JJH Siden E, Zoratti MJ, Dron L, Harari O, Singer J, Lester RT, et al. Systematic review of basket trials, umbrella trials, and platform trials: a landscape analysis of master protocols. *Trials.* (2019) 20:572. doi: 10.1186/s13063-019-3664-1

75. Ruggieri L, Landi A. *Innovative Research Methodologies Application in Paediatric Orphan Medicines XV Foresight Training Course - Boosting Research and Innovation in a Changing Regulatory framework.* Bari: Fondazione pr la Ricerca Farmacologica Gianni Benzi Onlus (2022).

76. Ruggieri L, Ceci A, Bartoloni F, Elie V, Felisi M, Jacqz-Aigrain E, et al. Paediatric clinical research in Europe: an insight on experts' needs and perspectives. *Contemp Clin Trials Commun.* (2021) 21:100735. doi: 10.1016/j.conctc.2021.100735

77. European Commission. *Inception Impact Assessment Ref. Ares (2020)7081640* (2020). Available online at: https://eur-lex.europa.eu/legal-content/EN/TXT/?uri=pi_com:Ares(2020)7081640

Frontiers in Medicine

Translating medical research and innovation into improved patient care

A multidisciplinary journal which advances our medical knowledge. It supports the translation of scientific advances into new therapies and diagnostic tools that will improve patient care.

Discover the latest Research Topics

See more →

Frontiers

Avenue du Tribunal-Fédéral 34
1005 Lausanne, Switzerland
frontiersin.org

Contact us

+41 (0)21 510 17 00
frontiersin.org/about/contact